EXHIBIT 5

Docket No. 108
Filed: 2/2/24

JACS
JOURNAL OF THE AMERICAN CHEMICAL SOCIETY
Article
pubs.acs.org/JACS

Efficient Liver Targeting by Polyvalent Display of a Compact Ligand for the Asialoglycoprotein Receptor

Carlos A. Sanhueza,[†,‡] Michael M. Baksh,[†,‡] Benjamin Thuma,[§] Marc D. Roy,[∥] Sanjay Dutta,[‡] Cathy Préville,[§] Boris A. Chrunyk,[§] Kevin Beaumont,[⊥] Robert Dullea,[#] Mark Ammirati,[§] Shenping Liu,[§] David Gebhard,[§] James E. Finley,[∥] Christopher T. Salatto,[#] Amanda King-Ahmad,[§] Ingrid Stock,[§] Karen Atkinson,[§] Benjamin Reidich,[#] Wen Lin,[§] Rajesh Kumar,[▽] Meihua Tu,[⊥] Elnaz Menhaji-Klotz,[⊥] David A. Price,[⊥] Spiros Liras,[⊥] M. G. Finn,*[,†,‡] and Vincent Mascitti*[,§]

[†]School of Chemistry & Biochemistry, Georgia Institute of Technology, 901 Atlantic Avenue, Atlanta, Georgia 30332, United States
[‡]Department of Chemistry and The Skaggs Institute for Chemical Biology, The Scripps Research Institute, 10550 N. Torrey Pines Road, La Jolla, California 92037, United States
[§]Pfizer Medicine Design, Eastern Point Road, Groton, Connecticut 06340, United States
[∥]Pfizer Drug Safety R&D, Eastern Point Road, Groton, Connecticut 06340, United States
[⊥]Pfizer Medicine Design, Main Street, Cambridge, Massachusetts 02139, United States
[#]Pfizer CVMET Biology, Main Street, Cambridge, Massachusetts 02139, United States
[▽]Pfizer Medicinal Sciences, Eastern Point Road, Groton, Connecticut 06340, United States

Supporting Information

ABSTRACT: A compact and stable bicyclic bridged ketal was developed as a ligand for the asialoglycoprotein receptor (ASGPR). This compound showed excellent ligand efficiency, and the molecular details of binding were revealed by the first X-ray crystal structures of ligand-bound ASGPR. This analogue was used to make potent di- and trivalent binders of ASGPR. Extensive characterization of the function of these compounds showed rapid ASGPR-dependent cellular uptake in vitro and high levels of liver/plasma selectivity in vivo. Assessment of the biodistribution in rodents of a prototypical Alexa647-labeled trivalent conjugate showed selective hepatocyte targeting with no detectable distribution in nonparenchymal cells. This molecule also exhibited increased ASGPR-directed hepatocellular uptake and prolonged retention compared to a similar GalNAc derived trimer conjugate. Selective release in the liver of a passively permeable small-molecule cargo was achieved by retro-Diels–Alder cleavage of an oxanorbornadiene linkage, presumably upon encountering intracellular thiol. Therefore, the multicomponent construct described here represents a highly efficient delivery vehicle to hepatocytes.

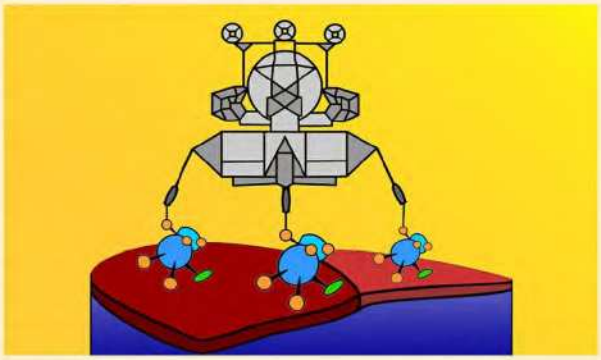

INTRODUCTION: AN OPTIMIZED ASGPR LIGAND MOTIF

By virtue of its extraordinary rates of transport, the asialoglycoprotein receptor (ASGPR) is an attractive target for the importation of diagnostic and therapeutic molecules into hepatocytes.[1−3] However, monosaccharide ligands of the ASGPR usually bind with low affinity (K_d in the high μM to low mM range),[4] and so multimerization of these species is used to achieve levels of affinity thought to be required for the delivery of therapeutic cargos.[5−9] To our knowledge, the relationship of high-affinity binding to transport (that is, to binding, membrane translocation, and release) has not been extensively explored.

We previously described several series of ASGPR ligands based on substituent variations at the anomeric, 2-, 5-, and 6-positions of the galactosamine (GalNAc) skeleton.[10] This work, along with previous studies of Ernst and co-workers[4,11] and others,[12] shows that substantial variations can be tolerated as long as the C3−C4 diol is presented in the proper orientation for interaction with a proximal calcium ion of the receptor.[13] Although it is possible to access analogues of improved affinity in this way, such compounds often suffer from a dramatic decrease in ligand efficiency (LE),[14−17] as shown for examples **1**−**3** in Figure 1. In combination with their multistep and low-

Received: December 21, 2016

DOI: 10.1021/jacs.6b12964
J. Am. Chem. Soc. XXXX, XXX, XXX−XXX

yielding synthesis, this makes them suboptimal alternatives as ASGPR-targeting ligands.

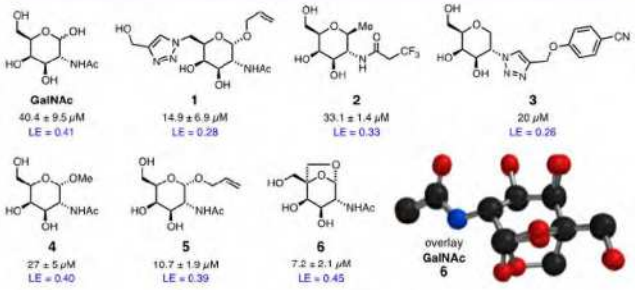

Figure 1. ASGPR ligands with ($1/K_{ads}$) values for immobilized ASGPR measured by surface plasmon resonance, plus calculated ligand efficiency (LE) values. (Bottom right) Overlay of the calculated minimum-energy conformations of GalNAc and compound **6**, showing close overlap of the pyranose rings and substituents between the two structures. Values for **1**, **2**, and **5** are from ref 10; compound **3** is found in ref 4.

Examination of the published X-ray crystal structure of ASGPR binding domain (PDB: 1dv8)[25] led us to postulate that one could potentially optimize the interaction between the hydrophobic α-face of the pyranose and the tryptophan residue Trp 243.[18] In order to improve both affinity and LE, we reasoned that a bridged ketal structure such as **6** should lock in a conformation in which the α-face is accessible and the 6-hydroxymethyl and 2-*N*-acetyl groups retain their positions (Figure 1). Molecular mechanics calculations showed the lowest-energy conformation of **6** to match that of GalNAc, but with ~1.6 kcal/mol separating it from the next-higher-energy structure. In contrast, five distinct low-energy conformations of GalNAc are within 0.5 kcal/mol of each other, suggesting that **6** should exhibit a much greater occupancy of the favored ASGPR-binding conformation than GalNAc. This is purchased at the cost of the addition of only a single extra methylene group compared to GalNAc, thereby potentially leading to an increase in LE. Similar bridged ketal ring systems were reported during the development of the antidiabetes medication ertugliflozin.[19,20]

Compound **6** was initially prepared in relatively low overall yield as shown in Figure 2A. Treatment of commercially available methyl-α-D-2-acetamido-2-deoxygalactopyranoside **4** in the presence of galactose oxidase and catalase in a phosphate buffer produced the corresponding intermediate aldehyde,[21]

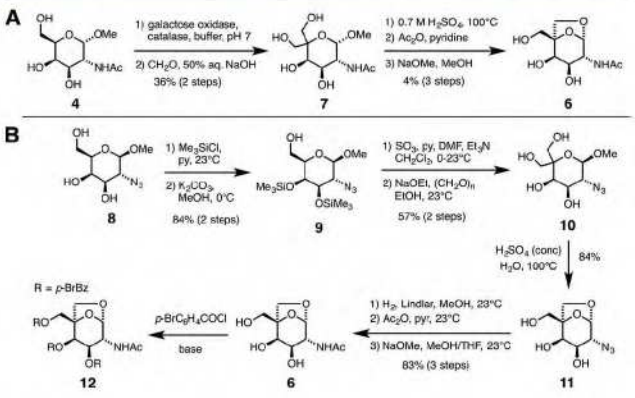

Figure 2. Initial (A) and improved (B) synthetic routes to **6**.

which was subjected without purification to aldol-Cannizzaro conditions to give polyol intermediate **7** in 36% yield over two steps.[22] Acid-promoted bridged ketal formation followed by peracetylation and saponification gave the desired product in sufficient quantities for measurement of binding to immobilized ASGPR by surface plasmon resonance (SPR) as described earlier.[10] These measurements provide Langmuir adsorption coefficients (K_{ads}), the reciprocals of which represent experimental approximations of dissociation constants.[23] Compound **6** exhibited almost 6-fold better affinity than GalNAc ($1/K_{ads}$ = 7.2 vs 40 μM), giving a calculated ligand efficiency (0.45) greater than that of the natural ligand (0.41).

The synthetic route shown in Figure 2B was developed to allow access to multigram quantities of this lead structure and derivatives for further in vitro and in vivo profiling. Persylilation of azide **8**[24] followed by base-promoted regioselective deprotection of the primary hydroxyl group gave **9**. Sequential Parikh–Doering oxidation and aldol-Cannizzaro reactions cleanly installed the desired tetrasubstituted carbon at C-5 (compound **10**). Stereoselective bridged ketal formation under acidic conditions gave **11** in good yield. Finally, azide reduction followed by peracetylation/saponification provided **6** as a white solid. This route provided access to **6** in 8 steps and 33% overall yield, as well as to other derivatives. Single-crystal X-ray diffraction analysis of derivative **12** was used to confirm the bridged ketal structure of **6** (Supporting Information).

SPR measurements of ASGPR binding (Figure 3) confirmed the importance of both the *N*-acetyl group (compound **13** vs **6**)

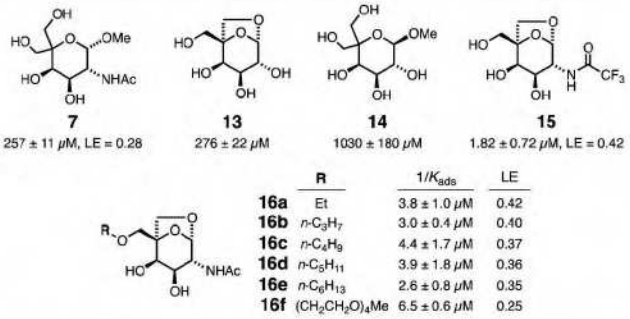

	R	$1/K_{ads}$	LE
16a	Et	3.8 ± 1.0 μM	0.42
16b	*n*-C_3H_7	3.0 ± 0.4 μM	0.40
16c	*n*-C_4H_9	4.4 ± 1.7 μM	0.37
16d	*n*-C_5H_{11}	3.9 ± 1.8 μM	0.36
16e	*n*-C_6H_{13}	2.6 ± 0.8 μM	0.35
16f	$(CH_2CH_2O)_4Me$	6.5 ± 0.6 μM	0.25

Figure 3. ASGPR ligands discussed in the text with $1/K_{ads}$ values for ASGPR determined by surface plasmon resonance.

and the bicyclic nature of the core structure (**7** vs **6** and **14** vs **13**). We had previously established for other GalNAc analogues that a trifluoroacetamide unit at C2 improved binding by 3–10-fold relative to acetamide,[10] and this trend was also observed here (compound **15** vs **6**). (Compound **6** was used for the in vivo studies described below because of uncertainty associated with the long-term metabolic stability of the trifluoroacetamide group.) Alkylation of the C6-hydroxyl was envisioned as a way to attach this motif to cargo molecules, and alkyl and oligo(glycol) ethers **16a–f** derived from **6** retained full affinity for the receptor.

Atomic Resolution Structure of ASGPR–Ligand Complexes. Although the crystals used for the reported structure of the ASGPR carbohydrate-binding H1 domain (PDB: 1dv8) were grown in the presence of 20 mM lactose, the sugar does not appear in the structure.[25] Therefore, we and others have relied on docking calculations, which show that the GalNAc-binding region is shallow and a difficult target for high-affinity monomeric ligands,[26] a conclusion reinforced by

DOI: 10.1021/jacs.6b12964
J. Am. Chem. Soc. XXXX, XXX, XXX–XXX

structures of GalNAc bound to homologous mannose receptor derivatives (PDB: 1bch, 1bcj, 1fif, and 1fih).[27,28] We were able to secure more direct structural information by crystallizing the ASGPR carbohydrate-binding domain with lactose and with compound **6**, and obtaining diffraction data with well-resolved ligand densities. The resulting structures are shown in Figure 4.

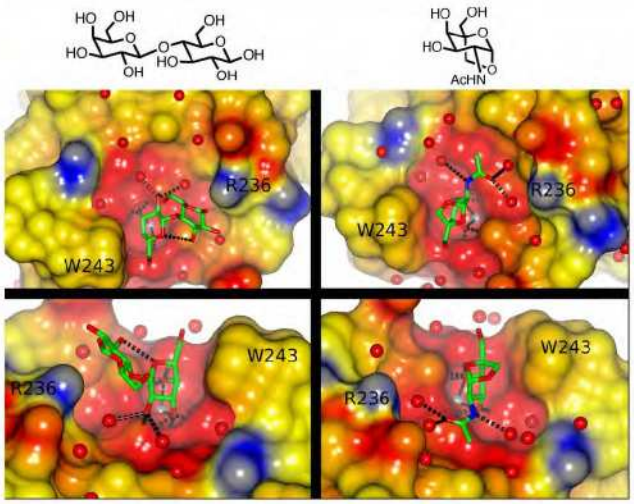

Figure 4. X-ray crystal structures of the ASGPR carbohydrate-binding domain with (left) lactose (PDB: 5JPV) and (right) compound **6** (PDB: 5JQ1). The top panels show the shallow binding pocket from above; the bottom panels show a side view highlighting hydrophobic interactions with Trp 243 and interactions with the acetamide group of **6** along the bottom of the pocket. Red = negative surface charge, blue = positive surface charge, and yellow = hydrophobic surface. Hydrogen bonds and bonds to metal ion (gray sphere) are shown in dashes. Small red spheres represent bound water molecules identified crystallographically.

These structures provide the first high-resolution look at the ASGPR–galactose-binding interaction. The sugar-binding mode was found to be consistent with previous analogue structures and predictions, showing interactions of the hydroxyls at C-3 and C-4 of the β-D-galactose ring with the required calcium ion.

Comparisons of affinity and LE of **6** versus its uncyclized precursors **4** and **7** support the hypothesis of a productive van der Waals interaction with Trp 243. Such an interaction is apparent in both structures, with ASGPR·**6** exhibiting a more extensive pyranose–indole overlap at a measured distance of 4 Å (Figure 4). The acetamide group of **6** conforms nicely to the channel floor (defined by Tyr 272, His256, Asn264, and Asp266 residues), whereas the 6-hydroxymethyl substituent extends away from the protein, allowing for cargo attachment. The structural details of the binding of other ligands reported previously, which have substituents at various places around the *N*-acetylgalactose core,[10] will be discussed elsewhere.

■ MULTIVALENT LIGANDS

The use of galactosyl-based ligands for the targeting of liver cells where ASGPR expression is highest has relied for many years on the creation of multivalent molecules to enhance receptor binding beyond the low-micromolar level,[29−32] with recent reports of targeted siRNA and antisense DNA delivery being especially exciting.[33−35] Multimerization of the bicyclic ASGPR-binding motif was accomplished by a convergent design relying on azide–alkyne cycloaddition to connect an azide-terminated version of ligand **6** to propargylic ethers of mono-, di-, and trivalent ethanolamines (Figure 5). The amino

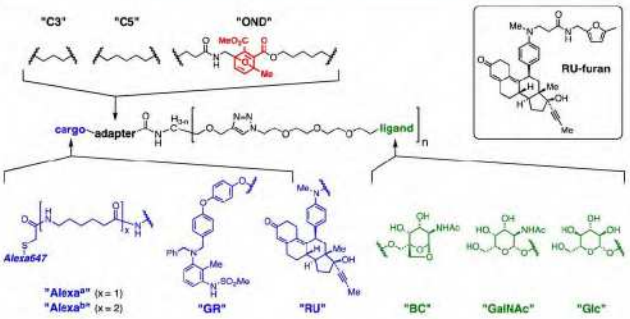

Figure 5. Modular composition of the multivalent compounds discussed in the text.

group was used to connect to the carboxylic acid derivatives of candidate "cargo" molecules: a fluorescent probe (Alexa-Fluor647, with two different linker lengths, designated "Alexa^a" and "Alexa^b") and two model drug-like compounds, a nonsteroidal glucocorticoid receptor modulator (designated "GR"),[36] and the steroidal glucocorticoid antagonist RU-486 (mifepristone, designated "RU"). Analogous compounds bearing the natural GalNAc and glucose (Glc) ligands in place of the bicyclic derivative were prepared by the same modular approach.

With the expectation that drug release from ASGPR-targeting motifs would be necessary, we also prepared variants incorporating the thiol-sensitive oxanorbornadiene (OND)[37,38] linker by the route shown in the Supporting Information. This system relies on a two-step Michael addition/retro-Diels–Alder sequence that is programmed to occur rapidly in the presence of intracellular levels of reduced thiols such as glutathione. Thus, the various molecules explored here are referred to in the form "cargo-adapter-ligand", as in "**GR-C3-(BC)$_2$**" for a compound bearing two bicyclic bridged ketal ASGPR ligands, connected to a GR cargo by a simple propyl (C_3) chain. The labeling scheme is shown in Table 1. Not all of the possible combinations of ligand, cargo, and valence were explored.

Table 1. Binding and Activity Results for Selected Compounds

compound	$1/K_{ads}$	compound	$1/K_{ads}$
Alexa^a-C3-(BC)$_1$	4.1 μM	**Gr-C3-(BC)$_1$**	nonspecific
Alexa^a-C3-(BC)$_2$	0.96 ± 0.01 nM	**Gr-C3-(BC)$_2$**	0.49 ± 0.01 nM
Alexa^a-C3-(BC)$_3$	30 ± 5 pM	**Gr-C3-(BC)$_3$**	71 ± 30 pM
Ru-C3-(BC)$_2$	1.48 ± 0.05 nM		

The ASGPR-binding ability of a subset of multivalent conjugates was measured by surface plasmon resonance (SPR), with results summarized in Table 1. The monovalent conjugate **Alexa^a-C3-(BC)$_1$** bound with low micromolar affinity, consistent with values for the parent bicyclic **6** and analogues shown in Figure 3 (**15**, **16a–f**). The corresponding GR modulator adduct, **GR-C3-(BC)$_1$**, exhibited competing nonspecific interactions in the SPR assay, perhaps to be expected given the hydrophobic nature of the cargo. Bivalent structures **Alexa^a-C3-(BC)$_2$**, **GR-C3-(BC)$_2$**, and **RU-C3-(BC)$_2$** all showed ~1000-fold improvement in avidity (binding

DOI: 10.1021/jacs.6b12964
J. Am. Chem. Soc. XXXX, XXX, XXX–XXX

constants approximately 1 nM), and the trivalent analogues (**Alexa^a-C3-(BC)$_3$** and **GR-C3-(BC)$_3$**) showed a further 7−30-fold improvement to the midpicomolar range. After binding to immobilized ASGPR on the SPR chip at pH 7.4, **Alexa^a-C3-(BC)$_3$** was rapidly released upon exposure to buffer at pH 5.2 or 5.7; whereas at pH 6.5, much less release was observed (Figure S3). This is consistent with the reported pH dependence of ASGPR binding to monomeric natural ligands.[39,40]

ASGPR Engagement In Vitro. The ability of representative conjugates to engage the ASGPR was assessed by fluorescence microscopy in cultured HepG2 and SK-Hep cells. These cell lines have some of the properties of hepatocytes and are standard in vitro models; while both exhibit lower levels of asialoglycoprotein receptor compared to primary hepatocytes, the HepG2 line expresses a much higher density of ASGPR on the cell surface than SK-Hep cells. This was verified prior to use by antibody staining (Figure S4). Cargo uptake by HepG2 cells was found to be extensive for di- and trivalent AlexaFluor conjugates of the bicyclic motif **6**, but much less pronounced with the monovalent analogue (Figures S8 and S10). Dye-labeled asialoorosomucoid (ASOR), commonly used as a positive control for ASGPR-mediated endocytosis, was taken into HepG2 cells better than the monovalent **Alexa^a-C3-(BC)$_1$** compound, but to a significantly lesser degree than the di- and trivalent analogues. Little or no uptake into HepG2 cells was observed for the analogous glucosyl derivatives (Figure S5), and SK-Hep cells were very poorly targeted by any of these compounds (Figure S9). These results were confirmed by quantitative flow cytometry (Figure 6, which of course measures total internalized signal, both

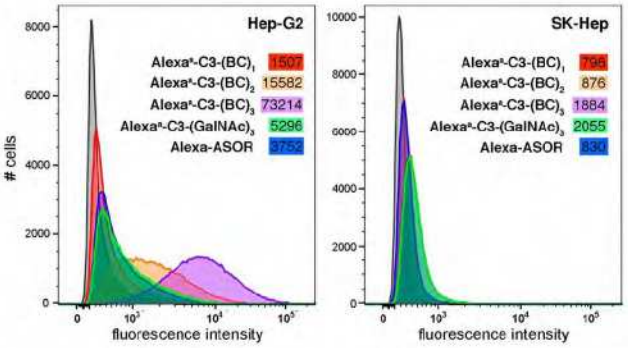

Figure 6. Flow cytometry analysis of the indicated cells treated with the indicated molecules (100 nM, 30 min, room temperature). Numerical values are the average number of dye-labeled molecules taken up per cell, derived from comparison to standardized samples.

cytosolic and endolysosomal), revealing a 10-fold increase in uptake of dye-labeled **Alexa^a-C3-(BC)$_3$** versus **Alexa^a-C3-(GalNAc)$_3$** by ASGPR-rich cells.

As shown in the Supporting Information, dye-labeled **Alexa^a-C3-(BC)$_n$** conjugates internalized into HepG2 cells appeared to be both colocalized with endosomes and in the cytosol. Furthermore, uptake of these compounds was found to be blocked in the presence of a low concentration of chlorpromazine, known to inhibit clathrin-mediated endocytosis,[41] as expected.[42,43]

ASGPR ligand valency also had a strong effect on the rate of receptor-mediated cellular uptake. Figure 7A shows marked differences for HepG2 cells in the presence of 100 nM solutions

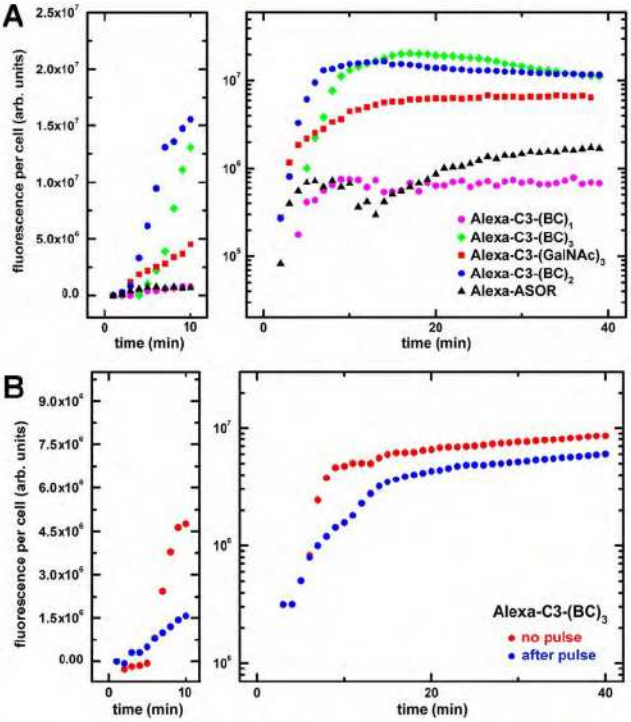

Figure 7. (A) Mean fluorescence intensity (MFI) per cell, measured by fluorescence microscopy, for HepG2 cells treated with 100 nM of the indicated molecule. (B) Pulse-chase experiment in which HepG2 cells were treated with 100 nM of a tripodal ligand lacking a cargo [**(BC)$_3$-NH$_2$**] for 30 min, washed three times, and then treated with 100 nM of the dye-labeled trimer (starting at time = 0). For comparison, uptake curves for the dye-labeled compounds alone (100 nM) are shown in red ("no pulse"). The first 10 min of the experiment is shown on the left on a linear fluorescence intensity scale; on the right is the full experiment on a logarithmic scale. Analogous results with other chase compounds are shown in Figure S11.

of dye−cargo conjugates, in the order BC dimer ≈ BC trimer > GalNAc trimer > ASOR ≈ BC monomer. To further probe effects on receptor recycling, a series of pulse-chase experiments was performed in which HepG2 cells were saturated with an unlabeled trivalent BC conjugate **(BC)$_3$-NH$_2$** (Supporting Information), followed by treatment with Alexa-labeled variants (100 nM), and uptake kinetics were compared to the direct treatments of dye-labeled compounds described earlier. Figure 7B shows an example in which the chase compound is **Alexa^a-C3-(BC)$_3$**. In this and analogous experiments (Figure S11), pretreatment with trivalent BC ligand induced a modest delay in follow-on internalization but no significant change in overall uptake, showing that this high-affinity molecule has a slightly delayed off-rate but does not abrogate receptor function. Similar results were observed when chasing with Alexa-labeled ASOR and **Alexa^a-C3-(GalNAc)$_3$**. These observations are consistent with the assumption that internalization rates and behavior of the di- and trivalent BC conjugates generally resemble that of the natural high-valent and high-affinity asialoorosomucoid ligand,[44] with higher affinity bestowed by the optimized nature of the bicyclic ligand.

To further explore the relative activity and potential translational impact of the compact bicyclic ligand versus GalNAc, human primary hepatocytes were treated with the triantennary versions of each, conjugated to AlexaFluor647. Figure 8 shows representative fluorescence microscopy images

DOI: 10.1021/jacs.6b12964
J. Am. Chem. Soc. XXXX, XXX, XXX−XXX

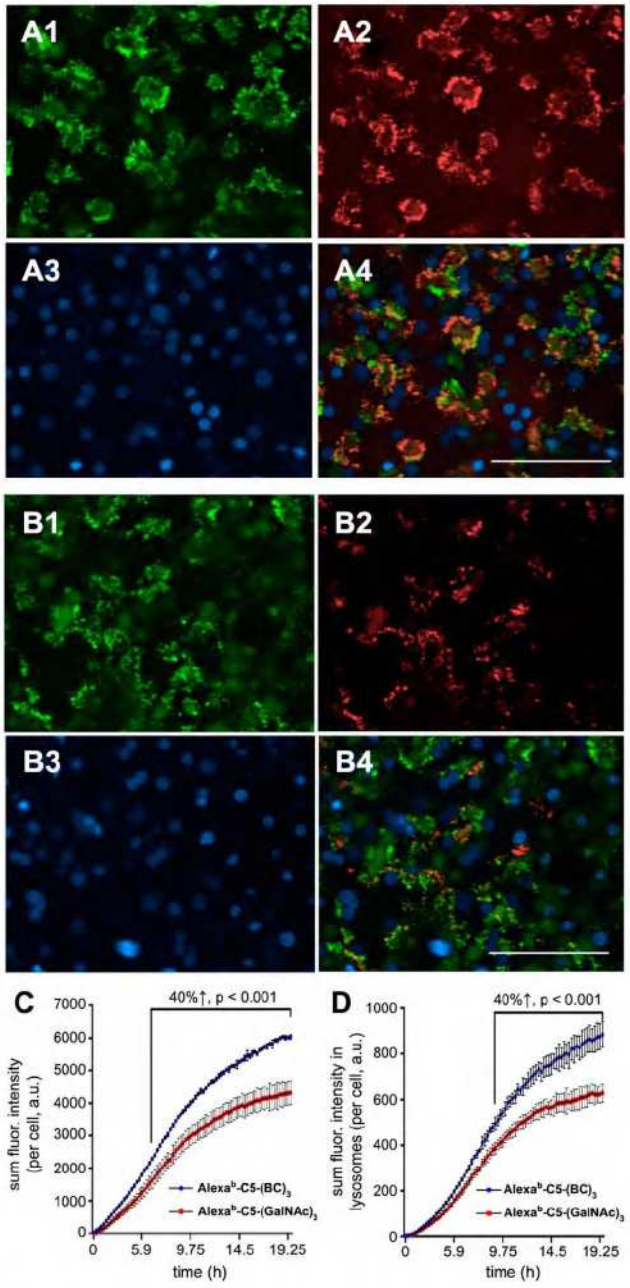

Figure 8. Human primary hepatocytes treated with (A) **Alexa^b-C5-(BC)$_3$** or (B) **Alexa^b-C5-(GalNac)$_3$** for 20 h at 1 μM. Staining: 1 = endolysosomal (pHrodo dextran); 2 = AlexaFluor647 (ASGPR-targeted compounds); 3 = nuclear (DAPI); 4 = composite overlaid images. Scale bar =100 μm. Wider-field images are shown in Figure S14. Quantification of intracellular (C) and lysosomal (D) accumulation. In each case, a statistically significant increase (~40%) was observed for the tripodal **BC** ligand vs the analogous **GalNAc** ligand.

after prolonged exposure, demonstrating more efficient uptake of the BC analogue and strong endolysosomal colocalization for both compounds. It should be noted that these dye-labeled compounds were derived from a commercial Alexa-thiol reagent, with two different connector lengths employed during the course of these studies, designated Alexa^a and Alexa^b and defined in Figure 5. No differences were noted in the behavior of conjugates having connectors of different lengths.

Liver Targeting. The glucocorticoid receptor modulator RU-486 was chosen as a model drug to illustrate the liver-targeting potential of these novel ASGPR ligands. Indeed, hepatoselective delivery of such modulators could be desirable for Type 2 diabetes treatment while minimizing risks of side effects associated with exposure of such compounds in peripheral tissues. We determined the liver/plasma ratios for various RU-486 conjugates in rats under steady-state intravenous infusion. Under these conditions, a molecule with high passive permeability (like RU-486 or RU-furan) should achieve a 1:1 unbound plasma to unbound liver concentration ratio, so long as there is no active uptake into or efflux from the liver. An unbound liver/plasma ratio greater than 1 reflects active uptake of that compound.

All compounds (except the hydrophobic **RU-furan**)[45] were formulated in 0.9% saline at 0.2 mg/mL and constantly infused into 4 male Wistar-Han rats at a rate of 10 $\mu g \cdot min^{-1} \cdot kg^{-1}$ over 7 h (total dose = 4.2 mg/kg, 21 mL/kg total volume). During this time, blood samples were taken at 0.1, 0.25, 0.5, 1, 2, 4, and 7 h following the start of the infusion, and compound concentrations were measured in the derived plasma. Steady-state values (reached within 1 h and maintained over the full 7 h in each case) are shown in Table 2; representative runs are shown

Table 2. In Vivo Results for the Distribution of Certain Adducts of RU-486 with Mono- and Multivalent ASGPR Ligand-Targeting Agents

	RU-C3-(BC)$_1$	RU-C3-(BC)$_2$	RU-C3-(BC)$_3$	RU-C3-(GalNac)$_2$	RU-C3-(GalNac)$_3$
fraction unbound, liver	0.089	0.11	0.065	0.079	0.22
fraction unbound, plasma	0.265	0.27	0.283	0.298	0.55
unbound liver:plasma ratio	0.39	9	144	0.87	8.7
	RU-C3-(Glc)$_2$	**RU-C3-(Glc)$_3$**	**RU-OND-(BC)$_2$[a]**	**RU-OND-(BC)$_3$[a]**	**RU-OND-(Glc)$_2$[a]**
fraction unbound, liver	0.13	0.12	nd[b]	nd[b]	nd[b]
fraction unbound, plasma	0.49	0.68	nd[b]	nd[b]	nd[b]
unbound liver:plasma ratio	0.22	0.02	93[c]	41[c]	0.9[c]

[a]OND = cleavable oxanorbornadiene linker (see Figure 5) releasing **RU-furan** (as shown in Figure 10). [b]Not determined due to decomposition. [c]Liver/plasma ratio determined for released **RU-furan**.

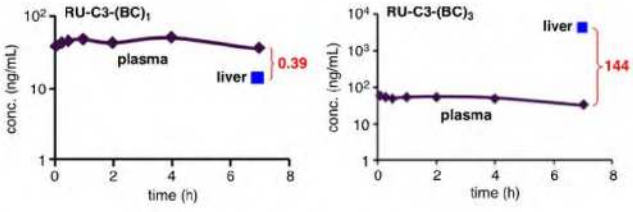

Figure 9. Representative intravenous infusion results in rat showing concentrations of free (unbound) plasma concentrations of the indicated compounds and the endpoint concentration in liver.

DOI: 10.1021/jacs.6b12964
J. Am. Chem. Soc. XXXX, XXX, XXX−XXX

in Figure 9. After 7 h of infusion, each animal was sacrificed, the liver was removed, and the compound concentration was determined in that organ. In addition to these values of total plasma and liver concentrations, in vitro equilibrium dialysis was used to determine the binding of these compounds in these environments (Table 2), as only unbound compound is available to exert a pharmacological effect. See Supporting Information for detailed procedures and analytical methods.

In general, all of the compounds tested showed higher binding (lower fraction unbound) in liver homogenate than in plasma. The aforementioned measurements of ASGPR-binding avidity and in vitro cell uptake proved to be predictive of the observed liver/plasma ratio, with increasing valency showing dramatic enhancements in each case (Figure 9 and Table 2). Thus, the noncleavable series [**RU-C3-(BC)$_n$**] showed values of 0.4, 9, and 144 for monomer, dimer, and trimer conjugates, respectively, with the last value representing an unusually high figure. The same trend, but lower absolute values, was observed for the weaker-binding GalNAc ligand (0.87 vs 8.7 for dimer vs trimer). The liver/plasma ratios for the glucosyl conjugates were <1.0, consistent with the expected poor permeability and lack of receptor-mediated uptake of these compounds. Further analysis of the significance of the differences in liver/plasma ratios for **BC** and **GalNAc** conjugates (which rely on detection of the parent compounds by mass spectrometry) would require a complete assessment of their metabolism, which may differ.

The cleavable ASGPR-binding OND conjugate was also effective in delivering small-molecule cargo to hepatocytes (Figure 10 and Table 2). OND linkers undergo facile Michael addition by free thiol compounds, inducing subsequent retro-Diels–Alder fragmentation of the resulting adducts.[37,38] The bivalent and trivalent OND conjugates **RU-OND-(BC)$_2$** and **RU-OND-(BC)$_3$** partitioned nicely into liver and released their cargo **RU-furan** with high liver/plasma ratios of 93 and 41, respectively. **RU-furan** alone showed no such selectivity (liver/plasma ratio = 0.7) as would be expected from a freely permeable small molecule. While **RU-OND-(BC)$_n$** compounds can react in principle with serum albumin or undergo ester hydrolysis,[46] these molecules showed good serum and plasma stability (Supporting Information). The majority of **RU-furan** release therefore presumably occurs after cellular internalization via ASGPR-mediated uptake and exposure to intracellular thiol (principally glutathione).

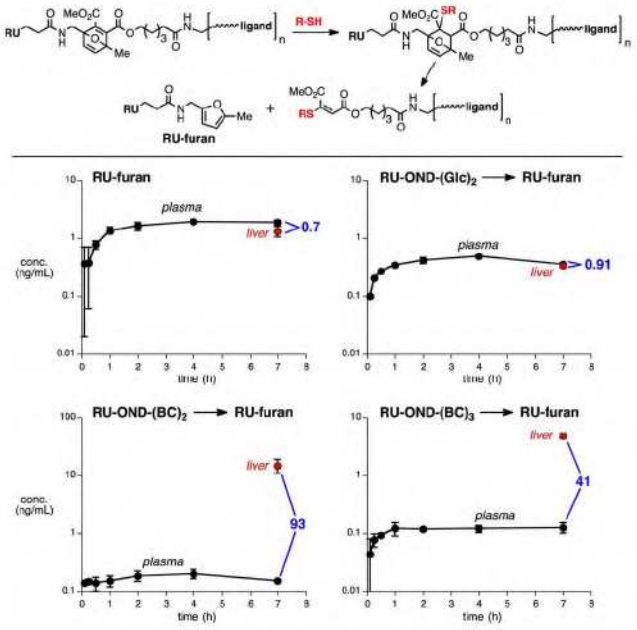

Figure 10. (Top) Thiol-triggered release of **RU-furan** cargo. (Bottom) Delivery of **RU-furan** by steady-state infusion of the indicated conjugates. Values in blue represent the free liver/plasma ratio at 7 h.

Hepatic Distribution. To further characterize the liver-targeting function of these molecules and compare both GalNAc- and BC-derived conjugates for hepatoselective delivery of therapeutic modalities, we conducted an in vivo biodistribution study in C57BL/6N mice using prototypical Alexa647-labeled conjugates **Alexa^b-C5-(BC)$_3$** and **Alexa^b-C5-(GalNAc)$_3$**. Both tripodal variants were shown to achieve similar systemic exposure at an early time point (15 min after tail vein injection) and then were rapidly cleared (Supporting Information).[47] The hepatic exposure and cellular distribution of these compounds were evaluated at 1, 2, and 4 h postdose using confocal microscopy. Representative images at each time point are shown in Figure 11 and visually demonstrate the elevated liver accumulation of **Alexa^b-C5-(BC)$_3$** relative to **Alexa^b-C5-(GalNAc)$_3$** at each time point. This was confirmed by image analysis quantification of liver exposure, showing 8–350 fold increase in the percentage of liver tissue area positive for the dye (Figure 11H). In addition, liver tissue area positive

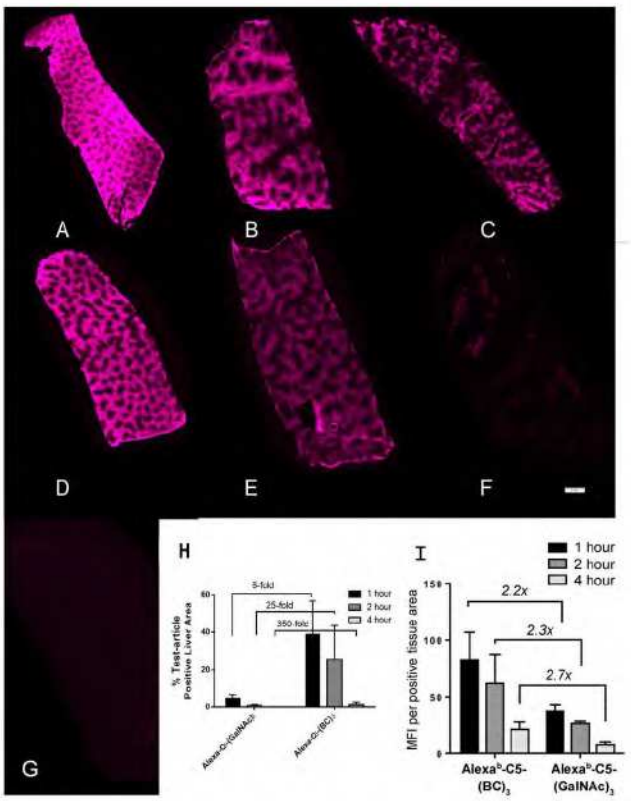

Figure 11. Whole tissue scans of mouse livers treated with (A–C) **Alexa^b-C5-(BC)$_3$** for 1, 2, and 4 h, respectively; (D–F) **Alexa^b-C5-(GalNAc)$_3$** for 1, 2, and 4 h, respectively; (G) vehicle only. Scale bar = 1 mm. Compound exposure in liver sections quantified by fluorescence microscopy: (H) percent of liver tissue area positive for dye and (I) mean fluorescence intensity of dye-positive tissue area representing relative exposure levels.

DOI: 10.1021/jacs.6b12964
J. Am. Chem. Soc. XXXX, XXX, XXX–XXX

for **Alexa^b-C5-(BC)$_3$** had, on average, ~2–3-fold greater mean fluorescence intensity (MFI) compared to **Alexa^b-C5-(GalNAc)$_3$** positive tissue area (Figure 11I). All other tissues evaluated were negative for **Alexa^b-C5-(GalNAc)$_3$** and **Alexa^b-C5-(BC)$_3$** exposure.

Characterization of both **Alexa^b-C5-(GalNAc)$_3$** and **Alexa^b-C5-(BC)$_3$** distribution within the liver (Figure 12) revealed

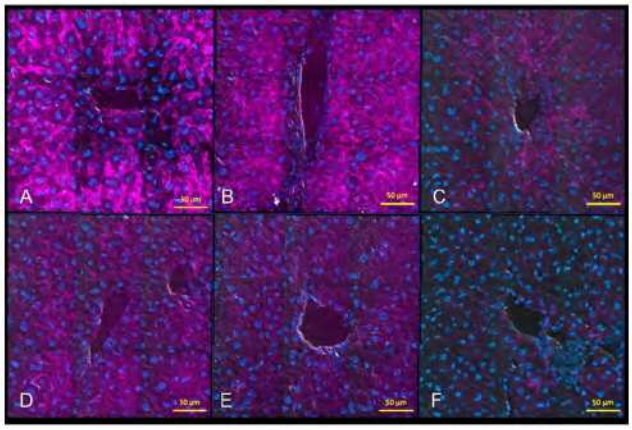

Figure 12. High-magnification composite images of perivenous regions of liver, from mice dosed with **Alexa^b-C5-(BC)$_3$** (panels A–C = 1, 2, 4 h) or **Alexa^b-C5-(GalNAc)$_3$** (panels D–F = 1, 2, 4 h). Purple color is fluorescence of the dosed compound, while nuclei are stained blue (scale bars = 50 μm).

centrilobular accumulation, correlating with reported ASPGR expression across the hepatic lobule in rodents.[48] These observations further support a receptor-mediated mechanism of cellular uptake within the liver. To further evaluate the cellular distribution of the tripodal ligands, high-resolution images were captured using confocal microscopy. Figure 13B shows the greater level of **Alexa^b-C5-(BC)$_3$** accumulation within the cytoplasm of liver cells compared to **Alexa^b-C5-(GalNAc)$_3$** at 4 h (Figure 13A). **Alexa^b-C5-(BC)$_3$** accumulation was associated with cytoplasmic puncta within hepatocytes (Figure 13C) that are not present in nonparenchymal cells. Intracellular accumulation of both ASGPR ligands within nonparenchymal cell types was not obvious.

Alexa^b-C5-(GalNAc)$_3$ and **Alexa^b-C5-(BC)$_3$** accumulation in hepatocytes was also measured by flow cytometry at 4 h. On average, hepatocytes isolated from mice treated with **Alexa^b-C5-(BC)$_3$** had an 8-fold greater positive population compared to hepatocytes isolated from **Alexa^b-C5-(GalNAc)$_3$** treated mice (Figure 14A). In addition, hepatocytes positive for **Alexa^b-C5-(BC)$_3$** had, on average, ~40% greater mean fluorescence intensity (MFI) compared to **Alexa^b-C5-(GalNAc)$_3$** positive hepatocytes (Figure 14B), confirming elevated intrahepatocellular levels of **Alexa^b-C5-(BC)$_3$** at this time point. This latter observation also correlates nicely with in vitro uptake results obtained with human primary hepatocytes (Figure 8).

■ CONCLUSIONS

Consideration of the likely intermolecular interactions that allow ASGPR to recognize *N*-acetylgalactosamine residues led to the design and synthesis of a bicyclic compound (**6**, or "**BC**") with superior ligand efficiency and binding affinity. The first reported X-ray crystal structures of ligand-bound ASGPR

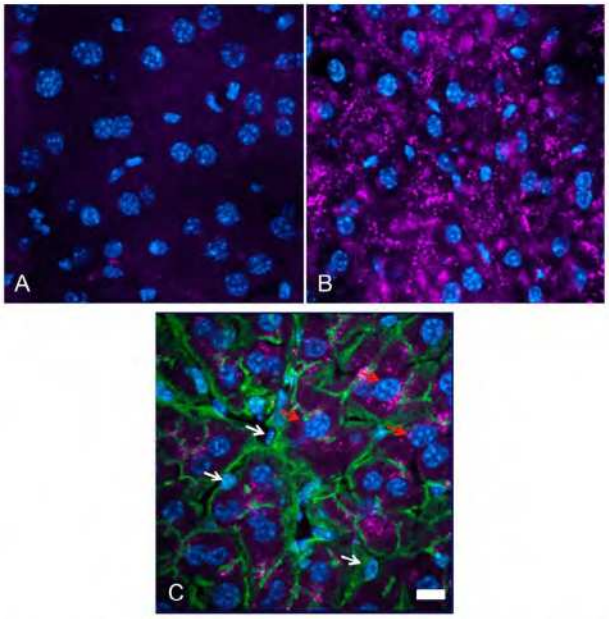

Figure 13. High-magnification images of cellular liver distribution, 4 h after dosing, demonstrating more efficient uptake of the construct based on bicyclic ligand **6**. (A) **Alexa^b-C5-(GalNAc)$_3$** and (B, C) **Alexa^b-C5-(BC)$_3$**. In panel C, the fluorescent compound is associated with hepatocytes (red arrows), while accumulation in nonparenchymal cells (white arrows) is not apparent (scale bar = 10 μm). Purple = dosed compound (AlexaFluor 647); blue = nuclei (DAPI); and green = actin (AlexaFluor 488).

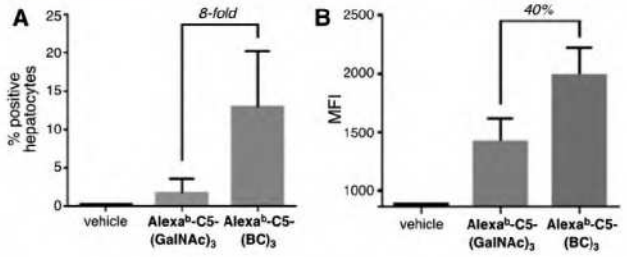

Figure 14. (A, B) Hepatic exposure of trivalent compounds quantified by flow cytometry. (A) Percent of isolated hepatocytes positive for each dosed compound. At 4 h, animals dosed with **Alexa^b-C5-(BC)$_3$** had 8-fold greater population of positive hepatocytes, compared to animals dosed with **Alexa^b-C5-(GalNAc)$_3$**. (B) Mean fluorescence intensity (MFI) of the indicated compound in hepatocytes positive for Alexa647 dye at 4 h. At this time point, hepatocytes positive for **Alexa^b-C5-(BC)$_3$** had 40% greater intracellular levels compared to positive hepatocytes from animals dosed with **Alexa^b-C5-(GalNAc)$_3$**.

were obtained, validating these predictions and the models used by others.

A modular synthetic approach enabled the synthesis of mono-, di-, and trivalent versions of this ligand (and of comparison GalNAc and glucose moieties), each carrying a single copy of a "cargo" compound. The performance of these molecules in binding ASGPR, mediating internalization into cultured cell lines and primary cells, and mediating trafficking and targeting in vivo was assessed by a variety of techniques. A consistent relationship was observed, with ASGPR avidity correlating with all the functional assays, with the bicyclic structure superior to GalNAc in the rate and extent of cellular uptake in vitro. This cellular uptake was dominated by ASGPR, and trivalent structures involving the bicyclic ligand were

DOI: 10.1021/jacs.6b12964
J. Am. Chem. Soc. XXXX, XXX, XXX–XXX

usually found to exceed the reported outstanding affinity and uptake exhibited by the natural asialoorosomucoid ligand while retaining the natural ligand's ability to allow for rapid receptor recycling.

As has been previously observed,[29] multimerization of ASGPR ligands (usually GalNAc) is a potent strategy for enhancement of binding to hepatocytes in vitro[5−8,49,50] and for delivery to the liver.[32−34,51−53] Because multiantennary displays of galactosyl ligands are effective agents in binding a number of different cell types,[54,55] it was important to verify[56,57] that, indeed, a prototypical trimer derivative (**Alexa^b-C5-(BC)$_3$**) of the novel bicyclic ligand **6** mediates predominant delivery to hepatocytes versus nonparenchymal cells (Kupffer, stellate) in vivo. In addition, the hepatic distribution of this representative compound appeared to be perivenous, with the greatest accumulation around the central vein of hepatic lobules.

By all measures, derivatives of bicyclic analogue **6** exhibited superior hepatoselective delivery compared to GalNAc. Quantification of **Alexa^b-C5-(GalNAc)$_3$** and **Alexa^b-C5-(BC)$_3$** liver exposure by multiple methods showed that, upon administration in mice, the trivalent conjugate of **6** facilitated increased ASGPR-directed hepatocellular uptake and prolonged retention compared to the GalNAc conjugate. Lastly, very high liver/plasma ratios were obtained in rats for the delivery of derivatives of the drug RU-486. In particular, we were able to take advantage of this phenomenon to release a passively permeable small-molecule cargo (**RU-furan**) via a triggered cleavable linker (the retro-Diels−Alder release from oxanorbornadienes) to achieve excellent liver/plasma distribution after intravenous infusion. This distribution would be impossible to achieve for the small molecule alone. Pharmacodynamics studies involving such molecular cargo will be explored and described separately. We anticipate that the highly efficient ASGPR-targeting ligands described here, coupled with triggered release and endosomal escape functions when needed, provide an exciting way to reduce dose, modulate the pharmacology of liver targeting, and improve pharmacological selectivity of hepatocytic therapeutics.

■ ASSOCIATED CONTENT

Supporting Information

The Supporting Information is available free of charge on the ACS Publications website at DOI: 10.1021/jacs.6b12964.

Details and additional data concerning small-molecule syntheses, assembly of multivalent conjugates, and studies of binding (surface plasmon resonance), cellular uptake (flow cytometry, fluorescence microscopy, and pulse-chase experiments), serum stability, biodistribution, and molecular structure (X-ray crystallography) (PDF)
CIF file of compound **6** (CIF)

■ AUTHOR INFORMATION

Corresponding Authors

*mgfinn@gatech.edu
*Vincent.Mascitti@pfizer.com

ORCID

M. G. Finn: 0000-0001-8247-3108

Notes

The authors declare the following competing financial interest(s): All authors, except Finn, Sanhueza, Dutta, and Baksh were employed by Pfizer, Inc. at the time this work was done.

■ ACKNOWLEDGMENTS

This work was supported by the Georgia Institute of Technology, The Skaggs Institute for Chemical Biology at The Scripps Research Institute, and Pfizer Global R&D. We thank Dr. Brian Samas (Pfizer) for assistance with the single-crystal X-ray diffraction analysis of compound **12**. All work with animals was approved by the IACUC and was conducted in the Pfizer, Inc., Groton laboratories.

■ REFERENCES

(1) Zelensky, A. N.; Gready, J. E. *FEBS J.* **2005**, *272*, 6179−6217.
(2) Lepenies, B.; Lee, J.; Sonkaria, S. *Adv. Drug Delivery Rev.* **2013**, *65*, 1271−1281.
(3) See ref 4 for citations to various examples.
(4) Stokmaier, D.; Khorev, O.; Cutting, B.; Born, R.; Ricklin, D.; Ernst, T. O. G.; Boni, F.; Schwingruber, K.; Gentner, M.; Wittwer, M.; Spreafico, M.; Vedani, A.; Rabbani, S.; Schwardt, O.; Ernst, B. *Bioorg. Med. Chem.* **2009**, *17*, 7254−7264 and references therein.
(5) Valentijn, A. R. P. M.; van der Marel, G. A.; Sliedregt, L. A. J. M.; van Berkel, T. J. C.; Biessen, E. A. L.; van Boom, J. H. *Tetrahedron* **1997**, *53*, 759−770.
(6) Sliedregt, L. A. J. M.; Rensen, P. C. N.; Rump, E. T.; van Santbrink, P. J.; Bijsterbosch, M. K.; Valentijn, A. R. P. M.; van der Marel, G. A.; van Boom, J. H.; van Berkel, T. J. C.; Biessen, E. A. L. *J. Med. Chem.* **1999**, *42*, 609−618.
(7) Khorev, O.; Stokmaier, D.; Schwardt, O.; Cutting, B.; Ernst, B. *Bioorg. Med. Chem.* **2008**, *16*, 5216−5231.
(8) Lee, R. T.; Lee, Y. C. *Glycoconjugate J.* **2000**, *17*, 543−551.
(9) Pathak, P. O.; Nagarsenker, M. S.; Barhate, C. R.; Padhye, S. G.; Dhawan, V. V.; Bhattacharyya, D.; Viswanathan, C. L.; Steiniger, F.; Fahr, A. *Carbohydr. Res.* **2015**, *408*, 33−43.
(10) Mamidyala, S. K.; Dutta, S.; Chrunyk, B. A.; Préville, C.; Wang, C.; Withka, J. M.; McColl, A.; Subashi, T. A.; Hawrylik, S. J.; Griffor, M. C.; Kim, S.; Pfefferkorn, J. A.; Price, D. A.; Menhaji-Klotz, E.; Mascitti, V.; Finn, M. G. *J. Am. Chem. Soc.* **2012**, *134*, 1978−1981.
(11) Riva, C. Targeting the liver via the asialoglycoprotein-receptor: Synthesis of directed small molecule libraries for the H1-CRD. Ph.D. Thesis, University of Basel, 2006.
(12) Wong, T. C.; Townsend, R. R.; Lee, Y. C. *Carbohydr. Res.* **1987**, *170*, 27−46.
(13) Kolatkar, A. R.; Weis, W. I. *J. Biol. Chem.* **1996**, *271*, 6679−6685.
(14) Rees, D. C.; Congreve, M.; Murray, C. W.; Carr, R. *Nat. Rev. Drug Discovery* **2004**, *3*, 660−672.
(15) Hopkins, A. L.; Groom, C. R.; Alex, A. *Drug Discovery Today* **2004**, *9*, 430−431.
(16) Kuntz, I. D.; Chen, K.; Sharp, K. A.; Kollman, P. A. *Proc. Natl. Acad. Sci. U. S. A.* **1999**, *96*, 9997−10002.
(17) Andrews, P. R.; Craik, D. J.; Martin, J. L. *J. Med. Chem.* **1984**, *27*, 1648−1657.
(18) For a discussion of the influence of van der Waals interactions in the ability of the rat hepatic lectin (RHL1) to bind GalNAc better than Gal, see: Kolatkar, A. R.; Leung, A. K.; Isecke, R.; Brossmer, R.; Drickamer, K.; Weis, W. I. *J. Biol. Chem.* **1998**, *273*, 19502−19508.
(19) Mascitti, V.; Thuma, B. A.; Smith, A. C.; Robinson, R. P.; Brandt, T.; Kalgutkar, A. S.; Maurer, T. S.; Samas, B.; Sharma, R. *MedChemComm* **2013**, *4*, 101−111.
(20) Mascitti, V.; Maurer, T. S.; Robinson, R. P.; Bian, J. W.; Boustany-Kari, C. M.; Brandt, T.; Collman, B. M.; Kalgutkar, A. S.; Klenotic, M. K.; Leininger, M. T.; Lowe, A.; Maguire, R. J.; Masterson, V. M.; Miao, Z.; Mukaiyama, E.; Patel, J. D.; Pettersen, J. C.; Preville, C.; Samas, B.; She, L.; Sobol, Z.; Steppan, C. M.; Stevens, B. D.; Thuma, B. A.; Tugnait, M.; Zeng, D. X.; Zhu, T. *J. Med. Chem.* **2011**, *54*, 2952−2960.
(21) Osuga, D. T.; Feather, M. S.; Shah, M. J.; Feeney, R. E. *J. Protein Chem.* **1989**, *8*, 519−528.
(22) Schaffer, R. *J. Am. Chem. Soc.* **1959**, *81*, 5452−5454.
(23) Smith, E. A.; Thomas, W. D.; Kiessling, L. L.; Corn, R. M. *J. Am. Chem. Soc.* **2003**, *125*, 6140−6148.

DOI: 10.1021/jacs.6b12964
J. Am. Chem. Soc. XXXX, XXX, XXX−XXX

(24) Paulsen, H.; Paal, M. *Carbohydr. Res.* **1984**, *135*, 53−69.
(25) Meier, M.; Bider, M. D.; Malashkevich, V. N.; Spiess, M.; Burkhard, P. *J. Mol. Biol.* **2000**, *300*, 857−865.
(26) The GalNAc binding pocket in the ASGPR receptor has a theoretical maximal binding affinity of 1.3 μM based on a computational druggability assessment. For this method, see: Cheng, A. C.; Coleman, R. G.; Smyth, K. T.; Cao, Q.; Soulard, P.; Caffrey, D. R.; Salzberg, A. C.; Huang, E. S. *Nat. Biotechnol.* **2007**, *25*, 71−75.
(27) Kolatkar, A. R.; Leung, A. K.; Isecke, R.; Brossmer, R.; Drickamer, K.; Weis, W. I. *J. Biol. Chem.* **1998**, *273*, 19502−19508.
(28) Feinberg, H.; Torgersen, D.; Drickamer, K.; Weis, W. I. *J. Biol. Chem.* **2000**, *275*, 35176−35184.
(29) Lodish, H. F. *Trends Biochem. Sci.* **1991**, *16*, 374−377.
(30) Chiu, M. H.; Thomas, V. H.; Stubbs, H. J.; Rice, K. G. *J. Biol. Chem.* **1995**, *270*, 24024−24031.
(31) Kim, E. M.; Jeong, H. J.; Park, I. K.; Cho, C. S.; Moon, H. B.; Yu, D. Y.; Bom, H. S.; Sohn, M. H.; Oh, I. J. *J. Controlled Release* **2005**, *108*, 557−567.
(32) Torres, S.; Martins, J. A.; Andre, J. P.; Neves, M.; Santos, A. C.; Prata, M. I. M.; Geraldes, C. *Radiochim. Acta* **2007**, *95*, 343−349.
(33) Rajeev, K. G.; Nair, J. K.; Jayaraman, M.; Charisse, K.; Taneja, N.; O'Shea, J.; Willoughby, J. L. S.; Yucius, K.; Nguyen, T.; Shulga-Morskaya, S.; Milstein, S.; Liebow, A.; Querbes, W.; Borodovsky, A.; Fitzgerald, K.; Maier, M. A.; Manoharan, M. *ChemBioChem* **2015**, *16*, 903−908.
(34) Nair, J. K.; Willoughby, J. L. S.; Chan, A.; Charisse, K.; Alam, M. R.; Wang, Q.; Hoekstra, M.; Kandasamy, P.; Kel'in, A. V.; Milstein, S.; Taneja, N.; O'Shea, J.; Shaikh, S.; Zhang, L.; van der Sluis, R. J.; Jung, M. E.; Akinc, A.; Hutabarat, R.; Kuchimanchi, S.; Fitzgerald, K.; Zimmermann, T.; van Berkel, T. J. C.; Maier, M. A.; Rajeev, K. G.; Manoharan, M. *J. Am. Chem. Soc.* **2014**, *136*, 16958−16961.
(35) Yu, R. Z.; Graham, M. J.; Post, N.; Riney, S.; Zanardi, T.; Hall, S.; Burkey, J.; Shemesh, C. S.; Prakash, T. P.; Seth, P. P.; Swayze, E. E.; Geary, R. S.; Wang, Y.; Henry, S. *Mol. Ther.−Nucleic Acids* **2016**, *5*, e317.
(36) Link, J. T.; Sorensen, B.; Patel, J.; Grynfarb, M.; Goos-Nilsson, A.; Wang, J. H.; Fung, S.; Wilcox, D.; Zinker, B.; Nguyen, P.; Hickman, B.; Schmidt, J. M.; Swanson, S.; Tian, Z. P.; Reisch, T. J.; Rotert, G.; Du, J.; Lane, B.; von Geldern, T. W.; Jacobson, P. B. *J. Med. Chem.* **2005**, *48*, 5295−5304.
(37) Kislukhin, A. A.; Higginson, C. J.; Hong, V. P.; Finn, M. G. *J. Am. Chem. Soc.* **2012**, *134*, 6491−6497.
(38) Hong, V.; Kislukhin, A.; Finn, M. G. *J. Am. Chem. Soc.* **2009**, *131*, 9986−9994.
(39) Hudgin, R. L.; Pricer, W. E. J.; Ashwell, G.; Stockert, R. J.; Morell, A. G. *J. Biol. Chem.* **1974**, *249*, 5536−5543.
(40) Ashwell, G.; Morell, A. G. *Adv. Enzymol. Relat. Areas Mol. Biol.* **1974**, *41*, 99−128.
(41) Vercauteren, D.; Vandenbroucke, R. E.; Jones, A. T.; Rejman, J.; Demeester, J.; De Smedt, S. C.; Sanders, N. N.; Braeckmans, K. *Mol. Ther.* **2010**, *18*, 561−569.
(42) D'Souza, A. A.; Devarajan, P. V. *J. Controlled Release* **2015**, *203*, 126−139.
(43) Weigel, P. H.; Yik, J. H. N. *Biochim. Biophys. Acta, Gen. Subj.* **2002**, *1572*, 341−363.
(44) Schwartz, A. L.; Fridovich, S. E.; Lodish, H. F. *J. Biol. Chem.* **1982**, *257*, 4230−4237.
(45) This compound was administered in a formulation of DMSO/PEG-400/12.5% SBE−cyclodextrin in water (1/10/89 v/v). The mixture was filtered prior to dosing to avoid the injection of undissolved compound; analysis of three 20 μL aliquots established the measured dose as 1.5 mg/kg.
(46) Higginson, C. J.; Eno, M. R.; Khan, S.; Cameron, M. D.; Finn, M. G. *ACS Chem. Biol.* **2016**, *11*, 2320−2327.
(47) Shemesh, C. S.; Yu, R. Z.; Gaus, H. J.; Greenlee, S.; Post, N.; Schmidt, K.; Migawa, M. T.; Seth, P. P.; Zanardi, T. A.; Prakash, T. P.; Swayze, E. E.; Henry, S. P.; Wang, Y. *Mol. Ther.−Nucleic Acids* **2016**, *5*, e319.
(48) Voorschuur, A. H.; Kuiper, J.; Neelissen, J. A. M.; Boers, W.; Van Berkel, T. J. C. *Biochem. J.* **1994**, *303*, 809−816.
(49) Griffith, L. G.; Lopina, S. *Biomaterials* **1998**, *19*, 979−986.
(50) Lai, C. H.; Lin, C. Y.; Wu, H. T.; Chan, H. S.; Chuang, Y. J.; Chen, C. T.; Lin, C. C. *Adv. Funct. Mater.* **2010**, *20*, 3948−3958.
(51) Yang, Y. S.; Thomas, V. H.; Man, S. C.; Rice, K. G. *Glycobiology* **2000**, *10*, 1341−1345.
(52) Prata, M. I. M.; Santos, A. C.; Torres, S.; Andre, J. P.; Martins, J. A.; Neves, M.; Garcia-Martin, M. L.; Rodrigues, T. B.; Lopez-Larrubia, P.; Cerdan, S.; Geraldes, C. *Contrast Media Mol. Imaging* **2006**, *1*, 246−258.
(53) Matsuda, S.; Keiser, K.; Nair, J. K.; Charisse, K.; Manoharan, R. M.; Kretschmer, P.; Peng, C. G.; Kel'in, A. V.; Kandasamy, P.; Willoughby, J. L. S.; Liebow, A.; Querbes, W.; Yucius, K.; Nguyen, T.; Milstein, S.; Maier, M. A.; Rajeev, K. G.; Manoharan, M. *ACS Chem. Biol.* **2015**, *10*, 1181−1187.
(54) David, A.; Kopeckova, P.; Minko, T.; Rubinstein, A.; Kopecek, J. *Eur. J. Cancer* **2004**, *40*, 148−157.
(55) Gomez-Valades, A. G.; Molas, M.; Vidal-Alabro, A.; Bermudez, J.; Bartrons, R.; Perales, J. C. *J. Controlled Release* **2005**, *102*, 277−291.
(56) Rozema, D. B.; Lewis, D. L.; Wakefield, D. H.; Wong, S. C.; Klein, J. J.; Roesch, P. L.; Bertin, S. L.; Reppen, T. W.; Chu, Q.; Blokhin, A. V.; Hagstrom, J. E.; Wolff, J. A. *Proc. Natl. Acad. Sci. U. S. A.* **2007**, *104*, 12982−12987.
(57) Biessen, E. A. L.; Bakkeren, H. F.; Beuting, D. M.; Kuiper, J.; Van Berkel, T. J. C. *Biochem. J.* **1994**, *299*, 291−296.

DOI: 10.1021/jacs.6b12964
J. Am. Chem. Soc. XXXX, XXX, XXX−XXX

EXHIBIT 6

Bioorganic & Medicinal Chemistry 17 (2009) 7254–7264

Contents lists available at ScienceDirect

Bioorganic & Medicinal Chemistry

journal homepage: www.elsevier.com/locate/bmc

Design, synthesis and evaluation of monovalent ligands for the asialoglycoprotein receptor (ASGP-R)

Daniela Stokmaier, Oleg Khorev, Brian Cutting, Rita Born, Daniel Ricklin, Thomas O. G. Ernst, Fabienne Böni, Kathrin Schwingruber, Martin Gentner, Matthias Wittwer, Morena Spreafico, Angelo Vedani, Said Rabbani, Oliver Schwardt, Beat Ernst *

Institute of Molecular Pharmacy, Pharmacenter, University of Basel, Klingelbergstrasse 50, CH-4056 Basel, Switzerland

ARTICLE INFO

Article history:
Received 14 July 2009
Revised 24 August 2009
Accepted 25 August 2009
Available online 29 August 2009

Keywords:
Asialoglycoprotein receptor (ASGP-R)
Competitive binding assay
Competitive NMR binding experiments
Triazolyl D-galactosamine derivatives

ABSTRACT

A series of novel aryl-substituted triazolyl D-galactosamine derivatives was synthesized as ligands for the carbohydrate recognition domain of the major subunit H1 (H1-CRD) of the human asialoglycoprotein receptor (ASGP-R). The compounds were biologically evaluated with a newly developed competitive binding assay, surface plasmon resonance and by a competitive NMR binding experiment. With compound **1b**, a new ligand with a twofold improved affinity to the best so far known D-Gal*N*Ac was identified. This small, drug-like ligand can be used as targeting device for drug delivery to hepatocytes.

1. Introduction

The asialoglycoprotein receptor (ASGP-R) is a C-type,[1] i.e. a Ca^{2+}-dependent lectin and is expressed exclusively by parenchymal hepatocytes, which contain 100,000–500,000 binding sites per cell. These receptors are randomly distributed over the sinusoidal plasma membrane facing the capillaries. Their main function is to maintain serum glycoprotein homeostasis by recognition, binding, and endocytosis of asialoglycoproteins (ASGPs). After internalization via receptor-mediated endocytosis, the ASGPs dissociate in the acidic environment of the endosomes and are finally degraded, while the receptor is recycled back to the cell surface.[2–5]

The human ASGP-R consists of two homologous subunits, designated H1 and H2, which form a non-covalent heterooligomeric complex by α-helical coiled coil domains with an estimated ratio of 2–5:1, respectively.[6,7] Both subunits are single-spanning membrane proteins with a calcium-dependent D-Gal/D-Gal*N*Ac recognition domain.[8] Whereas the recognition of the carbohydrate moiety is mediated via the H1-subunit, the H2-subunit accounts for the functional configuration of the native receptor.[9–12] Recently, the X-ray crystal structure of the carbohydrate recognition domain (CRD) of the major H1-subunit was solved.[13]

Beyond the specificity for terminal D-galactose and *N*-acetyl-D-galactosamine residues, binding to the ASGP receptor strongly depends on the valency of the ligand. Whereas the affinity of a single D-galactose residue is only in the millimolar range, bi-, tri- and tetraantennary desialylated glycoproteins bind with dissociation constants of 10^{-6}, 5×10^{-9}, and 10^{-9} M, respectively.[14,15] Furthermore, Lee and co-workers demonstrated that the ASGP-R exhibits an approximately 10–50-fold higher affinity for D-Gal*N*Ac versus D-Gal monosaccharides[16] and for terminal D-Gal*N*Ac versus D-Gal cluster glycosides,[17] respectively. As a result, research efforts for the design of high affinity ligands were focused on oligovalent ligands, containing primarily D-Gal*N*Ac but also D-Gal or D-Lac as terminal recognition elements. Their use as homing devices in liver-specific drug[18,19] and gene delivery[20–24] is well documented.

By contrast, only moderate research efforts were directed towards the discovery of potent monovalent ligands. Lee et al.[25] showed that the replacement of the acetamido group in D-Gal*N*Ac by a propanamido or trifluoroacetamido group did not lead to an alteration of the inhibitory effect regarding ^{125}I-asialo-orosomucoid binding to rat hepatocytes. However, with the bulkier benzamido or phthalimido groups an up to 10-fold drop in affinity was observed, indicating the impact of sterical factors on binding affinity. Later on, Weis and co-workers[26,27] provided a sophisticated model based on the mannose-binding protein to explain

Abbreviations: ABTS, 2,2′-azino-bis(3-ethylbenzthiazoline-6-sulfonic acid); AIBN, azo-bis-isobutyronitrile; ASGP, asialoglycoprotein; CRD, carbohydrate recognition domain; DCM, dichloromethane; D-Gal, D-galactose; D-Gal*N*Ac, *N*-acetyl-D-galactosamine; D-Lac, D-lactose; DMSO, dimethyl sulfoxide; EDTA, ethylenediaminetetraacetic acid; K_D, dissociation constant; NMR, nuclear magnetic resonance; PAA, polyacrylamide; SPR, surface plasmon resonance; Tf, trifluormethanesulfonyl.

* Corresponding author. Tel.: +41 61 2671550; fax: +41 61 2671552.
E-mail address: beat.ernst@unibas.ch (B. Ernst).

0968-0896/$ - see front matter © 2009 Elsevier Ltd. All rights reserved.
doi:10.1016/j.bmc.2009.08.049

the preferential binding of D-GalNAc compared with D-Gal as well as for the selectivity of different *N*-acyl derivatives.

For our investigation, we designed a directed library of easy accessible and metabolically stable D-galactosamine derivatives for mono- or oligovalent applications, for example, for the incorporation into trivalent drug carriers previously developed.[28] Furthermore, for the efficient evaluation of binding affinities the hitherto used radio-labeled competitive binding assay[29–31] was replaced by a non-radioactive, polymer-based assay format. Finally, surface plasmon resonance and NMR experiments allowed an independent validation of the binding affinities.

2. Results and discussion

2.1. Design of ASGP-R H1 ligands

Docking D-GalNAc to the crystal structure of the H1-CRD (Fig. 1A and B, PDB code 1DV8)[13] clearly reveals the pharmacophoric groups involved in this carbohydrate–lectin interaction. The 3- and 4-hydroxyl groups of D-GalNAc coordinate to the Ca^{2+} ion, requiring their equatorial and axial orientation (Fig. 1B).[32] Due to steric reasons, methylation of these hydroxyls leads to a substantial loss in affinity.[25] The hydrophobic patch formed by the circular arrangement of ring C–H bonds on the α-face of D-GalNAc establishes a lipophilic contact with the indole side chain of Trp243 (Fig. 1A). The pharmacophoric requirements are summarized in Figure 1C.

A closer look at the protein surface in the area of the 2-*N*-acetyl group reveals a dumbbell-shaped cavity (Fig. 1D) that on the one hand quickly leads to a steric clash with bulky substituents,[25] but on the other hand can host a wide variety of linear substituents. Finally, the β-anomeric as well as the 6-OH point into the solvent and could therefore serve as attachment points for conjugation to oligovalent carriers, fluorescent labels, etc.

Based on these evidences, a directed library of small, drug-like D-GalNAc derivatives was designed where (i) the anomeric OH was removed, since it could act as a metabolic 'soft-spot'[33] and (ii) the 2-acetamido group was replaced by a 4-substituted 1,2,3-triazole moiety. Docking of the test compound **1a** to the H1-CRD revealed a perfect accommodation of the triazole substituent by the dumbbell-shaped hydrophobic binding pocket (Fig. 1D).

2.2. Synthesis of triazole derivatives 1a–f, h

In anti-substituted triazoles as **1a**, the substituent in the 4-position of the heterocycle perfectly points into the dumbbell-shaped binding pocket. Anti-substituted triazoles are obtained highly regioselectively by a copper(I)-catalyzed Huisgen 1,3-dipolar cycloaddition.[34,35] For the synthesis of the azido component **7** used in the cycloaddition reaction (Scheme 1), peracetylated D-GalNAc (**2**) was used as starting material. Its treatment with $TiCl_4$ in DCM yielded glycosyl chloride **3** in 89%. Reductive dehalogenation using Bu_3SnH and AIBN in refluxing toluene gave **4** in quantitative yield. Deacetylation (→**5**), followed by amine-azide exchange[36]

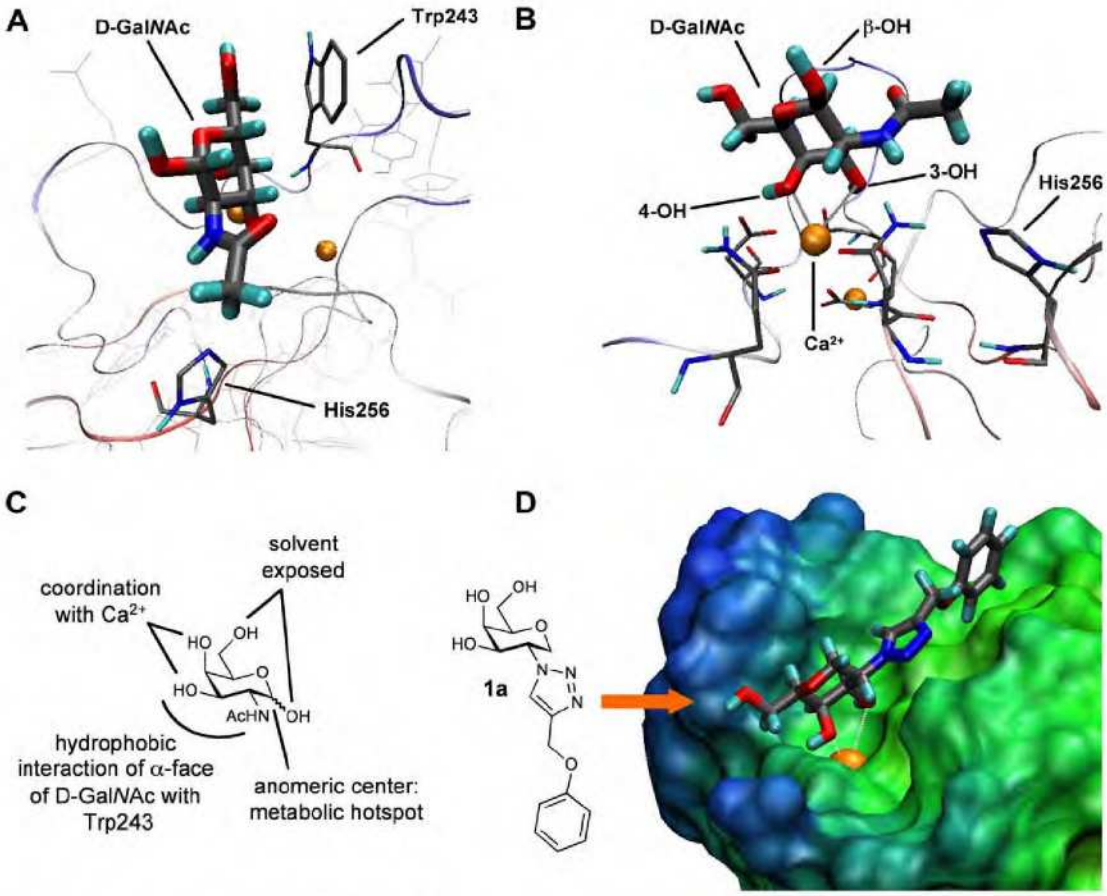

Figure 1. (A) Manual docking (MacYeti 7.05) of β-D-GalNAc into the H1-CRD of the ASGP-R (PDB code 1DV8).[13] Illustration of the hydrophobic interactions between Trp243 and the α-face of D-GalNAc and the *N*-acetate group with His256;[27] (B) coordination of the equatorial 3- and axial 4-hydroxyl group of D-GalNAc with Ca^{2+}; (C) summary of the important interactions of D-GalNAc with the binding site of the H1-CRD; (D) a model of the H1-CRD interacting with the D-GalNAc derivative **1a**, with the 3- and 4-OH groups coordinating Ca^{2+} (orange) and the triazole substituent well accommodated by a dumbbell-shaped hydrophobic binding pocket.

(→**6**) and subsequent re-acetylation gave **7** in 76% yield over three steps. For affinity testing, a small sample of **7** was deprotected under standard Zemplén conditions to yield **6** quantitatively.

Whereas acetylene **10a** (Scheme 2) is commercially available, **10b–d** and **10g** were easily synthesized following known procedures.[37–40] **10e** was obtained quantitatively by propargylation of 4-hydroxybenzoic acid (**8**) and **10f** in 69% by sulfonylation of **9**[37] with triflic anhydride (Scheme 1).

Cu(I)-catalyzed click conditions,[34,35] i.e. $CuSO_4$ and sodium ascorbate as reducing agent to obtain the catalytically active

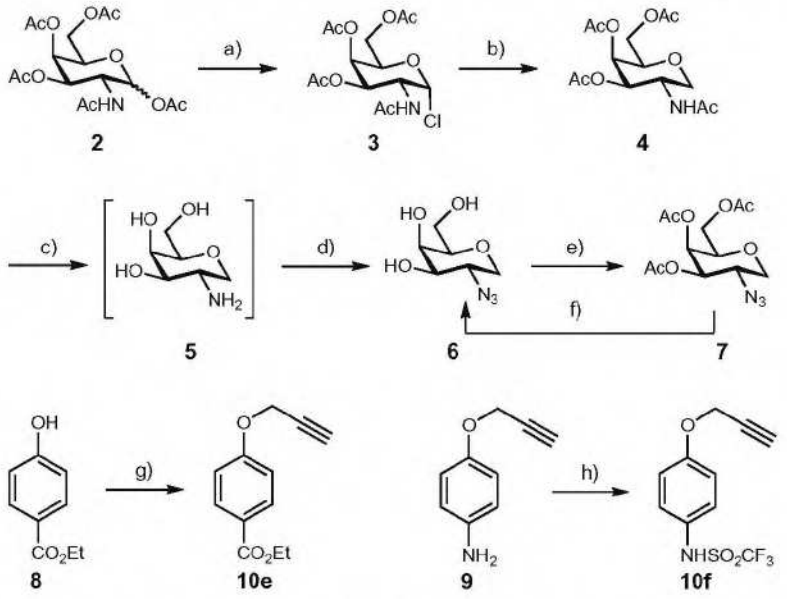

Scheme 1. Synthesis of building blocks. Reagents and conditions: (a) $TiCl_4$, DCM, rt, 3 d, 89%; (b) Bu_3SnH, AIBN, PhMe, reflux, 1 h 20 min, quant.; (c) KOH, 18-crown-6, dioxane/H_2O, reflux, 6.5 h; (d) TfN_3, $NaHCO_3$, $CuSO_4{\cdot}5H_2O$, H_2O/PhMe/MeOH, rt, 24 h; (e) Ac_2O, pyridine, rt, 24 h, 76% (three steps); (f) NaOMe/MeOH, rt, 3 h, quant.; (g) propargyl bromide, K_2CO_3, acetone, reflux, 5 h, 73%; (h) Tf_2O, Et_3N, DCM, 0 °C→rt, 24 h, 69%.

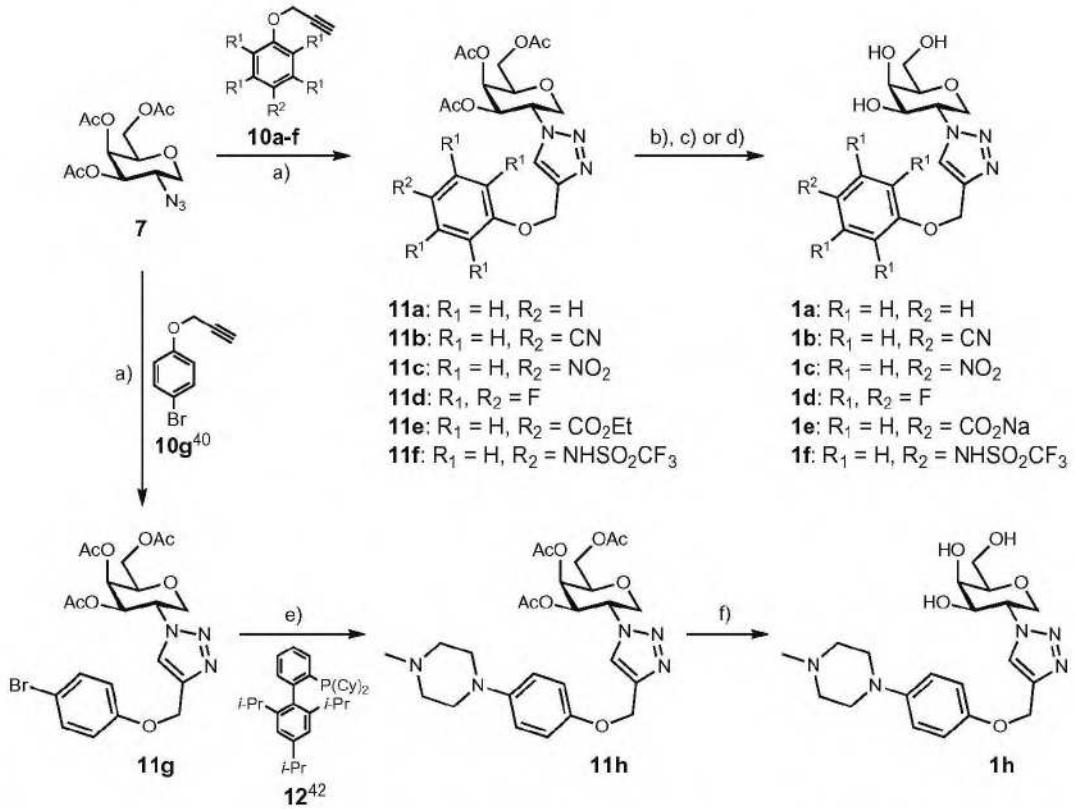

Scheme 2. Synthesis of triazoles. Reagents and conditions: (a) CuCl, Et_3N, DCM, rt, 24 h, **10a** (→**11a**, 93%), **10b**[38] (→**11b**, 98%), **10c**[37] (→**11c**, 95%), **10d**[39] (→**11d**, 73%), **10e** (→**11e**, 82%), **10f** (→**11f**, 41%), or **10g**[40] (→**11g**, 84%); (b) NaOMe/MeOH, rt, 3 h (**1a**, 45%; **1c**, 33%; **1d**, 68%; **1f**, 73%); (c) H_2O/MeOH/Et_3N (5:5:1), rt, 24 h (**1b**, 81%); (d) NaOH, H_2O/MeOH, rt, 24 h (**1e**, 74%); (e) *N*-methylpiperazine, $Pd_2(dba)_3$, Cs_2CO_3, PhMe, 80 °C, 24 h; (f) NaOMe/MeOH, rt, 24 h (44%, two steps).

Cu(I), led only to low yields of anti-substituted triazoles and in some cases even failed completely. However, with an alternative procedure, involving CuCl as the direct source of Cu(I) and triethylamine as base, the cycloaddition reactions of azide **7** with the phenyl propargyl ethers **10a–f** yielded the protected *anti*-substituted triazoles **11a–f** in 41–98% yield and after deprotection the test compounds **1a–f** (Scheme 2). To further explore the dumbbell-shaped binding site and to improve solubility of the test compound, a piperazinylphenyl derivative was synthesized. Click chemistry (→**11g**) and Pd-catalyzed Buchwald–Hartwig coupling using the biaryl monophosphine ligand **12** (→**11h**)[41] followed by deacetylation by Zemplén conditions yielded **1h**.

2.3. Expression of H1-CRD

A truncated form of the H1-subunit of the human hepatic ASGP-R consisting of the whole CRD domain (amino acid residues 147–291) was recombinantly expressed in *Escherichia coli* and purified to homogeneity by affinity chromatography.[43] The monomeric and dimeric forms were subsequently purified by ion exchange chromatography. The purified proteins were analyzed by SDS–PAGE and immuno-blot (Fig. 2).

2.4. Competitive binding assay

For the characterization of the H1-CRD ligands, a cell-free, competitive binding assay based on a polyacrylamide (PAA) glycoconjugate was established analog to binding assays reported for selectin antagonists.[44,45] For this assay, a microtiter plate coated with the H1-CRD is incubated with biotinylated D-Gal*N*Ac-PAA conjugated to streptavidin-horseradish peroxidase. Then, after incubation with the analyte at various concentrations and washing with HBS-buffer, the remaining PAA glycoconjugate is quantified by a colorimetric reaction using the enzyme's substrate 2,2′-azino-bis(3-ethylbenzthiazoline-6-sulfonic acid (ABTS). PAAs containing β-D-Glc or sLe^a are not recognized, whereas H1-CRD efficiently bound β-D-Gal*N*Ac-PAA and to a lesser extent β-D-Gal-PAA (Fig. 3A). Since the interaction is Ca^{2+}-dependent, D-Gal*N*Ac-polymer binding is completely inhibited in the presence of 1 mM EDTA in the assay buffer (Fig. 3B).

For a further validation of the binding assay, the IC_{50}'s of a number of monosaccharides were compared with K_D values derived from surface plasmon resonance (SPR, Biacore) measurements, were the H1-CRD was immobilized on a CM5 chip by amine coupling, and IC_{50}'s reported in literature.[16]

Interestingly, consistently negative sensorgrams in the surface plasmon resonance experiments, that is, a net decrease in resonance units, were obtained with the monosaccharides reported in Table 1. When fitted to a binding isotherm, these negative sensorgrams appear to clearly result from specific receptor–ligand interactions. Numerous factors such as the buffer capacity, the ion-strength of the buffer and matrix type of the sensor chip could be excluded as direct cause of the negative sensorgrams. A possible explanation is a ligand-induced conformational change of the

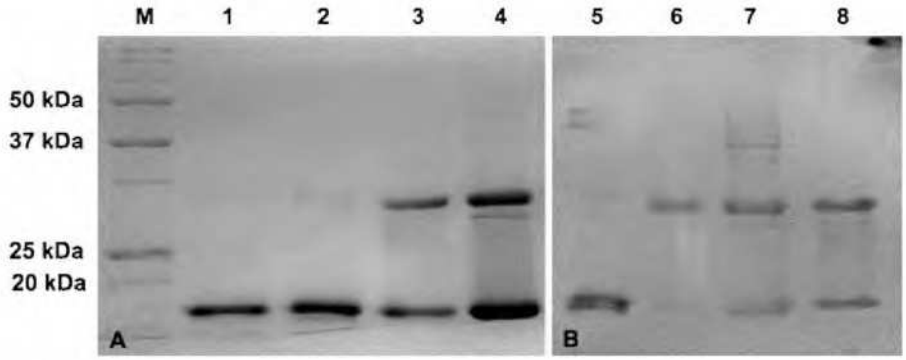

Figure 2. SDS–PAGE and immuno-blot analysis. (A) Monomeric and dimeric forms of H1-CRD were separated on a non-reducing 15% SDS–PAGE and visualized by coomassie staining. M: molecular weight marker, 1 and 2: H1-CRD monomer, 3 and 4: H1-CRD monomer and dimer; (B) Immuno-blot analysis was performed with IgY polyclonal anti-H1-CRD antibodies and alkaline phosphatase coupled rabbit anti-chicken IgG. 5: H1-CRD monomer, 6: H1-CRD dimer, 7 and 8: H1-CRD monomer and dimer.

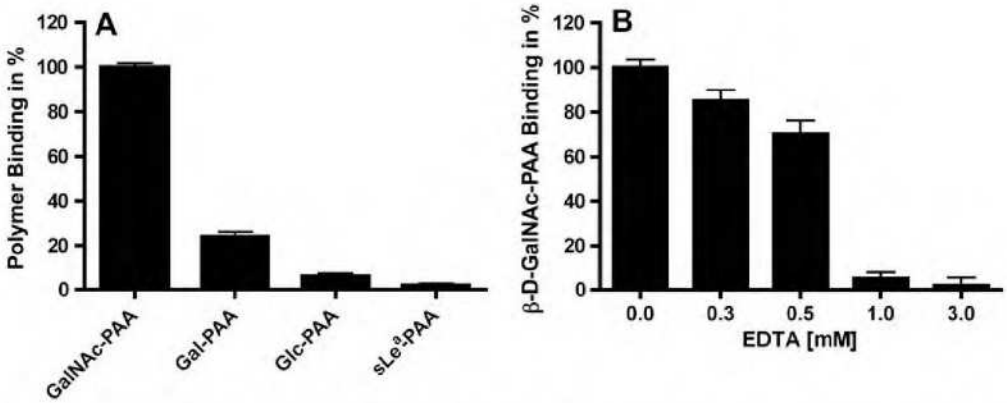

Figure 3. (A) Specificity of the binding assay. Comparison of H1-CRD binding of β-D-Gal*N*Ac-PAA and β-D-Gal-PAA and the negative controls β-D-Glc-PAA and sLe^a-PAA; (B) effect of EDTA on β-D-Gal*N*Ac-PAA binding to H1-CRD.

Table 1
Affinity data obtained by the competitive binding assay (IC_{50}) and surface plasmon resonance (K_D)

Monosaccharides	Competitive binding assay[a] (human H1)		Surface plasmon resonance (human H1)		Literature data[16] (rabbit ASGP-R)	
	$IC_{50} \pm SD$ [μM]	rIC_{50}	$K_D \pm SD$ [μM]	rK_D	IC_{50} [μM]	rIC_{50}
D-GalNAc	113 ± 13	1	150 ± 0.9	1	90	1
D-Gal	1049 ± 101	9.3	1460 ± 10	9.7	1700	18.9
β-D-GalOMe	1828 ± 169	16	2200 ± 40	14.7	1000	11.1
α-D-GalOMe	2831 ± 140	25	2760 ± 60	18	1600	17.8
D-Glc	>30,000	n.d.	>10,000	n.d.	60,000	667

IC_{50} defines the molar concentration of the test compound that reduces the maximal specific binding of D-GalNAc-PAA to H1-CRD by 50%. The relative IC_{50} (rIC_{50}) is the ratio of the IC_{50} of the test compound to the IC_{50} of the reference compound D-GalNAc. SD: standard deviation. Literature data describe the inhibition of ^{125}I-asialoorosomucoid binding to isolated rabbit hepatic lectin.[16]

[a] Compounds tested in triplicates, each at six different concentrations. The coefficient of variation, which is defined as the standard deviation divided by the mean, was 13.8% for unspecific binding and 4.8% for specific binding. These results demonstrate the low variability of the assay, making it suitable for the characterization of H1-CRD ligands.

immobilized receptor leading to a decrease of its hydrodynamic radius and, as a consequence, yielding a negative refraction index.[46] Since the negative refraction index correlates with the analyte concentration, we mirrored the negative sensorgrams by multiplication of each data point with −1. The K_Ds obtained correlate nicely with affinity data derived from the competitive binding assay and from the literature values (Table 1).

All three assay formats revealed a 10–20-fold higher affinity for D-GalNAc compared to D-Gal. Interestingly, methyl β-D-galactoside binds with slightly higher affinity than the corresponding α-anomer, although according to docking studies (see Fig. 1B) both aglycons point to the solvent. Furthermore, D-Glc-binding was beyond the detection limit, supporting the importance of the coordination of the 3- and 4-hydroxyls to Ca^{2+}. Overall, the three assay formats gave consistently comparable results, confirming the reliability of our new competitive binding assay.

The affinities of the triazoles are summarized in Table 2 and Figure 4. Compounds that were not soluble in HBS-buffer were dissolved in DMSO prior to dilution with buffer. The final DMSO concentration in the diluted samples did not exceed 5% and was well tolerated in the assay (data not shown).

Not unexpectedly, the azide scaffold **6** (Table 2, entry 2) exhibited an approximately 14-fold decrease in affinity compared to D-GalNAc (entry 1), because the proposed hydrophobic contact of the *N*-acetate group with His256[27] is no longer present. On the other hand, compound **1a** (entry 3), bearing a phenyloxymethyl-substituted triazole, had an affinity close to the one of D-GalNAc (rIC_{50} 1.1), indicating that the rather bulky substituent in the 2-position is tolerated. Only the *p*-cyano derivative **1b** (entry 4) and the *p*-nitro-derivative **1c** (entry 5) showed clearly better affinities than D-GalNAc. Despite its bulkiness, the *N*-methylpiperazine derivative **1h** exhibited a slightly improved rIC_{50} compared to D-GalNAc. This result further supports our hypothesis that compounds extended at the 2-position of the amino pyranose ring can interact with the dumbbell-shaped binding pocket (see Fig. 1D).

2.5. Competitive NMR binding experiments

For an independent assessment of the binding affinities, competitive binding experiments by NMR[47,48] were performed with D-GalNAc as a reference compound and **1b** as competitor. In a first step, binding of D-GalNAc to the H1-CRD was demonstrated by the large difference in transverse relaxation times in the absence and presence of the lectin (Fig. 5A).

Table 2
Determination of the relative IC_{50} (rIC_{50}) values for the triazolyl D-galactosamine derivatives

Entry	Compound	$rIC_{50} \pm SD$
1	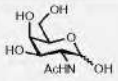	1.0
2	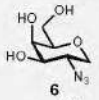 6	13.7 ± 4.3
3	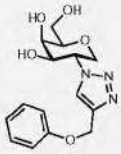 1a	1.1 ± 0.2
4	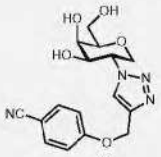 1b	0.5 ± 0.1
5	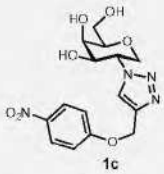 1c	0.8 ± 0.2
6	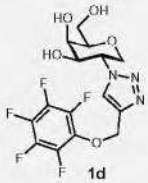 1d	1.4 ± 0.3
7	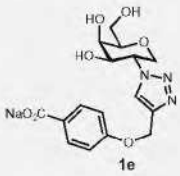 1e	8.7
8	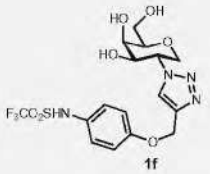 1f	–[a]
9	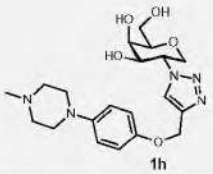 1h	0.9 ± 0.1

SD: standard deviation.

[a] Compound not soluble in the 10% DMSO/buffer stock solution used in the assay.

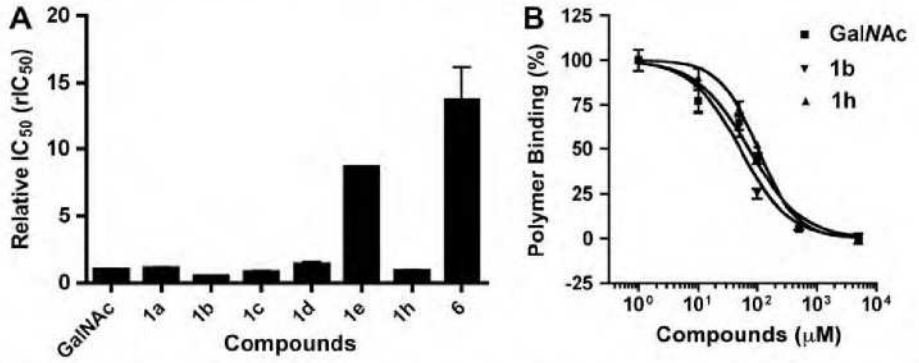

Figure 4. (A) Relative IC_{50}s derived from the competitive solid-phase binding assay; (B) Plot of D-Gal*N*Ac-PAA inhibition versus concentration. Inhibition of D-Gal*N*Ac-PAA binding to H1-CRD by Gal*N*Ac and derivatives. Microtiter plates were coated with a 3 μg/mL solution of monomeric H1-CRD. After washing steps a serial dilution of the test compound solution and 0.5 μg/mL of streptavidin-peroxidase coupled D-Gal*N*Ac-PAA were added to the protein. After 2 h incubation the plates were washed and the colorimetric reaction was developed and quantified as described in experimental section. (■) Gal*N*Ac, (▼) **1b**, (▲) **1h**.

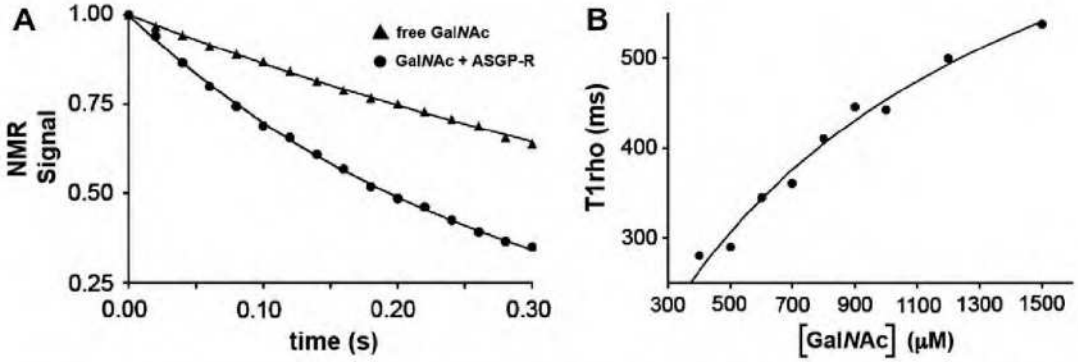

Figure 5. (A) Transverse relaxation of D-Gal*N*Ac, either in the presence (circles) or in the absence (triangles) of ASGP-R H1-CRD. T1rho experiments;[47] (B) Titration of ASGP-R H1-CRD with D-Gal*N*Ac and the corresponding T1rho time constants. The leftmost point, at 400 μM D-Gal*N*Ac, is the T1rho time constant determined for the data in Figure 5B. Additional points correspond to the identical analysis with increasing D-Gal*N*Ac concentrations.

For the quantitative evaluation of the relative affinity of **1b** relative to D-Gal*N*Ac, a titration curve documenting the changes in the transverse relaxation times of D-Gal*N*Ac was required. The T1rho time constants were therefore measured for different concentrations of D-Gal*N*Ac and fit to a one-site binding model (Fig. 5B). The relative affinities were then determined in a two-step process. In a first step, a NMR sample with H1-CRD and the concentration of D-Gal*N*Ac corresponding to the initial point of the titration curve (400 μM) was investigated, indicating a high degree of reproducibility according to the nearly identical T1rho time constants for the first and second sample (282 ± 2 ms and 280 ± 3 ms, respectively). The second step consisted of mixing a small amount of the competitor with the second sample (H1-CRD, 400 μM of D-Gal*N*Ac) and measuring the resulting T1rho time constant, from which the apparent concentration of D-Gal*N*Ac was determined by means of the titration curve. When 200 μM of **1b** were added, the T1rho time constant increased to 401 ± 2 ms. Interpolating this value on the titration curve in Figure 5B indicates an apparent concentration of D-Gal*N*Ac of 785 μM. By subtracting the actual concentration for D-Gal*N*Ac from its apparent concentration and dividing through the concentration of **1b** a relative affinity of 1.9 with respect to D-Gal*N*Ac was obtained, a result almost identical to that received by the competitive solid-phase assay.

3. Conclusion

Based on docking studies of D-Gal*N*Ac to the crystal structure of the H1-CRD of the ASGP-R, a directed library of aryl-substituted triazole derivatives was synthesized and biologically evaluated. For that purpose, a competitive binding assay allowing the determination of Ca^{2+}-dependent binding of potential ligands to the H1-CRD was developed. The reliability of this sensitive, rapid and simple assay was confirmed by a comparison with IC_{50}'s reported in literature and K_D values derived from SPR measurements.

The presented triazolyl galactosamine derivatives which are synthetically easily accessible and hydrolytically stable have drug-like properties. Thus, **1b** may be used instead of D-Gal*N*Ac for oligovalent drug-carriers directed to the ASGP-R, for example, with the scaffold we recently published.[28] Eventually, improved affinity may be realized by further modifications of the substituents of the triazole ring. These follow-up experiments are currently being performed.

It remains to be seen whether the new ligands selectively bind to the H1-CRD of the ASGP-R or bind equally well to the three other D-Gal/D-Gal*N*Ac-receptors of the C-type lectin family,[49] the Kupffer cell receptor, the macrophage galactose lectin, and the scavenger receptor C-type lectin (SRCL).[50–53]

4. Experimental

4.1. General methods

NMR spectra were recorded on a Brucker Avance DRX-500 (500 MHz) spectrometer. Assignment of ^1H and ^{13}C NMR spectra was achieved using 2D methods (COSY, HSQC, TOCSY). Chemical shifts are expressed in ppm using residual $CHCl_3$, CHD_2OD and

HDO as references. NMR solvents were purchased from Sigma–Aldrich ($CDCl_3$), Armar Chemicals (MeOH-d_4, D_2O) and Cambridge Isotope Laboratories (Tris-d_{11}, DMSO-d_6). Optical rotations were measured using a Perkin–Elmer Polarimeter Model 341. The LC/HR-MS analysis were carried out using a Agilent 1100 LC equipped with a photodiode array detector and a Micromass QTOF I. Reactions were monitored by TLC using glass plates coated with Silica Gel 60 F_{254} (Merck). Carbohydrate-containing compounds were visualized by charring with a molybdate solution (0.02 M solution of ammonium cerium sulfate dihydrate and ammonium molybdate tetrahydrate in aqueous 10% H_2SO_4). All other compounds were visualized with $KMnO_4$ solution (2% $KMnO_4$ and 4% $NaHCO_3$ in water). Column chromatography was performed on Silica Gel 60 (Fluka, 0.040–0.060 mm). Methanol (MeOH) was dried by refluxing with sodium methoxide and distilled immediately before use. Pyridine was freshly distilled under argon over CaH_2. Dichloromethane (DCM) was dried by filtration over Al_2O_3 (Fluka, type 5016 A basic). Dioxane and toluene were dried by refluxing with sodium and benzophenone. Molecular sieves (4 Å) were activated in vacuo at 500 °C for 2 h immediately before use.

The vector pET3b encoding the amino acid residues 147–291 of H1-subunit, was kindly provided by M. Spiess (University of Basel, Switzerland). *E. coli* strain AD494 (DE3) was purchased from Novagen (Lucerne, Switzerland). Bacto-Yeast extract, Bacto-Agar and Bacto-Tryptone for LB (Luria-Bertani) and TB (Terrific Broth) culture media were purchased from Becton Dickinson (Allschwil, Switzerland). IPTG (isopropyl β-D-thiogalactopyranoside) was from AppliChem. Sepharose-4B column material, kanamycin, carbenicillin and protein-standard BSA solution were obtained from Sigma (Buchs, Switzerland). The Shodex IEC-DEAE column was from Brechtbühler (Schlieren, Switzerland). Biotinylated polyacrylamide polymers (D-Gal*N*Ac-, D-Gal-PAA) were obtained from Lectinity (Moscow, Russia). HEPES [4-(2-hydroxyethyl)-piperazine-1-ethanesulfonic acid], oxalic acid, $CaCl_2$ and methyl β-D-glucopyranoside were from Fluka (Buchs, Switzerland). Methyl α- and β-D-galactopyranoside and bovine serum albumin (BSA) were from Sigma (Buchs, Switzerland). Lactose, *N*-acetyl-D-galactosamine and D-galactosamine were obtained from Pfanstiehl Laboratories (Ohio, USA). Streptavidin-peroxidase conjugate was from Roche Applied Science (Switzerland). Fetal bovine serum (FBS) was from Invitrogen. The peroxidase substrate kit ABTS [2,2′-azino-di-(3-ethylbenzthiazoline-6-sulfonic acid)] was obtained from BioRad (California, USA) and MaxiSorp 96-well microtiter plates were from Nunc (Roskilde, Denmark). Anti-H1-CRD polyclonal antibodies were produced in chicken and purified from their eggs after PEG-precipitation[56] by affinity chromatography on a agarose-immobilized H1-CRD column. Surface plasmon resonance experiments were performed on a Biacore 3000 machine using CM5 chips (Biacore AB, Uppsala, Sweden).

4.1.1. 2-Acetamido-3,4,6-tri-*O*-acetyl-2-deoxy-α-D-galactopyranosyl chloride (3)

Titanium tetrachloride (185 μL, 1.69 mmol) was added to a suspension of **2** (500 mg, 1.28 mmol) in dry DCM (5 mL). The mixture was stirred at rt under argon for 3 d. The solvent was removed in vacuo, and the residue was purified by flash chromatography on silica gel (petrol ether/EtOAc 2:3→1:4), yielding **3** (419 mg, 89%). The analytical data were identical to those found in the literature.[54]

4.1.2. 2-Acetamido-3,4,6-tri-*O*-acetyl-1,5-anhydro-2-deoxy-D-galactitol (4)

A solution of **3** (2.24 g, 6.12 mmol) in dry toluene (33 mL) was degassed in an ultrasound bath under a steady flow of argon for 30 min. Tributyltin hydride (2.14 g, 7.35 mmol) and AIBN (ca. 25 mg) were added and the mixture was refluxed under argon for 80 min. The solvent was removed in vacuo, and the residue was purified by flash chromatography on silica gel (toluene/EtOAc (1:4→1:9→0:1), yielding **4** (2.03 g, quant).

^{1}H NMR (500 MHz, $CDCl_3$): δ 1.93 (s, 3H, NHAc), 2.02, 2.04, 2.14 (3s, 9H, 3 OAc), 3.15 (t, J = 11.1 Hz, 1H, H-1ax), 3.76 (m, 1H, H-5), 4.06 (m, 2H, H-6), 4.18 (dd, J = 5.2, 11.3 Hz, 1H, H-1eq), 4.40 (m, 1H, H-2), 4.92 (dd, J = 3.3, 11.2 Hz, 1H, H-3), 5.35 (m, 1H, H-4), 5.69 (d, J = 8.0 Hz, 1H, NH); ^{13}C NMR (125 MHz, $CDCl_3$): δ 20.6, 20.7, 20.8 (3 OCO*C*H$_3$), 23.2 (NHCO*C*H$_3$), 46.5 (C-2), 62.2 (C-6), 67.1 (C-4), 68.6 (C-1), 71.5 (C-3), 75.0 (C-5), 170.25, 170.3, 170.5, 171.4 (4 CO); Anal. Calcd for $C_{14}H_{21}NO_8$: C, 50.75; H, 6.39; N, 4.23. Found: C, 51.07; H, 6.49; N, 4.12.

4.1.3. 2-Amino-1,5-anhydro-D-galactitol (5)

To a solution of **4** (3.17 g, 9.58 mmol) in dioxane (8.5 mL) were subsequently added water (6.5 mL), 18-crown-6 (21.1 mg) and potassium hydroxide (840 mg, 15.0 mmol). The reaction mixture was refluxed for 5 h. Another 5 equiv (2.10 g) of potassium hydroxide was then added, and the mixture was refluxed for another 1.5 h. The solvent was removed in vacuo and the crude product **5** (3.91 g) was used without further purification in the next step.

4.1.4. 3,4,6-Tri-*O*-acetyl-1,5-anhydro-2-azido-2-deoxy-D-galactitol (7)

Triflyl azide stock solution preparation: Sodium azide (3.49 g, 53.7 mmol) was dissolved in water (8.7 mL). Toluene was added, and the mixture was cooled to 0 °C with stirring. Then triflic anhydride (5.8 mL, 34.4 mmol) was added dropwise. The biphasic reaction mixture was stirred vigorously at 0 °C for 1 h and at 10 °C for another 2 h. The reaction mixture was neutralized with satd aq $NaHCO_3$. The phases were separated, and the aqueous phase extracted with toluene (2 × 8 mL). The organic layers were combined to give the triflyl azide stock solution.

Amine-azide exchange: Compound **5** (1.56 g, 9.56 mmol), $NaHCO_3$ (319 mg, 38.0 mmol) and $CuSO_4 \cdot H_2O$ (95.0 mg, 380 μmol) were dissolved in water (6.4 mL). The triflyl azide stock solution (21 mL, 9.56 mmol) was added and the biphasic reaction mixture was made homogenous by the dropwise addition of MeOH. The mixture was stirred at rt overnight during that time the color of the mixture turned from blue to green. The solvent was removed in vacuo and the residue containing **6** (1.81 g) was taken up in dry pyridine (36 mL, 447 mmol), and acetic anhydride (8.2 mL, 86.2 mmol) was added. The reaction mixture was stirred at rt under argon overnight. The solvent was removed in vacuo and the crude product was purified by flash chromatography (petrol ether/EtOAc 20:1→9:1) to give **7** (2.31 g, 76%).

$[\alpha]_D$ +0.04 (*c* 1.00, $CHCl_3$); ^{1}H NMR (500 MHz, $CDCl_3$): δ 2.09, 2.16, 2.22 (3s, 9H, 3 OAc), 3.24 (t, J = 11.3 Hz, 1H, H-1ax), 3.79 (dt, J = 0.9, 6.5 Hz, 1H, H-5), 3.93 (m, 1H, H-2), 4.08 (d, J = 6.5 Hz, 2H, H-6), 4.12 (dd, J = 5.4, 11.6 Hz, 1H, H-1eq), 4.91 (dd, J = 3.3, 10.4 Hz, 1H, H-3), 5.40 (d, J = 0.9 Hz, 1H, H-4); ^{13}C NMR (125 MHz, $CDCl_3$): δ 20.6, 20.8, 22.1 (3 CO*C*H$_3$), 55.9 (C-2), 61.9 (C-6), 67.1 (C-4), 68.1 (C-1), 73.4 (C-3), 74.9 (C-5); Anal. Calcd for $C_{12}H_{17}N_3O_7$: C, 45.72; H, 5.43; N, 13.33. Found: C, 45.90; H, 5.44; N, 13.18.

4.1.5. 1,5-Anhydro-2-azido-2-deoxy-D-galactitol (6)

Compound **7** (20.0 mg, 63.4 μmol) was dissolved in MeOH (2 mL) and sodium metal (10 mg) was added. The resulting solution was stirred overnight, the solvent was removed in vacuo and the residue was purified on an RP-C18 column (H_2O/MeOH 20:0→9:1, stepwise gradient) yielding **6** (12.0 mg, quant).

$[\alpha]_D$ −0.12 (*c* 1.00, MeOH); ^{1}H NMR (500 MHz, CD_3OD): δ 3.07 (t, J = 11.1 Hz, 1H, H-1ax), 3.38 (m, 1H, H-5), 3.50 (dd, J = 3.3, 9.9 Hz, 1H, H-3), 3.62–3.72 (m, 3H, H-2, H-6), 3.83 (d, J = 3.0 Hz, 1H, H-4), 3.95 (dd, J = 5.4, 11.2 Hz, 1H, H-1eq); ^{13}C NMR (125 MHz, $CDCl_3$): δ 60.6 (C-2), 62.9 (C-6), 69.1 (C-1), 70.6 (C-4),

75.3 (C-3), 81.0 (C-5); HR-MS Calcd for $C_6H_{11}N_3NaO_4$ $[M+Na]^+$: 212.0647; Found 212.0650.

4.1.6. Ethyl 4-(2-propynyloxy)-benzoate (10e)

Ethyl 4-hydroxybenzoate (**8**, 500 mg, 3.01 mmol) was dissolved in dry acetone (5 mL), and K_2CO_3 (580 mg, 4.21 mmol) was added, followed by propargyl bromide (651 μL, 6.02 mmol), and the mixture was refluxed for 3 h. The mixture was then diluted with DCM (50 mL), washed with H_2O (25 mL) and brine (25 mL), dried (Na_2SO_4), and the solvent was removed in vacuo. The residue was purified by flash chromatography on silica gel (petrol ether/EtOAc 20:1→4:1), yielding **10e** (452 mg, 73%).

^{1}H NMR (500 MHz, $CDCl_3$): δ 1.36 (t, J = 7.2 Hz, 3H, OCH_2CH_3), 2.55 (t, J = 2.4 Hz, 1H, CH), 4.33 (q, J = 7.2 Hz, 2H, OCH_2CH_3), 4.73 (d, J = 2.4 Hz, 2H, CH_2, propynyl), 6.98, 8.00 (AA′, BB′ of AA′BB′, J = 9.0 Hz, 4H, C_6H_4); ^{13}C NMR (125 MHz, $CDCl_3$): δ 14.3 (OCH_2CH_3), 55.7 (OCH_2), 60.5 (OCH_2CH_3), 76.0 (CH), 77.8 (C_Q), 114.4, 123.7, 131.4, 161.0 (6C, C_6H_4), 166.2 (CO); Anal. Calcd for $C_{12}H_{12}O_3$: C, 70.58; H, 5.92. Found: C, 70.58; H, 5.93.

4.1.7. 1-Trifluoromethylsulfonamido-4-(2-propynyloxy)benzene (10f)

Compound **9**[37] (100 mg, 679 μmol) was dissolved in dry DCM (3 mL). Triethylamine (103 μL, 747 μmol) was added, followed by the dropwise addition of triflic anhydride (123 μL, 747 μmol) at 0 °C. The solution was allowed to reach rt and stirred under argon overnight. The solvent was removed in vacuo and the residue was purified by flash chromatography on silica gel (petrol ether/EtOAc 19:1→9:1), yielding **10f** (130 mg, 69%).

^{1}H NMR (500 MHz, $CDCl_3$): δ 2.54 (t, J = 2.4 Hz, 1H, CH); 4.69 (d, J = 2.4 Hz, 2H, OCH_2); 6.97, 7.23 (AA′, BB′ of AA′BB′, J = 8.9 Hz, 4H, C_6H_4); ^{13}C NMR (125 MHz, $CDCl_3$): δ 56.1 (OCH_2), 76.1 (CH), 77.9 (C_Q), 119.8 (J = 322.8 Hz, CF_3), 115.8, 126.6, 126.9, 157.2 (C_6H_4); Anal. Calcd for $C_{10}H_8NO_3F_3S$: C, 43.01; H, 2.89; N, 5.02. Found: C, 42.95; H, 3.00; N, 4.97.

4.1.8. 1-(3,4,6-Tri-O-acetyl-1,5-anhydro-2-deoxy-D-galactitol-2-yl)-4-phenoxymethyl-1,2,3-triazole (11a)

Compound **7** (50.0 mg, 158 μmol) was dissolved in dry DCM (3 mL). The mixture was degassed in an ultrasound bath under a flow of argon for 20 min. Copper(I) chloride (31.2 mg, 316 μmol), DIPEA (54.4 μL, 316 μmol) and **10a** (40.6 μL, 316 μmol) were added. The mixture was stirred under argon at rt for 24 h. The solvent was removed in vacuo, and the crude mixture was purified by flash chromatography (petrol ether/EtOAc 3:2) to yield compound **11a** (66.5 mg, 93%).

^{1}H NMR (500 MHz, $CDCl_3$): δ 1.81, 2.08, 2.19 (3s, 9H, 3 OAc), 4.00–4.07 (m, 2H, H-1ax, H-5), 4.15 (d, J = 6.4 Hz, 2H, H-6), 4.33 (dd, J = 5.1, 11.6 Hz, 1H, H-1eq), 4.92 (dt, J = 5.0, 11.0 Hz, 1H, H-2), 5.22 (s, 2H, CH_2OPh), 5.50 (dd, J = 3.2, 11.0 Hz, 1H, H-3), 5.54 (d, J = 2.5 Hz, 1H, H-4), 6.95–6.99, 7.26–7.30 (m, 5H, C_6H_5), 7.62 (s, 1H, H-5 triazole); ^{13}C NMR (125 MHz, $CDCl_3$): δ 20.3, 20.7, 20.7 (3 $COCH_3$), 56.0 (C-2), 61.8 (2C, CH_2OPh, C-6), 67.0 (C-4), 68.7 (C-1), 71.5 (C-3), 75.3 (C-5), 114.7, 121.4, 122.7, 129.6 (6C, C_6H_5), 118.5 (C-5 triazole), 144.3 (C-4 triazole), 169.3, 170.0, 170.5 (3 CO); HR-MS Calcd for $C_{21}H_{26}N_3O_8$ $[M+H]^+$: 448.1720; Found: 448.1725.

4.1.9. 1-(3,4,6-Tri-O-acetyl-1,5-anhydro-2-deoxy-D-galactitol-2-yl)-4-(4-cyanophenoxy)methyl-1,2,3-triazole (11b)

Prepared according to the procedure described for **11a**, using **7** (50.0 mg, 158 μmol) **10b**[38] (49.7 mg, 316 μmol). The compound was purified by flash chromatography (petrol ether/EtOAc 1:1→0:1) to give **11b** (73.0 mg, 98%).

^{1}H NMR (500 MHz, $CDCl_3$): δ 1.79, 2.04, 2.16 (3s, 9H, 3 $COCH_3$), 3.99–4.04 (m, 2H, H-1ax, H-5), 4.12 (d, J = 6.4 Hz, 2H, H-6), 4.30 (dd, J = 5.0, 11.6 Hz, 1H, H-1eq), 4.92 (dt, J = 4.9, 10.7 Hz, 1H, H-2), 5.22 (s, 2H, CH_2OAr), 5.48–5.52 (m, 2H, H-3, H-4), 7.01, 7.56 (m, 4H, C_6H_4), 7.67 (s, 1H, H-5 triazole); ^{13}C NMR (125 MHz, $CDCl_3$): δ 20.2, 20.5, 20.6 (3 $COCH_3$), 56.1 (C-2), 61.7, 61.9 (C-6, CH_2OAr), 66.9 (C-4), 68.6 (C-1), 71.3 (C-3), 75.2 (C-5), 115.4 (2C, 2 C-*ortho*), 118.8 (C-*para*), 123.0 (C-5 triazole), 134.0 (2C, 2 C-*meta*), 142.9 (C-4 triazole), 161.2 (C-*ipso*), 169.2, 169.8, 170.4 (3 CO); HR-MS Calcd for $C_{22}H_{24}N_4O_8$ $[M+H]^+$: 473.1672; Found: 473.1667.

4.1.10. 1-(3,4,6-Tri-O-acetyl-1,5-anhydro-2-deoxy-D-galactitol-2-yl)-4-(4-nitrophenyloxy) methyl-1,2,3-triazole (11c)

Prepared according to the procedure described for **11a**, using **7** (50.0 mg, 158 μmol) and **10c**[37] (49.7 mg, 316 μmol). The compound was purified by flash chromatography (petrol ether/EtOAc 1:1) to give **11c** (74.0 mg, 95%).

^{1}H NMR (500 MHz, $CDCl_3$): δ 1.80, 2.03, 2.15 (3s, 9H, 3 $COCH_3$), 3.99–4.04 (m, 2H, H-1ax, H-5), 4.12 (d, J = 6.4 Hz, 2H, H-6), 4.30 (dd, J = 5.0, 11.6 Hz, 1H, H-1eq), 4.93 (m, 1H, H-2), 5.26 (s, 2H, CH_2OAr), 5.49–5.52 (m, 2H, H-3, H-4), 7.02 (AA′ of AA′BB′, J = 9.3 Hz, 2H, C_6H_4), 7.70 (s, 1H, H-5 triazole), 8.15 (BB′ of AA′BB′, J = 9.3 Hz, 2H, C_6H_4); ^{13}C NMR (125 MHz, $CDCl_3$): δ 20.3, 20.6, 20.7 (3 $COCH_3$), 56.2 (C-2), 61.9, 62.3 (C-6, CH_2OAr), 67.0 (C-4), 68.6 (C-1), 71.4 (C-3), 75.3 (C-5), 114.8 (2C, 2 C-*ortho*), 123.2 (C-5 triazole), 125.9 (2C, 2 C-*meta*), 141.9 (C-*para*), 142.8 (C-4 triazole), 163.0 (C-*ipso*), 169.3, 170.0, 170.5 (3 CO); HR-MS Calcd for $C_{21}H_{24}N_4O_{10}$ $[M+H]^+$: 493.1571; Found: 493.1579.

4.1.11. 1-(3,4,6-Tri-O-acetyl-1,5-anhydro-2-deoxy-D-galactitol-2-yl)-4-(pentafluorophenoxy) methyl-1,2,3-triazole (11d)

Prepared according to the procedure described for **11a**, using **7** (50.0 mg, 158 μmol) and **10d**[39] (70.2 mg, 316 μmol). The compound was purified by flash chromatography (petrol ether/EtOAc 4:1→1:1) to give **11d** (62.0 mg, 73%).

^{1}H NMR (500 MHz, $CDCl_3$): δ 1.85, 2.05, 2.18 (3s, 9H, 3 $COCH_3$), 3.97–4.02 (m, 2H, H-1ax, H-5), 4.13 (d, J = 6.4 Hz, 2H, H-6), 4.29 (dd, J = 5.0, 11.6 Hz, 1H, H-1eq), 4.95 (dt, J = 5.0, 11.0 Hz, 1H, H-2), 5.27 (s, 2H, CH_2OAr), 5.49–5.53 (m, 2H, H-3, H-4), 7.74 (m, 1H, H-5 triazole); ^{13}C NMR (125 MHz, $CDCl_3$): δ 20.1, 20.5, 20.6 (3 $COCH_3$), 56.1 (C-2), 61.8 (C-6), 66.9 (C-4), 67.6 (CH_2OAr), 68.6 (C-1), 71.3 (C-3), 75.2 (C-5), 123.6 (C-5 triazole), 136.9, 139.0, 141.1, 142.9 (6C, C_6F_5), 142.5 (C-4 triazole), 169.3, 169.9, 170.4 (3 CO); HR-MS Calcd for $C_{21}H_{21}F_5N_3O_8$ $[M+H]^+$: 538.1249; Found: 538.1252.

4.1.12. 1-(3,4,6-Tri-O-acetyl-1,5-anhydro-2-deoxy-D-galactitol-2-yl)-4-(4-ethoxycarbonylphenoxy)methyl-1,2,3-triazole (11e)

Prepared according to the procedure described for **11a**, using **7** (50.0 mg, 160 μmol) and **10e** (64.5 mg, 316 μmol). The compound was purified by flash chromatography (hexane/EtOAc 3:2→2:3) to give **11e** (62.0 mg, 82%).

^{1}H NMR (500 MHz, $CDCl_3$): δ 1.35 (t, J = 7.1 Hz, 3H, CH_2CH_3), 1.79, 2.05, 2.16 (3s, 9H, 3 $COCH_3$), 3.99–4.10 (m, 2H, H-1ax, H-5), 4.13 (d, J = 6.4 Hz, 2H, H-6), 4.29–4.34 (m, 3H, H-1eq, CH_2CH_3), 4.92 (dt, J = 4.9, 10.9 Hz, 1H, H-2), 5.23 (s, 2H, CH_2OAr), 5.49–5.53 (m, 2H, H-3, H-4), 6.95 (AA′ of AA′BB′, J = 8.9 Hz, 2H, C_6H_4), 7.66 (s, 1H, H-5 triazole), 7.96 (BB′ of AA′BB′, J = 8.9 Hz, 2H, C_6H_4); ^{13}C NMR (125 MHz, $CDCl_3$): δ 14.3 (CH_2CH_3), 20.2, 20.5, 20.6 (3 $COCH_3$), 56.0 (C-2), 60.6 (CH_2CH_3), 61.8 (2C, C-6, CH_2OAr), 66.9 (C-4), 68.6 (C-1), 71.4 (C-3), 75.2 (C-5), 114.2 (2C, 2 C-*ortho*), 122.9 (C-5 triazole), 131.5 (2C, 2 C-*meta*), 131.6 (C-*para*), 143.5 (C-4 triazole), 161.5 (C-*ipso*), 169.2, 169.9, 170.4 (3 CO); HR-MS Calcd for $C_{24}H_{30}N_3O_{10}$ $[M+H]^+$: 520.1931; Found: 520.1937.

4.1.13. 1-(3,4,6-Tri-*O*-acetyl-1,5-anhydro-2-deoxy-D-galactitol-2-yl)-4-(trifluoromethylsulfonamidophenyloxy)methyl-1,2,3-triazole (11f)

Prepared according to the procedure described for **11a**, using **7** (50.0 mg, 158 μmol) and **10f** (88.2 mg, 316 μmol). The compound was purified by flash chromatography (petrol ether/EtOAc 3:1→1:1) to give **11f** (39.0 mg, 41%).

^{1}H NMR (500 MHz, $CDCl_3$): δ 1.81, 2.06, 2.18 (3s, 9H, 3 $COCH_3$), 4.00–4.05 (m, 2H, H-1ax, H-5), 4.14 (d, J = 6.4 Hz, 2H, H-6), 4.32 (dd, J = 5.0, 11.6 Hz, 1H, H-1eq), 4.95 (m, 1H, H-2), 5.12 (s, 2H, CH_2OAr), 5.50–5.53 (m, 2H, H-3, H-4), 6.88, 7.22 (AA′, BB′ of AA′BB′, J = 8.8 Hz, 4H, C_6H_4), 7.68 (s, 1H, H-5 triazole), 8.56 (s, 1H, NH); ^{13}C NMR (125 MHz, $CDCl_3$): δ 20.2, 20.6, 20.7 (3 $COCH_3$), 56.3 (C-2), 61.7, 61.9 (C-6, CH_2OAr), 67.0 (C-4), 68.6 (C-1), 71.4 (C-3), 75.2 (C-5), 115.4 (2C, 2 C-*ortho*), 119.84 (q, J = 323.1 Hz, CF_3), 123.2 (C-5 triazole), 126.6 (2C, 2 C-*meta*), 127.1 (C-*para*), 143.5 (C-4 triazole), 157.3 (C-*ipso*), 169.5, 170.1, 170.6 (3 CO); HR-MS Calcd for $C_{22}H_{25}F_3N_4NaO_{10}$ [M+Na]$^+$: 617.1141; Found: 617.1150.

4.1.14. 1-(3,4,6-Tri-*O*-acetyl-1,5-anhydro-2-deoxy-D-galactitol-2-yl)-4-(4-bromophenoxy) methyl-1,2,3-triazole (11g)

Prepared according to the procedure described for **11a**, using **7** (200 mg, 634 μmol) and **10g**[40] (267 mg, 1.07 mmol). The compound was purified by flash chromatography (hexane/EtOAc 1:1) to give **11g** (279 mg, 84%).

^{1}H NMR (500 MHz, $CDCl_3$): δ 1.74, 2.00, 2.11 (3s, 9H, 3 $COCH_3$), 3.93–4.00 (m, 2H, H-1ax, H-5), 4.07 (d, J = 6.4 Hz, 2H, H-6), 4.24 (dd, J = 5.0, 11.6 Hz, 1H, H-1eq), 4.86 (dt, J = 5.0, 11.0 Hz, 1H, H-2), 5.10 (s, 2H, CH_2OAr), 5.43–5.47 (m, 2H, H-3, H-4), 6.77, 7.30 (AA′, BB′ of AA′BB′, J = 8.9 Hz, 4H, C_6H_4), 7.57 (s, 1H, H-5 triazole); ^{13}C NMR (125 MHz, $CDCl_3$): δ 20.2, 20.5, 20.6 (3 $COCH_3$), 56.0 (C-2), 61.8, 61.9 (C-6, CH_2OAr), 66.9 (C-4), 68.6 (C-1), 71.4 (C-3), 75.2 (C-5), 113.5 (C-Br), 116.5 (2C, 2 C-*ortho*), 122.8 (C5 triazole), 132.3 (2C, 2 C-*meta*), 143.7 (C-4 triazole), 157.0 (C-*ipso*), 169.2, 169.9, 170.4 (3 CO); HR-MS Calcd for $C_{21}H_{25}BrN_3O_8$ [M+H]$^+$: 526.0825; Found: 526.0818.

4.1.15. 1-(1,5-Anhydro-2-deoxy-D-galactitol-2-yl)-phenoxymethyl-1,2,3-triazole (1a)

Compound **11a** (65.0 mg, 145 μmol) was dissolved in dry MeOH (5 mL) and sodium metal (20.0 mg, 869 μmol) was added. The solution was stirred at rt under argon for 3 h, after which the solvent was removed in vacuo and the residue was purified by preparative LC-MS to give **1a** (21.0 mg, 45%).

$[\alpha]_D$ +36.4 (*c* 0.17, MeOH); ^{1}H NMR (500 MHz, CD_3OD): δ 3.31 (t, J = 1.6 Hz, 1H, H-5), 3.61–3.81 (m, 2H, H-6), 3.84 (t, J = 11.1 Hz, 1H, H-1ax), 3.99 (d, J = 3.0 Hz, 1H, H-4), 4.14–4.18 (m, 2H, H-1eq, H-3), 4.81 (dt, J = 5.0, 10.8 Hz, 1H, H-2), 5.16 (s, 2H, CH_2OPh), 6.93–7.01, 7.26–7.30 (m, 5H, C_6H_5), 8.14 (s, 1H, H-5 triazole); ^{13}C NMR (125 MHz, CD_3OD): δ 60.7 (C-2), 62.3 (CH_2OPh), 62.9 (C-6), 69.8 (C-1), 70.4 (C-4), 73.5 (C-3), 81.5 (C-5), 122.2, 125.8, 130.6, 159.8 (6C, C_6H_5), 115.9 (C-5 triazole), 144.53 (C-4 triazole); HR-MS Calcd for $C_{15}H_{20}N_3O_5$ [M+H]$^+$: 322.1403; Found: 322.1401.

4.1.16. 1-(1,5-Anhydro-2-deoxy-D-galactitol-2-yl)-4-(4-cyanophenoxy)methyl-1,2,3-triazole (1b)

Compound **11b** (73.0 mg, 155 μmol) was dissolved in H_2O/MeOH/Et_3N (5:5:1, 5.5 mL) and stirred at rt overnight. The solvent was removed in vacuo and the residue was purified by flash chromatography (DCM/MeOH 9:1) to give **1b** (44.0 mg, 81%).

^{1}H NMR (500 MHz, CD_3OD): δ 3.62 (m, 1H, H-5), 3.73 (dd, J = 4.9, 11.4 Hz, 1H, H-6a), 3.80 (dd, J = 7.1, 11.4 Hz, 1H, H-6b), 3.84 (t, J = 11.1 Hz, 1H, H-1ax), 3.99 (d, J = 3.0 Hz, 1H, H-4), 4.14–4.18 (m, 2H, H-1eq, H-3), 4.82 (dt, J = 5.0, 10.9 Hz, 1H, H-2), 5.36 (s, 2H, CH_2OAr), 7.17, 7.67 (AA′, BB′ of AA′BB′, J = 9.0 Hz, 4H, C_6H_4), 8.19 (s, 1H, H-5 triazole); ^{13}C NMR (125 MHz, CD_3OD): δ 60.7 (C-2), 62.6 (CH_2OAr), 62.9 (C-6), 69.7 (C-1), 70.3 (C-4), 73.5 (C-3), 80.5 (C-5), 105.3 (CN), 116.8 (2C, 2 C-*ortho*), 120.0 (C-*para*), 126.2 (C-5 triazole), 135.2 (2C, 2 C-*meta*), 143.5 (C-4 triazole), 163.2 (C-*ipso*); HR-MS Calcd for $C_{16}H_{19}N_4O_5$ [M+H]$^+$: 347.1355; Found: 347.1358.

4.1.17. 1-(1,5-Anhydro-2-deoxy-D-galactitol-2-yl)-4-(4-nitrophenoxy)methyl-1,2,3-triazole (1c)

Compound **11c** (74.0 mg, 150 μmol) was deacetylated according to the procedure described for **1a**. The final product was purified by LC-MS to give **1c** (18.0 mg, 33%).

^{1}H NMR (500 MHz, CD_3OD): δ 3.76–3.87 (m, 2H, H-5, H-6a), 3.90 (t, J = 11.2 Hz, 1H, H-1ax), 4.10 (m, 2H, H-6b, H-4), 4.24 (dd, J = 5.1, 11.2 Hz, 1H, H-1eq), 4.28 (dd, J = 3.2, 10.6 Hz, 1H, H-3), 4.87 (m, 1H, H-2), 5.38 (s, 2H, CH_2OAr), 7.23 (AA′ of AA′BB′, J = 9.3 Hz, 2H, C_6H_4), 8.29 (m, 3H, C_6H_4, H-5 triazole); ^{13}C NMR (125 MHz, CD_3OD): δ 60.3 (C-2), 62.5, 62.6 (C-6, CH_2OAr), 69.3 (C-1), 69.8 (C-4), 72.9 (C-3), 81.0 (C-5), 116.1 (2C, 2 C-*ortho*), 126.5 (C-5 triazole), 127.0 (2C, 2 C-*meta*), 142.6 (C-*para*), 143.3 (C-4 triazole), 164.5 (C-*ipso*); HR-MS Calcd for $C_{15}H_{19}N_4O_7$ [M+H]$^+$: 367.1254; Found: 367.1255.

4.1.18. 1-(1,5-Anhydro-2-deoxy-D-galactitol-2-yl)-4-(pentafluorophenoxy)methyl-1,2,3-triazole (1d)

Compound **11d** (60.0 mg, 111 μmol) was deacetylated according to the procedure described for **1a**. The crude product was purified by LC-MS to give **1d** (31.0 mg, 68%).

^{1}H NMR (500 MHz, CD_3OD): δ 3.59 (m, 1H, H-5), 3.69 (dd, J = 4.9, 11.4 Hz, 1H, H-6a), 3.75-3.90 (m, 2H, H-1ax, H-6b), 3.97 (m, 1H, H-4), 4.10-4.14 (m, 2H, H-1eq, H-3), 4.78 (dt, J = 5.0, 10.8 Hz, 1H, H-2), 5.20 (m, 2H, CH_2OAr), 8.10 (m, 1H, H-5 triazole); ^{13}C NMR (125 MHz, CD_3OD): δ 60.7 (C-2), 62.9 (C-6), 68.4 (CH_2OAr), 66.5 (C-1), 70.4 (C-4), 73.5 (C-3), 81.5 (C-5), 126.9 (C-5 triazole), 142.9 (C-4 triazole); HR-MS Calcd for $C_{15}H_{15}F_5N_3O_5$ [M+H]$^+$: 412.0932; Found: 412.0934.

4.1.19. 1-(1,5-Anhydro-2-deoxy-D-galactitol-2-yl)-4-(sodium 4-carboxyphenoxy)methyl-1,2,3-triazole (1e)

Compound **11e** (62.0 mg, 119 μmol) was dissolved in MeOH/H_2O (4 mL, 1:1), and NaOH (170 mg, 4.72 mmol) was added. The solution was stirred at rt for 24 h, after which the solvent was removed in vacuo, and the residue was purified by flash chromatography (DCM/MeOH 5:1→2:1) to give **1e** (32.0 mg, 74%).

^{1}H NMR (500 MHz, CD_3OD): δ 3.62 (m, 1H, H-5), 3.73 (m, 2H, H-6), 3.81 (t, J = 11.3 Hz, 1H, H-1ax), 3.99 (d, J = 3.0 Hz, 1H, H-4), 4.11-4.17 (m, 2H, H-3, H-1eq), 4.80 (m, 1H, H-2), 5.20 (s, 2H, CH_2OAr), 7.02, 7.93 (AA′, BB′ of AA′BB′, J = 8.8 Hz, 4H, C_6H_4), 8.19 (s, 1H, H-5 triazole); ^{13}C NMR (125 MHz, CD_3OD): δ 60.6 (C-2), 62.4 (CH_2OAr), 62.9 (C-6), 69.7 (C-4), 70.5 (C-1), 73.3 (C-3), 81.2 (C-5), 115.1 (2C, 2 C-*ortho*), 126.0 (C-5 triazole), 127.5 (C-*para*), 132.5 (2C, 2 C-*meta*), 144.1 (C-4 triazole), 162.8 (C-*ipso*), 173.7 (CO); HR-MS Calcd for $C_{16}H_{19}N_3NaO_7$ [M+H]$^+$: 388.1121; Found: 388.1128.

4.1.20. 1-(1,5-Anhydro-2-deoxy-D-galactitol-2-yl)-4-(4-trifluoromethylsulfonamidophenoxy) methyl-1,2,3-triazole (1f)

Compound **11f** (39.0 mg, 61.6 μmol) was deacetylated according to the procedure described for **1a**. The final product was purified by flash chromatography on silica gel (DCM/MeOH 10:1) to give **1f** (21.2 mg, 73%).

^{1}H NMR (500 MHz, CD_3OD): δ 3.58 (m, 1H, H-5), 3.68 (dd, J = 4.8, 11.4 Hz, 1H, H-6a), 3.73–3.81 (m, 2H, H-1ax, H-6b), 3.95 (d, J = 3.0 Hz, 1H, H4), 4.10–4.13 (m, 2H, H-1eq, H-3), 4.77 (dt, J = 5.1, 10.8 Hz, 1H, H-2), 5.11 (s, 2H, CH_2OAr), 6.94, 7.13 (AA′ of AA′BB′, J = 9.0 Hz, 2H, C_6H_4), 8.11 (s, 1H, H-5 triazole); ^{13}C NMR (125 MHz, CD_3OD): δ 60.7 (C-2), 62.6 (CH_2OAr), 62.9 (C-6), 69.7

(C-1), 70.4 (C-4), 73.4 (C-3), 81.4 (C-5), 116.3 (2C, 2 C-*ortho*), 121.9 (q, J = 323.9 Hz, CF_3), 125.9 (C-5 triazole), 126.8 (2C, 2 C-*meta*), 131.4 (C-*para*), 144.3 (C-4 triazole), 158.0 (C-*ipso*); HR-MS Calcd for $C_{16}H_{19}F_3N_4O_7SNa$ $[M+Na]^+$: 491.0824; Found: 491.0828.

4.1.21. 1-(3,4,6-Tri-*O*-acetyl-1,5-anhydro-2-deoxy-D-galactitol-2-yl)-4-[(4-methyl-piperazin-1-yl)-phenoxymethyl]-1,2,3-triazole (11h)

Compound **11g** (75.0 mg, 142 μmol) and Cs_2CO_3 (64.8 mg, 199 μmol) were azeotropically dried with toluene, and Pd_2dba_3 (3.00 mg, 2.89 μmol), X-phos[42] (**12**, 1.35 mg, 2.84 μmol), *N*-methylpiperazine (17.0 μL, 157 μmol) and dry toluene (3 mL) were added. The resultant mixture was stirred at 80 °C under argon for 24 h. The solvent was removed in vacuo, and the residue purified by flash chromatography (EtOAc/MeOH 9:1→4:1) to give **11h**, which was still slightly impure according to NMR. The compound was used without further purification in the next step.

4.1.22. 1-(1,5-Anhydro-2-deoxy-D-galactitol-2-yl)-4-[(4-methyl-piperazin-1-yl)-phenoxymethyl]-1,2,3-triazole (1h)

Compound **11h** (35.1 mg, 64.3 μmol) was deacetylated according to the procedure described for **1a**. The final product was purified by flash chromatography (DCM/MeOH 9:1→7:3) to give **1h** (12.0 mg, 44%).

^{1}H NMR (500 MHz, CD_3OD): δ 2.63 (s, 3H, NCH_3), 3.02 (m, 4H, $(CH_2)_2NCH_3$), 3.18 (m, 4H, $(CH_2)_2NPh$), 3.59 (m, 1H, H-5), 3.69 (dd, J = 4.9, 11.4 Hz, 1H, H-6a), 3.74–3.82 (m, 2H, H-1ax, H-6b), 3.95 (d, J = 3.0 Hz, 1H, H-4), 4.10-4.13 (m, 2H, H-1eq, H-3), 4.02 (dd, J = 3.0, 10.5 Hz, 1H, H-3), 4.76 (m, 1H, H-2), 5.07 (s, 2H, CH_2OAr), 6.92 (m, 4H, C_6H_4), 8.09 (s, 1H, H-5 triazole); ^{13}C NMR (125 MHz, CD_3OD): δ 44.7 (NCH_3), 49.5 (2C, $(CH_2)_2NCH_3$), 55.4 (2C, $(CH_2)_2NPh$), 60.7 (C-2), 62.8 (2C, C-6, CH_2OAr), 69.7 (C-1), 70.4 (C-4), 73.4 (C-3), 81.4 (C-5), 116.7 (2C, 2 C-*ortho*), 119.9 (2C, 2 C-*meta*), 125.8 (C-5 triazole), 144.6 (C-*para*), 146.4 (C-4 triazole), 154.7 (C-*ipso*); HR-MS Calcd for $C_{20}H_{30}N_5O_5$ $[M+H]^+$: 420.2247; Found: 420.2252.

4.2. Expression and purification of recombinant H1-CRD

The vector pET3b encoding the amino acid residues 147–291 of the H1-subunit was transformed into *E. coli* strain AD494 (DE3). Following IPTG (0.4 mM) induction, the protein was accumulated as inclusion bodies. After collection and lysis of the cells the protein extract was denatured under reducing conditions and dialyzed against Tris/HCl buffer (20 mM TrisCl, 120 mM NaCl, 20 mM $CaCl_2$, pH 7.8). The correctly folded H1-CRD was purified by affinity chromatography on a D-Gal-Sepharose column attached to an FPLC-system (Bio-Rad). In a second step the monomer and dimer fractions were separated by ion exchange HPLC (Agilent 1100) on a DEAE column. The monomeric fraction was quantified by a Bradford assay[55] and immediately used for the binding assay or stored at −20 °C. The purity and identity of the purified protein were verified by SDS–PAGE and immuno-blot analysis, respectively. For the immuno-blot analysis, polyclonal (IgY) anti-H1-CRD antibodies were used. The antibodies were produced in chicken and purified from their eggs after PEG-precipitation[56] by affinity chromatography on a agarose-immobilized H1-CRD column.

4.3. Competitive solid-phase binding assay

Flat-bottom 96-well microtiter plates were coated with 100 μL/well of a 3 μg/mL solution of monomeric H1-CRD in 20 mM HEPES, 150 mM NaCl and 1 mM $CaCl_2$, pH 7.4 (HBS-buffer) overnight at 4 °C. The coating solution was discarded and the wells were blocked with 150 μL/well of 1% BSA in HBS-buffer for 2 h at 4 °C. After three washing steps with 150 μL/well of HBS-buffer, 50 μL/well of the test compound solution (6 μM to 2 mM) and 50 μL of a 0.5 μg/mL of streptavidin-peroxidase coupled PAA-glycopolymers (D-Gal*N*Ac-, D-Gal-PAA) were added. The plates were incubated for 2 h at rt and 250 rpm. The plates were then carefully washed twice with 150 μL/well HBS-buffer. After the addition of 100 μL/well of ABTS-substrate, the colorimetric reaction was allowed to develop for 2 min. The reaction was stopped by the addition of 2% aqueous oxalic acid and the optical density (OD) was measured at 415 nm on a microplate-reader (Spectramax 190, Molecular Devices, California, USA). The IC_{50} values of the compounds tested in triplicates in three independent experiments were calculated with PRISM software (GraphPad Software, Inc, La Jolla, USA). The data set was normalized to percentage of binding by setting background binding (D-Gal*N*Ac-PAA binding to wells without H1-CRD) as 0% and control binding (maximal D-Gal*N*Ac-PAA binding to H1-CRD) as 100%. The nonlinear fit of the normalized data was calculated with a four-parameter logistic equation with the bottom of the curve constraint to zero and the top to 100. The IC_{50} defines the molar concentration of the test compound that reduces the maximal specific binding of D-Gal*N*Ac-PAA to H1-CRD by 50%. The relative IC_{50} (rIC_{50}) is the ratio of the IC_{50} of the test compound to the IC_{50} of D-Gal*N*Ac.

4.4. Surface Plasmon Resonance Experiments (Biacore)

The analyses were performed on a Biacore 3000 machine (Biacore AB, Uppsala, Sweden) using CM5 chips. After activating the surface of the chip for 5–10 min at a flow rate of 5 μL/min using a standard amine coupling procedure, H1-CRD, diluted in 10 mM acetate buffer pH 4.5 to a final concentration of 20 μg/mL, was injected for 5–15 min and the surface was deactivated for a time corresponding to the activation phase. The obtained surface densities ranged from 1800 to 2500 RUs. HBS-N buffer (10 mM HEPES pH 7.4, 50 mM $CaCl_2$) was used as running buffer. The screening of the compounds was performed by the injection of twofold serial dilutions between 5 mM and 5 μM as randomized triplicates. Each sample was injected for 30 s with an undisturbed dissociation phase of 20 s and 50 μL/min. No regeneration or washing steps were applied. Five buffer blanks were injected at the beginning and one between the triplicate series. Signals of an untreated flow cell and averaged blank injections were subtracted from the sample sensorgrams. Since referenced sensorgrams showed negative SPR signals, the whole data set was mirrored by multiplication of each data point with −1. Mirrored steady state data were evaluated between 10 and 20 s of the injection period and were fitted to a single site-binding model. Data processing and equilibrium binding constant determinations were accomplished with SCRUBBER software Version 2.

4.5. NMR experiments

Shigemi NMR tubes were used to reduce the sample volume, and therefore protein consumption, needed for measurement to 250 μL. The ASGP-R protein was present at 17 μM, as determined by a Bradford assay. The buffer consisted of 1 mM $CaCl_2$ in D_2O (Armar Chemicals), maintained at pH 7.5 with 25 mM Tris-d_{11}. A stock solution of D-Gal*N*Ac was prepared in D_2O at 50 mM. A stock solution of **1b** in DMSO-d_6 was prepared at 50 mM.

All NMR experiments were carried out at 300 K on a Bruker DRX500 spectrometer, equipped with *Z*-gradient SEI probe. The pulse sequence used for the T1rho relaxation was slightly modified from that described by Hajduk.[57] Following the 90° non-selective pulse, a continuous-wave spin-lock of 2 kHz was applied for a various duration to monitor the T1rho relaxation. The pulse sequence terminated with the DPFGSE water suppression sequence to suppress the magnetization from the residual protons in the D_2O

solvent.[58] For each T1rho time constant measurement, 15 experiments were performed with different durations of the spin-lock which started at 20 ms to a final value of 300 ms, in intervals of 20 ms. For concentrations of D-Gal*N*Ac that were less than 600 μM, 16 scans were measured, preceded by eight dummy scans, and a recovery delay of 10 s between successive scans. For concentrations of D-Gal*N*Ac that were 600 μM or greater, the identical procedure was followed, except that only eight scans were measured. Prior to the measurement upon addition of a competing compound, a 1 h incubation time for equilibration was allowed.

The NMR data were analyzed using XWINNMR version 3.5 operating on a PC running under Linux OS. The spectra were apodized with an exponential decay function with 2 Hz line broadening. The inversion recovery data, as well as the one-site binding model, were fit using PRISM 4 (GraphPad Software Inc., San Diego, USA).

Acknowledgment

The authors would like to thank the Swiss National Science Foundation (SNF) for funding the research.

Supplementary data

Supplementary data (^{1}H NMR spectra of target compounds **1a–f**, **1h** and **6**) associated with this article can be found, in the online version, at doi:10.1016/j.bmc.2009.08.049.

References and notes

1. Drickamer, K.; Taylor, M. E. *Annu. Rev. Cell. Biol.* **1993**, *9*, 237.
2. Hubbard, A. L.; Sturenbrok, H. *J. Cell Biol.* **1979**, *83*, 56.
3. Spiess, M. *Biochem.* **1990**, *29*, 10009.
4. Geffen, I.; Spiess, M. *Int. Rev. Cytol.* **1992**, *137B*, 181.
5. Weigel, P. H.; Yik, J. H. *Biochim. Biophys. Acta* **2002**, *1572*, 341.
6. Yik, J. H.; Saxena, A.; Weigel, P. H. *J. Biol. Chem.* **2002**, *277*, 23076.
7. Henis, Y. I.; Katzir, Z.; Shia, M. A.; Lodish, H. F. *J. Cell. Biol.* **1990**, *111*, 1409.
8. Bider, M. D.; Wahlberg, J. M.; Kammerer, R. A.; Spiess, M. *J. Biol. Chem.* **1996**, *271*, 31996.
9. Tozawa, R.; Ishibashi, S.; Osuga, J.; Yamamoto, K.; Yagyu, H.; Ohashi, K.; Tamura, Y.; Yahagi, N.; Iizuka, Y.; Okazaki, H.; Harada, K.; Gotoda, T.; Shimano, H.; Kimura, S.; Nagai, R.; Yamada, N. *J. Biol. Chem.* **2001**, *276*, 12624.
10. Ishibashi, S.; Hammer, R. E.; Herz, J. *J. Biol. Chem.* **1994**, *269*, 27803.
11. Bider, M. D.; Spiess, M. *FEBS Lett.* **1998**, *434*, 37.
12. Shia, M. A.; Lodish, H. F. *Proc. Natl. Acad. Sci. U.S.A.* **1989**, *86*, 158.
13. Meier, M.; Bider, M. D.; Malashkevich, V. N.; Spiess, M.; Burkhard, P. *J. Mol. Biol.* **2000**, *300*, 857.
14. Lee, Y. C.; Townsend, R. R.; Hardy, M. R.; Lonngren, J.; Arnarp, J.; Haraldsson, M.; Lönn, H. *J. Biol. Chem.* **1983**, *258*, 199.
15. Lee, R. T.; Lee, Y. C. *Glycoconj. J.* **2000**, *17*, 543.
16. Connolly, D. T.; Townsend, R. R.; Kawaguchi, K.; Bell, W. R.; Lee, Y. C. *J. Biol. Chem.* **1982**, *257*, 939.
17. Lee, R. T.; Lee, Y. C. *Bioconj. Chem.* **1997**, *8*, 762.
18. Biessen, E. A.; Beuting, D. M.; Vietsch, H.; Bijsterbosch, M. K.; Van Berkel, T. J. *J. Hepatol.* **1994**, *21*, 806.
19. Biessen, E. A.; Vietsch, H.; Rump, E. T.; Fluiter, K.; Kuiper, J.; Bijsterbosch, M. K.; van Berkel, T. J. *Biochem. J.* **1999**, *340*, 783.
20. Wu, G. Y.; Wu, C. H. *J. Biol. Chem.* **1991**, *263*, 14621.
21. Hara, T.; Aramaki, Y.; Takada, S.; Koike, K.; Tsuchiya, S. *Gene Ther.* **1995**, *2*, 784.
22. Hara, T.; Aramaki, Y.; Takada, S.; Koike, K.; Tsuchiya, S. *Gene* **1995**, *159*, 167.
23. Hara, T.; Kawasawa, H.; Aramaki, Y.; Takada, S.; Koike, K.; Ishidate, K.; Kato, H.; Tsuchiya, S. *Biochim. Biophys. Acta* **1996**, *1278*, 51.
24. Kawakami, S.; Yamashita, F.; Nishikawa, M.; Takakura, Y.; Hashida, M. *Biochem. Biophys. Res. Commun.* **1998**, *252*, 78.
25. Wong, T. C.; Townsend, R. R.; Lee, Y. C. *Carbohydr. Res.* **1987**, *170*, 27.
26. Kolatkar, A. R.; Weis, W. I. *J. Biol. Chem.* **1996**, *271*, 6679.
27. Kolatkar, A. R.; Leung, A. K.; Isecke, R.; Brossmer, R.; Drickamer, K.; Weis, W. I. *J. Biol. Chem.* **1998**, *273*, 19502.
28. Khorev, O.; Stokmaier, D.; Schwardt, O.; Cutting, B.; Ernst, B. *Bioorg. Med. Chem.* **2008**, *16*, 5216; and references cited therein.
29. Hudgin, R. L.; Pricer, W. E.; Ashwell, G.; Stockert, R. J.; Morell, A. G. *J. Biol. Chem.* **1974**, *249*, 5536.
30. Quesenberry, M. S.; Drickamer, K. *Glycobiology* **1991**, *1*, 615.
31. Park, E. I.; Manzella, S. M.; Baenziger, J. U. *J. Biol. Chem.* **2003**, *278*, 4597.
32. Lee, R. T. *Biochem.* **1982**, *21*, 1045.
33. Trunzer, M.; Faller, B.; Zimmerlin, A. *J. Med. Chem.* **2009**, *52*, 329.
34. (a) Tornøe, C. W.; Meldal, M. In *Peptides: The Wave of the Future: Proceedings of the Second International and the Seventeenth American Peptide Symposium*; Lebl, M., Houghten, R. A., Eds.; Springer, 2001; p 263; (b) Tornøe, C. W.; Christensen, C.; Meldal, M. *J. Org. Chem.* **2002**, *67*, 3057.
35. Kolb, H. C.; Sharpless, K. B. *Angew. Chem., Int. Ed.* **2001**, *40*, 2004.
36. Titz, A.; Radic, Z.; Schwardt, O.; Ernst, B. *Tetrahedron Lett.* **2006**, *47*, 2383.
37. Li, H.; Cheng, F.; Duft, A. M.; Adronov, A. *J. Am. Chem. Soc.* **2005**, *127*, 14518.
38. Argentini, M.; dos Santos, D. F.; Weinreich, R.; Hansen, H.-J. *Inorg. Chem.* **1998**, *37*, 6018.
39. Brooke, G. M. *J. Chem. Soc., Perkin Trans. 1* **1974**, 233.
40. Kotsuki, H.; Araki, T.; Miyazaki, A.; Iwasaki, M.; Datta, P. K. *Org. Lett.* **1999**, *1*, 499.
41. Wolfe, J. P.; Wagaw, S.; Buchwald, S. L. *J. Am. Chem. Soc.* **1996**, *118*, 7215.
42. Huang, X.; Anderson, K. W.; Zim, D.; Jiang, L.; Klapars, A.; Buchwald, S. L. *J. Am. Chem. Soc.* **2003**, *125*, 6653.
43. Fornstedt, N.; Porath, J. *FEBS Lett.* **1975**, *57*, 187.
44. Weitz-Schmidt, G.; Stokmaier, D.; Scheel, G.; Nifant'ev, N. E.; Tuzikov, A. B.; Bovin, N. V. *Anal. Biochem.* **1996**, *238*, 184.
45. Thoma, G.; Magnani, J. L.; Oehrlein, R.; Ernst, B.; Schwarzenbach, F.; Duthaler, R. O. *J. Am. Chem. Soc.* **1997**, *119*, 7414.
46. Gestwicki, J. E.; Hsieh, H. V.; Pitner, J. B. *Anal. Chem.* **2001**, *73*, 5732.
47. Dalvit, C.; Flocco, M.; Knapp, S.; Mostardini, M.; Perego, R.; Stockman, B. J.; Veronesi, M.; Varasi, M. *J. Am. Chem. Soc.* **2002**, *124*, 7702.
48. Lepre, C. A.; Moore, J. M.; Peng, J. W. *Chem. Rev.* **2004**, *104*, 3641.
49. Coombs, P. J.; Taylor, M. E.; Drickamer, K. *Glycobiology* **2006**, *16*, 1C.
50. Li, M.; Kurata, H.; Itoh, N.; Yamashina, I.; Kawasaki, T. *J. Biol. Chem.* **1990**, *265*, 11295.
51. Nakamura, K.; Funakoshi, H.; Miyamoto, K.; Tokunaga, F.; Nakamura, T. *Biochem. Biophys. Res. Commun.* **2001**, *280*, 1028.
52. Hoyle, G. W.; Hill, R. L. *J. Biol. Chem.* **1988**, *263*, 7487.
53. Wu, J.; Nantz, M. H.; Zern, M. A. *Front. Biosci.* **2002**, *7*, d717.
54. Tarasiejska, Z.; Jeanloz, R. W. *J. Am. Chem. Soc.* **1958**, *80*, 6325.
55. Bradford, M. M. *Anal. Biochem.* **1976**, *72*, 248.
56. Polson, P.; Coetzer, T.; Kruger, J.; von Maltzahn, E.; van der Merwe, K. *J. Immin. Invest.* **1985**, *14*, 323.
57. Hajduk, P. J.; Olejniczak, E. T.; Fesik, S. W. *J. Am. Chem. Soc.* **1997**, *119*, 12257.
58. Hwang, T.-. L.; Shaka, A. J. *J. Magn. Reson. Ser. A* **1995**, *112*, 275.

EXHIBIT 7

US006172045B1

(12) United States Patent
Theodore et al.

(10) Patent No.: US 6,172,045 B1
(45) Date of Patent: *Jan. 9, 2001

(54) **CLUSTER CLEARING AGENTS**

(75) Inventors: **Louis J. Theodore**, Lynnwood; **Donald B. Axworthy**, Brier, both of WA (US)

(73) Assignee: **NeoRx Corporation**, Seattle, WA (US)

(*) Notice: This patent issued on a continued prosecution application filed under 37 CFR 1.53(d), and is subject to the twenty year patent term provisions of 35 U.S.C. 154(a)(2).

Under 35 U.S.C. 154(b), the term of this patent shall be extended for 0 days.

This patent is subject to a terminal disclaimer.

(21) Appl. No.: **08/659,761**

(22) Filed: **Jun. 6, 1996**

Related U.S. Application Data

(63) Continuation-in-part of application No. 08/350,551, filed on Dec. 7, 1994, now Pat. No. 6,075,010.

(51) **Int. Cl.**[7] **A01N 43/04**; A61K 31/70

(52) **U.S. Cl.** **514/24**; 514/23; 514/25

(58) **Field of Search** 424/178.1; 514/23, 514/24, 25, 53, 54, 61, 62

(56) **References Cited**

U.S. PATENT DOCUMENTS

4,179,337		12/1979	Davis et al. .
4,358,439		11/1982	Sieber et al. .
4,410,688		10/1983	Denkewalter et al. .
4,507,466		3/1985	Tomalia et al. .
4,678,667		7/1987	Meares et al. .
4,732,863		3/1988	Tomasi et al. .
4,863,713		9/1989	Goodwin et al. .
4,902,502		2/1990	Nitecki et al. .
4,904,481		2/1990	Fathman et al. .
4,923,985		5/1990	Gansow et al. .
5,089,261		2/1992	Nitecki et al. .
5,141,966		8/1992	Poratli .
5,183,660		2/1993	Ikeda et al. .
5,215,927		6/1993	Berenson et al. .
5,256,395		10/1993	Barbet et al. .
5,281,698		1/1994	Nitecki .
5,342,940		8/1994	Ono et al. .

FOREIGN PATENT DOCUMENTS

031 303		7/1981	(EP) .
0251494		1/1988	(EP) .
0451824		10/1991	(EP) .
0496074		7/1992	(EP) .
519 554		12/1992	(EP) .
8900427	*	3/1989	(GB) .
8910140		11/1989	(WO) .
WO 89/10140		11/1989	(WO) .
9012050		10/1990	(WO) .
WO 92/12730		8/1992	(WO) .
9514493	*	6/1993	(WO) .
WO 93/15210		8/1993	(WO) .
9325240	*	12/1993	(WO) .
WO 94/04702		3/1994	(WO) .
WO 94/11398		5/1994	(WO) .
9515978	*	6/1995	(WO) .
WO 95/15770		6/1995	(WO) .
WO 95/15979		6/1995	(WO) .

OTHER PUBLICATIONS

Axworthy et al., "Antibody Pretargeting For Radioimmunotherapy: A Three–Step Approach In Tumored Nude Mice," *The Journal Of Nuclear Medicine*; Proceedings Of The 39th Annual Meeting 33: p. 880, Abstract No. 234, 1992.

Sanderson et al., "Preparation And Characterization Of Biotin Conjugates Of Anti–Pan–Carcinoma NR–LU–10 Monoclonal Antibody For A Three Step Radioimmunotherapy," *The Journal Of Nuclear Medicine*; Proceedings Of The 39th Annual Meeting 33: p. 880, Abstract No. 233, 1992.

Schmidt et al., "Synthesis of peptide alkaloids. 5. New method for synthesis of ansa peptides. Amino acids and peptides. 34," *J. Org. Chem. 47*(17):3261–3264, 1982.

Abuchowski et al., "Alteration of Immunological Properties of Bovine Serum Albumin by Covalent Attachment of Polyethylene Glycol," *J. of Biological Chem. 252*(11):3578–3581, 1997.

Abuchowski et al., "Cancer Therapy with Chemically Modified Enzymes. I. Antitumor Properties of Polyethylene Glycol–Asparaginase Conjugates," *Can. Biochem. Biophys. 7*:175–186, 1984.

Basch et al., in *Journal of Immunological Methods 56*:269–280, 1983.

Beauchamp et al., "A New Procedure for the Synthesis of Polyethylene Glycol–Protein Adducts; Effects on Function, Receptor Recognition, and Clearance of Superoxide Dismutase, Lactoferrin, and α_2–Macroglobulin," *Analytical Biochem 131*:25–33, 1983.

Bodenmuller et al., in *Embo J. 5*(8):1825–9, 1986.

Boehringer Mannheim Catalog—1991, pp. 49–59.

Chen et al., "Properties of Two Urate Oxidases Modified by the Covalent Attachment of Poly (ethylene Glycol)," *Biochemica et Biophysica Acta 660*:293–298, 1981.

Davis et al., "Alteration of the circulating life and antigenic properties of bovine adenosine deaminase in mice by attachment of polyethylene glycol," *Clin. Exp. Immunol. 46*:649–652, 1981.

Goodwin and Hnatowich, Letter to the Editor/Reply, in *J. Nucl. Med. 32*(4):750–751, 1991.

(List continued on next page.)

Primary Examiner—Patricia A. Duffy
(74) *Attorney, Agent, or Firm*—Seed Intellectual Property Law Group PLLC

(57) **ABSTRACT**

Cluster clearing agents (CCAs) and the use thereof are discussed. CCAs are composed of a hepatic clearance directing moiety which directs the biodistribution of a CCA-containing construct to hepatic clearance; and a binding moiety which mediates binding of the CCA to a compound for which rapid hepatic clearance is desired.

8 Claims, 16 Drawing Sheets

OTHER PUBLICATIONS

Goodwin et al., "Pharmacokinetics of Biotin–Chelate Conjugates for Pretargeted Avidin–Biotin Immunoscintigraphy," *J. Nucl. Med.*, p. 880, Abstract No. 232, 1992.

Green, "The Use of [^{14}C] Biotin for Kinetic Studies and for Assay," *Biochem. J. 89*:585, 1963.

Hnatowich et al., "Investigations of Avidin and Biotin for Imaging Applications," 28(8):1294–1302, 1987.

Hubbard et al., "Suppression of the Anti–DNP IgE Response with Tolerogenic Conjugates of DNP with Polyvinyl Alcohol," *J. of Immunology 126*(2), 1981.

Kalofonos et al., "Imaging of Tumor in Patients with Indium–111–Labeled Biotin and Streptavidin–Conjugated Antibodies: Preliminary Communication," *J. Nucl. Med. 31*(11):1791–1796, 1990.

Koch and Macke, "^{99m}Tc Labeled Biotin Conjugate in a Tumor 'Pretargeting' Approach with Monoclonal Antibodies," *Angew. Chem. Intl. Ed. Engl. 31*(11):1507 1509, 1992.

Krull et al., "Solid–phase derivatization reactions for biomedical liquid chromatography," *J. Chromatography B: Biomedical Applications 659*:19–50, 1994.

Lee et al., "Abrogation of the Antibenzylpencilloyl (BPO) IgE Response with BPO–Polyvinyl Alcohol Conjugates," *Int. Archs Allergy appl. Immun. 63*:1–13, 1980.

Lee et al., "New Synthetic Cluster Ligands for Galactose/N–Acetylgalactosamine–Specific Lectin of Mammalian Liver," *Biochemistry 23*:4255–4261, 1984.

Lee et al., "Suppresion of Reaginic Antibodies with Modified Allergens," *Int. Arch Allergy appl. Immun. 63*:1–13, 1980.

Leonard et al., "Synthesis of monomethoxypolyoxyethylene–Bound haemoglobins," *Tetrahedron 40*(9):1581–1584, 1984.

Ling et al., "A General Study of the Binding and Seperation in Partition Affinity Ligand Assay. Immunoassay of β_2–Microglobulin," *J. Immunological Methods 59*:327–337, 1983.

Mattes, J., "Biodistribution of Antibodies After Intraperitoneal or Intravenous Injection and Effect of Carbohydrate Modifications," 79(4):855–863, 1987.

Mauk et al., "Targeting of lipid vesicles: Specificity of carbohydrate receptor analogues for leukocytes in mice," *Proc. Natl. Acad. Sci. USA 77*:4430–4434, 1980.

Mauk et al., "Vesicle Targeting: Timed Release and Specificity for Leukocytes in Mice by Subcutaneous Injection," *Science 207*(18), 1980.

Paganelli et al., "Intraperitoneal Radio–Localization of Tumors Pre–Targeted by Biotinylated Monoclonal Antibodies," *Int J. Cancer 45*:1184–1189, 1990.

Paganelli et al. "Monoclonal Antibody Pretargeting techniques for Tumour Localization: The Avidin–Biotin System," *Nuclear Medicine Communications 121*:211–234, 1991.

Pierce Biochemicals, in *Immunotechnology 1*, 1990.

Ponpipom et al., "Cell Surface carbohydrates for targeting studies," 58:214, 1980.

Ponpipom et al., "Cell–Specific Ligands for Selecting Drug Delivery to Tissues and Organs," *J. Med. Chem. 24*(12):1388–1395, 1981.

Rosario et al., "Bolton–Hunter and Biotin Derivatized Polylysine: A New Multi–Valent Peptide Reagent for In Vivo Pre–Targeting with Streptavidin Conjugates," *J. Nucl. Med. 32*(5):p. 993, Abstract No. 356, 1991.

Rosebrough, "Plasma Stability and Pharmacokinetics of Radio–Labeled Deferoxamine–Biotin Derivatives" *J. Nucl. Med.*, p. 880, Abstract No. 235, 1992.

Savoca et al., "Preparation of a Non–Immunogenic Arginase by the Covalent Attachment of Polyethylene Glycol," *Biochemica et Biophysica Acta 578*:47–53, 1979.

Schnaar et al., "Adhesion of Chicken Hepatocytes to Polycrylamide Gels Derivatized with N–Acetylglucosamine," *Journal of Biological Chemistry 253*(21):7940–7951, 1978.

Schulling, H. et al., "Design of Compounds Having Enhanced Tumour Uptake, Using Serum Albumin as a Carrier, Part 2," *Nucl. Med. Biol. 19*:6, 685–695, 1992.

Sharon and Lis, "Carbohydrates in Cell Recognition," *Scientific American 268*(1):82–89, 1993.

Sheldon et al., "Targeting of [^{111}In] Biocytin to Cultured Ovarian Adenocarcinoma Cells Using Covalent Monoclonal Antibody–Streptavidin Conjugates," *Appl. Radiat. Isot. 43*(11):1399–1402, 1992.

Sigma Catalogue—1984, p. 250.

Sinn, H. et al., "Design of Compounds Having an Enhanced Tumour Uptake, Using Serum Albumin as a Carrier, Part 1," *Nucl. Med. Biol. 17*:8, 819–827, 1990.

Tolleshaug, "Binding and Internalization of Asialoglycoproteins by Isolated Rat Hepatocytes," *Int. J. Biochem. 13*:45–51, 1981.

Virzi et al., "The Preparation and Evaluation of 12 Biotin Derivatives Labeled with Tc–99M," *J. Nucl. Med.*, 920, Abstract No. 403, 1992.

Weigel, "Endocytic Components: Identification and Characterization," *Subcellular Biochemistry*, vol. 19, Chapter 5, Endocytosis and Function of the Hepatic Asialoglycoprotein Receptor, edited by Bergeron et al., New York, pp. 125–161, 1993.

Weigel, "GlycoConjugates Composition, Structure and Function," Chapter 14, Mechanisms and Control of Glycoconjugate Turnover, edited by Allen et al, Marcel Dekker, Inc., NY, pp 421–497, 1992.

Sprengard et al Bioorganic and Medicinal Chemistry Letters 6(5) 509–514 (1996).

Doris A. Wall et al., The Galactose–Specific Recognition System of Mammalian Liver: the Route of Ligand Internalization in Rat Hepatocytes, *Cell 25*, 79–93, Aug. 1980.

Yuan Chuan Lee et al., 2–Imino–2–methoxyethyl 1–Thioglycosides: New Reagents for Attaching Sugars to Proteins, *Biochemistry 15*:18, 3956–3962, 1976.

Mark J. Krantz et al., Attachment of Thioglycosides to Proteins: Enhancement of Liver Membrane Binding, *Biochemistry 15*:18, 3963–3968, 1976.

Peter van der Sluijs et al., Drug Targeting to the Liver with Lactosylated Albumins: Does Glycoprotein Target the Drug or Is the Drug Targeting the Glycoprotein?, *Hepatology 6*::4, 723–728, 1986.

Anatol G. Morell et al., the Role of Sialic Acid in Determining the Survival of Glycoproteins in the Circulation, *Journal of Biological Chemistry 246*:5, 1461–1467, 1971.

G. Galli et al., A Radiopharmaceutical for the Study of the Liver: ^{99m}Tc–DTPA–Asialo–Orosomucoid, *The Journal of Nuclear Medicine and Allied Sciences*, 110–116, Apr.–Jun. 1988.

S.K. Sharma et al., Inactivation and clearance of an anti–CEA carboxypeptidase G2 conjugate in blood after localisation in a xenograft model, *Br. J. Cancer 61*, 659–662, 1990.

Robert W. Jansen et al., Hepatic Endocytosis of Various Types of Mannose–terminated Albumins, *The Journal of Biological Chemistry 266*:5, 3343–3348, 1991.

D. A. Goodwin et al., New Methods for Localizing Infection: A Role for Avidin–Biotin?, *The Jounral of Nuclear Medicine 33*:10, 1816–1818, Oct. 1992.

David A. Goodwin et al., Pretargeted Immunoscintigraphy: Effect of Hapten Valency on Murine Tumor Uptake, *The Journal of Nuclear Medicine 33*:11, 2006–2103, Nov. 1992.

Paul F. Sieving et al., Preparation and Characterization of Paramagnetic Polychelates and Their Protein Conjugates, *Bioconjugate Chem 1*, 65–71, 1990.

G. Paganelli et al., Monoclonal antibody pretargeting techniques for tumour localization: the avidin–biotin system, *Nuclear Medicine Communications 12*, 211–234, 1991.

David R. Vera et al., Tc–99m Galactosyl–Neoglycoalbumin: In Vitro Characterization of Receptor Mediated Binding, *J Nucl Med 25*:7, 779–787, 1984.

Jean Haensler et al., Synthesis and Characterization of a Trigalactosylated Bisacridine Compound to Target DNA to Hepatocytes, *Bioconjugate Chem. 4*, 85–93, 1993.

C. Wu et al., Investigations of N–linked Macrocycles for ^{111}In and ^{90}Y Labeling of Proteins, *Nucl. Med. Biol, 19*:2, 239–244, 1992.

Paul H. Weigel, Endocytosis and Function of the Hepatic Asialoglycoprotein Receptor, *Endocytosis and Functin of GalNAc Receptor*, Chapter 5,125–161.

Reiko T. Lee, New Synthetic Cluster Ligands for Galactose/N–Acetylgalactosamine–Specific Lectin of Mammalian Liver, *Biochemistry 23*, 4255–4261, 1984.

Erik A. L. Biessen et al., Synthesis of Cluster Galatosides with High Affinity for the Hepatic Asialoglycoprotein Receptor, *J. Med. Chem. 38*, 1538–1546, 1995.

June Rae Merwin et al., Targeted Delivery of DNA Using YEE(GalNAcAH)$_{X\beta}$, a Synthetic Glycopeptide Ligand for the Asialoglycoprotein Receptor, *Bioconjugate Chem. 5*, 612–620, 1994.

Mark A. Findeis, Stepwise systhesis of a GalNAc–containing cluster glycoside ligand of the asialoglycoprotein receptor, *Int. J. Peptide Protein Res. 43*, 477–485, 1994.

Reiko T. Lee et al., Preparation of Cluster Glycosides of N–Acetylgalactosamine That Have Subnanomolar Binding Constants Towards the Mammalian Hepatic Gal/GalNAc–specific Receptor, *Glycoconjugate J 4*, 317–328, 1987.

Timothy D. McKee et al., Preparation of Asialoorosomucoid–Polylysine Conjugates, *Bioconjugate Chem. 5*, 306–311, 1994.

Samar E. Makhlouf et al., Antisera Specificities to β–D–Galactopyranoside Cluster Ligands, *Carbohydrate Research 132*, 93–103, 1984.

A.S. Chaudhari et al., Coupling of Amino Acids and Amino Sugars with Cyanuric Chloride (2,4,6–Trichloro–s–triazine)[1], *Canadian Journal of Chemistry 50*:13, 1987–1990, Jul. 1, 1972.

Paul H. Weigel, Mechanisms and Control of Glycoconjugate Turnover, *Glycoconjugatges*, Chapter 14, 421–497, 1992.

Christian Plank et al., Gene Transfer into Hepatocytes Using Asialoglycoprotein Receptor Mediated Endocytosis of DNA Complexed with an Artificial Tetra–Antennary Galactose Ligand, *Bioconjugate Chem. 3*, 533–539, 1992.

* cited by examiner

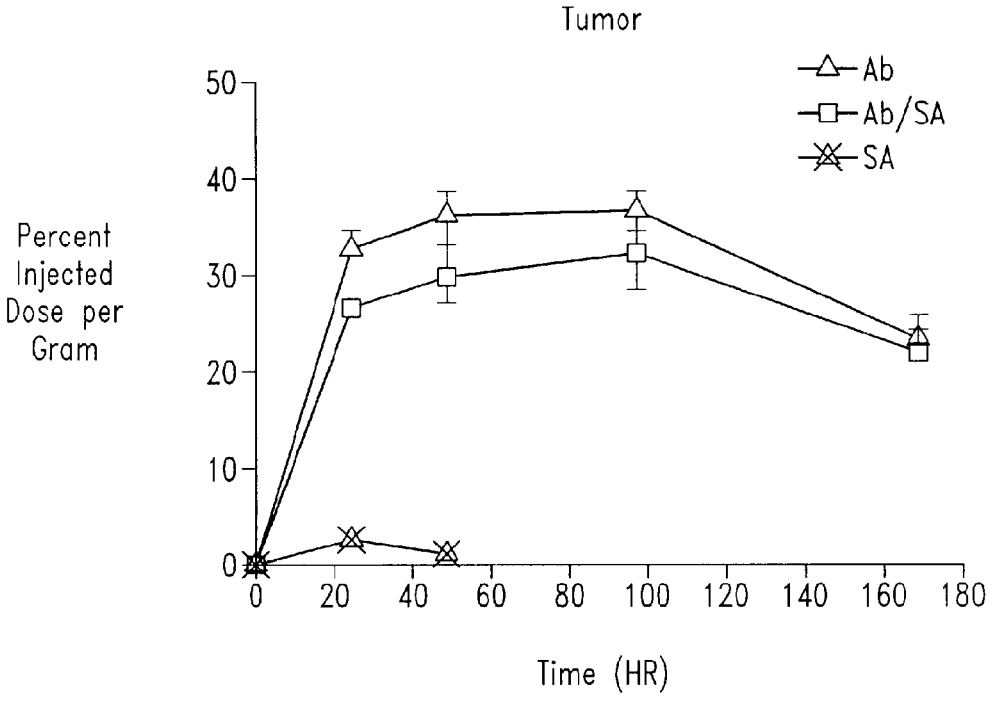
Tumor
Ab
Ab/SA
SA
Percent Injected Dose per Gram
50
40
30
20
10
0
0
20
40
60
80
100
120
140
160
180
Time (HR)

Fig. 1

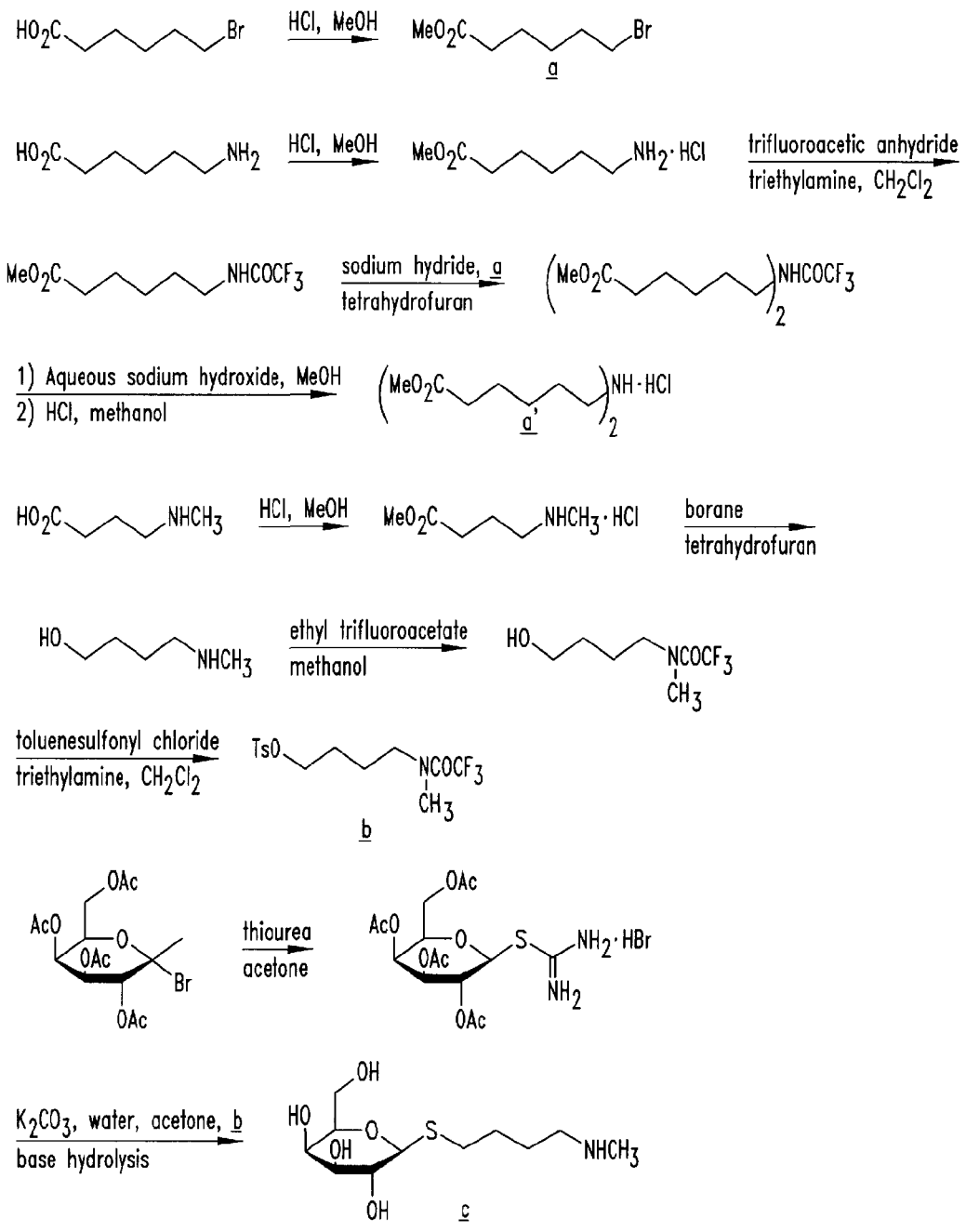
HO2C
Br
HCl, MeOH
MeO2C
Br
a
HO2C
NH2
HCl, MeOH
MeO2C
NH2·HCl
trifluoroacetic anhydride
triethylamine, CH2Cl2
MeO2C
NHCOCF3
sodium hydride, a
tetrahydrofuran
(MeO2C
NHCOCF3)2
1) Aqueous sodium hydroxide, MeOH
2) HCl, methanol
(MeO2C
NH·HCl)2
a'
HO2C
NHCH3
HCl, MeOH
MeO2C
NHCH3·HCl
borane
tetrahydrofuran
HO
NHCH3
ethyl trifluoroacetate
methanol
HO
NCOCF3
CH3
toluenesulfonyl chloride
triethylamine, CH2Cl2
TsO
NCOCF3
CH3
b
AcO
OAc
O
OAc
Br
OAc
thiourea
acetone
AcO
OAc
O
OAc
S
NH2·HBr
NH2
OAc
K2CO3, water, acetone, b
base hydrolysis
HO
OH
O
OH
S
NHCH3
OH
c

Fig. 2A

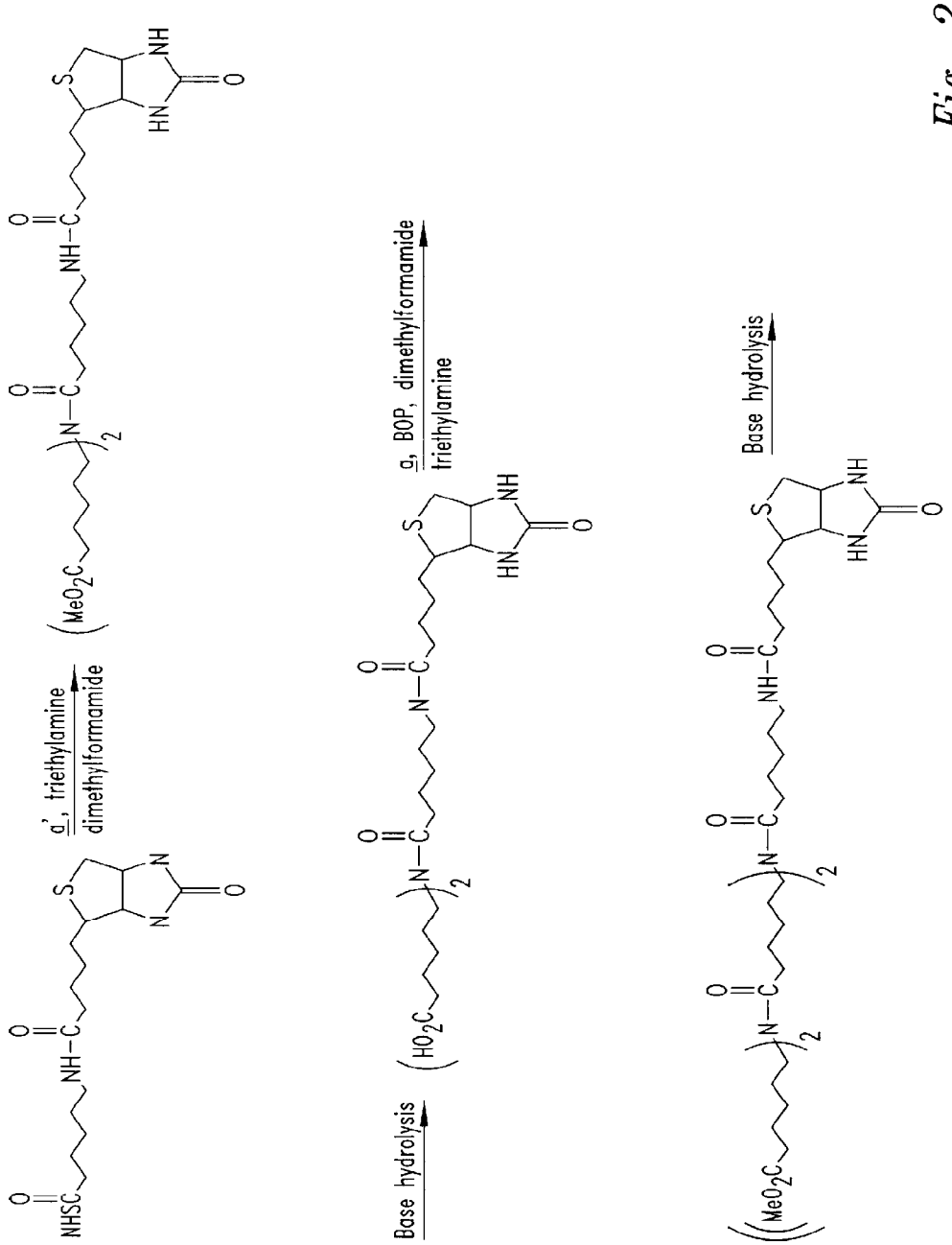

Fig. 2B

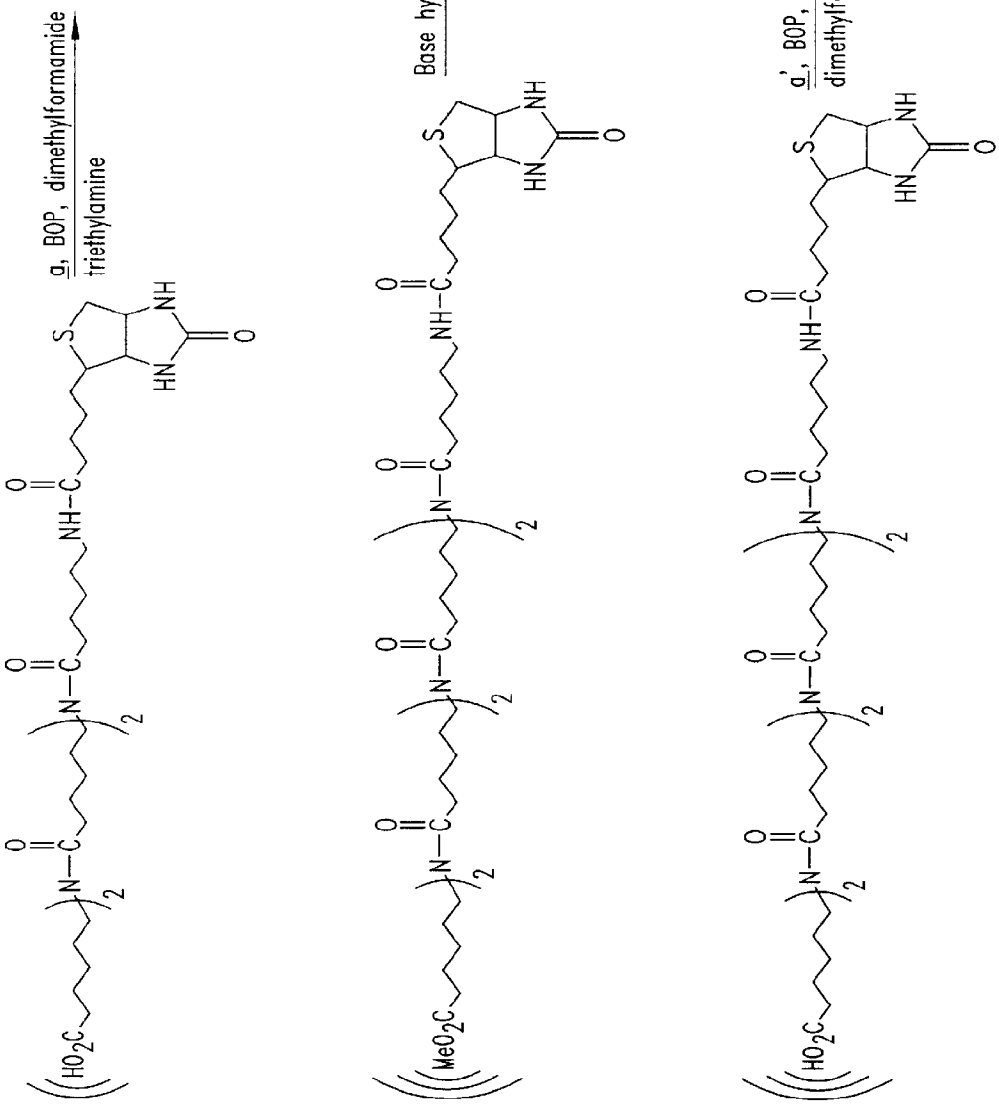

Fig. 2B (Continued)

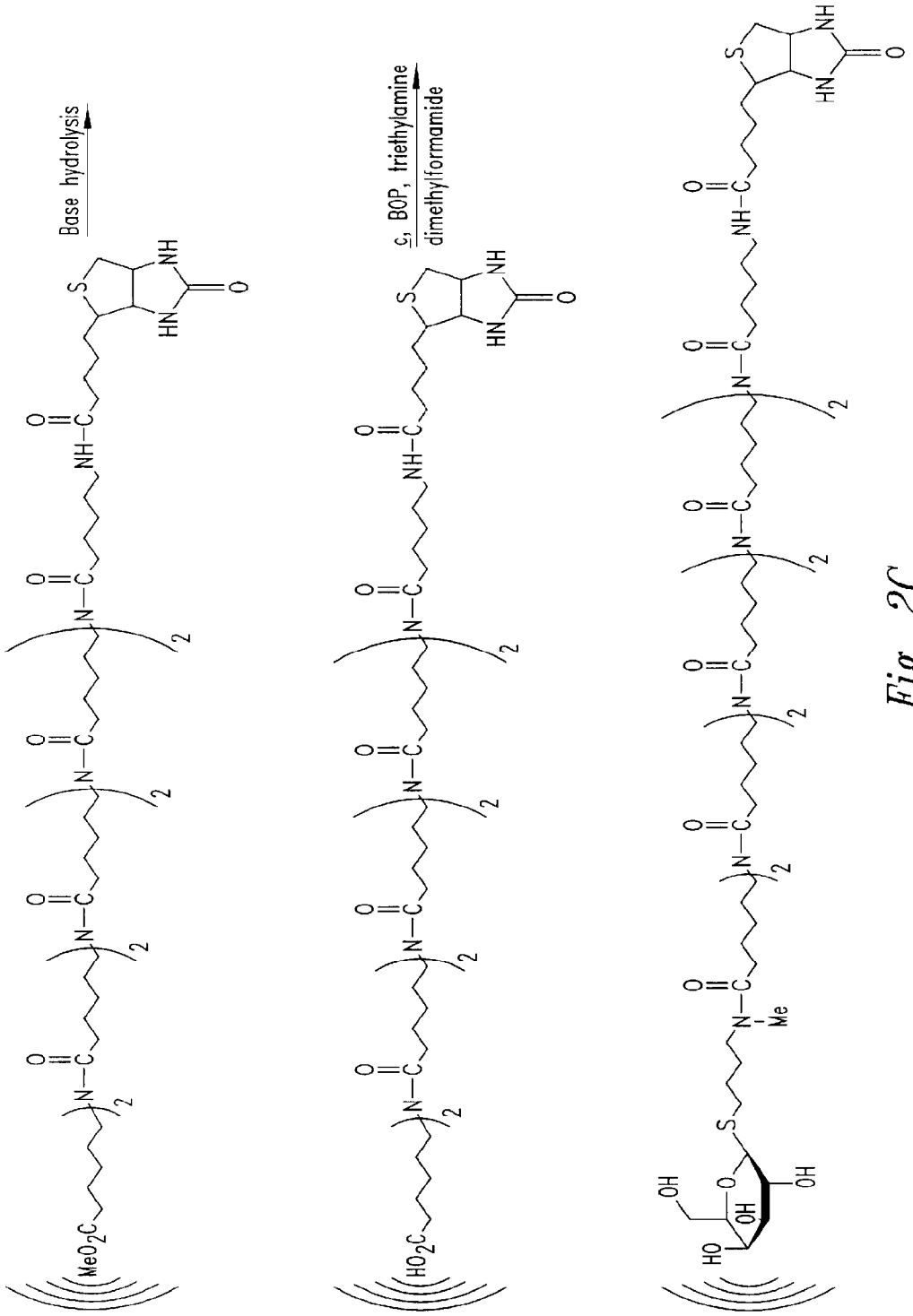

Fig. 2C

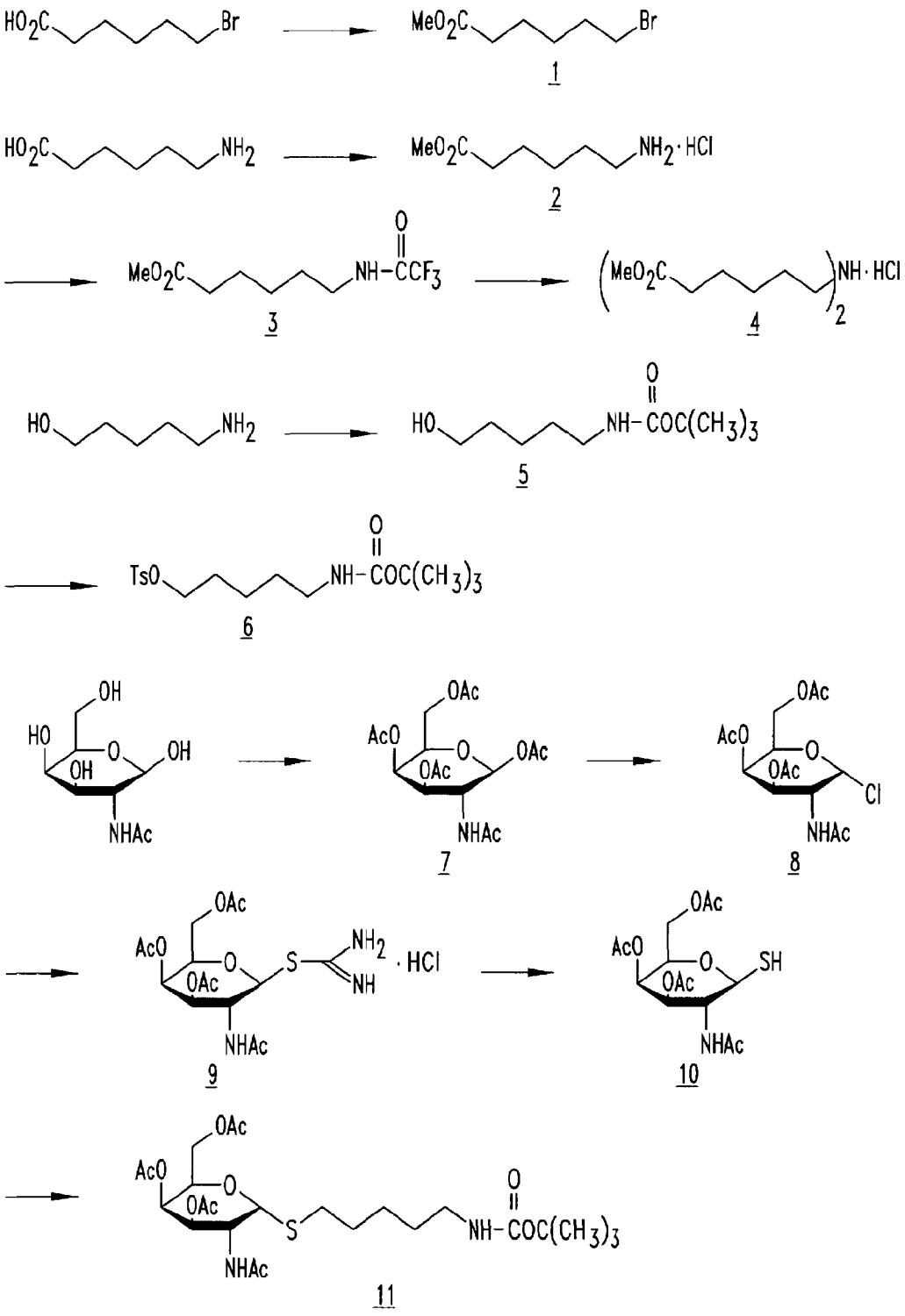
HO2C
Br
MeO2C
Br
1
HO2C
NH2
MeO2C
NH2·HCl
2
MeO2C
NH-CCF3
3
MeO2C
NH·HCl
2
4
HO
NH2
HO
NH-COC(CH3)3
5
TsO
NH-COC(CH3)3
6
HO
OH
OH
OH
NHAc
7
AcO
OAc
OAc
OAc
NHAc
8
AcO
OAc
OAc
Cl
NHAc
AcO
OAc
OAc
S
NH2
NH
·HCl
NHAc
9
AcO
OAc
OAc
SH
NHAc
10
AcO
OAc
OAc
S
NH-COC(CH3)3
NHAc
11

Fig. 3A

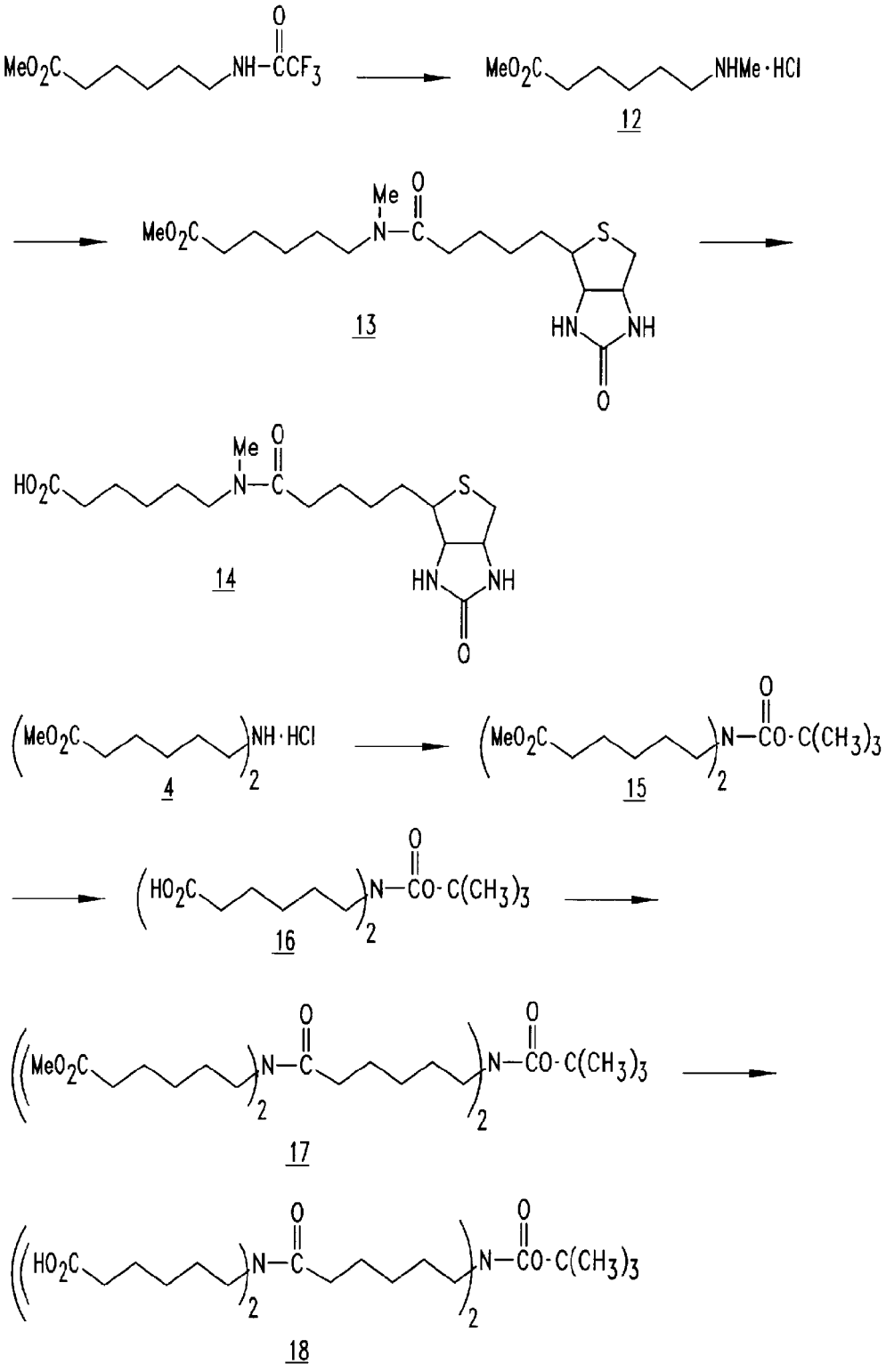
MeO2C
NH–CCF3
NHMe·HCl
12
Me
13
HO2C
14
NH·HCl
4
N–CO·C(CH3)3
15
16
17
18

Fig. 3B

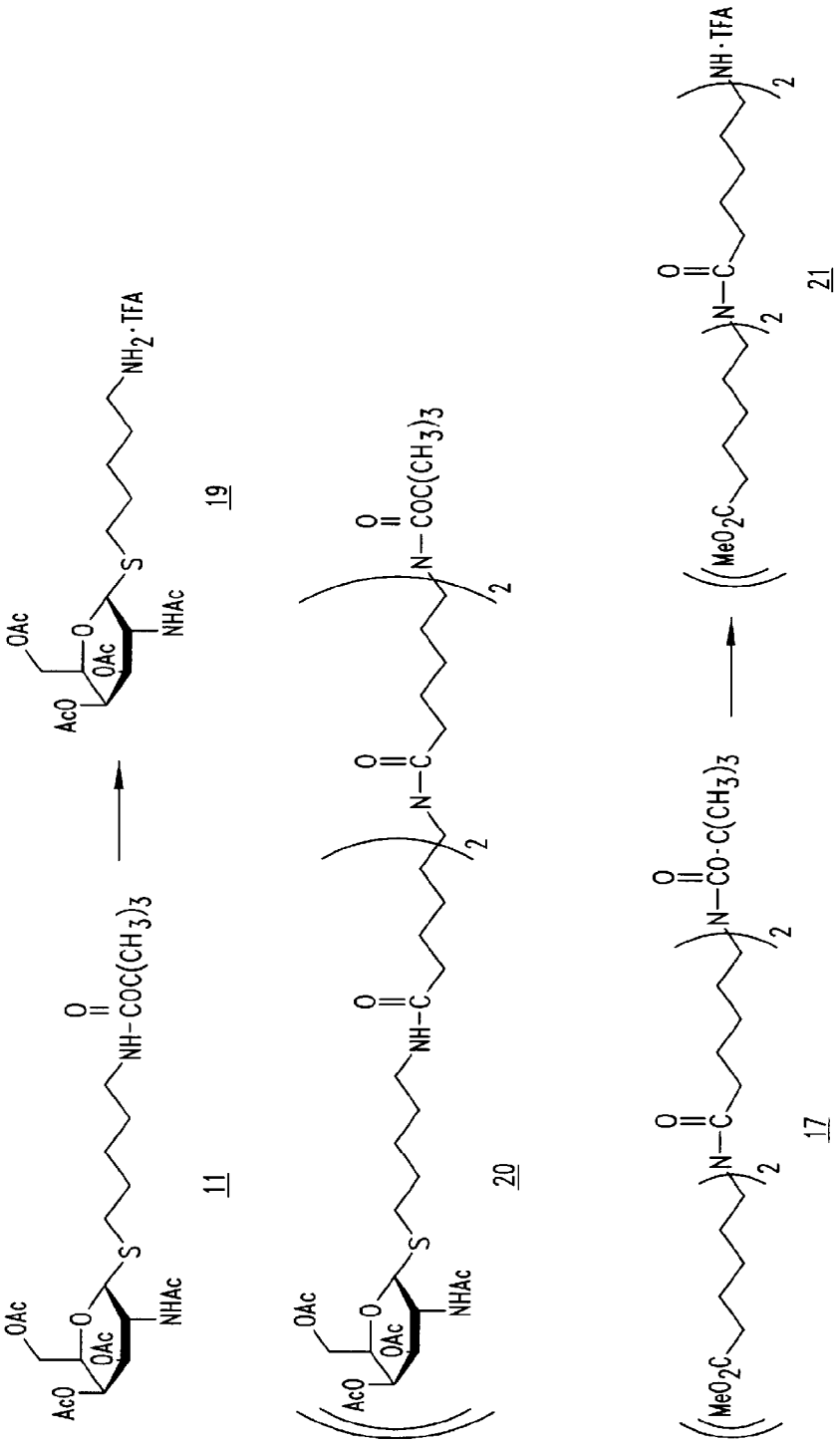
OAc
AcO
OAc
O
S
NHAc
NH-COC(CH3)3
O
11
NH2·TFA
19
20
N-COC(CH3)3
NH-C
MeO2C
NH·TFA
21
17
N-CO·C(CH3)3

Fig. 3C

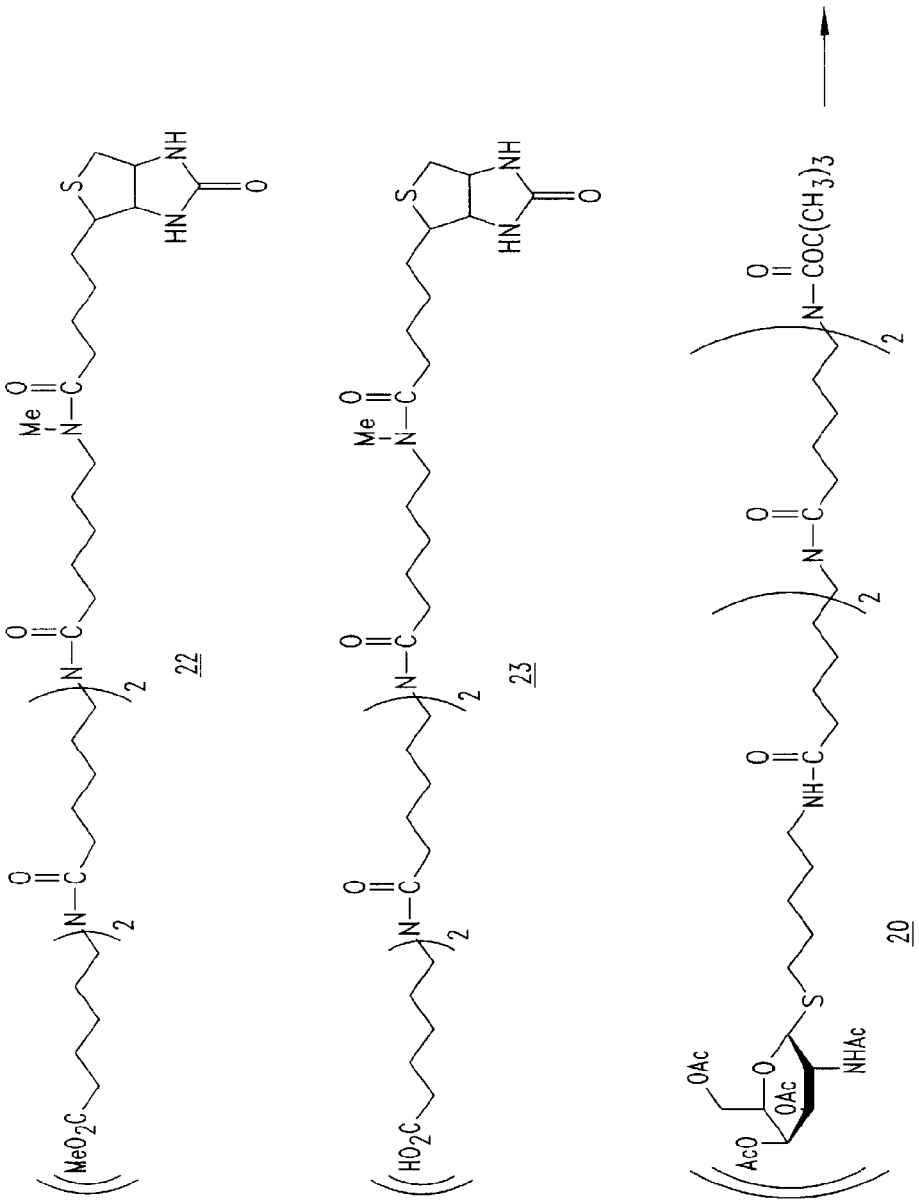

Fig. 3D

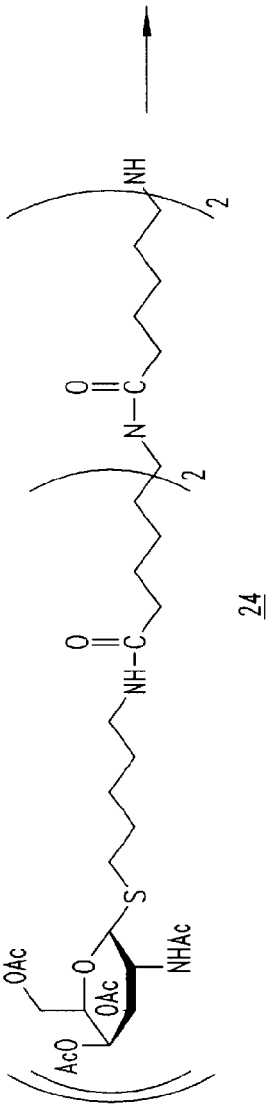

24

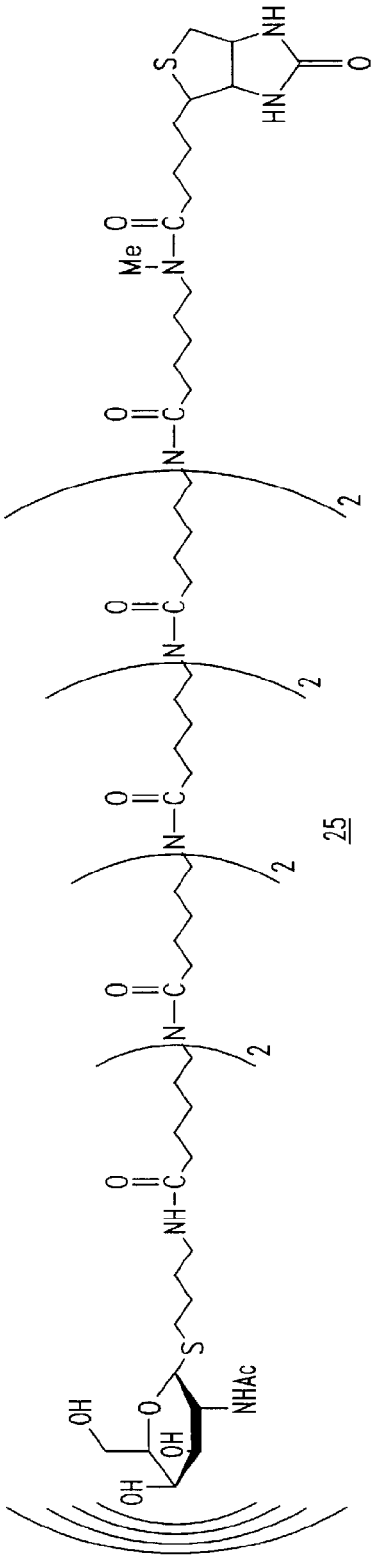

25

Fig. 3E

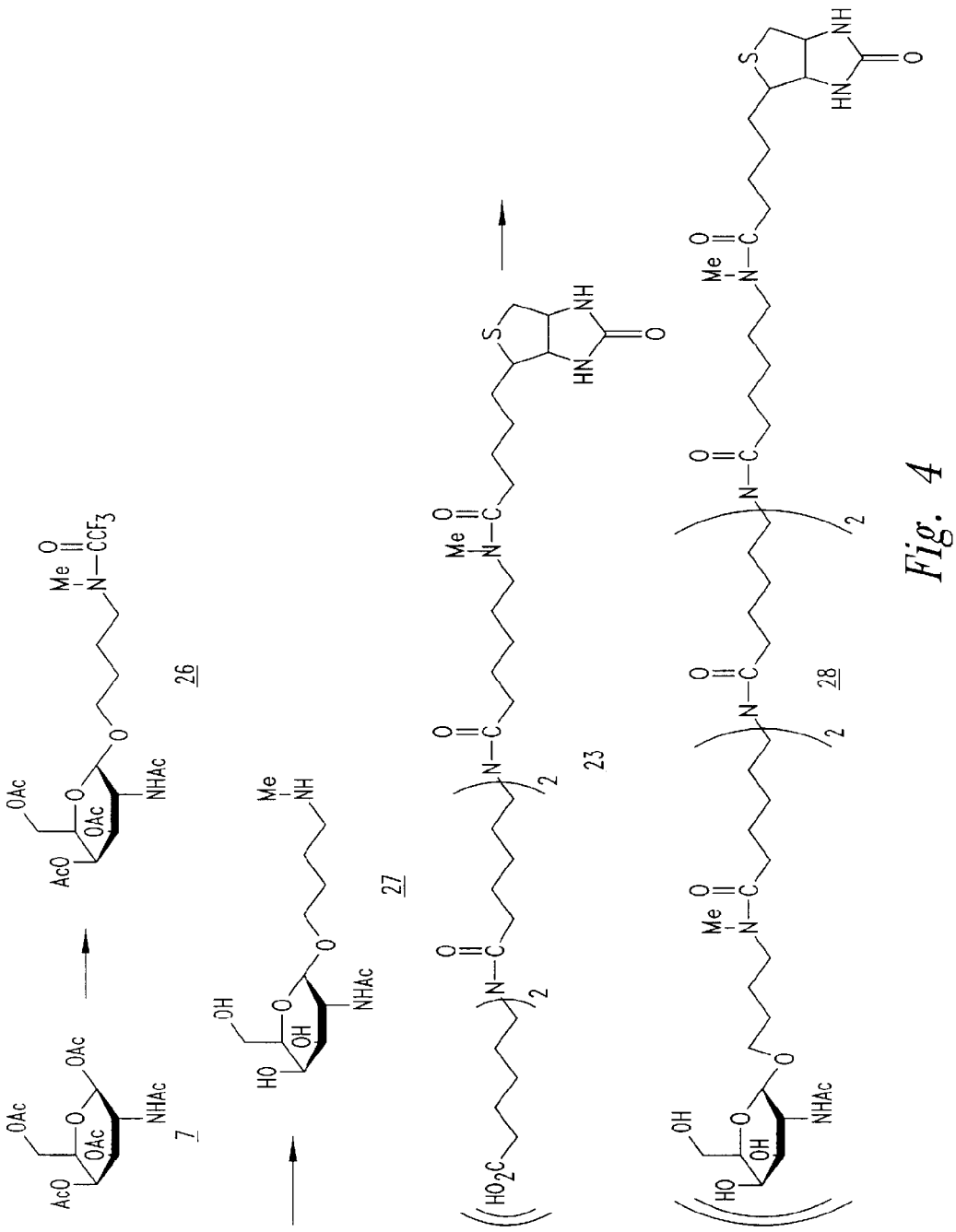

Fig. 4

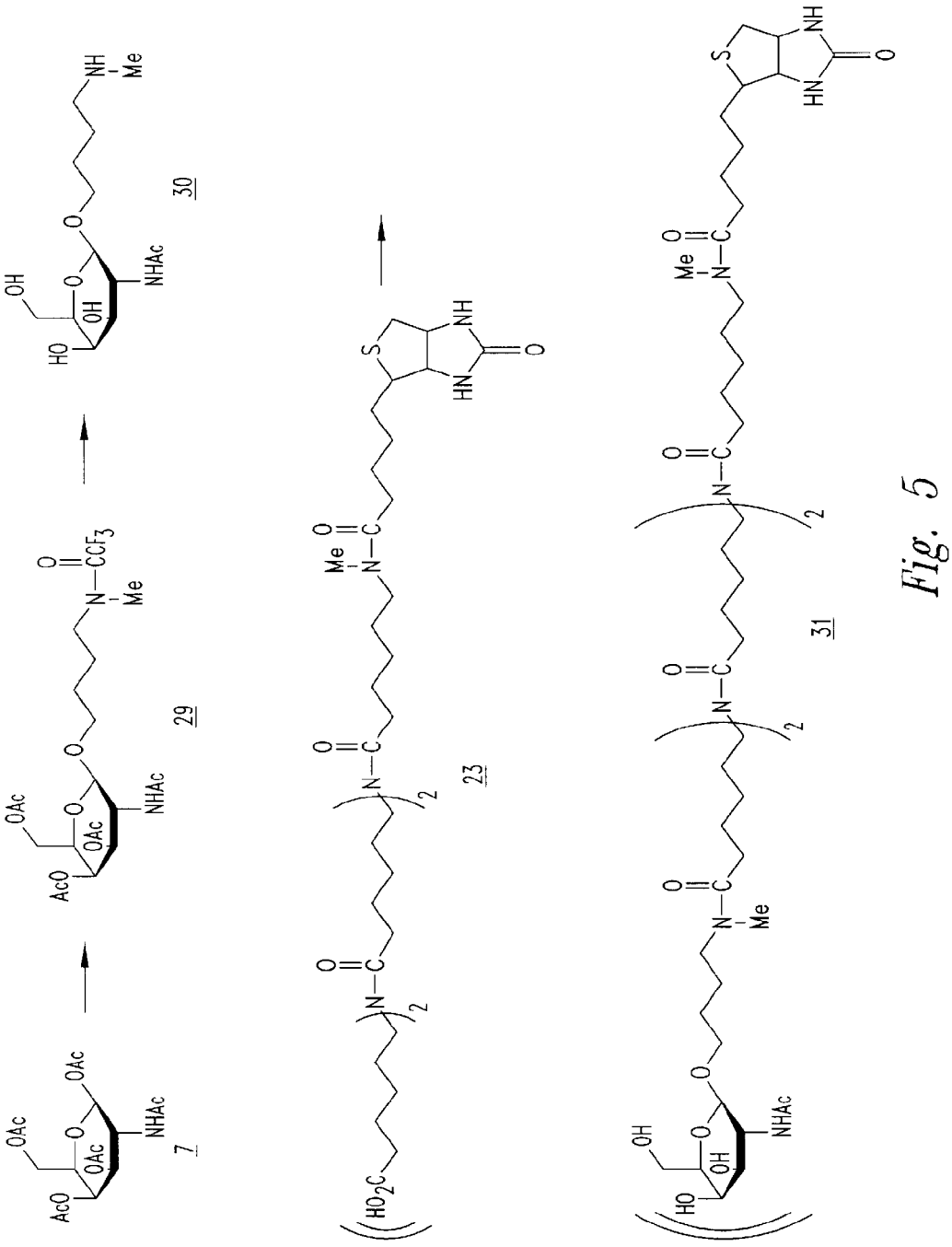

Fig. 5

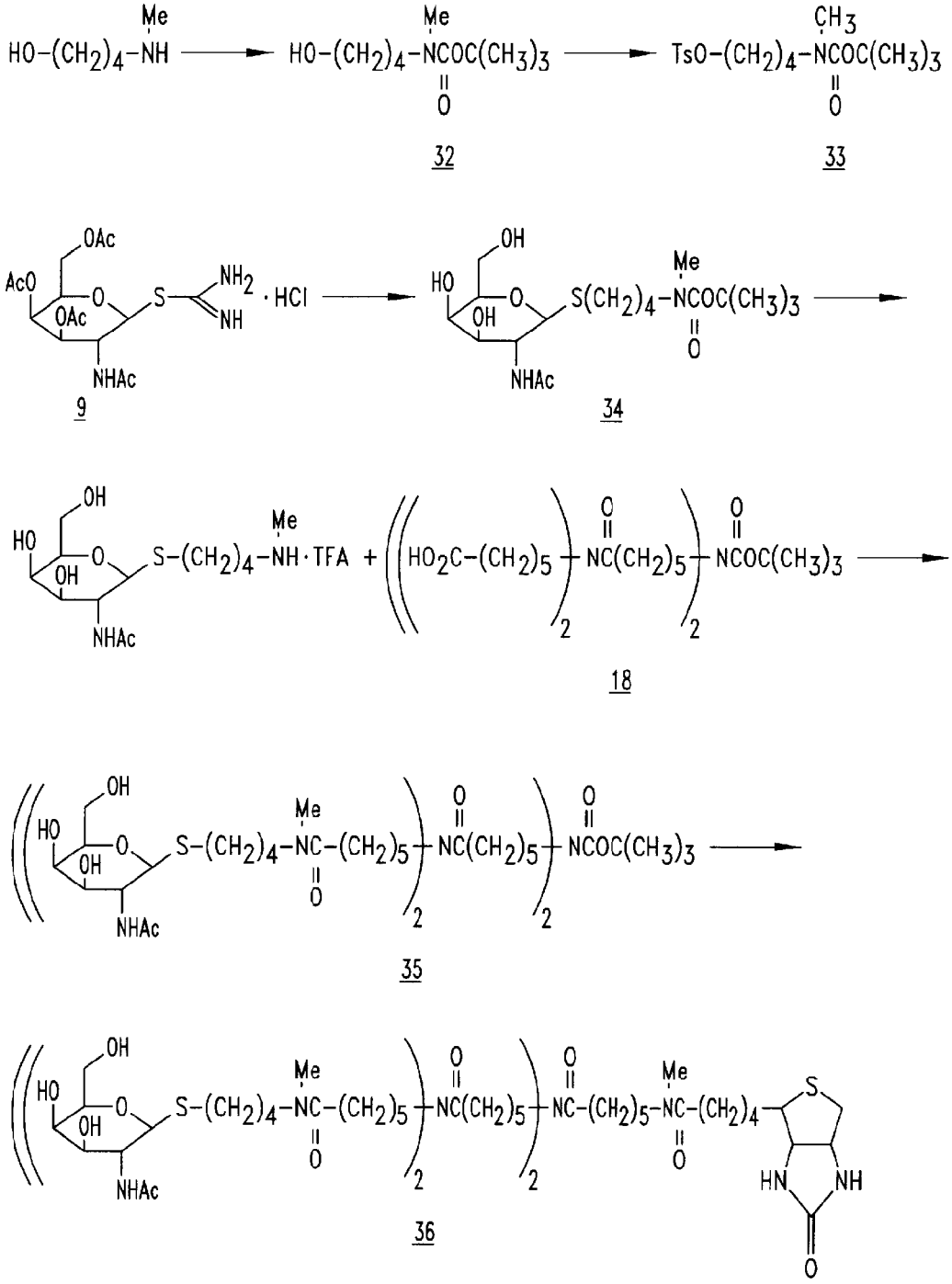
HO-(CH2)4-NH
Me
HO-(CH2)4-NCOC(CH3)3
TsO-(CH2)4-NCOC(CH3)3
CH3
32
33
AcO
OAc
NHAc
9
· HCl
HO
S(CH2)4-NCOC(CH3)3
34
S-(CH2)4-NH · TFA
HO2C-(CH2)5
NC(CH2)5
NCOC(CH3)3
18
S-(CH2)4-NC-(CH2)5
35
HN
NH
36

Fig. 6

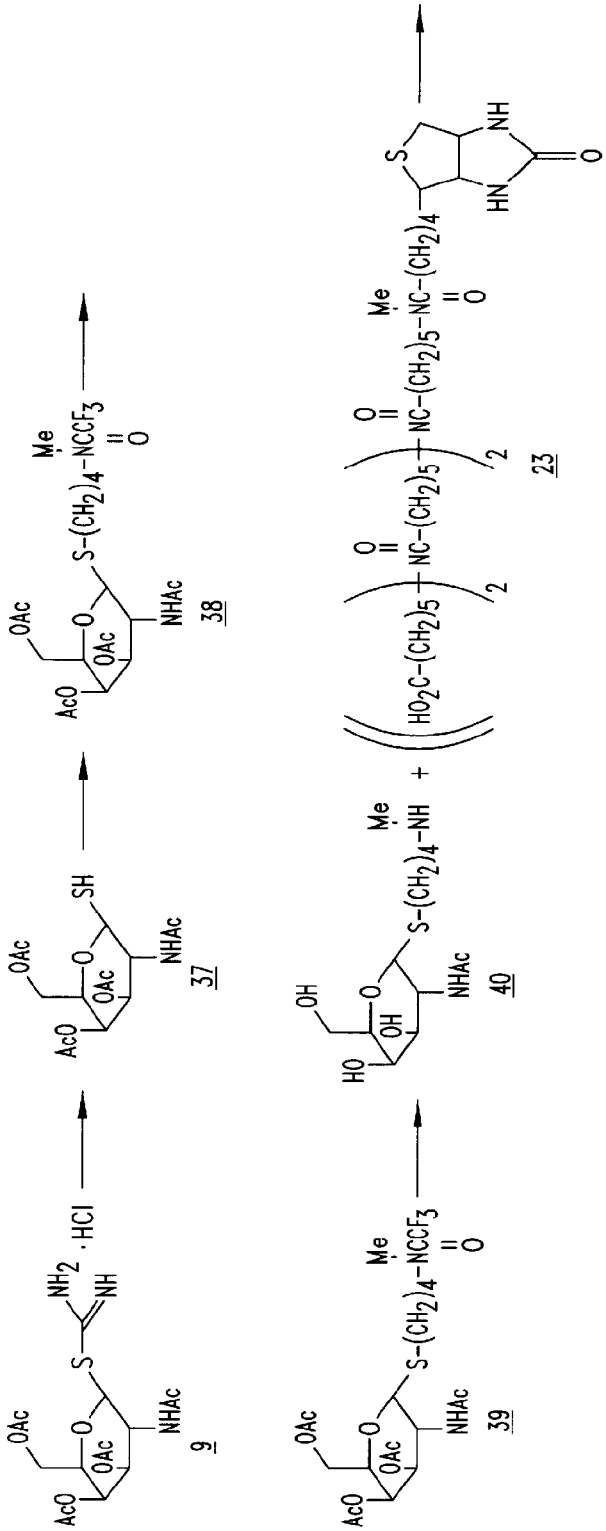

Fig. 7

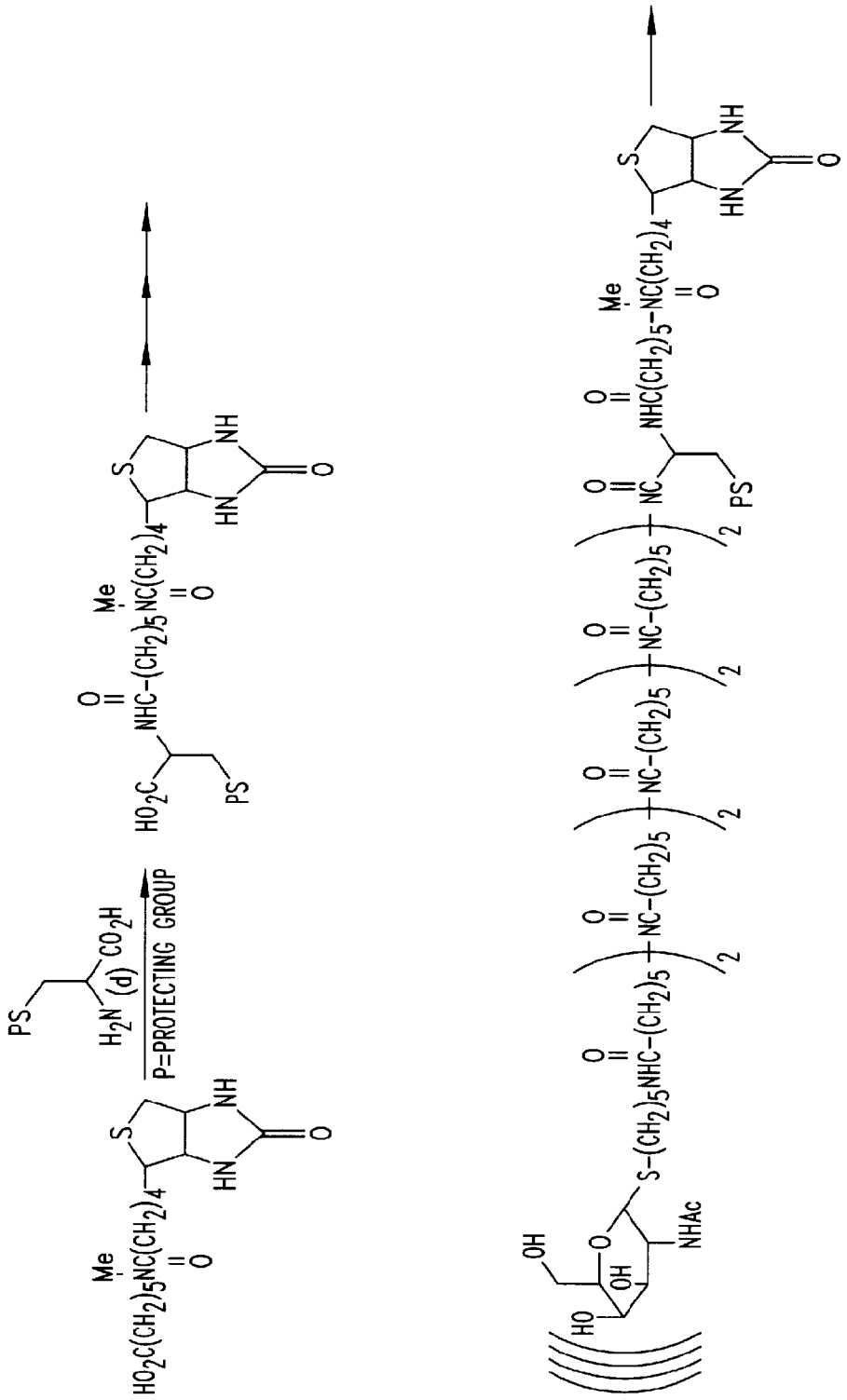
PS
H2N (d) CO2H
P=PROTECTING GROUP
HO2C(CH2)5NC(CH2)4
Me
O
NH
HN
S
O
HO2C
PS
NHC-(CH2)5NC(CH2)4
Me
O
NHC(CH2)5-NC(CH2)4
Me
O
NC
PS
2
NC-(CH2)5
S-(CH2)5NHC-(CH2)5
NHAc
OH
HO

Fig. 8

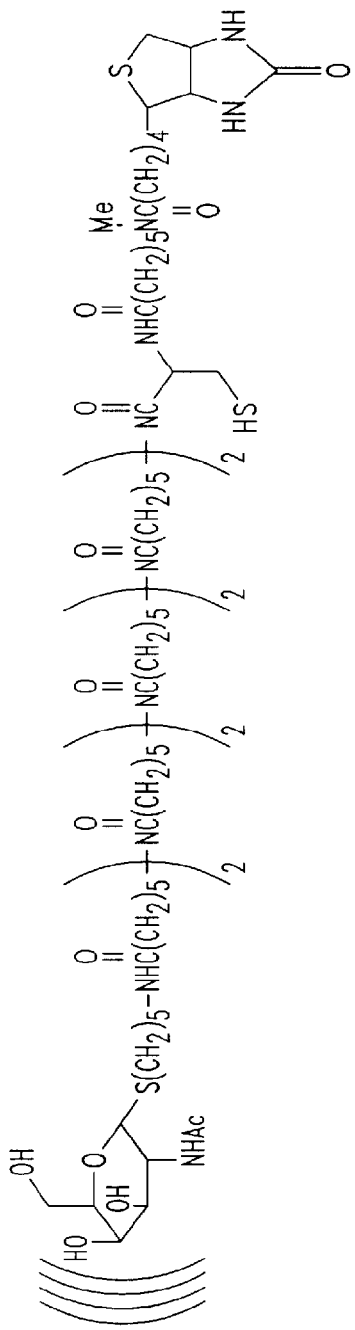

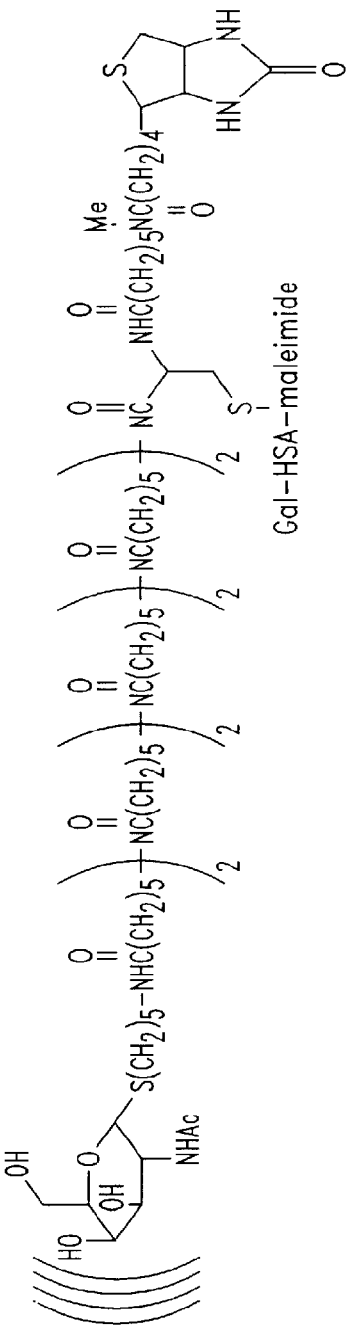

Fig. 8 (Continued)

CLUSTER CLEARING AGENTS

CROSS-REFERENCE TO RELATED APPLICATIONS

This application is a continuation-in-part of U.S. application Ser. No. 08/350,551, filed Dec. 7, 1994 now U.S. Pat. No. 6,075,010 for PRETARGETING METHODS AND COMPOUNDS.

TECHNICAL FIELD

The present invention relates to cluster clearing agents (CCAs), reagents for the preparation thereof and associated methods and compositions. CCAs impact the elimination and biodistribution of constructs that incorporate or become associated with such agents in a manner resulting in increased elimination via a hepatic route. The CCA-associated constructs also generally exhibit a decreased serum half-life in comparison to counterpart compounds which do not incorporate or become associated with CCAs.

BACKGROUND OF THE INVENTION

Conventional cancer therapy is limited by the problem that the generally attainable targeting ratio (ratio of administered dose of active agent localizing to tumor versus administered dose circulating in blood) is low. This limitation is generally encountered in systemic administration of chemotherapeutic agents as well as in administration of monoclonal antibody-active agent conjugates. Systemic administration involves exposure of healthy tissue to the active agent. Also, as a result of the relatively long half life of a monoclonal antibody, non-target tissue is exposed to circulating antibody-active agent conjugate. Improvement in targeting ratio is therefore sought.

A method employed to improve targeting ratio is referred to generally as pretargeting. In pretargeting, a targeting moiety is formed of a targeting agent and a receptor. The active agent is associated with a ligand for the receptor. The targeting moiety is administered to a recipient, and permitted to localize to the target site with binding at that site mediated by the targeting agent. When target site localization and sufficient elimination of circulating targeting moiety is achieved by the recipient's metabolism, the active agent-ligand is administered. The ligand component of the construct binds to the pretargeted receptor, thereby delivering the active agent to the target.

Pretargeting is made more efficient by administration of a clearing agent to facilitate elimination of circulating targeting moiety. Various clearing agents have been disclosed. Galactose-human serum albumin (HSA)-biotin clearing agents have been employed in pretargeting protocols employing a monoclonal antibody-streptavidin targeting moiety and a biotin-active agent construct. Such clearing agents are discussed in PCT/US93/05406. Derivatization by galactose facilitates elimination of complexes of monoclonal antibody-streptavidin-biotin-HSA-galactose via Ashwell receptors in the liver. These clearing agents rapidly decrease circulating monoclonal antibody-streptavidin levels in patients. Since pretargeting methods are enhanced using clearing agents, improvements in such clearing agents are sought.

SUMMARY OF THE INVENTION

The present invention is directed to low molecular weight cluster clearing agents (CCAs) which meet certain performance criteria and are amenable to scale up for commercial production. Preferred CCAs of the present invention preferably exhibit one or more of the following characteristics:

- rapid, efficient complexation with serum-associated targeting moiety-ligand (or anti-ligand) conjugate in vivo;
- rapid clearance from the blood of serum-associated targeting moiety conjugate capable of binding a subsequently administered complementary anti-ligand or ligand containing molecule;
- high capacity for clearing (or inactivating) large amounts of serum-associated targeting moiety conjugate; and
- low immunogenicity.

In addition, CCAs of the present invention are preferably capable of achieving circulating targeting moiety clearance without compromising the binding potential of the pretargeted targeting moiety, either directly by binding of the CCA thereto or indirectly by binding of CCA metabolites thereto. The present invention also contemplates CCAs of defined chemistry to facilitate characterization, manufacturing and quality control. The CCAs of this invention are also designed to be effective over a broad dose range to avoid the desirability of extensive dose optimization. The present invention further provides CCAs of increased efficiency in clearance of circulating targeting moiety.

Preferred CCAs of present invention incorporate (1) a cluster hepatic clearance directing moiety; and (2) a binding moiety incorporating a member of a ligand/anti-ligand pair or a lower affinity form thereof. The cluster hepatic clearance directing moiety is composed of a cluster of sugar residues arranged on a cluster backbone and mediates hepatic clearance of the CCA via recognition of the sugar clusters by a hepatocyte receptor. The ligand or anti-ligand binding moiety facilitates binding to targeting moiety-ligand/anti-ligand conjugate. Preferably, CCAs of the present invention range in molecular weight from between about 1,000 and about 20,000 daltons, more preferably from about 2,000 to 16,000daltons. Such preferred CCAs generally incorporate between about 4 and about 32 sugar residues, with about 16 sugar residues more preferred.

More preferred CCAs of the present invention are characterized by one or more of the following:

- Unnatural orientation of ligand (e.g., 1-biotin) and anti-ligand (e.g., streptavidin formed from d-amino acids);
- Secondary amide connecting a sugar residue to the cluster backbone of the CCA;
- High affinity sugar for binding to the Ashwell receptor (e.g., N-acetylgalactosamine);
- Orientation for sugar attachment (e.g., alpha-orientation sugar attachment is generally preferred for N-acetylgalactosamine hexoses, and beta-orientation sugar attachment is generally preferred for galactose hexoses);
- Appropriate linking atom for sugar attachment (e.g., sulfur linker atoms are generally preferred with regard to metabolic stability of CCAs);
- Optimized spacer between the linker atom and the nitrogen atom of the amide connecting the sugar residue to the cluster backbone of the CCA;

Tertiary amine adjacent to the ligand or anti-ligand component to enhance in vivo stability of the CCA; and

Extended linker between the cluster backbone and the ligand or anti-ligand to improve the bioavailability of said ligand or anti-ligand.

CCAs of the present invention may also be employed to remove toxic or potentially toxic moieties from a recipient's circulation or extravascular space. In this embodiment, the CCA comprises a hepatic clearance directing moiety and a binding moiety capable of recognizing a component or an epitope associated with the toxic or potentially toxic moieties.

Another embodiment of the present invention is a CCA-protein clearing agent. For example, HSA may be derivatized with one or more CCAs, preferably 1 or 2 CCAs, and optionally derivatized by hexose residues. By virtue of the synthetic nature of the CCA and the methylated amide bond(s) incorporated in the linker/extender between the cluster and their binding moiety, the CCA is resistant to metabolic degradation. Consequently, any CCA-biotin metabolites of this proteinaceous clearing agent are likely to be retained n liver hepatocytes.

BRIEF DESCRIPTION OF THE DRAWINGS

FIG. **1** illustrates the tumor uptake profile of antibody-streptavidin conjugate (Ab/SA) and control profiles of native whole antibody (Ab) and streptavidin (SA).

FIGS. **2***a*, **2***b* and **2***c* schematically depict the preparation of a sixteen galactose cluster-biotin CCA.

FIGS. **3***a*, **3***b*, *3c*, **3***d* and **3***e* schematically depict the preparation of a sixteen N-acetyl-galactosamine (alpha-S) cluster-biotin CCA (compound 25).

FIG. **4** schematically depicts the preparation of a four N-acetyl-galactosamine (alpha-O) cluster-biotin CCA (compound 28).

FIG. **5** schematically depicts the preparation of a four n-acetyl-galactosamine (beta-O) cluster-biotin CCA (compound 31).

FIG. **6** schematically depicts the preparation of a four N-acetyl-galactosamine (beta-S) cluster-biotin CCA (compound 36).

FIG. **7** schematically depicts the preparation of a four N-acetyl-galactosamine (alpha-S) cluster-biotin CCA (compound 41).

FIG. **8** schematically depicts the preparation of a CCA-protein clearing agent of the present invention.

DETAILED DESCRIPTION OF THE INVENTION

Prior to setting forth the invention, it may be helpful to set forth definitions of certain terms to be used within the disclosure.

Targeting moiety: A molecule that binds to a defined population of cells. The targeting moiety may bind a receptor, an oligonucleotide, an enzymatic substrate, an antigenic determinant, or other binding site present on or in the target cell population. Antibody is used throughout the specification as a prototypical example of a targeting moiety. Tumor is used as a prototypical example of a target in describing the present invention.

Ligand/anti-ligand pair: A complementary/anti-complementary set of molecules that demonstrate specific binding, generally of relatively high affinity. Exemplary ligand/anti-ligand pairs include zinc finger protein/dsDNA fragment, enzyme/inhibitor, hapten/antibody, lectin/carbohydrate, ligand/receptor, S-protein/S-peptide, head activator protein (which binds to itself), cystatin-C/cathepsin B, and biotin/avidin. Biotin/avidin is used throughout the specification as a prototypical example of a ligand/anti-ligand pair.

Anti-ligand: As defined herein, an "anti-ligand" demonstrates high affinity, and preferably, multivalent binding of the complementary ligand. Preferably, the anti-ligand is large enough to avoid rapid renal clearance, and is multivalent to bind a greater number of ligands. Univalent anti-ligands are also contemplated by the present invention. Anti-ligands of the present invention may exhibit or be derivatized to exhibit structural features that direct the uptake thereof, e.g., galactose residues that direct liver uptake. Avidin and streptavidin are used herein as prototypical anti-ligands.

Avidin: As defined herein, "avidin" includes avidin, streptavidin and derivatives and analogs thereof that are capable of high affinity, multivalent or univalent binding of biotin.

Ligand: As defined herein, a "ligand" is a relatively small, soluble molecule that binds with high affinity by anti-ligand and preferably exhibits rapid serum, blood and/or whole body clearance with administered intravenously in an animal or human. Biotin constructs are used as prototypical ligands.

Lower Affinity Ligand or Lower Affinity Anti-Ligand: A ligand or anti-ligand that binds to its complementary ligand-and-ligand pair member with an affinity that is less than the affinity with which native ligand or anti-ligand binds the complementary member. Preferably, lower affinity ligands and anti-ligands exhibit between from about 10^{-6} to 10^{-10}M binding affinity for the native form of the complementary anti-ligand or ligand. For avidin/streptavidin and other extremely high affinity binding molecules, however, lower affinity may range between 10^{-6} to 10^{-13}M. Lower affinity ligands and anti-ligands may be employed in clearing agents of the present invention.

Active Agent: A diagnostic or therapeutic agent ("the payload"), including radionuclides, drugs, anti-tumor agents, toxins and the like. Radionuclide therapeutic agents are used as prototypical active agent. Attachment of such radionuclide active agents to other moieties, either directly or via chelaton technology, may be accomplished as described herein or as known in the art.

Pretargeting: As defined herein, pretargeting involves target site localization of a targeting moiety that is conjugated with one member of a ligand/anti-ligand pair; after a time period sufficient for optimal target-to-non-target accumulation of this targeting moiety conjugate, active agent conjugated to the opposite member of the ligand/anti-ligand pair is administered and is bound (directly or indirectly) to the targeting moiety conjugate at the target site (two-step pretargeting). Three-step and other related methods described herein are also encompassed.

Clearing Agent: An agent capable of binding, complexing or otherwise associating with an administered moiety (e.g.,

targeting moiety-ligand, targeting moiety-anti-ligand or anti-ligand alone) present in the recipient's circulation, thereby facilitating circulating moiety clearance from the recipient's body, removal from blood circulation, or inactivation thereof in circulation. The clearing agent is preferably characterized by physical properties, such as size, charge, reduced affinity, configuration or a combination thereof, that limit clearing agent access to the population of target cells recognized by a targeting moiety used in the same treatment protocol as the clearing agent.

Conjugate: A conjugate encompasses chemical conjugates (covalently or non-covalently bound), fusion proteins and the like.

Cluster Clearing Agent (CCA): A moiety capable of directing the clearance of a moiety to which it is bound upon administration or of a component to which it becomes associated with in vivo. CCAs of the present invention direct clearance via a hepatic pathway. Preferred CCAs of the present invention are characterized by a cluster hepatic clearance directing moiety and a binding moiety such as a ligand, an anti-ligand or a lower affinity derivative thereof. Preferred cluster hepatic clearance directing moieties are attached to the binding moiety via a single point of attachment.

Cluster Hepatic Clearance Directing Moiety: A plurality of sugar residues preferably arranged in a branched configuration along a cluster backbone in a manner in which the sugar residues are recognized by a hepatocyte receptor. Hepatic clearance directing moieties preferably contain from 3 to about 100 sugar residues, with from 3 to about 50 sugar residues preferred. Preferably, he branching network consists of two or three pronged branches, i.e., consists of 2, 4, 8, 16, 32 or 64 sugar residues or consists of 3, 9, 27, or 81 sugar residues. Two branched structures with 8, 16 or 32 sugar residues are more preferred as cluster hepatic clearance directing moieties of the present invention.

Cluster Backbone: A chemical framework to which sugar residues are bound. Preferably, the cluster backbone is formed of repetitive bifunctional units configured in a two or three pronged branching arrangement. Preferably he branching structure is iterative, such that 2-pronged units form 4, 8, 16, 32, etc, hexose bearing CCAs and 3-pronged units form 9, 27, 81, etc. hexose bearing CCAs. Aminocaproyl ($HOOC—(CH_2)_5—NH_2$) units are set forth herein as prototypical building blocks of cluster backbones, wherein the nitrogen atom provides the two-pronged attachment with the hydrogen atoms displaced by the formation of amide bonds. Other moieties useful as cluster backbone components are those bearing trivalent, tetravalent or higher valency atoms. The cluster is formed by derivatization of the available site son such trivalent, tetravalent or higher valency atoms. For example, nitrogen is trivalent, and therefore iterative, two-branched CCAs can be constructed with nitrogen bearing moieties, such as $HOOC—(CH_2)_n—NH_2$, wherein n is between from about 3 and about 8, heterobifunctional PEG structures, such as $HOOC—CH_2—(O(CH_2)_2)_nO(CH_2)_2—NH_2$, $HOOC—(CH_2)_2—(O(CH_2)_2)_nO(CH_2)_2—NH_2$ where n ranges from 1 to 5, and the like. Carbon is tetravalent, and therefore iterative, three-branched CCAs can be constructed with carbon bearing moieties, such as that described herein. Alternative base atoms and cluster backbone structures can be used, and skilled chemists are capable of identifying and synthesizing appropriate structures.

Binding Moiety: A ligand, anti-ligand or other moiety capable of in vivo association with a previously administered molecule (bearing the complementary ligand or anti-ligand, for example) or with another toxic or potentially toxic molecule present in the recipient's circulation or extravascular fluid space via recognition by the binding moiety of an epitope associated with the previously administered moiety or with the toxic or potentially toxic molecule.

The CCAs of the present invention are preferably employed in pretargeting protocols. "Two-step" pretargeting procedures feature targeting moiety-ligand or targeting moiety-anti-ligand (targeting moiety-receptor) administration, followed by administration of active agent conjugated to the opposite member of the ligand-anti-ligand pair. As step "1.5" in the two-step pretargeting methods of the present invention, a CCA is administered to facilitate the clearance of circulating targeting moiety-receptor conjugate.

In the two-step pretargeting approach, the clearing agent preferably does not become bound to the target cell population, either directly or through the previously administered and target cell bound targeting moiety-anti-ligand or targeting moiety-ligand ligand conjugate. An example of two-step pretargeting involves the use of biotinylated human transferrin as a clearing agent for avidin-targeting moiety conjugate, wherein the size of the clearing agent results in liver clearance of transferrin-biotin-circulating avidin-targeting moiety complexes and substantially precludes association with the avidin-targeting moiety conjugates bound at target cell sits. (See, Goodwin, D. A. , *Antibod. Immunoconj. Radiopharm.,* 4:427–34, 1991).

CCAs of the present invention contain a cluster hepatic clearance directing moiety and a binding moiety. Thus, CCAs of the present invention are bispecific in that the cluster hepatic clearance directing moiety mediates binding with the molecule to be cleared. These bispecific CCAs are capable of in vivo binding or association with molecules to be cleared and interaction with hepatic receptors to effect clearance of CCA-containing constructs by that route. Preferred CCAs of the present invention are suitable for use as a clearing agent in pretargeting protocols, including two step protocols.

Clearing agents useful in the practice of the present invention preferably exhibit one or more of the following characteristics:

- rapid, efficient complexation with serum-associated targeting moiety-ligand (or anti-ligand) conjugate in vivo;
- rapid clearance from the blood of serum-associated targeting moiety conjugate capable of binding a subsequently administered complementary anti-ligand or ligand containing molecule;
- high capacity for clearing (or inactivating) large amounts of serum-associated targeting moiety conjugate; and
- low immunogenicity.

Clearing agents previously developed by the assignee of this patent application, incorporated human serum albumin (HSA), a plurality of hexoses and a plurality of ligands, as follows:

$(Hexose)_m—Human\ Serum\ Albumin\ (HSA)—(Ligand)_n$, wherein n is an integer from 1 to about 10 and m is an integer

from 1 to about 45 and wherein the hexose is recognized by a liver receptor (e.g., Ashwell receptors).

The exposed hexose residues direct the clearing agent to rapid clearance by endocytosis into the liver through specific receptors therefor. These receptors bind the clearing agent or clearing agent-containing complexes, and induce endocytosis into the hepatocyte, leading to fusion with a lysosome and recycle of the receptor back to the cell surface. This clearance mechanism is characterized by high efficiency, high capacity and rapid kinetics. The rapid kinetics of hexose-mediated liver uptake, coupled with a relatively high affinity interaction between the binding moiety, such as a ligand, and the compound to be cleared, provide for rapid and efficient clearance, facilitating the use of intermediate or low molecular weight clearing agents such as the CCAs of the present invention.

CCAs of the present invention are designed to meet the four criteria set forth above as well. Three additional performance criteria were instituted for CCAs:

metabolic stability in at least one of the following physiological environments, serum, urine and liver;

low ability to compromise pretargeted receptor; and

chemically defined structure.

Preferred CCAs may be characterized as small molecule clearing agents with regard to molecular weight (less than about 20,000 daltons) and structural homogeneity. More preferred CCAs or small molecule clearing agents, composed of biotin or a lower affinity biotin analog and a branched multi-sugar residue cluster hepatic clearance directing moiety, have utility for the clearance of streptavidin- or avidin-targeting moiety conjugates from non-target sites, e.g., the circulation, extravascular space, etc.

Other embodiments of the present invention involve the preparation and use of CCAs in clearance of other previously administered molecules or toxic or potentially toxic molecules generated in vivo, which compounds to be cleared are present in a patient's circulation or extravascular fluid space. Previously administered molecules may include active agent-containing conjugates (e.g., radionuclide-chelate-antibody which can be cleared by a CCA containing an anti-chelate or anti-antibody binding moiety; or radionuclide-chelate-antibody-biotin binding protein which can be cleared by a biotin-containing CCA); targeting moiety-receptor conjugates; or the like.

Preferred CCAs of the present invention are administered, permeate the circulation and penetrate the extravascular fluid space. Consequently, previously administered compounds or toxic or potentially toxic moieties that are present in the circulation or in the extravascular fluid space are accessible to the CCAs of the present invention. Circulating compounds are removed via association with the CCA and processing by liver receptors. Previously administered compounds or toxic or potentially toxic moieties, present in extravascular fluid space but not associated with a target cell or epitope, are removed via liver receptors as such compounds diffuse back into the circulation in association with CCAs.

CCA bound to a pretargeted agent (targeting moiety-anti-ligand conjugate, for example) dissociates and reassociates over time. Following dissociation and prior to reassociation, the pretargeted agent is available for binding to active agent-containing constructs. Binding of such active agent-containing constructs is expected to be favored due to a concentration gradient (i.e., higher concentration of active agent-containing construct than target-associated CCA). Another CCA embodiment of the present invention exhibits a favorable biodistribution which avoids such compromise of pretargeted receptor via direct receptor-CCA or CCA metabolite association. A preferred alternative CCA embodiment of the present invention incorporates a lower affinity binding moiety, which can be more easily replaced at the pretargeted receptor by subsequently administered active agent-higher affinity binding moiety construct.

Toxic or potentially toxic molecules that may be removed from a recipient's circulation or extravascular fluid space include: chemotherapeutics e.g., alkylators, heavy metals and the like. Binding moieties capable of associating with toxic or potentially toxic molecules present in the recipient's circulation or extravascular fluid space include antibodies or fragments thereof directed to epitopes that are characteristic of such toxin or potential toxin. Other useful binding moieties include oligonucleotides, ligands or anti-ligands.

Characteristics of useful binding moieties are discussed below. The binding between the binding moiety of the CCAs of the present invention and the molecule to be cleared from the circulation or extravascular fluid space need only be transient, i.e., exists for a sufficient amount of time to clear the molecule from circulation or extravascular fluid space to the liver. Also, it should be noted that the binding constant of the binding component is determined with regard to the CCA as a whole. That is, a biotin-containing CCA is expected to bind to avidin or streptavidin with a binding constant less than that of biotin itself. Experimentation has revealed that biotin-containing CCAs of the present invention are capable of clearance.

In general, the binding constant characterizing the interaction of the binding moiety of the CCA and the molecule to be bound thereby should be low enough to keep short the residence time of any CCA accreting to target sites. Also, the binding constant must be sufficiently high to capture the molecule to be bound and traffic that molecule to the liver. Consequently, CCA binding moieties having a binding constant in excess of about 10^8 are preferred.

Binding moieties of the present invention include ligands, anti-ligands, and other target epitope-recognizing moieties. One skilled in the art can substitute acceptable moieties for the binding moieties discussed specifically herein. Preferred binding moieties are characterized by a molecular weight of a Fab fragment of a monoclonal antibody or lower. Such binding moieties may also be modified to include suitable functional groups to allow for attachment of other molecules of interest, e.g., peptides, proteins, nucleotides, and other small molecules.

Lower molecular weight bispecific CCA molecules, designed to contain appropriately spaced hexoses and biotin, when formulated, quickly cleared streptavidin-containing conjugate from circulation. Examples of such biotin-containing CCAs are set forth below.

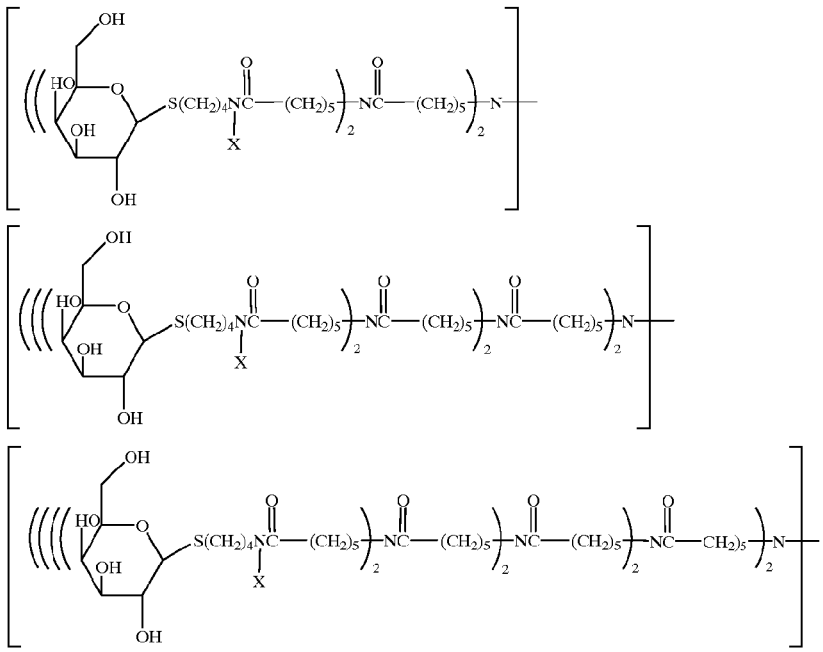

where X is H, methyl, lower alkyl or lower alkyl with heteroatoms. The term lower alkyl refers to moieties of straight or branched construction having from 1 to about 10 carbon atoms, with from 1 to about 6 carbon atoms preferred. The term herteroatom refers to sulfur, oxygen or nitrogen. The above structures bear 4, 8 and 16 galactose residues respectively. Further iteration in the branching allows expansion to include 32, 64, etc., galactose residues.

CCAs of the present invention are designed to interact with hepatic receptors to facilitate clearance of CCA-containing constructs via that route. Hepatocyte receptors which provide for effective clearance include in particular Ashwell receptors, mannose receptors associated with endothelial cells and/or Kupffer cells of the liver, the mannose 6-phosphate receptor, and the like. Hexoses which may be employed in the CCA structure include by way of example galactose, mannose, mannose 6-phosphate, N-acetylgalactosamine, pentamannosyl-phosphate, and the like. Hexoses recognized by Ashwell receptors include glucose, galactose, galactosamine, N-acetylgalactosamine, pentamannosyl phosphate, mannose-6-phosphate and thioglycosides of galactose, galactosides, galactosamine, N-acetylgalactosamine, and mannosyl-6-phosphate and the like. A sufficient number of hexose residues are attached to biotin or to the selected biotin analog to provide for effective clearance, e.g., via the Ashwell receptors located on the surface of hepatocytes.

Preferably, CCAs are of a low enough molecular weight to provide for efficient diffusion into the extravascular space, thus providing for binding to both circulating and non-circulating conjugate. This molecular weight will preferably range from about 1,000 to about 20,000 daltons, more preferably about 2,000 to 16,000 daltons.

Preferable cluster hepatic clearance directing moieties of CCAs of the present invention are characterized by at least 3 hexose residues, e.g., glactose residue or N-acetylgalactosmaine residues. However, the invention is not limited thereby and embraces the attachment of any number of hexose residues or mixture thereof which results in an efficacious bispecific CCA.

The design of the cluster hepatic clearance directing component of the CCA, containing a hexose such as galactose or N-acetylgalactosamine, also depends upon a number of factors including:

(i) The number of hexose residues, e.g., galactose or N-acetylgalactosamine residues:

The literature suggests that galactose receptors are grouped on the surface of human hepatocytes as heterotrimers and possible bis-heterotrimers. Thus, for optimal affinity, the CCA should possess at least three galactose residues, and preferably more, to provide for "galactose clusters." In general, the CCA will contain from about 3 to about 50 galactose residues, preferably from about 3 to 32, and most preferably 16 galactose residues.

(ii) Distance between hexose residues:

Each galactose receptor is separated by a distance of 15, 22 and 25 Å. Thus, the galactose residues within each CCA should preferably be separated by a flexible linker which provides for a separation distance of at least 25 Å, to enable the sugars to be separated by at least that distance. It is expected that this minimum spacing will be more significant as the number of sugar residues, e.g., galactoses, are decreased. This is because larger number of galactoses will likely contain an appropriate spacing between sugars that are not immediately adjacent to one another, thus providing for the desired receptor interaction.

Assuming an average bond length of about 1.5 Å, this would mean that the sugar residues should ideally be separated by a spacer of not less than about 10 bond lengths, with at least 25 bond lengths being more preferred.

For example, galactoses or other sugar residues may be attached in a branched arrangement as follows, which is based on bis-homotris:

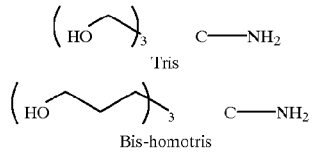

Preferably, each arm is extended, and terminates in a carboxylic acid terminus as follows:

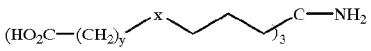

where x = S or O
y = 1–10

Exemplary clearing agents having such an arrangement are set forth below:

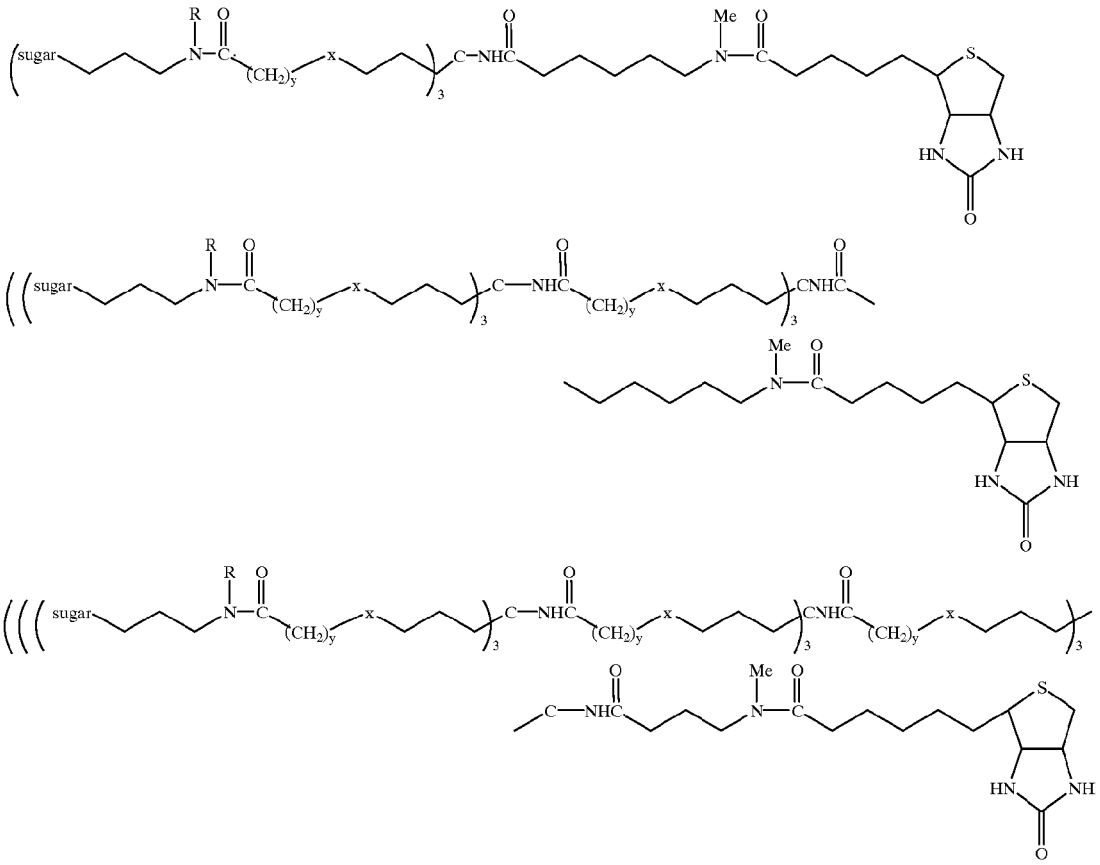

where R = H or Me; y = 1–10; x = 0 or S

Such an arrangement, with 0, 1 or 2 branched iterations, allows for the incorporation of 3, 9 or 27 sugars. Other iterative structures may be based upon the constructs, such as Asp (bis-LAC AHT)$_2$, set forth by Lee et al., *Biochemistry,* 23:4255–4261, 1984.

(iii) Distance between the cluster hepatic clearance directing moiety and the binding moiety of the CCA.

If many galactose or other sugar residues are linked to the biotin species, then the linker should be long enough to alleviate adverse steric effects which may result in diminished binding of the CCA to the molecule to be cleared and/or diminished binding of the complex to the hepatocyte receptor.

While the following parameters appear to be optimal for galactose it should be noted that these factors may vary with other hexoses or mixtures thereof, which may or may not bind to the same receptors, or may bind differently. For example, the inventors have now conducted a series of experiments and developed a second generation of CCAs based upon the hexosse N-acetylgalactosamine. In this development effort, the three design parameters discussed above were re-evaluated and additional design parameters were investigated.

With regard to criteria (i), the number of hexose residues, it was discovered that a smaller number of N-acetylgalactosamine hexose residues can be employed to achieve equivalent levels of clearance of targeting moiety-receptor. It appears therefore that N-acetylgalactosamine exhibits higher affinity for the Ashwell receptor than galactose.

Regarding criteria (ii), the distance between hexose residues, it was discovered that an increase in distance between the sugar residue and the cluster backbone (from four carbons to five carbons) resulted in enhanced affinity for Ashwell receptors. This enhancement is believed to be the result of greater conformational flexibility. Further increases in that distance provided additional enhancement in affinity but adversely impacted the solubility of the resulting CCAs. Consequently, chemical modification of such extended CCAs to improve solubility may be necessary. Such chemical modifications are within the ordinary skill in the chemical arts.

With respect to criteria (iii), the distance between the cluster hepatic clearance directing moiety and the binding moiety, the use of an extender which is stabilized against metabolic degradation between those moieties provided the following advantages: (1) relief from steric hindrance impacting binding moiety association with the compound it is designed to clear; and (2) enhanced in vivo stability against formation of binding moiety-containing CCA metabolites. However, some steric hindrance may be advantageous with regard to biotin-containing CCAs, because binding thereof to pretargeted receptor will likely be reduced. Consequently, selection of optimal structure in this regard involves an analysis of the affinity required to clear versus the affinity displacement by non-sterically hindered biotin-active agent constructs.

As an extender between the binding moiety and the cluster hepatic clearance directing moiety, a bifunctional linker is employed which is preferably characterized by one or more of the following characteristics: flexibility, ability to access all binding sites available on the moiety to be cleared (e.g., targeting moiety-anti-ligand conjugate), metabolic stability and the like. One such linker incorporates a simple linear carbon chain between two functional groups, such as aminocaproate (—CO—$(CH_2)_5$—NH—). Alternatively, linear or branched carbon chains containing heteroatoms, polymeric moieties containing heteroatoms, and the like may be used to link two functional groups. One such extender is —CO—$(CH_2)_2$—(O—$(CH_2)_2$—O)$_n$—$(CH_2)_2$—NX—, wherein n ranges from 1 to about 20 and X is hydrogen or branched or straight chain lower alkyl of 1 to about 6 carbon atoms, phenyl, benzyl, or a 2 to about 6 carbon lower alkyl group substituted with a phenyl moiety. The extender may be generated using a polyethylene glycol polymer and affords the advantage of metabolic stability, increased aqueous solubility, increased access to the construct to be cleared and greater hydrodynamic extension. Also, alternative functional groups may be selected by a person of ordinary skill in the art to link the extender to the binding moiety and to the cluster hepatic clearance directing moiety. Alternative extenders include, polymers such as dextran, poly-D-amino acids (formed of lysine, glutamic acid or the like), poly-amino-phosphonates (e.g., based upon alpha-phosphonomethyl amino acid compounds, such as the following:

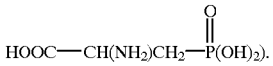

Non-polymeric molecules such as aminoalkylhalides, capable of forming an amide with biotin or other binding component and a tertiary amine with the hexose cluster, and the like, may also be used as extenders in the practice of the present invention.

Further structural/functional studies were conducted on the N-acetylgalactosamine second generation CCAs in an effort to design an optimal CCA. As a result of this effort, more preferred CCAs of the present invention are characterized by one or more of the following structural features.

(A) Unnatural orientation of ligand (e.g., (L)-biotin) and anti-ligand (e.g., streptavidin formed from (D)-amino acids) impart enhanced stability to metabolic degradation.

(B) Secondary amide bond between sugar residues and the cluster backbone appears to contribute to higher affinity sugar-Ashwell receptor binding.

(C) Appropriate orientation for sugar attachment appears to impact affinity, and appropriate linking heteroatom appears to impact stability and affinity. For an oxygen linking heteroatom, a 1-beta linkage is preferred for galactose-containing CCAs, while a 1-alpha linkage is preferred for N-acetylgalactosamine-containing CCAs. Overall, sulfur linkers are preferred (appear to improve stability), and 1-alpha-S linkers are most preferred for N-acetylgalactosamine-containing CCAs.

(D) Tertiary amine adjacent to the binding moiety, such as a ligand or an anti-ligand, enhances in vivo stability of the CCA.

Examples of specific embodiments of preferred CCAs of the present invention are shown below:

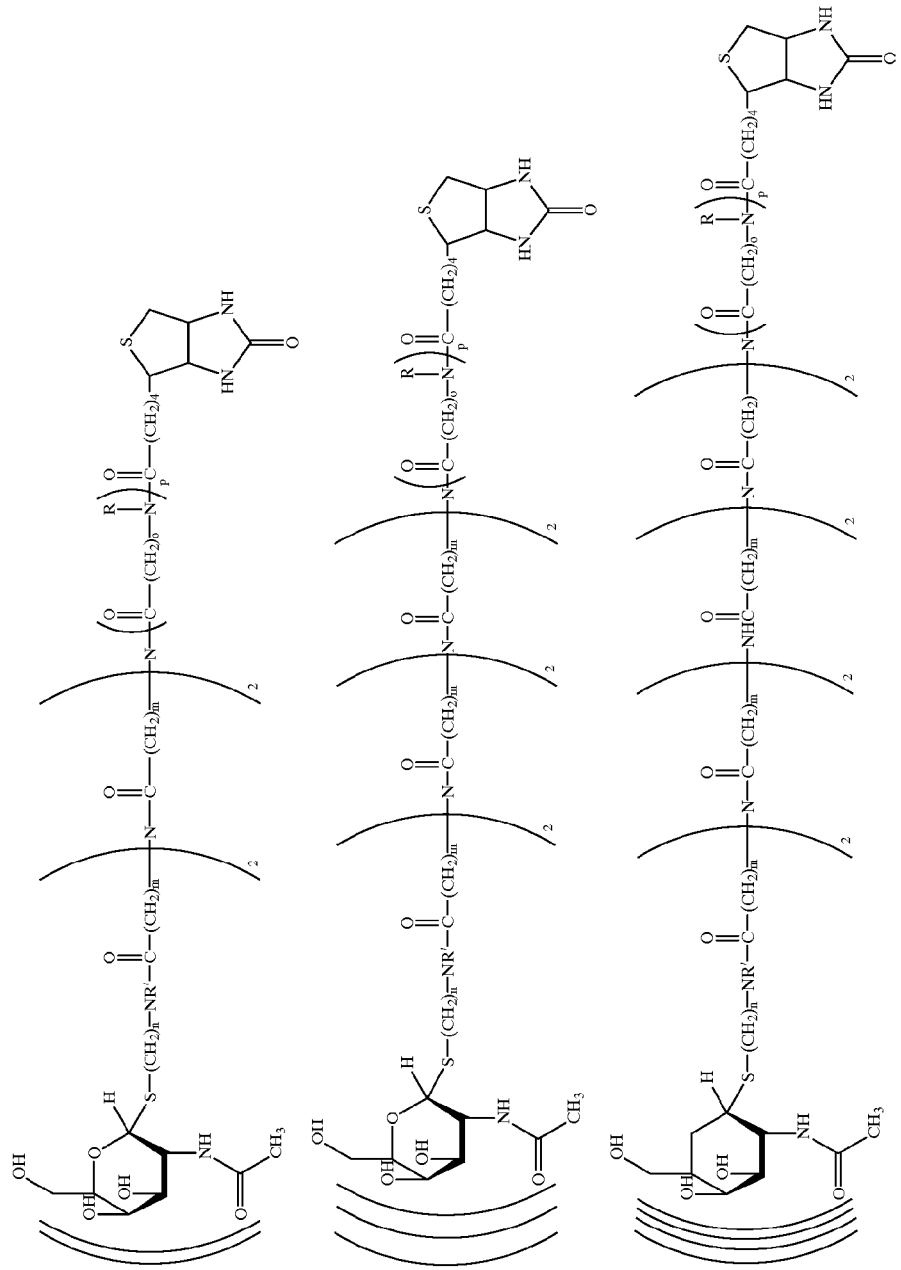

where n is an integer ranging from 1 to about 10, with from about 4 to about 8 preferred and with from about 4 to about 5 still more preferred; m is an integer ranging from about 3 to about 6, with 5 preferred; wherein o is an integer ranging from about 3 to about 6, with 5 preferred; p is an integer ranging from 1 to about 10, with from 1 to about 6 preferred and with from 1 to about 3 more preferred; and R is a straight or branched chain lower alkyl of from 1 to about 6 carbon atoms, phenyl, benzyl, or a 2 to about 6 carbon lower alkyl group substituted with a phenyl moiety.

At higher administered doses of CCA characterized by greater distance between the binding moiety (e.g., biotin) and the cluster hepatic clearance directing moiety, blockage of pretargeted receptor sites by the CCA is more likely. In this case, lower affinity biotin analogs may be employed as is more fully discussed below. An alternative way to diminish the affinity of the biotin ligand is to provide greater steric hindrance to biotin-avidin or biotin-streptavidin binding (in contrast to general bias for decreased steric hindrance as discussed above). On method to provide increased steric hindrance is by increasing the size, and therefore the steric impact, of the substituent used to form a tertiary amine on the amide nitrogen next adjacent to biotin in the CCA structure. For example, N-propyl, N-butyl, N-benzyl or like substitutions can be employed. Persons skilled in the art are familiar with substitutions of this type.

Given the teachings in this application one skilled in the art can, using available synthesis techniques, attach biotin to other hexose residues, or a mixture of different hexose residues via a cluster backbone and the ascertain those constructs which provide acceptable clearance.

Also, one skilled in the art can additionally substitute other complementary ligands for biotin, ideally those having small molecular weight. Such ligands may also be modified to include suitable functional groups to allow for the attachment of other molecules of interest, e.g., peptides, proteins, nucleotides, and other small molecules. Examples of suitable functional groups include, e.g., maleimides, activated esters, isocyanates, alkyul halides (e.g., iodoacetate), hydrazides, thiols, imidates and aldehydes.

In addition to the described therapeutic advantages of the described CCAs, they also afford cost, regulatory and safety advantages. The CCAs of the present invention are chemically well defined and therefore are amenable to relatively precise characterization. Also, such CCAs can be produced reproducible from readily available or easily synthesizable components.

One embodiment of the present invention provides CCAs having physical properties facilitating use for in vivo complexation and blood clearance of anti-ligand/ligand (e.g., avidin/biotin)-targeting moiety (e.g., antibody) conjugates. These CCAs are useful in improving the target:blood ratio of targeting moiety-containing conjugate. One application in which the target:blood ratio improvement is sought is in solid tumor imaging and therapy.

Other applications of these CCAs include lesional imaging or therapy involving blood clots and the like, employing antibody or other targeting vehicle-active agent delivery modalities. For example, an efficacious anti-clotting agent provides rapid target localization and high target:non-target ratio. Active agents administered in pretargeting protocols of the present invention using efficient clearing agents are targeted in the desirable manner and are, therefore, useful in the imaging/therapy of conditions such as pulmonary embolism and deep vein thrombosis.

The present invention provides methods of increasing active agent localization at a target cell site of a mammalian recipient, which methods include:

- administering to the recipient a first conjugate comprising a targeting moiety and a member of a ligand-anti-ligand binding pair;
- thereafter administering to the recipient a CCA incorporating a cluster hepatic clearance directing component, capable of directing the clearance of circulating first conjugate via hepatocyte receptors of the recipient, and a binding component; and
- subsequently administering to the recipient a second conjugate comprising an active agent and a ligand/anti-ligand binding pair member, wherein the second conjugate binding pair member is complementary to that of its first conjugate.

The present invention also provides methods for decreasing the background active agent concentration in otherwise conventional imaging protocols. These methods involve:

- administering to the recipient a first conjugate including a targeting moiety, a member of a ligand-anti-ligand pair and an active imaging agent; and
- thereafter administering to the recipient a CCA incorporating a cluster hepatic clearance directing component, capable of directing the clearance of circulating first conjugate via hepatocyte receptors of the recipient, and a binding component capable of binding to the first conjugate,

wherein upon administration of the CCA, serum-associated first conjugate is cleared and therefore the image background is diminished. In this manner, the quality of diagnostic images can be improved.

Another improvement of the present invention incorporates a CCA into a proteinaceous clearing agent. For example, HSA may be derivatized with one or more CCAs, preferably 1 or 2 CCAs and optionally by hexose residues. By virtue of the synthetic nature of the CCA and the methylated amide bond(s) incorporated in the linker/extender between the cluster and the binding moiety, the CCA is resistant to metabolic degradation. Consequently, any CCA-biotin metabolites of this proteinaceous clearing agent are likely to be retained in liver hepatocytes. One such construct, illustrated in the synthetic scheme of FIG. **8** incorporates a D-cysteine residue in the extender between biotin and the cluster which serves to donate a reactive thiol. The cysteine thiol may then be employed to bind to hexose-derivatized or non-hexose-derivatized HSA which is derivatized with a maleimide residue.

Clearing agent evaluation experimentation involving galactose- and biotin-derivatized clearing agents is detailed in Example III. The specific clearing agents examined during the Example III experimentation are human serum albumin derivatized with galactose and biotin and a 70,000 dalton molecular weight dextran derivatized with both biotin and galactose. The experimentation showed that proteins and polymers are derivatizable to contain both galactose and biotin and that the resultant derivatized molecule is effective in removing circulating streptavidin-protein conjugate from the serum of the recipient. Biotin loading was varied to determine the effects on both clearing the blood pool of

circulating avidin-containing conjugate and the ability to deliver a subsequently administered biotinylated isotope to a target site recognized by the streptavidin-containing conjugate. The effect of relative doses of the administered components with respect to clearing agent efficacy was also examined. Experimentation relating to first generation hexose cluster-bearing moieties is set forth in Example V below. Experimentation involving second generation CCAs is set forth in Example VII below.

The present invention provides CCAs that incorporate ligand derivatives or anti-ligand derivatives, wherein such derivatives exhibit a lower affinity than the native form of the compound, employed in the same construct, for the complementary ligand/anti-ligand pair member (i.e., lower affinity ligands or anti-ligands). In embodiments of the present invention employing a biotin-avidin or biotin-streptavidin ligand/anti-ligand pair, preferred CCAs incorporate either lower affinity biotin (which exhibits a lower affinity for avidin or streptavidin than native biotin) or lower affinity avidin or a streptavidin (which exhibits a lower affinity for biotin than native avidin or streptavidin).

In two-step pretargeting protocols employing the biotin-avidin or biotin-streptavidin ligand-anti-ligand pair, lower affinity biotin, lower affinity avidin or lower affinity streptavidin may be employed. Exemplary lower affinity biotin molecules, for example, exhibit the following properties: bind to avidin or streptavidin with an affinity less than that of native biotin (10^{-15}); retain specificity for binding to avidin or streptavidin; are non-toxic to mammalian recipients; and the like. Exemplary lower affinity avidin or streptavidin molecules, for example, exhibit the following properties: bind to biotin with an affinity less than native avidin or streptavidin; retain specificity for binding to biotin; are non-toxic to mammalian recipients; and the like.

Exemplary lower affinity biotin molecules include 2'-thiobiotini; 2'-iminobiotin; 1'-N-methoxycarbonyl-biotin; 3' -N-methoxycarbonylbiotin; 1-oxy-biotin; 1-oxy-2'-thiobiotin; 1-oxy-2'-iminobiotin; 1-sulfoxide-biotin; 1-sulfoxide-2'-thiobiotin; 1-sulfoxide-2'-iminobiotin; 1-sulfone-biotin; 1-sulfone-2'-thio-biotin; 1-sulfone-2'-iminobiotin; imidazolidone derivatives such as desthiobiotin (d and dl optical isomers), dl-desthiobiotin methyl ester, dl-desthiobiotinol, D-4-n-hexyl-imidazolidone, L-4-n-hexylimidazolidone, dl-4-n-butyl-imidazolidone, dl-4-n-propylimidazolidone, dl-4-ethyl-imidazolidone, dl-4-methylimidazolidone, imidazolidone, dl-4,5-dimethylimidazolidone, meso-4,5-dimethylimidazolidone, dl-norleucine hydantoin, D-4-n-hexyl-2-thiono-imidazolidine, d-4-n-hexyl-2-imino-imidazolidine and the like; oxazolidone derivatives such as D-4-n-hexyl-oxazolidone, D-5-n-hexyloxazolidone and the like; [5-(3,4-diamino-thiophan-2-yl] pentanoic acid; lipoic acid; 4-hydroxy-azobenzene-2'-carboxylic acid; and the like. Preferred lower affinity biotin molecules for use in the practice of the present invention are 2'-thiobiotin, desthiobiotin, 1-oxy-biotin, 1-oxy-2'-thiobiotin, 1-sulfoxide-biotin, 1-sulfoxide-2'-thiobiotin, 1-sulfone-biotin, 1-sulfone-2'-thiobiotin, lipoic acid and the like. These exemplary lower affinity biotin molecules may be produced substantially in accordance with known procedures therefor. Incorporation of the exemplary lower affinity biotin molecules into CCAs proceeds substantially in accordance with procedures described herein in regard to biotin incorporation.

Much has been reported about the binding affinity of different biotin analogs to avidin. Based upon what is known in the art, the ordinary skilled artisan could readily select or use known techniques to ascertain the respective binding affinity of a particular biotin analog to streptavidin, avidin or a derivative thereof.

The present invention further provides methods of increasing active agent localization at a target cell site of a mammalian recipient, which methods include:

administering to the recipient a first conjugate comprising a targeting moiety and a member of a ligand-anti-ligand binding pair;

thereafter administering to the recipient a CCA incorporating a cluster hepatic clearance directing moiety capable of directing the clearance of circulating first conjugate via hepatocyte receptors of the recipient, wherein the CCA also incorporates a lower affinity complementary member of the ligand-anti-ligand binding pair employed in the first conjugate; and

subsequently administering to the recipient a second conjugate comprising an active agent and a ligand/anti-ligand binding pair member, wherein the second conjugate binding pair member is complementary to that of the first conjugate and, preferably, constitutes a native or high affinity form thereof.

The "targeting moiety" of the present invention binds to a defined target cell population, such as tumor cells. Preferred targeting moieties useful in this regard include antibody and antibody fragments, peptides, and hormones. Proteins corresponding to known cell surface receptors (including low density lipoproteins, transferrin and insulin), fibrinolytic enzymes, anti-HER2, platelet binding proteins such as annexins, and biological response modifiers (including interleukin, interferon, erythropoietin and colony-stimulating factor) are also preferred targeting moieties. Also, anti-EGF receptor antibodies, which internalize following binding to the receptor and traffic to the nucleus to an extent, are preferred targeting moieties for use in the present invention to facilitate delivery of Auger emitters and nucleus binding drugs to target cell nuclei. Oligonucleotides, e.g., antisense oligonucleotides that are complementary to portions of target cell nucleic acids (DNA or RNA), are also useful as targeting moieties in the practice of the present invention. Oligonucleotides binding to cell surfaces are also useful. Analogs of the above-listed targeting moieties that retain the capacity to bind to a defined target cell population may also be used within the claimed invention. In addition, synthetic targeting moieties may be designed.

Functional equivalents of the aforementioned molecules are also useful as targeting moieties of the present invention. One targeting moiety functional equivalent is a "mimetic" compound, an organic chemical construct designed to mimic the proper configuration and/or orientation for targeting moiety-target cell binding. Another targeting moiety functional equivalent is a short polypeptide designated as a "minimal" polypeptide, constructed using computer-assisted molecular modeling and mutants having altered binding affinity, which minimal polypeptides exhibit the binding affinity of the targeting moiety.

Preferred targeting moieties of the present invention are antibodies (polyclonal or monoclonal), peptides, oligonucle-

otides or the like. Polyclonal antibodies useful in the practice of the present invention are polyclonal (Vial and Callahan, *Univ. Mich. Med. Bull.,* 20:284–6, 1956), affinity-purified polyclonal or fragments thereof (Chao et al., *Res. Comm. in Chem. Path. & Pharm.,* 9:749–61, 1974).

Monoclonal antibodies useful in the practice of the present invention include whole antibody and fragments thereof. Such monoclonal antibodies and fragments are producible in accordance with conventional techniques, such as hybridoma synthesis, recombinant DNA techniques and protein synthesis. Useful monoclonal antibodies and fragments may be derived from any species (including humans) or may be formed as chimeric proteins which employ sequences from more than one species. See, generally, Kohler and Milstein, *Nature*, 256: 495–97, 1975; *Eur. J. Immunol.,* 6: 511-19, 1976.

Human monoclonal antibodies or "humanized" murine antibody are also useful as targeting moieties in accordance with the present invention. For example, murine monoclonal antibody may be "humanized" by genetically recombining the nucleotide sequence encoding the murine Fv region (i.e., containing the antigen binding sites) or the complementarity determining regions thereof with the nucleotide sequence encoding a human constant domain region and an Fc region , e.g., in a manner similar to that disclosed in European Patent Application No. 0,411,893 A2. Some murine residues may also be retained within the human variable region framework domains to ensure proper target site binding characteristics. Humanized targeting moieties are recognized to decrease the immunoreactivity of the antibody or polypeptide in the host recipient, permitting an increase in the half-life and a reduction in the possibility of adverse immune reactions.

Types of active agents (diagnostic or therapeutic) useful herein include toxins, anti-tumor agents, drugs and radionuclides. Several of the potent toxins useful within the present invention consist of an A and a B chain. The A chain is the cytotoxic portion and the B chain is the receptor-binding portion of the intact toxin molecule (holotoxin). Because toxin B chain may mediate non-target cell binding, it is often advantageous to conjugate only the toxin A chain to a targeting protein. However, while elimination of the toxin B chain decreases non-specific cytotoxicity, it also generally leads to decreased potency of the toxin A chain-targeting protein conjugate, as compared to the corresponding holotoxin-targeting protein conjugate.

Preferred toxins in this regard include holotoxins, such as abrin, ricin, modeccin, Pseudomonas exotoxin A, Diphtheria toxin, pertussin toxin and Shiga toxin; and A chain or "A chain-like" molecules, such as ricin A chain, abrin A chain, modeccin A chain, the enzymatic portion of Pseudomonas exotoxin A, Diphtheria toxin A chain, the enzymatic portion of pertussis toxin, the enzymatic portion of Shiga toxin, gelonin, pokeweed antiviral protein, saporin, tritin, barley toxin and snake venom peptides. Ribosomal inactivating proteins (RIPs), naturally occurring protein synthesis inhibitors that lack translocating and cell-binding ability, are also suitable for use herein. Extremely highly toxic toxins, such as palytoxin and the like, are also contemplated for use in the practice of the present invention.

Preferred drugs suitable for use herein include conventional chemotherapeutics, such as vinblastine, doorubicin, bleomysin, methotrexate, 5-fluorouracil, 6-thioguanine, cytarabine, cyclophosphamide and cis-platinum, as well as other conventional chemotherapeutics as described in *Cancer: Principles and Practice of Oncology*, 2d ed., V. T. DeVita, Jr., S. Hellman, S. A. Rosenberg, J. B. Lippincott Co., Philadelphia, Pa. 1985, Chapter 14. A particularly preferred drug within the present invention is a trichothecene.

Trichothecenes are drugs produced by soil fungi of the class *Fungi imperfecti* or isolated from *Baccharus megapotamica* (Bamberg, J. R. *Proc. Molec. Subcell. Biol.* 8:41–110, 1983; Jarvis & Mazzola, *Acc. Chem. Res.* 15:338–395, 1982). They appear to be the most toxic molecules that contain only carbon, hydrogen and oxygen (Tamm, C. *Fortschr. Chem. Org. Naturst.* 31:61–117, 1974). They are all reported to act at the level of the ribosome as inhibitors of protein synthesis at the initiation, elongation, or termination phases.

There are two broad classes of trichothecenes: those that have only a central sesquiterpenoid structure and those that have an additional macrocyclic ring (simple and macrocyclic trichothecenes, respectively). The simple trichothecenes may be subdivided into three groups (i.e., Group A, B, and C) as described in U.S. Pat. Nos. 4,744,981 and 4,906,452 (incorporated herein by reference). Representative examples of Group A simple trichothecenes include: Scirpene, Roridin C, dihydrotrichothecene, Scirpen-4, 8-diol, Verrucarol, Scirpentriol, T-2 tetraol, pentahydroxyscirpene, 4-deacetylneosolaniol, trichodermin, deacetylcalonectrin, calonectrin, diacetylverrucarol, 4-monoacetoxyscirpenol, 4,5-diacetoxyscirpenol, 7-hydroxydiacetoxyscirpenol, 8-hydroxydiacetoxy-scirpenol (Neosolaniol), 7,8-dihydroxydiacetoxyscirpenol, 7-hydroxy-8-acetyldiacetoxyscirpenol, 8-acetylneosolaniol, NT-1, NT-2, HT-2, T-2, and acetyl T-2 toxin.

Representative examples of Group B simple trichothecenes include: Trichothecolone, Trichothecin, deoxynivalenol, 3-acetyldeoxynivalenol, 5-acetyldeoxynivalenol, 3,15-diacetyldeoxynivalenol, Nivalenol, 4-acetylnivalenol (Fusarenon-X), 4,15-idacetylnivalenol, 4,7,15-triacetylnivalenol, and tetra-acetylnivalenol. Representative examples of Group C simple trichothecenes include: Crotocol and Crotocin. Representative macrocyclic trichothecenes include Verrucarin A, Verrucarin B, Verrucarin J (Satratoxin C), Roridin A, Roridin D, Roridin E (Satratoxin D), Roridin H, Satratoxin F, Satratoxin G, Satratoxin H, Vertisporin, Mytoxin A, Mytoxin C, Mytoxin B, Myrotoxin A, Myrotoxin B, Myrotoxin C, Myrotoxin D, Roritoxin A, Roritoxin B, and Roritoxin D. In addition, the general "trichothecene" sesquiterpenoid ring structure is also present in compounds termed "baccharins" isolated from the higher plant *Baccharis megapolamica*, and these are described in the literature, for instance as disclosed by Jarvis et al. (Chemistry of Alleopathy, ACS Symposium Series No. 268: ed. A. C. Thompson, 1984, pp. 149–159).

Experimental drugs, such as mercaptopurine, N-methylformamide, 2-amino-1,3,4-thiadiazole, melphalan, hexamethylmelamine, gallium nitrate, 3% thymidine, dichloromethotrexate, mitoguazone, suramin, bromodeoxyuridine, iododeoxyuridine, semustine, 1-(2-chloroethyl)-3-(2,6-dioxo-3-piperidyl)-1nitrosourea, N,N'-

hexamethylene-bis-acetamide, azacitidine, dibromodulcitol, Erwinia asparaginase, ifosfamide, 2-mercaptoethane sulfonate, teniposide, taxol, 3-deazauridine, soluble Baker's antifol, homoharringtonine, cyclocytidine, acivicin, ICRF-187, spiromustine, levamisole, chlorozotocin, aziridinyl benzoquinone, spirogermanium, aclarubicin, pentostatin, PALA, carboplatin, amsacrine, caracemide, iproplatin, misonidazole, dihydro-5-azacytidine, 4'-deoxy-doxorubicin, menogaril, triciribine phosphate, fazarabine, tiazofurin, teroxirone, ethiofos, N-(2-hydroxyethyl)-2-nitro-1H-imidazole-1-acetamide, mitoxantrone, acodazole, amonafide, fludarabine phosphate, pibenzimol, didemnin B, merbarone, dihydrolenperone, flavone-8-acetic acid, oxantrazole, ipomeanol, trimetrexate, deoxyspergualin, echinomycin, and dideoxycytidine (see *NCI Investigational Drugs, Pharmaceutical Data* 1987 NIH Publication No. 88-2141, Revised November 1987) are also preferred.

Radionuclides useful within the present invention include gamma-emitters, positron-emitters, Auger electron-emitters, X-ray emitters and fluorescence-emitters, with beta- or alpha-emitters preferred for therapeutic use Radionuclides are well-known in the art and include ^{123}I, ^{125}I, ^{130}I, ^{131}I, ^{133}I, ^{135}I, ^{47}Sc, ^{72}As, ^{72}Se, ^{90}Y, ^{88}Y, ^{97}Ru, ^{100}Pd, ^{101m}Rh, ^{119}Sb, ^{128}Ba, ^{197}Hg, ^{211}At, ^{212}Bi, ^{153}Sm, ^{169}Eu, ^{212}Pb, ^{109}Pd, ^{111}In, ^{67}Ga, ^{68}Ga, ^{64}Cu, ^{67}Cu, ^{75}Br, ^{76}Br, ^{77}Br, ^{99m}Tc, ^{11}C, ^{13}N, ^{15}O, ^{166}Ho and ^{18}F. Prefered therapeutic radionuclides include ^{188}Re, ^{186}Re, ^{203}Pb, ^{212}Pb, ^{212}Bi, ^{109}Pd, ^{64}Cu, ^{67}Cu, ^{90}Y, ^{125}I, ^{131}I, ^{77}Br, ^{211}At, ^{97}Ru, ^{105}Rh, ^{198}Au and ^{199}Ag, ^{166}Ho or ^{177}Lu.

Other anti-tumor agents, e.g., agents active against proliferating cells, are administrable in accordance with the present invention. Exemplary anti-tumor agents include cytokines, such as IL-2, tumor necrosis factor or the like, lectin inflammatory response promoters (selectins), such as L-selectin, E-selectin, P-selectin or the like, and like molecules.

Ligands suitable for use within the present invention include biotin, haptens, lectins, epitopes, dsDNA fragments, enzyme inhibitors and analogs and derivatives thereof. Useful complementary anti-ligands include avidin (for biotin), carbohydrates (for lectins) and antibody, fragments or analogs thereof, including mimetics (for haptens and epitopes) and zinc finger proteins (for dsDNA fragments) and enzymes (for enzyme inhibitors). Preferred ligands and anti-ligands bind to each other with an affinity of at least about k_D 10^9M. Other useful ligand/anti-ligand systems include S-protein/S-peptide, head activator protein (which binds to itself), cystatin-C/cathepsin B, and the like.

One preferred chelate system for use in the practice of the present invention is based upon a 1,4,7,10-tetraazacyclododecane-N,N',N",N'"-tetra acetic acid (DOTA) construct. Because DOTA strongly binds Y-90 and other radionuclides, it has been proposed for use in radioimmunotherapy. For therapy, it is very important that the radionuclide be stably bound within the DOTA chelate and that the DOTA chelate be stably attached to an effector, such as a ligand or an anti-ligand.

The strategy for design of preferred DOTA molecules incorporating biotin for use in the practice of embodiments of the present invention involved three primary considerations:

1) in vivo stability (including biotinidase and general peptidase activity resistance), with an initial acceptance criterion of 100% stability for 1 hour;

2) renal excretion; and

3) ease of synthesis.

The same or similar criteria are applicable to alternative binding moieties, such as ligands or anti-ligands, as can be readily ascertained by one of ordinary skill in the art.

The DOTA-biotin conjugates that are preferably employed in the practice of the present invention reflect the implementation of one or more of the following strategies:

1) substitution of the carbon adjacent to the cleavage susceptible amide nitrogen;

2) alkylation of the cleavage susceptible amide nitrogen;

3) substitution of the amide carbonyl with an alkyl amino group;

4) incorporation of D-amino acids as well as analogs or derivatives thereof; or

5) incorporation of thiourea linkages.

DOTA-biotin conjugates in accordance with the present invention are described in published PCT Patent Application No. PCT/US/93/05406. A method of preparing preferred DOTA-biotin embodiments is described in Example II hereof.

The preferred linkers are useful to produce DOTA-biotin or other DOTA-small molecule conjugates having one or more of the following advantages:

bind avidin or streptavidin with the same or substantially similar affinity as free biotin;

bind metal M^{+3} ions efficiently and with high kinetic stability;

are excreted primarily through the kidneys into urine;

are stable to endogenous enzymatic or chemical degradation (e.g., bodily fluid amidases, peptidases or the like);

penetrate tissue rapidly and bind to pretargeted avidin or streptavidin; and

are excreted rapidly with a whole body residence half-life of less than about 5 hours.

One component to be administered in a preferred two-step pretargeting protocol is a targeting moiety-anti-ligand or a targeting moiety-ligand conjugate. Streptavidin-proteinaceous targeting moiety conjugates are preferably prepared as described in Example I below, with the preparation involving the steps of preparation of SMCC-derivitized streptavidin; preparation of DTT-reduced proteinaceous targeting moiety; conjugation of the two prepared moieties; and purification of the monosubstituted or disubstituted (with respect to streptavidin) conjugate from crosslinked (antibody-streptavidin-antibody) and aggregate species and unreacted starting materials. The purified fraction is preferably further characterized by one or more of the following techniques: HPLC size exclusion, SDS-PAGE, immunoreactivity, biotin binding capacity and in vivo studies.

CCAs of the present invention may be administered in single or multiple doses or via continuous infusion. A single dose of a biotin-containing CCA, for example, produces a rapid decrease in the levelof circulating targeting moiety-streptavidin, followed by a small increase in that level, presumably caused, at least in part, by re-equilibration of

targeting moiety-streptavidin within the recipient's physiological compartments. A second or additional CCA doses may then be employed to provide supplemental clearance of targeting moiety-streptavidin. Alternatively, CCA may be infused intravenously for a time period sufficient to clear targeting moiety-streptavidin in a continuous manner.

The dose of CCAs of the present invention will depend upon numerous patient-specific and clinical factors, which clinicians are uniquely qualified to assess. In general, the dose of the CCA to be administered will depend on the dose of the targeting conjugate or other previously administered component to be cleared that is either measured or expected to remain in the serum compartment at the time the CCA is administered. Alternatively, the dose of the CCA will depend on the measured or expected level of toxic agent to be cleared. Generally, a single CCA dose will range from about 20 mg to about 500 mg, with from about 50 mg to about 200 mg preferred. It is important to note that preclinical testing of CCA agents has revealed that great latitude exists in effective CCA dose range.

One embodiment of the present invention in which rapid acting CCAs are useful is in the delivery of Auger emitters, such as I-125, I-123, Er-165, Sb-119, Hg-197, Ru-97, Tl-201 and Br-77, or nucleus-binding drugs to target cell nuclei. In these embodiments of the present invention, targeting moieties that localize to internalizing receptors on target cell surfaces are employed to deliver a targeting moiety-containing conjugate (i.e., a targeting moiety-anti-ligand conjugate in the preferred two-step protocol) to the target cell population. Such internalizing receptors include EGF receptors, transferrin receptors, HER2 receptors, IL-2 receptors, other interleukins and cluster differentiation receptors, somatostatin receptors, other peptide binding receptors and the like.

After the passage of a time period sufficient to achieve localization of the conjugate to target cells, but insufficient to induce internalization of such targeted conjugates by those cells through a receptor-mediated event, a rapidly acting CCA is administered. In a preferred two-step protocol, an active agent-containing ligand or anti-ligand conjugate, such as a biotin-Auger emitter or a biotin-nucleus acting drug, is administered as soon as the CCA has been given an opportunity to complex with circulating targeting moiety-containing conjugate, with the time lag between CCA and active agent administration being less than about 24 hours. In this manner, active agent is readily internalized through target cell receptor-mediated internalization. While circulating Auger emitters are thought to be non-toxic, the rapid, specific targeting afforded by the pretargeting protocols of the present invention increases the potential of shorter half-life Auger emitters, such as I-123, which is available and capable of stable binding.

The invention is further described through presentation of the following examples. These examples are offered by way of illustration, and not by way of limitation.

EXAMPLE I

Targeting Moiety-Anti-Ligand Conjugate for Two-Step Pretargeting In Vivo

A. Preparation of SMCC-derivitized streptavidin.

31 mg (0.48 mol) streptavidin was dissolved in 9.0 ml PBS to prepare a final solution at 3.5 mg/ml. The pH of the solution was adjusted to 8.5 by addition of 0.9 ml of 0.5 M borate buffer, pH 8.5. A DMSO solution of SMCC (3.5 mg/ml) was prepared, and 477 l (4.8 mol) of this solution was added dropwise to the vortexing protein solution. After 30 minutes of stirring was purified by G-25 (PD-10, Pharmacia, Picastaway, N.J.) column chromatography to remove unreacted or hydrolyzed SMCC. The purified SMCC-derivitized streptavidin was isolated (28 mg, 1.67 mg/ml).

B. Preparation of DTT-reduced NR-LU-10. To 77 mg NR-LU-10 (0.42 mol) in 15.0 ml PBS was added 1.5 ml of 0.5 M borate buffer, pH 8.5. A DTT solution, at 400 mg/ml (165 l) was added to the protein solution. After stirring at room temperature for 30 minutes, the reduced antibody was purified by G-25 size exclusion chromatography. Purified DTT-reduced NR-LU-10 was obtained (74 mg, 2.17 mg/ml).

C. Conjugation of SMCC-streptavidin to DTT-reduced NR-LU-10. DTT-reduced NR-LU-10 (63 mg, 29 ml, 0.42 mol) was diluted with 44.5 ml PBS. The solution of SMCC-streptavidin (28 mg, 17 ml, 0.42 mol) was added rapidly to the stirring solution of NR-LU-10. Total protein concentration in the reaction mixture was 1.0 mg/ml. The progress of the reaction was monitored by HPLC (Zorbax® GF-250, available from MacMod). After approximately 45 minutes, the reaction was quenched by adding solid sodium tetrathionate to a final concentration of 5 mM.

D. Purification of conjugate. For small scale reactions, monosubstituted or disubstituted (with regard to streptavidin) conjugate was obtained using HPLC Zorbax (preparative) size exclusion chromatography. The desired monosubstituted or disubstituted conjugate product eluted at 14.0–14.5 min (3.0 ml/min flow rate), while unreacted NR-LU-10 eluted at 14.5–15 min and unreacted derivitized streptavidin eluted at 19–20 min.

For larger scale conjugation reactions, monosubstituted or disubstituted adduct is isolatable using DEAE ion exchange chromatography. After concentration of the crude conjugate mixture, free streptavidin was removed therefrom by eluting the column with 2.5% xylitol in sodium borate buffer, pH 8.6. The bound unreacted antibody and desired conjugate were then sequentially eluted from the column using an increaseing salt gradient in 20 mM diethanolamine adjusted to pH 8.6 with sodium hydroxide.

E. Characterization of Conjugate.

1. HPLC size exclusion was conducted as described above with respect to small scale purification.
2. SDS-PAGE analysis was performed using 5% polyacrylamide gels under non-denaturing conditions. Conjugates to be evaluated were not boiled in sample buffer containing SDS to avoid dissociation of streptavidin into its 15 kD subunits. Two product bands were observed on the gel, which correspond to the mono- and di-substituted conjugates.
3. Immunoreactivity was assessed, for example, by competitive binding ELISA is compared to free antibody. Values obtained were within 10% of those for the free antibody.
4. Biotin binding capacity was assessed, for example, by titrating a known quantity of conjugate with p-[I-125] iodobenzoylbiocytin. Saturation of the biotin binding sites was observed upon addition of 4 equivalences of the labeled biocytin.

5. In vivo studies are useful to characterize the reaction product, which studies include, for example, serum clearance profiles, ability of the conjugate to target antigen-positive tumors, tumor retention of the conjugate over time and the ability of a biotinylated moluclc to bind streptavidin conjugate at the tumor. These data facilitate determination that the synthesis resulted in the formation of a 1:1 streptavidin-NR-LU-10 whole antibody conjugate that exhibits blood clearance properties similar to native NR-LU-10 whole antibody, and tumor uptake and retention properties at least equal to native NR-LU-10.

For example, FIG. **1** depicts the tumor uptake profile of the NR-LU-10-streptavidin conjugate (Ab/SA, referred to in this example as LU-10-StrAv) in comparison to a control profile of native NR-LU-10 whole antibody and a control profile of streptavidin. LU-10-StrAv was radiolabeled on the streptavidin component only, giving a clear indication that LU-10-StrAv localizes to target cells as efficiently as NR-LU-10 whole antibody itself.

EXAMPLE II

Synthesis of DOTA-Biotin Conjugates

A. Synthesis of Nitro-Benzyl-DOTA.

The synthesis of aminobenzyl-DOTA was conducted substantially in accordance with the procedure of McMurry et al., *Bioconjugate Chem.*, 3: 108–117, 1992. The critical step in the prior art synthesis is the intermolecular cyclization betwen disuccinimidyl N-(tert-butoxycarbonyl) iminodiacetate and N-(2-aminoethyl)-4-nitrophenyl alaninamide to prepare 1(tert-butoxycarbonyl)-5-(4-nitrobenzyl)-3,6,11-trioxo-1,4,7,10-tetraazacyclododecane. In other words, the critical step is the intermolecular cyclization between the bis-NHS ester and the diamine to give the cyclized dodecane. McMurry et al. conducted the cyclization step on a 140 mmol scale, dissolving each of the reagents in 100 ml DMF and adding via a syringe pump over 48 hours to a reaction pot containing 4 liters dioxane.

A 5x scale-up of the McMurry et al. procedure was not practical in terms of reaction volume, addition rate and reaction time. Process chemistry studies revealed that the reaction addition rate could be substantially increased and that the solvent volume could be greatly reduced, while still obtaining a similar yield of the desired cyclization product. Consequently on a 30 mmol scale, each of the reagents was dissolved in 500 ml DMF and added via addition funnel over 27 hours to a reaction pot containing 3 liters dioxane. The addition rate of the method employed involved a 5.18 mmol/hour addition rate and a 0.047 M reaction concentration.

B. Synthesis of an N-methyl-glycine linked conjugate.

The N-methyl glycine-linked DOTA-biotin conjugate was prepared by an analogous method to that used to prepare D-analine-linked DOTA-biotin conjugates. N-methyl-glycine (trivial name carcosine, available from Sigma Chemical Co.) was condensed with biotin-NHS ester in DMF and triethylamine to obtain N-methyl glycyl-biotin. N-methyl-glycyl biotin was then activated with EDCI and NHS. The resultant NHS ester was not isolated and was condensed in situ with DOTA-aniline and excess pyridine. The reaction solution was heated at 60° C. for 10 minutes and then evaporated. The residue was purified by preparative HPLC to give [N-methyl-N-biotinyl)-N-glycyl]-aminobenzyl-DOTA.

1. Preparation of (N-methyl)glycyl biotin. DMF (8.0 ml) and triethylamine (0.61 ml, 4.35 mmol) were added to solids N-methyl glycine (182 mg, 2.05 mmol) and N-hydroxy-succinimidl biotin (500 mg, 1.46 mmol). The mixture was heated for 1 hour in an oil bath at 85° C. during which time the solids dissolved producing a clear and colorless solution. The solvents were then evaporated. The yellow oil residue was acidified with glacial acetic acid, evaporated and chromatographed on a 27 mm column packed with 50 g silica, eluting with 30% MeOH/EtOAc 1% HOAc to give the product as a white solid (383 mg) in 66% yield.
   H—NMR (DMSO): 1.18–1.25 (m, 6H, $(CH_2)_3$), 2.15, 2.35 (2 t's, 2H, CH_2CO), 2.75 (m, 2H, SCH_2), 2.80, 3.00 (2 s's, 3H, NCH_3), 3.05–3.15 (m, 1H, SCH), 3.95, 4.05 (2 s's, 2H, CH_2N), 4.15, 4.32 (2 m's, 2H, 2CHN's), 6.35 (s, NH), 6.45 (s, NH).
2. Preparation of [(N-methyl-N-biotinyl)glycyl] aminobenzyl-DOTA. N-hydroxysuccinimide (10 mg, 0.08 mmol) and EDCI (15 mg, 6.08 mmol) were added to a solution of (N-methylglycyl biotin (24 mg, 0.08 mmol) in DMF (1.0 ml). The solution was stirred at 23 C for 64 hours. Pyridine (0.8 ml) and aminobenzyl-DOTA (20 mg, 0.04 mmol) were added. The mixture was heated in an oil bath at 63° C. for 10 minutes, then stirred at 23 C for 4 hours. The solution was evaporated. The residue was purified by preparative HPLC to give the product as an off white solid (8 mg, 0.01 mmol) in 27% yield.
   H—NMR (D_2O): 1.30–1.80 (m, 6H), 2.40, 2.55 (2 t's, 2H, CH_2CO), 2.70–4.2 (complex multiplet), 4.35 (m, CHN), 4.55 (m, CHN), 7.30 (m, 2H, benzene hydrogens), 7.40 (m, 2H, benzene hydrogens).

EXAMPLE III

Clearing Agent Evaluation Experimentation

A. Galactose- and Biotin-Derivatization of Human Serum Albumin (HSA). HSA was evaluated because it exhibits the advantages of being both inexpensive and non-immunogenic. HSA was derivatized with varying levels of biotin (1-about 9 biotins/molecule) via analogous chemistry to that previously described with respect to AO. More specifically, to a solution of HSA available from Sigma Chemical Co. (5–10 mg/ml in PBS) was added 10% v/v 0.5 M sodium borate buffer, pH 8.5, followed by dropwise addition of a DMSO solution of NHS—LC-biotin (Sigma Chemical Co.) to the stirred solution at the desired molar offering (relative molar equivalents of reactants). The final percent DMSO in the reaction mixture should not exceed 5%. After stirring for 1 hour at room temperature, the reaction was complete. A 90% incorporation efficiency for biotin on HSA was generally observed. As a result, if 3 molar equivalences of the NHS ester of LC-biotin was introduced, about 2.7 biotins per HSA molecule were obtained. Unreacted biotin reagent was removed from the biotin-derivatized HSA using G-25 size exclusion chromatography. Alternatively, the crude material may be directly galactoxylated. The same chemistry is applicable for biotinylating non-previously biotinylated dextran.

HSA-biotin was then derivatized with from 12 to 45 galactoses/molecule. Galactose derivatization of the bioti-

nylated HSA was performed according to the procedure of Lee, et al., *Biochemistry*, 15: 3956, 1976. More specifically, a 0.1 M methanolic solution of cyanomethyl-2,3,4,6-tetra-O-acetyl-1thio-D-galactopyranoside was prepared and reacted with a 10% v/v 0.1 M NaOMe in methanol for 12 hours to generate the reactive galactosyl thioimidate. The galactosylation of biotinylated HSA began by initial evaporation of the anhydrous methanol from a 300 fold molar excess of reactive thioimidate. Biotinylated HSA in PBS, buffered with 10% v/v 0.5 M sodium borate, was added to the oily residue. After stirring at room temperature for 2 hours, the mixture was stored at 4° C. for 12 hours. The galactosylated HSA-biotin was then purified by G-25 size exclusion chromatography or by buffer exchange to yield the desired product. The same chemistry is exploitable to galactosylating dextran. The incorporation efficiency of galactose on HSA is approximately 10%.

70 micrograms of Galactose-HSA-Biotin (G—HSA—B), with 12–45 galactose residues and 9 biotins, was administered to mice which had been administered 200 micrograms of StrAv—MAb or 200 microliters of PBS 24 hours earlier. Results indicated that G—IISA—B is effective in removing StrAv—MAb from circulation. Also, the pharmacokinetics of G—HSA—B is unperturbed and rapid in the presence or absence of circulating MAb—StrAv.

B. Non-Protein Clearing Agent. A commercially available form of dextran, molecular weight of 70,000 daltons, pre-derivatized with approximately 18 biotins/molecule and having an equivalent number of free primary amines was studied. The primary amine moieties were derivatized with a galactosylating reagent, substantially in accordance with the procedure therefor described above in the discussion of HSA-based clearing agents, at a level of about 9 galactoses/molecule. The molar equivalence offering ratio of galactose to IISA was about 300:1, with about one-third of the galactose being converted to active form. 40 Micrograms of galactose-dextran-biotin (GAL—DEX—BT) was then injected i.v. into one group of mice which had received 200 micrograms MAb—StrAv conjugate intravenously 24 hours earlier, while 80 micrograms of GAL—DEX—BT was injected into other such mice. GAL—DEX—BT was rapid and efficient at clearing StrAv—MAb conjugate, removing over 66% of circulating conjugate in less than 4 hours after clearing agent administrtion. An equivalent effect was seen at both clearing agent doses, which correspnd to 1.6 (40 micrograms) and 3.2 (80 micrograms) times the stoichiometric amount of circulating StrAv conjugate present.

C. Dose Ranging for G—HSA—B Clearing Agent. Dose ranging studies followed the following basic format:

200 micrograms MAb—StrAv conjugate administered;

24 hours later, clearing agent administered; and

2 hours later, 5.7 micrograms PIP-biocytin administerd.

Dose ranging studies were performed with the G—HSA—B clearing agent, starting with a loading of 9 biotins per molecule and 12–45 galactose residues per molecule. Doses of 20, 40, 70 and 120 micrograms were administerd 24 hours after a 200 microgram dose of MAb—StrAv conjugate. The clearing agent administrations were followed 2 hours later by administration of 5.7 micrograms of I-131-PIP-biocytin. Tumor uptake and blood retention of PIP-biotcytin was examined 44 hours after administration thereof (46 hours after clearing agent administration). The results showed that a nadir in blood retention of PIP-biocytin was achieved by all doses greater than or equal to 40 micrograms of G—HSA—B. A clear, dose-dependent decrease in tumor binding of PIP-biocytin at each increasing dose of G—HSA—B was present, however. Since no dose-dependent effect on the localization of MAb—StrAv conjugate at the tumor was observed, this data was interpreted as being indicative of relatively higher blocking of tumor-associated MAb—StrAv conjugate by the release of biotin from catabolized clearing agent. Similar results to those described earlier for the asialoorosomucoid clearing agent regarding plots of tumor/blood ratio were found with respect to G—HSA—B, in that an optimal belance between blood clearance and tumor retention occurred around the 40 microgram dose.

Because of the relatively large molar amounts of biotin that could be released by this clearing agent at higher doses, studies were undertaken to evaluate the effect of lower levels of biotinylation on the effectiveness of the clearing agent. G—HSA—B, derivatized with either 9, 5 or 2 biotins/molecule, was able to clear MAb—StrAv conjugate from blood at equal protein doses of clearing agent. All levels of biotinylation yielded effective, rapid clearance of MAb—StrAv from blood.

Comparison of these 9-, 5-, and 2-biotin-derivatized clearing agents with a single biotin G—HSA—B clearing agent was carried out in tumored mice, employing a 60 microgram dose of each clearing agent. This experiment showed each clearing agent to be substantially equally effective in blood clearance and tumor retention of MAb—StrAv conjugate 2 hours after clearing agent administration. The G—HSA—B with a single biotin was examined for the ability to reduce binding of a subsequently administered biotinylated small molecule (PIP-biocytin) in blood, while preserving tumor binding of PIP-biocytin to prelocalized MAb—StrAv conjugate. Measured at 44 hours following PIP-biocytin administration, tumor localization of both the MAb—StrAv conjugate and PIP-biocytin was well preserved over a broad dose range of G—HSA—B with one biotin/molecule (90 to 180 micrograms). A progressive decrease in blood retention of PIP-biocytin was achieved by increasing doses of the single biocytin G—HSA—B clearing agent, while tumor localization remained essentially constant, indicating that this clearing agent, with a lower level of biotinylation, is preferred. This preference arises because the single biotin G—HSA—B clearing agent is both effective at clearing MAb—StrAv over a broader range of doses (potentially eliminating the need for patient-to-patient titration of optimal dose) and appears to release less competing biotin into the systemic circulation than the same agent having a higher biotin loading level.

Another way in which to decrease the effect of clearing agent-released biotin on active agent-biotin conjugate binding to prelocalized targeting moiety-streptavidin conjugate is to attach the protein or polymer or other primary clearing agent component to biotin using a retention linker. A retention linker has a chemical structure that is resistant to agents that cleave peptide bonds and, optionally, becomes protonated when localized to a catabolizing space, such as a lysosome. Preferred retention linkers of the present inven-

tion are short strings of D-amino acids or small molecules having both of the characteristics set forth above. An exemplary retention linker of the present invention is cyanuric chloride, which may be interposed between an epsilon amino group of a lysine of a proteinaceous primary clearing agent component and an amine moiety of a reduced and chemically altered biotin carboxy moiety (which has been discussed above) to form a compound of the structure set forth below.

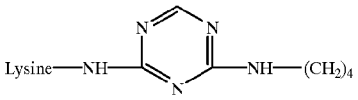

When the compound shown above is catabolized in a catabolizing space, the heterocyclic ring becomes protonated. The ring protonation prevents the catabolite from exiting the lysosome. In this manner, biotin catabolites containing the heterocyclic ring are restricted to the site(s) of catabolism and, therefore, do not compete with active-agent-biotin conjugate for prelocalized targeting moiety-streptavidin target sites.

Comparisons of tumor/blood localization of radiolabeled PIP-biocytin observed in the G—HSA—B dose ranging studies showed that optimal tumor to background targeting was achieved over a broad dose range (90 to 180 micrograms), with the results providing the expectation that even larger clearing agent doses would also be effective. Another key result of the dose ranging experimentation is that G—HSA—B with an average of only 1 biotin molecule is presumably only clearing the MAB—StrAv conjugate via the Ashwell receptor mechanism only, because too few biotins are present to cause cross-linking and aggregation of MAb—StrAv conjugates and clearing agents with such aggregates being cleared by the reticuloendothelial system.

D. Tumor Targeting Evaluation Using G—HSA—B. The protocol for this experiment was as follows:

Time 0: administer 400 micrograms MAb—StrAv conjugate;

Time 24 hours: administer 240 micrograms of G—HSA—B with one biotin and 12–45 galactoses and

Time 26 hours: administer 6 micrograms of

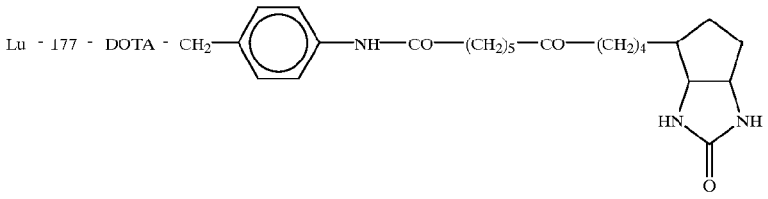

Lu-177 is complexed with the DOTA chelate using known techniques therefor.

Efficient delivery of the Lu177-DOTA-biotin small molecule was observed, 20–25% injected dose/gram of tumor. These values are equivalent with the efficiency of the delivery of the MAb—StrAv conjugate. The AUC tumor/AUC blood obtained for this non-optomized clearing agent dose was 300% greater than that achievable by comparable direct MAb-radiolabel administration. Subsequent experimentation has resulted in AUC tumor/AUC blood over 1000% greater than that achievable by comparable conventional MAb-radiolabel administration. In addition, the HSA-based clearing agent is expected to exhibit a low degree of immunogenicity in humans.

EXAMPLE IV

First Generation CCA (Small Molecule Clearing Agent) Preparation

This procedure is shown schematically in FIG. **2**.

Methyl 6-bromohexanoate. To a 1 L round bottom flask, charged with 20 g (102.5 mmol) of 6-bromohexanoic acid and 50 mL of methanol, was bubbled hydrogen chloride gas for 2–3 minutes. The mixture was stirred at room temperature for 4 hours and concentrated to afford 21.0 g of the product as a yellow oil (99%); ^{1}H—NMR (200 MHz, d_6-DMSO); 3.57 (s, 3H), 3.51 (t, 2H), 2.30 (t, 2H), 1.78 (pentet, 2H), and 1.62–1.27 (m, 4H) ppm.

Methyl 6-aminohexanoate hydrochloride. To a 1 L round bottom flask, charged with 40.0 g aminocaproic acid, was added 500 mL of methanol. Hydrogen chloride gas was bubbled through the mixture for 5 minutes, and the mixture was stirred at room temperature for 5 hours. The mixture was then concentrated via rotary evaporation and then under full vacuum pump pressure (<0.1 mm Hg) to afford 55 g of the product as a white solid (99%): ^{1}H—NMR (200 MHz, CD_3OD); 3.67 (s, 3H), 3.02 (t, 2H), 2.68 (s, 3H), 2.48 (t, 2H), and 2.03–1.87 (pentet, 2H) ppm.

Methyl 6-(trifluoroacetamido)-hexanoate: To a 1 L round bottom flask, charged with 25.0 g (138 mmol) of methyl 6-aminohexanoate hydrochloride and 500 mL of methylene chloride, was added 24 mL (170 mmol) trifluoroacetic anhydride. The mixture was cooled in an ice bath, and 42 mL (301 mmol) of triethylamine was added over a 25–30 minute period. The mixture was stirred at 0° C. to room temperature for 2 hours and then concentrated. The residue was diluted with 150 mL of diethyl ether and 150 mL of petroleum ether, and the resulting solution was washed first with 1 N aqueous HCl (3×150 mL) and then with saturated aqueous sodium bicarbonate (3×150 mL). The organic phase was dried over magnesium sulfate, filtered and concentrated to give 32.9 g of the product as a pale yellow oil (99%): ^{1}H—NMR (200 MHz, d_6-DMSO); 9.39 (m, 1H), 3.57 (s, 3H), 3.14 (q, 2H), 2.29 (t, 2H), 1.60–1.38 (m, 4H), and 1.32–1.19 (m, 2H) ppm.

N,N'-Bis(6-methoxycarbonylhexyl)amine hydrochloride. To a 500 mL dry round bottom flask, charged with 12.0 g (50.0 mmol) of the secondary amide, methyl 6-trifluoroacetamido)-hexanoate, and 250 mL of dry tetrahydrofuran, was added 2.2 g (55 mmol, 1.1 equiv) of

60% sodium hydride. The mixture was stirred at room temperature for 30 minutes and then 10.25 g (49.0 mmol, 0.98 equiv) of the alkyl bromide, methyl 6-bromohexanoate, was added. The mixture was stirred at reflux for 3 hours. an additional 5.80 g (27.7 mmol, 0.55 equiv) of methyl 6-bromohexanoate was added, and the mixture was stirred at reflux for 70 hours. The mixture was cooled, diluted with 150 mL of 1 N aqueous HCl and then extracted with ethyl acetate (3×100 mL). The organic extracts were combined, dried over magnesium sulfate, filtered and concentrated. The residue was diluted with 200 mL of methanol and then treated with 30 mL of 10 N aqueous sodium hydroxide. The mixture was stirred at room temperature for 18 hours and then concentrated. The residue was diluted with 200 mL of deionized water and acidified to pH 1–2 with 37% concentrated HCl. The solution was washed with diethyl ether (3×100 mL). The aqueous phase was concentrated. The residue was diluted with 200 mL of methanol and reconcentrated. The subsequent residue was diluted with 250 mL of methanol, and HCl gas was bubbled through for 2–3 minutes followed by stirring at room temperature for 3 hours. The mixture was concentrated. The residue was diluted with 300 mL of methanol and filtered to remove inorganic salts. The filtrate was treated with 3 g of activated charcoal, filtered through Celite (manufactured by J. T. Baker) and concentrated. The residue, an off-white solid, was recrystallized from 100 mL of 2-propanol to afford 7.0 g of the product as a white solid. Concentration of the filtrate and further recrystallization of the residue yielded an additional 1.65 g of the product for a total of 8.65 g (56%): ^{1}H—NMR (200 MHz, d_6-DMSO); 3.57 (s, 3H), 2.90–2.73 (m, 4H), 2.30 (t, 4H), 1.67–1.44 (m, 8H), and 1.37–1.20 (m, 4H) ppm.

Methyl 4-methylaminobutyrate hydrochloride. To a 1 L round bottom flask, charged with 30.0 g (195 mmol) of 4-methylaminobutyric acid and 500 mL of methanol, was bubbled HCl gas for 1–2 minutes. The mixture was stirred at room temperature for 3–4 hours and then concentrated to afford 32.5 g of the product as a foamy, off-white solid (99%): ^{1}H—NMR (200 MHz, CD_3OD); 3.67 (s, 3H), 3.03 (t, 2H), 2.68 (s, 3H), 2.48 (t, 2H), and 2.03–1.87 (pentet, 2H) ppm.

4-Methylaminobutanol. To a 1 L round bottom flask, charged with 32.5 g (194 mmol) of the ester, methyl 4-methylaminobutyrate hydrochloride, was added 500 mL of 1 M borane in tetrahydrofuran over a 1 hour period at 0° C. After the addition was complete, the mixture was refluxed for 20 hours, cooled to 0° C., and the excess borane was destroyed by careful addition of 100 mL of methanol. After all the methanol was added, the mixture was stirred at room temperature for 1 hour and then concentrated. The residue was diluted with 400 mL of methanol and then HCl gas was bubbled into the solution for 5 minutes. The mixture was refluxed for 16 hours. The mixture was cooled, concentrated and then diluted with 250 mL of deionized water. the product was initially free based by addition of 10 N aqueous sodium hydroxide, to a pH of 9–9.95, and then by addition of 70 g of AG 1 X-8 anion exchange resin (hydroxide form) commercially available from BioRad), and by stirring the solution for 2 hours. The resin was filtered off and washed with 150 mL of deionized water. The aqueous filtrates were combined and concentrated. The residue was diluted with 200 mL of 2-propanol and filtered. The collected solids were rinsed with 100 mL of 2-propanol. The organic filtrates were combined and concentrated. The residue was distilled under reduced pressure to afford 12.85 g of the product as a colorless oil (bp 68° C. at 0.1–0.2 mm HG; 64%): ^{1}H—NMR (200 MHz, D_2O); 3.52 (t, 2H), 2.56 (t, 2H), 2.31 (s, 3H), and 1.65–1.43 (m, 4H) ppm.

4-(N-Methyl-trifluoroacetamido)-1-butanol. To a 250 mL round bottom flask, charged with 10.0 g (96.9 mmol) of the amine, 4-methylaminobutanol, in 100 mL of dry methanol, was added 17.5 mL (147 mmol) of ethyl trifluoroacetate. The mixture was stirred at room temperature for 24 hours and then concentrated to afford 18.55 g of the product as a near colorless oil (96%): ^{1}H—NMR (200 MHz, D_2O); 3.63 and 3.50 (2t's, 4H), 3.20 and 3.05 (d and s, 3H), and 1.82–1.47 (m, 4H) ppm.

1-(p-Toluenesulfonyloxy)-4-(N-methyl-trifluoroacetamido)butane. To a 1 L dry round bottom blask; charged with 17.0 g (85.4 mmol) of the alcohol, 4-(N-methyl-trifluoroacetamido-1-butanol, in 400 mL of methylene chloride, was added 17.1 g (89.7 mmol, 1.05 equiv) of toluenesulfonyl chloride followed by 30 mL (213 mmol, 2.5 equiv) of triethylamine at 0° C. over a 10 minute period. The mixture was stirred at 0° C. to room temperature for 15 hours and then washed with 5% v/v aqueous HCl (3×200 mL). the organic phase was dried over magnesium sulfate, filtered and concentrated. The residue was chromatographed on silica gel, eluting with 50:50 hexane/methylene chloride and then with methylene chloride, to give 25.1 g of the product as a pale yellow oil (83%): ^{1}H—NMR (200 MHz, $CDCL_3$); 7.80 (d, 2H), 7.37 (d, 2H), 4.07 (m, 2H), 3.41 (m, 3H), 3.09 and 2.98 (q and s, 3H), 2.45 (s, 3H), and 1.68 (m, 4H) ppm: TLC (methylene chloride) R_f=0.31.

1-S-(2,3,4,6-tetra-O-acetyl-beta-D-galacto-pyranosyl)-2-thiopseudourea hydrobromide. To a 250 mL round bottom flask, charged with 5.08 g (60.3 mmol, 1.09 equiv) of thiourea and 36 mL of acetone, was added 25.0 g (66.7 mmo9l) of tetra-acetyl-alpha-D-galactopyranosyl bromide. The mixture ws stirred at reflux for 15–20 minutes and then cooled on ice. The mixture was filtered into a Buchner funnel and rinsed with 25 mL of ice cold acetone. The solids were treated with 50 mL of acetone, refluxed for 15 minutes, cooled on ice, and filtered. The solids were rinsed with 25 mL of cold acetone, air dried and then dried under vacuum to give 22.6 g of the product as a white solid (76%): ^{1}H—NMR (200 MHz, d_6-DMSO); 9.4–9.0 (broad d, 4H), 5.63 (d, 1H), 5.38 (d, 1H), 5.23 (dd, 1H), 5.09 (t, 1H), 4.40 (t, 1H, 4.04 (dd, 1H), 2.13 (s, 3H), 2.08 (s, 3H), 2.00 (s, 3H), 1.93 (s, 3H) ppm.

4-(N-Methylaminobutyl)-1-thio-beta-D-galactopyranoside. To a 500 mL round bottom flask, charged with 20.7 g (42.5 mmol, 1.07 equiv) of the thiopseudourea hydrobromide prepared as described above in 70 mL of deionized water, was added 6.4 g (46.3 mmol, 1.16 equiv) of potassium carbonate and 4.7 g (45.2 mmol, 1.13 equiv) of sodium bisulfite followed immediately by 14.1 g (39.9 mmol, 1.0 equiv) of the tosylate, 1-(p-toluenesulfonyloxy)-4-(N-methyl-trifluoroacetamido)butane in 70 mL of acetone. The mixture was stirred at room temperature for 16 hours. The mixture was diluted with 50 mL of brine and extracted

with ethyl acetate (3×200 mL). The organic extracts were combined, dried over magnesium sulfate, filtered and concentrated. The residue was chromatographed on silica gel, eluting first with 75% methylene chloride/hexane, followed by methylene chloride, then with 2% methanol/methylene chloride and finally with 10% methanol/methylene chloride. Fractions containing alkylation product with different degrees of acetylation were combined and concentrated. The residue was diluted with 250 mL of methanol and 150 mL of deionized water and treated with 110 g of AG-1 X-8 resin (hydroxide form; 2.6 m equiv/g dry weight) commercially available from BioRad. The mixture was stirred at room temperature for 18 hours. The mixture was filtered, and the resin was rinsed with methanol (2×150 mL). The filtrates were combined and concentrated to afford 6.1 g of product (54%): ^{1}H—NMR (200 MHz, D_2O); 4.38 (d, 1H), 3.88 (d, 1H), 3.69–3.41 (m, 5H), 2.82–2.64 (m, 4H), 2.43 (s, 3H), and 1.68–1.57 (, 4H) ppm.

Biotin bis-methyl ester: To a 50 mL round bottom flask, charged with 1.00 g (3.23 mmol, 1.13 equiv) of amine hydrochloride, N,N'-bis-(6-methoxycarbonyl-hexyl)amine hydrochloride), and 1.30 g (2.86 mmol) of caproamidobiotin-NHS-ester (preparable by standard methods or commercially available from Sigma Chemical Company) and 10 mL of dry dimethylformamide, was added 1.5 mL (10.6 mmol) of triethylamine. The mixture was stirred at 85° C. for 2 hours and then concentrated via reduced pressure rotary evaporation. The residue was chromatographed on silica gel, eluting with 75:25:0.05 ethyl acetate/methanol/acetic acid, to afford 1.63 g of the product as a white foamy solid (98%): ^{1}H—NMR (200 MHz d_6-DMSO); 7.72 (t, 1H), 6.41 (s, 1H), 6.34 (s, 1H), 4.29 (m, 1H, 4.11 (m, 1H), 3.57 (s, 6H), 3.23–2.91 (m, 7H) 2.81 (dd, 1H), 2.55 (d, 1H), 2.35–2.13 (m, 6H), 2.03 (t, 2H) 1.65–1.10 (m, 24H) ppm: TLC; R_f=0.58 (75:25:0.01 ethyl acetage/methanol/acetic acid).

Biotin bis-acid: To a 200 mL round botom flask, charged with 1.61 g (2.63 mmol) of biotin bis-methyl ester and 50 mL of methanol, was added 5 mL of 3 N aqueous sodium hydroxide. The mixture was stirred at 40° C. for 3 hours and then concentrated via reduced pressure rotary evaporation. The residue was diluted with 50 mL of deionized water, and then 3 N aqueous HCl was added until a pH of 1–2 was attained. The mixture was again concentrated. The residue was chromatographed on C-18 reverse phase silica gel, eluting first with 20:80:-0.1 acetonitrile/water/trifluoroacetic acid and then with 50:50:0.1 acetonitrile/water/trifluoroacetic acid. The fractions containing product were combined and concentrated. The residue was diluted with 40 mL of water and 20 mL of acetonitrile. The solution was frozen (−70° C.) and lyophilized to afford 1.42 g of the product as a fluffy white solid (92%): ^{1}H—NMR (200 MHz d_6-DMSO); 7.72 (t, 1H), 6.61 (broad s, 2H), 4.29 (m, 1H), 4.11 (m, 1H), 3.35–2.93 (m, 7H) 2.81 (dd, 1H), 2.55 (d, 1H), 2.28–2.12 (m, 6H), 2.03 (t, 2H), 1.68–1.10 (m, 24H) ppm: TLC; R_f=0.30 (50:50:0.01 acetonitrile/water/trifluoroacetic acid).

Biotin tetra-methyl ester: To a 50 mL round bottom flask, charged with 350 mg (0.599 mmol) of the biotin bis-acid, 402 mg (1.30 mmol, 2.16 equiv) of amine hydrochloride, N,N'-bis-(6-methoxycarbonyl-hexyl)amine hydrochloride), and 10 mL of dry dimethylformamide, was added 556 mg (1.26 mmol, 2.10 equiv) BOP and 500 microliters (3.54 mmol, 5.91 equiv) of triethylamine. The mixture was stirred at room temperature for 2 hours and then concentrated via reduced pressure rotary evaporation. The residue was chromatographed on C-18 reverse phase silica gel, eluting first with 50:50 methanol/water and then with 85:15 methanol/water, to afford 618 mg of the product as a foamy white solid (95%): ^{1}H—NMR (200 MHz d_6-DMSO); 7.71 (t, 1H), 6.1 (broad s, 2H), 4.29 (m, 1H), 4.11 (m, 1H), 3.57 (s, 12H, 3.25–2.91 (m, 15H) 2.81 (dd, 1H), 2.55 (d, 1H), 2.35–2.12 (m, 14H, 2.02 (t, 2H), 1.65–1.10 (m, 48H) ppm: TLC; R_f=0.48 (85:15 methanol/water).

Biotin tetra-acid: To a 50 mL round bottom flask, charged with 350 mg (0.319 mmol) of biotin tetra-methyl ester and 15 mL of methanol, was added 5 mL of 1 N aqueous sodium hydroxide and 5 mL of deionized water. The mixture was stirred at room temperature for 14 hours and then concentrated via reduced pressure rotary evaporation. The residue was diluted with 15 mL of deionized water, acidified to pH 1–2 by addition of 6 N aqueous HCl and then reconcentrated. The residue was chromatographed on C-18 reverse phase silica gel, eluting first with 50:50 methanol/water and then with 70:30 methanol/water. The fractions containing the product were combined and concentrated. The residue was diluted with 10 mL of water and 8 mL of acetonitrile. The solution was frozen (−70° C.) and lyophilized to afford 262 mg of the product as a fluffy white solid (79%): ^{1}H—NMR (200 MHz d_6-DMSO); 7.71 (t, 1H), 6.41 (s, 1H), 6.34 (s, 1H), 4.29 (m, 1H), 4.11 (m, 1H), 3.25–2.93 (m, 15H) 2.81 (dd, 1H), (dd, 1H), 2.55 (d, 1H), 2.31–2.10 (m, 14H), 2.02 (t, 2H), 1.63–1.09 (m, 48H) ppm: TLC; R_f=0.45 (70:30 methanol/water).

Biotin octa-methyl ester: To a 25 mL round bottom flask, charged with 220 mg (0.710 mmol, 4.93 equiv) of amine hydrochloride, N,N'-bis-(6-methoxycarbonyl-hexyl)amine hydrochloride), 150 mg (0.144 mmol) of the biotin tetra-acid, and 5 mL of dry dimethylformamide, was added 300 mg (0.678 mmol), 4.71 equiv) BOP followed by 500 microliters (3.54 mmol, 24.0 equiv) of triethylamine. The mixture was stirred at room temperature for 3 hours and then concentrated via reduced pressure rotary evaporation. The residue was chromatographed on C-18 reverse phase silica gel, eluting first with 60:40 methanol/water and then with 90:10 methanol/water, to afford 246 mg of the product as a foamy white solid (83%): ^{1}H—NMR (200 MHz d_6-DMSO); 7.71 (t, 1H), 6.41 (s, 1H), 6.34 (s, 1H), 4.29 (m, 1H), 4.11 (m, 1H), 3.57 (s, 24H), 3.25–2.91 (m, 31H) 2.81 (dd, 1H), (d, 1H), 2.32–2.12 (m, 30H), 2.02 (t, 2H), 1.65–1.08 (m, 96H) ppm: TLC; R_f=0.42 (90:10 methanol/water).

Biotin octa-acid. To a 50 mL round bottom flask, charged with 235 mg (0.114 mmol) of biotin octa-methyl ester and 10 mL of methanol, was added 5 mL of 1 N aqueous sodium hydroxide and 5 mL of deionized water. The mixture was stirred at room temperature for 14 hours and then concen-

trated via reduced pressure rotary evaporation. The residue was diluted with 10 mL of deionized water, acidified to pH 1–2 by addition of 6 N aqueous IICl and then reconcentrated. The residue was chromatographed on C-18 reverse phage silica gel, eluting first with 50:50 methanol/water and then with 75:25 methanol/water. The fractions containing the product were combined and concentrated. The residue was diluted with 20 mL of 1:1 (ratio by volume) acetonitrile/water. The solution was frozen (−70° C.) and lyophilized to afford 202 mg of the product as a fluffy white solid (91%): ^{1}H—NMR (200 MHz d_6-DMSO); 7.71 (t, 1H), 6.41 (s, 1H), 6.34 (s, 1H), 4.29 (m, 1H), 4.11 (m, 1H), 3.29–2.91 (m, 31H) 2.81 (dd, 1H), 2.55 (d, 1H), 2.31–2.10 (m, 30H), 2.03 (t, 2H), 1.65–1.09 (m, 96H) ppm: TLC; R_f=0.51 (75:25 methanol/water).

Biotin hexadeca-methyl ester: To a 25 mL round bottom flask, charged with 154 mg (0.497 mmol, 10.0 equiv) of amine hydrochloride, N,N'-bis-(6-methoxycarbonyl-hexyl) amine hydrochloride), 97 mg (0.0497 mmol) of the bioxin octa-acid, and 5 mL of dry dimethylformamide, was added 202 mg (0.457 mmol, 9.2 equiv) BOP followed by 500 microliters (3.54 mmol, 71.2 equiv) of triethylamine. The mixture was stirred at room temperature for 8 hours and then concentrated via reduced pressure rotary evaporation. The residue ws chromatographed on silica gel, eluting first with 70:30 methanol/water and then with 95:5 methanol/water, to afford 149 mg of the product as a foamy white solid (75%): ^{1}H—NMR (200 MHz d_6-DMSO); 7.71 (t, 1H), 6.41 (s, 1H), 6.34 (s, 1H), 4.29 (m, 1H), 4.11 (m, 1H), 3.57 (s, 48H), 3.25-2.92 (m, 63H) 2.81 (dd, 1H), 2.55 (d, 1H), 2.35-2.11 (m, 62H), 2.01 (t, 3H), 1.65-1.08 (m, 192H)ppm: TLC; R_f=0.31 (95:5 methanol/water).

Biotin hexadecyl-acid: To a 50 mL round bottom flask, charged with 141 mg (0.0353 mmol) of biotin hexadeca-methyl ester and 15 mL of methanol, was added 8 mL of 1N aqueous sodium hydroxide and 5 mL of deionized water. The mixture was stirred at room temperature for 14 hours and then concentrated via reduced pressure rotary evaporation. The residue was diluted with 15 mL of deionized water, acidified to pH 1–2 by addition of 6N aqueous HCl and then reconcentrated. The residue was chromatographed on C-18 reverse phase silica gel, eluting first with 60:40 methanol/water and then with 85:15 methanol/water. The fractions containing the product were combined and concentrated. The residue was diluted with 20 mL of 1:1 acetonitrile/water. The solution was frozen (−70° C.) and lyophilized to afford 130 mg of the product as a fluffy white solid (75%): ^{1}H-NMR (200 MHz d_6-DMSO); 7.71 (t, 1H), 6.41 (s, 1H), 6.34 (s, 1H), 4.29 (m, 1H), 4.11 (m, 1H), 3.26-2.92 (m, 63H) 2.81 (dd, 1H), 2.55 (d, 1H), 2.35-2.10 (m, 62H), 2.01 (t, 2H), 1.65-1.09 (m, 192H) ppm: TLC; R_f=0.64 (85:15 methanol/water).

Hexadeca-galactosyl biotin: To a 25 mL round bottom flask, charged with 125 mg (0.0332 mmol) of biotin hexadeca-acid, 179 mg (0.636 mmol, 19.2 equiv.) of galactose-amine, 4-(N-methylaminobutyl)-1-thio-beta-D-galactopyranoside, and 4 mL of dry methylformamide, was added 264 mg (0.587 mmol, 18.0 equiv) of BOP followed by 400 microliters (3.87 mmol, 86.5 equiv) of dry triethylamine. The mixture was stirred at room temperature for 17 hours and then concentrated via reduced pressure rotary evaporation. The residue was chromatographed on C-18 reverse phase silica gel, eluting first with 60:40 methanol/water and then with 75:25 methanol/water. The fractions containing the product were combined and concentrated and rechromatographed on C-18 reverse phase silica gel, eluting first with 40:60:01 acetonitrile/water/trifluoroacetic acid and then with 50:50:01 acetonitrile/water/trifluoroacetic acid. The fractions containing the product were again combined and concentrated. The residue was dissolved in 20 mL of water. The solution was frozen (−70° C.) and lyophilized to afford 173 mg of the product as a fluffy white solid (75%): ^{1}H-NMR (200 MHz D_2O); 4.52 (m, 1H), 4.37 (d, 15H), 3.90 (d, 16H), 3.70-3.42 (m, 80H), 3.41-3.05 (m, 95H), 2.98-2.82 (2s and 2m, 49H), 2.80-2.49 (m, 33H), 2.44-2.11 (m, 64H), 1.75-1.10 (m, 256H) ppm: TLC; R_f=0.53 (75:25 methanol/water).

The above procedure is designed for the formation of a galactose cluster of 16 galactose residues. The four or eight galactose versions can be made in accordance with this procedure by proceeding from the tetra acid or the octa acid to the galactose derivatization step, which was described above for the 16-galactose cluster. Similarly, 32, etc. galactose cluster constructs can be prepared in accordance with the present invention by introduction of more iterations of the methyl ester and acid formation steps. When the desired number of acid residues are formed, the galactose derivization step is employed, with the proportions of the components adjusted to accommodate the number of acid residues.

EXAMPLE V

First Generation CCA (Small Molecule Clearing Agent) Evaluation

In order to demonstrate the efficacy of the described small molecule clearing agents, a number of such conjugates were synthesized using a biotin binding moiety and galactose residue cluster directors. These conjugates were synthesized using different numbers of attached galactose residues. In addition, these conjugates contained either the long chain linker (LC=containing an aminocaproyl spacer between the amine associated with galactose and the carboxyl moiety associated with the biotin) or the short chain liner (SC= direct link between the amine associated with galactose and the carboxyl moiety associated with the biotin) as set forth below.

The conjugates involved in the testing are depicted below:

$(Galactosyl)_1$-SC-Biotin

MW: 507.64

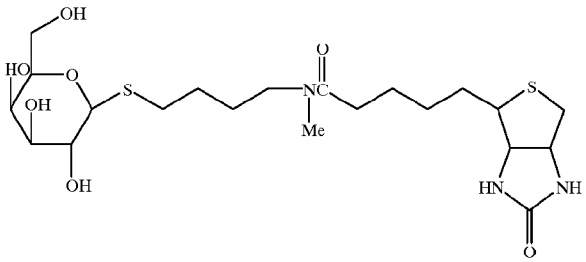

$(Galactosyl)_1$-LC-Biotin

MW: 620.80

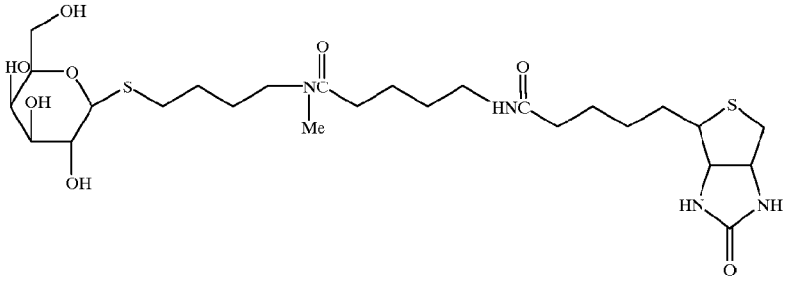

$(Galactosyl)_2$-SC-Biotin

MW: 998.27

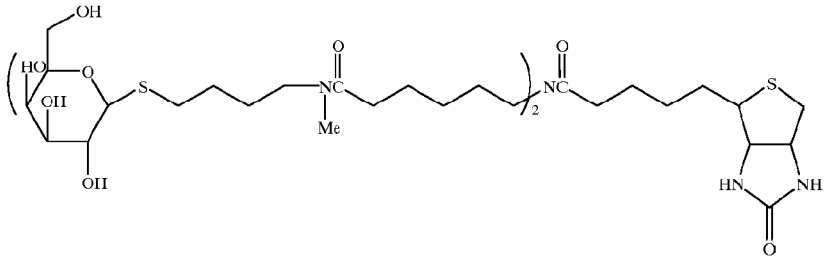

$(Galactosyl)_4$-SC-Biotin

MW: 1979.63

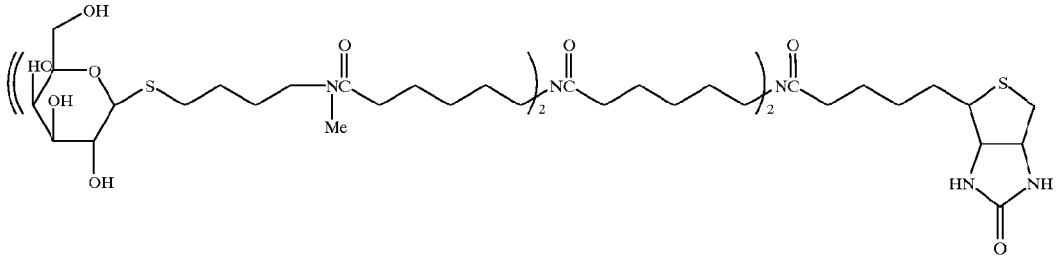

$(Galactosyl)_4$-LC-Biotin

MW: 2092.79

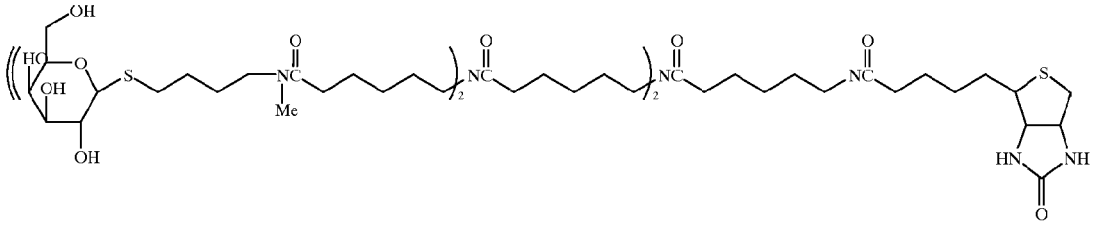

-continued

(Galactosyl)$_8$-SC-Biotin

MW: 3942.28

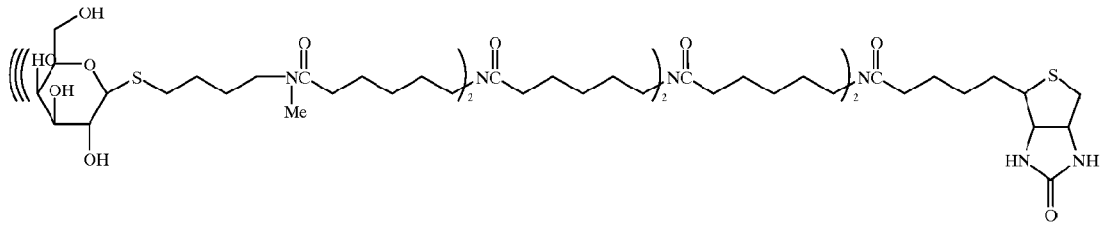

(Galactosyl)$_8$-LC-Biotin

MW: 4055.42

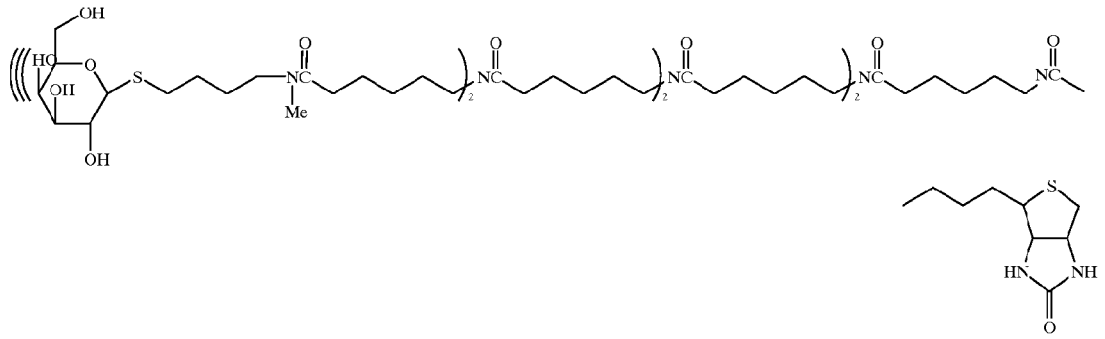

(Galactosyl)$_{16}$-LC-Biotin

MW: 7961.81

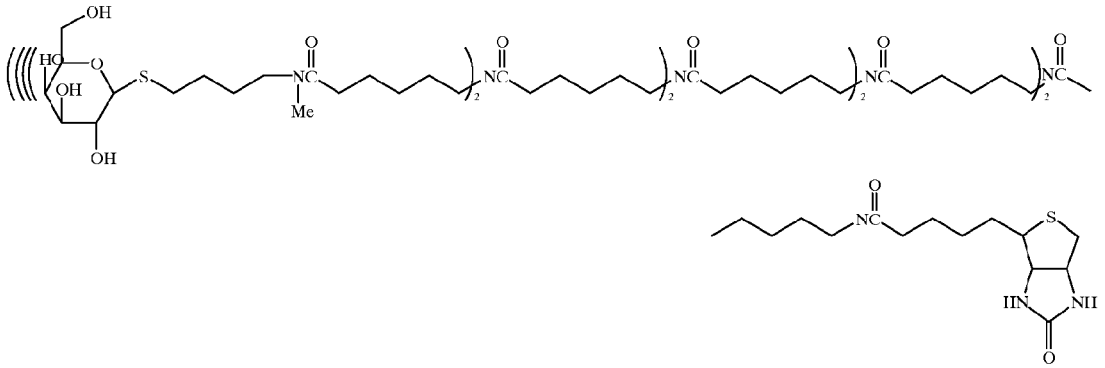

Some or all of these compounds were assayed for their clearance directing activity in two sets of experiments. The first set of experiments involved ex vivo preparation of a precomplexed monoclonal antibody-streptavidin-biotin-galactose cluster conjugate labeled with I-125, intravenous administration of the conjugate in a mouse model, and measuring serum levels of the conjugate over time. The second set of experiments involved intravenous administration of MAb-streptavidin conjugate followed by administration of biotin-galactose cluster conjugate.

NR-LU-10 antibody (MW 150 kD) was conjugated to streptavidin (MW 66 kD) (as described in Example II above), and radiolabeled with ^{125}I/PIP-NHS as described below. The antibody component of the conjugate was radioiodinated using p-aryltin phenylate NHS ester (PIP-NHS) and ^{125}I sodium iodide. In general, the experimentation involving the 2, 4 and 8 galactose-biotin constructs was conducted in an analogous manner to that for the 16 galactose-biotin construct as described below.

The data from these experiments indicates that no significant increase in serum clearance (in comparison to the MAb-Streptavidin conjugate itself) occurs until at least 4 galactose residues are attached to the biotin molecule. In addition, the data indicates that the longer linker separating the galactose cluster from the biotin molecule resulted in better clearance rates. This is consistent with the inventors' belief that the galactose cluster interferes with binding to the conjugate to be cleared if an appropriate length spacer is not used to minimize steric interactions or that sugar-hepatocyte interaction is sterically precluded.

In a third set of experiments conducted in vivo in the pretargeting format (e.g., administration of radiolabeled MAb-streptavidin conjugate followed by administration of clearing agent], the (galactosyl)$_8$-LC-biotin conjugate was also compared to galactose-HSA-biotin prepared as described above. This comparison was conducted in a Balb/c mouse model and was for the ability to clear an I-125 labeled monoclonal antibody-streptavidin conjugate (I-125 LU-10-

streptavidin) from circulation as a function of time. The results of this experiment indicate that the $(galactosyl)_8$-LC-biotin conjugate is comparable to galactosylated-HSA-biotin in its ability to clear the streptavidin-containing conjugate from circulation. Subsequent experiments have further shown that hepatic-directed compounds containing 16 galactose residues provide for even better clearance than those containing 8 galactose residues.

Experiments were designed and executed to evaluate a 16 galactose cluster-biotin construct without the stabilizing tertiary amine structure of the nitrogen of the amide closest to the biotin, the preparation of such a stabilized construct being described above in Example V.

BALB/c female mice (20–g) were injected i.v. with 120 micrograms of NR-LU-10-streptavidin conjugate radiolabeled with I-125, and blood was serially collected from n=3 mice. The clearance of the conjugate from the blood was measured of these control mice. Separate groups of mice were injected with either 120 or 12 micrograms of radiolabeled monoclonal antibody-streptavidin conjugate which had been precomplexed with the 16 galactose-biotin construct by mixing the biotin analog at a 20-fold molar excess with the antibody conjugate, and purifying the excess small molecule from the protein by size exclusion chromatography. Both doses of precomplexed conjugate showed extremely rapid clearance from the blood, relative to the antibody conjugate control.

Having shown that precomplexed material could clear rapidly and efficiently from the blood, experiments were conducted to measure the effectiveness of various doses of the 16 galactose-biotin construct to form rapidly clearing complexes in vivo. Mice received 400 micrograms of I-125 NR-LU-10-streptavidin conjugate intravenously, and approximately 22 hours later received the 16 galactose-biotin construct at doses of 100 50, or 10:1 (456, 28 and 45 micrograms, respectively) molar excess to circulating monoclonal antibody-streptavidin conjugate. While each dose was effective at clearing conjugate, the most effective dose (both kinetic and absolute) was the 10:1 dose. For the larger doses, there appears to be some saturation of the liver receptor, since both larger doses show a plateau in conjugate clearance for about 1 hour after administration of the 16 galactose-biotin construct. The larger doses may be sufficiently high to achieve competition between complexed and non-complexed 16-galactose-biotin for liver receptors, thereby precluding all but a small initial fraction of the complexed MAb-streptavidin conjugate from clearing via the liver. Following the plateau period, clearing of the conjugate remained slow and was eventually less complete than that achieve with the lower dose (approximately 10% of the conjugate remained in circulation at the higher doses, in comparison to 2% for the lower dose). An alternative explanation for this finding rests on the fact that the 16-galactose-biotin construct was not stabilized to potential biotinidase-mediated cleavage (e.g., the chemical synthesis did not incorporate a methyl, lower alkyl, carboxylic acid, lower alkyl carboxylic acid or like group was not bound to the amide nitrogen most closely adjacent the biotin rather than hydrogen). If the 16 galactose-biotin construct is unstable, sufficient biotin may be released at higher doses to that a significant portion of circulating conjugate became blocked thereby and, consequently, was not cleared via hepatic-mediated uptake.

Evident in all groups is the lack of a "rebound" or gradual increase in blood levels of circulating conjugate following disruption of the equilibrium between vascular and extravascular concentrations of conjugate. This constitutes the best evidence to date that galactose cluster-biotin constructs extravasate into extravascular fluid, and that conjugate which is complexed extravascularly clears very rapidly when it passes back into the vascular compartment.

Further experimentation in the same animal model compared $(galactose)_{35}$-HSA-$(biotin_2$ clearing agents prepared as described above and decreasing doses of 16 galactose-biotin construct as in vivo clearing agents. A 46 microgram dose of 16 galactose-biotin was found to be optimal and more effective than the previously optimized dose of $(galactose)_{35}$-HSA-$(biotin)_2$. Lower (12 and 23 microgram) and higher (228 microgram) doses of 16 galactose-biotin were less efficient at removing circulating conjugate, and the lower doses showed a significant rebound effect, indicating that incomplete complexation with circulating conjugate may have occurred.

Having shown that effective clearing could be achieved with the appropriate does of 16 galactose-biotin construct, studies were undertaken in tumored nude mice to evaluate the potential blockade of tumor-associated conjugate by the small 16 galactose-biotin. Mice bearing either SW-1222 colon tumor xenografts or SHT-1 small cell lung cancer (SCLC) tumor xenografts were pretargeted with NR-LU-1-streptavidin conjugate and, 22 hours later, received 46 micrograms of 16 galactose-biotin. After 2 hours, Y-90-DOTA-biotin prepared as described above was administered, and its uptake and retention in tumor and non-target tissues was evaluated by sacrifice and tissue counting for radioactivity 2 hours post-administration.

In comparison to historical controls employing $(galactose)_{35}$-HSA-$(biotin)_2$, tumor targeting was slightly lower in the high antigen-expressing colon xenograft and was slightly higher in the low antigen-expressing SCLC xenograft. Given the normal variability in such experiments, tumor uptake of radioactivity was assessed as roughly equivalent, a surprising result given the potential for target uptake of 16 galactose-biotin. Non-target organ uptake was comparable in all tissues except liver, where animals receiving 16 galactose-biotin showed slightly higher levels. The historical controls were conducted with a 3 hour time period between clearing agent and radioactivity administration. When such a 3 hour period was allowed between 16 galactose-biotin and radioactivity administration, the liver levels were lower and comparable to that of the HSA-containing agent (approximately 1% injected dose/gram).

Experiments were also carried out using I-125 labeled MAb-streptavidin conjugate and IN-111 labeled DOTA-biotin to assess the relative stoichiometry of those materials at the tumor target site using 16 galactose-biotin as a clearing agent. Previous studies with $(galactose)_{35}$-HSA-$(biotin)_2$ had shown that an expected 4:1 ratio of DOTA-biotin to MAb-streptavidin (streptavidin has 4 biotin binding sites) could be achieved at the tumor with an optimized dose of that clearing agent. When a similar protocol was employed with the 16 galactose-biotin construct, the ratio of

DOTA-biotin to MAb-streptavidin was only 2.65. This indicated that some filling of tumor-associated streptavidin may have occurred, although the nature of such blockage (16 galactose-biotin or biotin released therefrom) was undetermined. Experiments to assess the nature of this blockade are underway.

In summary, galactose cluster conjugates exhibited ability to clear circulating conjugate, provided the galactose cluster contains a sufficient number of appropriately spaced galactosyl residues. 16 Galactose-biotin has proven to be an effective construct for clearing MAb-streptavidin from the circulation (both vascular and extravascular spaces). Despite an apparent blockade of some pretargeted biotin binding sites at the tumor, efficient tumor targeting can still be achieved using this agent. Stabilization of the linkage between biotin and the galactose cluster may minimize any tumor-associated biotin binding site compromise by the galactose cluster-biotin construct.

EXAMPLE VI

Second Generation CCA Preparation

Preparation of second generation CCAs is shown schematically in FIGS. **3–7**.

A. Preparation of 16-N-AcetylGalactosamine-Biotin-CCA (alpha-sulfur) Corresponding to Compound 25 in FIG. **3**.

Preparation of Methyl 6-bromohexanoate (1)

To a 2 liter round bottomed flask, charged with 99.7 g (0.511 mol) of 6-bromohexanoate (Aldrich Chemical Co., Milwaukee, Wis.) and 1 liter of methanol, was bubbled hydrogen chloride gas for 1–2 minutes. The mixture was stirred at 20–30° C. for 18 h and then concentrated via rotary evaporation. The residue was diluted with 500 mL of diethyl ether and washed with 150 mL of de-ionized water, 200 mL of saturated sodium bicarbonate, and then once again with 200 mL of de-ionized water. The organic phase was dried over anhydrous magnesium sulfate, filtered and concentrated via rotary evaporation. The residue was distilled under vacuum to afford 99.6 g of the product (1) as a colorless oil (93%): b.p.=93–96° C. at 3 mm Hg: ^{1}H NMR (d_6-DMSO) d 3.57 (3H, s), 3.51 (2H, t), 2.30 (2H, t), 1.78 (2H, pentet) and 1.62-1.28 (4H, m) ppm.

Preparation of Methyl 6-Aminohexanoate Hydrochloride (2)

To a 2 liter round bottom flask, charged with 101.3 g (0.722 mol) of 6-aminohexanoate (Aldrich Chemical Co.) in 1 liter of methanol was bubbled hydrogen chloride gas for 3–4 minutes. the mixture was stirred at 20–30° C. for 16 h and then concentrated via rotary evaporation. The residue was twice diluted with 500 mL of methanol and re-concentrated (<0.5 mm Hg) to afford 140.1 g of the product (2) as a white solid (100%): ^{1}H NMR (d_6-DMSO) d 9.40 (1H, broad triplet), 3.57 (3H, s), 3.15 (2H, quartet), 2.29 (2H, t), 1.60-1.38 (4H, m) and 1.32-1.19 (2H, m) ppm.

Preparation of Methyl 6-(Trifluoroacetamido)hexanoate (3 3)

To a 2 liter round bottom flask, charged with 100.2 g (0.552 mol) of amine hydrochloride 2 and 1 liter of methanol was added 100 g (0.703 mol) of ethyl trifluoroacetate followed by 120 mL (0.861 mol) of triethylamine. The mixture was stirred at 20–30° C. for 19 h and then concentrated via rotary evaporation. The residue was diluted with 500 mL of diethyl ether and then filtered. The filtrate was washed with 3×300 mL aliquots of 1N aqueous HCl, 200 mL of de-ionized water, 2×200 mL aliquots of saturated aqueous sodium bicarbonate and finally with 200 mL of de-ionized water. The organic phase was dried over anhydrous magnesium sulfate, filtered and concentrated. The residue was distilled under vacuum to afford 115.8 g of the product (3) as a colorless oil: b.p.=113–116° C. at 120 mm Hg: ^{1}H NMR (d_6-DMSO) d 3.57 (3H, s), 2.75 (2H, m), 2.29 (2H, t), 1.60-1.40 (4H, m) and 1.37-1.19 (2H, m) ppm.

Preparation of N,N-Bis-(5-Methoxycarbonylpentyl)amine Hydrochloride (4)

To a 5 liter three neck flask equipped with a reflux condenser connected to a gas bubbler, charged with 20.9 g of 60% sodium hydride (0.523 mol) in 1 liter of anhydrous dioxane, was added 100 g (0.416 mol) of secondary amide 3 in 200 mL of dry dioxane over a 20 minute period. The mixture was stirred at 20–30° C. for 1 h, and then 130 g (0.622 mol) of bromide 1 in 100 mL of dioxane was added. The mixture was heated to reflux and stirred for 7 h. An additional 10 g of 1 was added and the resulting mixture stirred for 15 h more. The mixture was cooled and concentrated via rotary evaporation. The residue was diluted with 600 mL of 1N aqueous HCl and extracted with 1 liter of ethyl acetate. The organic phase was then washed with 250 mL of de-ionized water, 250 mL of 5% aqueous sodium metabisulfite, and finally with 250 mL of de-ionized water. The organic phase was dried over anhydrous magnesium sulfate, filtered and concentrated.

The residue was diluted with 300 mL of de-ionized water and 500 mL of methanol and treated with 200 mL of 10N aqueous sodium hydroxide. The mixture was stirred at 20–30° C. for 16 h and concentrated to a thick syrup via rotary evaporation. The residue was diluted with 800 mL of deionized water and acidified to pH 1–2 with 200 mL of concentrated HCl. The mixture was washed with 3×300 mL aliquots of diethyl ether and the aqueous phase then concentrated to a thick syrup via rotary evaporation. The residue was diluted with 1 liter of dry methanol and re-concentrated via rotary evaporation. The residue was diluted with 1 liter of dry methanol and then hydrogen chloride gas was bubbled into the mixture of 2–3 minutes. The mixture was stirred at 20–30° C. for 18 h, and then vacuum filtered through Celite (manufactured by J. T. Baker). The solids were rinsed with 200 mL of methanol. The combined filtrates were concentrated. The residue was diluted with 1 liter of methanol and hydrogen chloride gas again bubbled into the mixture for 2–3 minutes. The mixture was stirred for 3 h and then concentrated. The residue was diluted with 1 liter of methanol and 10 g of activated charcoal was added. The mixture was stirred for 30 minutes and then vacuum filtered through Celite. The solids were washed with 100 mL of methanol and the combined filtrates concentrated. The residue was dissolved in hot 2-propanol and then allowed to recrystallize, first at room temperature and then with the use of an ice bath. The solids were filtered and rinsed with 3×75 mL aliquots of cold 2-propanol. The solids were air dried to afford 70.5 g of the product (4) as a white solid. The filtrates were combined and concentrated. The residue was recrystallized from 200 mL of 2-propanol to afford an additional 15.3 g of product for a total of 85.8 g (67%): ^{1}H NMR (d_6-DMSO) d 8.69 (2H, broad), 3.57 (6H, s), 2.82 (4H, m), 2.30 (4H, t), 1.67-1.43 (8H, m) and 1.28-1.19 (4H, m) ppm;

^{1}H NMR (CD_3OD) d 3.66 (6H, s), 3.42 (4H, t), 2.34 (4H, t), 1.75-1.55 (8H, m) and 1.45-1.25 (4H, m) ppm.

Preparation of N-BOC-5-Aminopentanol (5)

To a 2 liter three neck round bottom flask, fitted in the center neck with 500 mL addition funnel and in a side neck with an adaptor venting to a gas bubbler, was added 40 g (0.388 mol) of 5 aminopentanol in 500 mL of dry acetonitrile. Then 84.5 g (0.387 mol) of di-t-butyl-dicarbonate in 400 mL of dry acetonitrile was added over a 50 minute period. The mixture was stirred at 20–30° C. for 15 h and then concentrated. The residue was diluted with 600 mL of ethyl acetate and washed with 2×200 mL aliquots of 0.5N aqueous HCl and 2×200 mL aliquots of de-ionized water. The organic phase was dried over anhydrous magnesium sulfate, vacuum filtered, and concentrated, first via rotary evaporation and then using full vacuum pump pressure (<0.5 mm Hg), to afford 74.5 g of the product (5) as a near colorless oil (88%): ^{1}H NMR (d_6-DMSO) d 6.72 (1H, broad triplet), 4.31 (1H, t), 3.43-3.27 (2H, m), 2.87 (2H, quartet), and 1.45-1.10 (15H, s and multiplet) ppm; ^{1}H NMR ($CDCl_3$) d 4.58 (1H, broad s), 3.65 (2H, t), 3.13 (2H, quartet), and 1.70-1.30 (15H, singlet and multiplet) ppm: Thin Layer Chromatography (Visualization with ninhydrin spray and heat); Silica Gel, R_f=0.28 (9⅝ methylene chloride/methanol).

Preparation of N-BOC-5-Aminopentyltoluenesulfonate (66)

To a 1 liter round bottom flask, charged with 74.5 g (0.366 mol) of N-BOC-aminopentanol (6) in 400 mL of methylene chloride, was added 45 mL of anhydrous pyridine followed by 74.1 g (0.389 mol) of p-toluenesulfonyl chloride. The mixture was stirred at room temperature for 17 h, diluted with 200 mL of methylene chloride and washed with 400 mL of 0.5N HCl, 2×200 mL aliquots of 0.5N HCl, and 2×100 mL aliquots of de-ionized water. The organic phase was dried over anhydrous magnesium sulfate, vacuum filtered, and concentrated. The residue was chromatographed on 11×23 cm of silica gel, eluting first with methylene chloride and then with 3:97 ethyl acetate/methylene chloride. The fractions containing product were combined and concentrated, first via rotary evaporation and then under full vacuum pump pressure (<0.5 mm Hg), to afford 82.13 g of the product (6) as a white solid: ^{1}H NMR ($CDCl_3$) d 7.77 (2H, d), 7.31 (2H, d), 4.45 (1H, broad s), 3.98 (2H, t), 3.03 (2H, t), 2.41 (3H, s), and 1.80-1.20 (15H, singlet and multiplet)ppm: Thin Layer Chromatography (Visualization with ninhydrin spray and heat); Silica Gel, R_f=0.50 (3:97 ethyl acetate/methylene chloride).

Preparation of 1-b,3,4,6-Tetra-O-Acetyl-N-Acetyl-Galactosamine (7)

To a 500 mL round bottom flask charged with 25.0 g (116 mmol) of galactosamine hydrochloride (Sigma Chemical Co., St. Louis, Mo.) was added 180 mL of anhydrous pyridine and then 115 mL of acetic anhydride (1.22 mol). The mixture was stirred at 20–30° C. for 44 h and then poured into a 2 liter beaker containing 600 g of ice and 600 mL of de-ionized water. The mixture was stirred at room temperature for 10–15 minutes and then vacuum filtered. The collected solids were rinsed with 4×100 mL aliquots of de-ionized water, air dried for 2 h and then dried under full vacuum pump pressure (<0.5 mm Hg) for 14 h to give 39.8 g of the product as a white sole (88%): ^{1}H NMR (d_6-DMSO) d 7.89 (1H, d), 5.63 (1H, d), 5.16 (1H, d), 5.07 (1H, dd), 4.28-3.92 (4H, m), 2.11 (3H, s), 2.02 (3H, s), 1.99 (3H, s), 1.90 (3H, s) and 1.88 (3H, s) ppm.

Preparation of 3,4,6-Tri-O-Acetyl-N-Acetyl-Galactosamine-1-b-Pseudothioure a Hydrochloride (9)

To a 1 liter round bottom flask, charged with 39.8 g (102 mmol) of 7, was added 400 mL of acetyl chloride. The mixture was stirred at 47–48° C. for 64 h. The mixture was concentrated and then twice diluted with 200 mL of methylene chloride and re-concentrated, first via rotary evaporation and then under full vacuum pump pressure (<0.5 mm Hg), to afford 40.2 g of the crude product (8) as a dark amber foamy solid: H NMR ($CDCl_3$) d 6.24 (1H, d), 5.61 (1H, d), 5.43 (1H, dd), 5.27 (1H, dd), 4.83-4.71 (1H, m), 4.48 (1H, t), 4.22-4.01 (2H, 2 dd's), 2.15 (3H, s), 2.02 (3H, s), 2.00 (3H, s) and 1.98 (3H, s) ppm. To the crude chloride (8), in a 1 liter round bottom flask, was added 9.3 g (122 mmol) of thiourea and 150 mL of acetone. The mixture was stirred at reflux for 40 minutes and then cooled in an ice bath for 30 minutes and then vacuum filtered. The collected solids were rinsed with 2×75 m aliquots of acetone. The solids were then air dried for 45 minutes and then dried further under full vacuum pump pressure (<0.5 mm Hg) for 2 h to afford 33.0 g of the product (9) as a light beige solide (74% overall yield from 7): ^{1}H NMR (d_6-DMSO) d 9.38 and 9.12 (2 broad s's, 3H), 8.36 (1H, d), 5.56 (1H, d), 5.34 (1H, d), 5.01 (1H, dd), 4.38 (1H, t), 4.22-4.00 (3H, m), 2.11 (3H, s), 2.01 (3H, s), 1.92 (3H, s) and 1.81 (3H, s) ppm.

Preparation of 1-b-Mercapto 3,4,6-Tri-O-Acetyl-N-Acetyl-Galactosamine (10)

To a 1 liter round bottom flask, charged with 30.0 g (67.9 mmol) of the pseudothiourea (9) in 175 mL of methylene chloride and 175 mL of de-ionized water was added 7.08 g (37.24 mmol) of sodium metabisulfite followed by careful addition of 10.2 g (74.5 mmol) of potassium carbonate. The mixture was stirred at room temperature for 40 minutes and the mixture then transferred to a 500 mL separatory funnel. The layers were separated and the aqueous phase was then extracted with 2×125 mL aliquots of methylene chloride. The organic extracts were combined, dried over anhydrous sodium sulfate, filtered and concentrated to give 24.2 g (10) of the product as a very pale yellow (off-white) solid (98%): ^{1}H NMR ($CDCl_3$) d 6.24 (1H, d), 5.61 (1H, d), 5.43 (1H, dd), 5.27 (1H, dd), 4.83-4.71 (1H, m), 4.48 (1H, t), 4.22-4.01 (2H, 2 dd's), 2.15 (3H, s), 2.02 (3H, s), 2.00 (3H, s) and 1.98 (3H, s) ppm.

Preparation of 3,4,6-Tri-O-Acetyl-N-Acetyl-Galactosamine-1-a-S-[5'-Thiopentyl-N-BOC-Amine] (11)

To a 1 liter round bottom flask, charged with 24.2 g (66.6 mmol) of the thiol (10) under nitrogen atmosphere, was added 350 mL of dry acetonitrile. The mixture was heated to 40–42° C., the solids eventually dissolving over a 20 minute period. 1,8-Diazabicyclo[5.4.0]undec-7-ene (DBU commercially available from Aldrich Chemical Company, 10.5 mL, 70.2 mmol) was then added and the mixture stirred for 20 minutes. Then, 24.0 g (67.1 mmol) of the tosylate 6 in 75 mL of acetonitrile was added over a 3–4 minute period. The resultant mixture was stirred at 40-25° C. for 1.5 h and then concentrated. The residue was diluted with 400 mL of methylene chloride and washed first with 250 mL of 0.5N aqueous HCl and then with 250 mL of 5% aqueous sodium bicarbonate. The organic phase was dried over anhydrous magnesium, vacuum filtered, and concentrated via rotary

evaporation. The residue was chromatographed on 21×7 cm of silica gel (manufactured by E. M. Merck), eluting with 55/42.5/2.5 ethyl acetate/hexane/ethanol. The fractions containing product were combined, concentrated and re-chromatographed on 21×7 cm of RP-18 silica gel (manufactured by J. T. Baker), eluting with 500 mL each of 50/50, 60/40, 65/35, and 70/30 methanol/water and then with 75/25 methanol/water until all of the desired product had eluted from the column. The fractions containing product were combined and concentrated. The residue was diluted with 500 mL of methylene chloride and treated with anhydrous magnesium sulfate. The mixture was vacuum filtered and the filtrate was concentrated, first via rotary evaporation and then under full vacuum pump pressure (<0.5 mm Hg) to afford 17.9 g of the product (11) as a foamy white solid: ^{1}H NMR (d_6-DMSO) d 9.38 and 9.12 (2 broad s's, 3H), 8.36 (1H, d), 5.56 (1H, d), 5.34 (1H, d), 5.01 (1H, dd), 4.38 (1H, t), 4.22-4.00 (3H, m), 2.11 (3H, s), 2.01 (3H, s), 1.92 (3H, s) and 1.81 (3H, s) ppm: Thin Layer Chromatography (Visualization with p-anisaldehyde spray and heat); Silica Gel, R_f=0.50 (57/40.5/2.5 ethyl acetate/hexane/ethanol); RP-18 Silica Gel, R_f=0.21 (65/35 methanol/water).

Preparation of Methyl-6-Methylaminohexanoate Hydrochloride (12)

To a 2 liter three neck round bottom flask, charged with 8.77 g of 60% NaH in mineral oil (219 mmol, 1.1 equiv.) in 500 mL of anhydrous tetrahydrofuran, was fitted a 500 mL addition funnel in the center neck. Then, 34.5 g (144 mmol) of secondary amide in 3 in 300 mL of anhydrous tetrahydrofuran was added over a 30 minute period. The mixture was stirred for 50 additional minutes and then 22.6 mL (363 mmol) of iodomethane was added. The mixture was stirred at room temperature for 23 h and then transferred to a 2 liter round bottom flask and concentrated via rotary evaporation. The residue was treated with 400 mL of 1N aqueous HCl and then extracted with 300 mL of ethyl acetate and then with 2×200 mL aliquots of ethyl acetate. The organic extracts were combined and first washed with 3×125 mL aliquots of 5% aqueous sodium thiosulfate and then with 100 mL of de-ionized water. The organic phase was dried over anhydrous magnesium sulfate, vacuum filtered, and concentrated. The residue was dissolved in 250 mL of methanol and re-concentrated. The residue was dissolved in 250 mL of methanol and treated with 50 mL of 10N aqueous sodium hydroxide followed by 100 mL of de-ionized water. The mixture was stirred at room temperature for 17 h, diluted with an additional 50 mL of de-ionized water and then washed with 3×200 mL aliquots of hexane. The aqueous phase was concentrated via rotary evaporation. The residue was diluted with 500 mL of methanol and hydrogen chloride gas was bubbled into the mixture for 2–3 minutes (10 g). The mixture was stirred at room temperature for 3 h and then vacuum filtered and concentrated via rotary evaporation. To the residue was added 500 mL of methanol and then hydrogen chloride gas was again bubbled into the mixture for 2–3 minutes (9.2 g). The mixture was stirred at room temperature for 18 h. The mixture was cooled in an ice bath and then vacuum filtered. The filtrate was concentrated by rotary evaporation. The residue was twice diluted with 250 mL of methanol and re-concentrated. The residue was diluted with 300 mL of 2-propanol and treated with 4 g of activated charcoal for 30 minutes. The mixture was vacuum filtered through Celite and the solids rinsed with 2×75 mL aliquots of 2-propanol. The filtrates were combined and concentrated, first via rotary evaporation and then under full vacuum pump pressure. The residue was diluted with 250 mL of methanol and re-concentrated, first via rotary evaporation and then under full vacuum pump pressure. The residue was diluted with 250 mL of methanol and hydrogen chloride gas was bubbled into the mixture for 1–2 minutes (5.0 g). The mixture was stirred at room temperature for 2 h and then concentrated via rotary evaporation. The residue was twice diluted with 250 mL of methanol and concentrated, first via rotary evaporation and finally under full vacuum pump pressure (<0.5 mm Hg) to afford 23.91 g of the product (12) as a very light yellow foamy solid (85%): ^{1}H NMR (d_6-DMSO) d 8.72 (2H, broad s), 3.58 (3H, s), 2.82 (2H, m), 2.49 (3H, s), 2.32 (2H, t), 1.68-1.45 (4H, m) and 1.39-1.21 (2H, m) ppm; ^{1}H NMR (CD_3OD) d 3.63 (3H, s), 2.97 (2H, t), 2.34 (2H, t), 1.75-1.56 (4H, m) and 1.49-1.31 (2H, m) ppm.

Preparation of N-Methyl-N-(5-Methoxycarbonylpentyl) Biotinamide (13)

To a 500 mL round bottom flask, charged with 9.00 g (36.8 mmol) of biotin (Sigma Chemical Company), 7.93 g (40.5 mmol, 1.1 equiv.) of amine hydrochloride 12, and 200 mL of anhydrous dimethylformamide was added 17 mL of triethylamine (120 mmol) followed by 17.1 g (38.7 mmol, 1.05 equiv.) of benzotriazolyloxytris(dimethylamino) phosphonium hexaphosphonate (BOP, commercially available from Aldrich Chemical Company and Chem-Impex International, Wood Dale, Ill.) coupling agent. The reaction was stirred at room temperature for 13 h and then concentrated. The residue was diluted with 100 mL of 2-propanol and 300 mL of methylene chloride and the resulting mixture was washed with 2×150 mL aliquots of 1N aqueous HCl and then with 150 mL of de-ionized water. The organic phase was dried with anhydrous magnesium sulfate and vacuum filtered. The solids were rinsed with 100 mL of 25% 2-propanol/methylene chloride. The combined filtrates were concentrated. The residue was chromatographed on 9×22 cm of silica gel, eluting with 20% methanol/ethyl acetate. The fractions containing product (13) were combined and concentrated via rotary evaporation. The residue was chromatographed on 7×18 cm of RP-18 silica gel, eluting with 800 mL of 50:50 methanol/water, 1 liter of 55:45 methanol/water and 2 liters of 60:40 methanol/water. The fractions containing product (13) were combined and concentrated, first via rotary evaporation and finally under full vacuum pump pressure (<0.5 mm Hg) to afford 11.58 of the product (13) as a near colorless oil: ^{1}H NMR (d_6-DMSO) d 6.42 (1H, s), 6.33 (1H, s), 4.29 (1H, m), 4.12 (1H, m), 3.57 (3H, s), 3.22 (2H, t), 3.09 (1H, m), 2.91 and 2.77 (3H, 2 s), 2.81 (1H, dd), 2.57 (1H, d), 2.34-2.19 (4H, m) and 1.70-1.10 (12H, m) ppm; ^{1}H NMR ($CD_{3pk\ OD)\ d}$ 4.48 (1H, dd), 4.29 (1H, dd), 3.63 and 3.62 (3H, 2 s), 3.34 (2H, t), 3.20 (1H, m), 3.02 and 2.88 (3H, 2 s), 2.91 (1H, dd), 2.68 (1H, d), 2.43-2.27 (4H, m) and 1.80-1.20 (12H, m) ppm; Thin Layer Chromatography (Visualization with p-aminocinnimaldehyde spray); Silica Gel, R_f=0.31 (8/2 ethyl acetate/methanol); RP-18 Silica Gel, R_f=0.29 (6/4 methanol/water).

Preparation of N-Methyl-N-(5-Hydroxycarbonylpentyl) Biotinamide (14)

To a 1 liter round bottom flask, charged with 11.58 g (30.0 mmol) of 13 in 100 mL of methanol was added 50 mL of 1N

aqueous sodium hydroxide. The mixture was stirred for 2–3 h and then concentrated via rotary evaporation. The residue was transferred to a 250 mL round bottom flask in a total of 75 mL of de-ionized water. With vigorous stirring, the pH of the solution was adjusted to 1.5–2 by addition of 1N aqueous HCl, the product precipitating out as a white solid in the process. The mixture was vacuum filtered. The collected solids were rinsed with 3×50 mL aliquots of ice cold de-ionized water. The solids were air dried for 3 h and then under full vacuum pump pressure (<0.5 mm Hg) for 21 h to afford 10.07 g of the product (14) as a white solid (90%): ^{1}H NMR (d_6-DMSO) d 6.43 (1H, s), 6.35 (1H, s), 4.30 (1H, m), 4.12 (1H, m), 3.23 (2H, t), 3.10 (1H, m), 2.91 and 2.78 (3H, 2 s), 2.81 (1H, dd), 2.57 (1H, d), 2.30-2.13 (4H, m) and 1.79-1.10 (12H, m) ppm; ^{1}H NMR (CD_3OD) d 4.48 (1H, dd), 4.29 (1H, dd), 3.35 (2H, t), 3.19 (1H, m), 3.02 and 2.88 (3H, 2 s), 2.91 (1H, dd), 2.68 (1H, d), 2.43-2.23 (4H, m) and 1.83-1.21 (12H, m) ppm; Thin Layer Chromatography (Visualization with p-aminocinnimaldehyde spray); RP-18 Silica Gel, R_f=0.50 (6⁰⁄₁₀ methanol/water).

Preparation of N-BOC-N,N-Bis-(5-Methoxycarbonylpentyl)amine (15)

To a 500 mL round bottom flask, charged with 6.43 g (29.1 mmol) of di-t-butyl-dicarbonate and 9.00 g (29.1 mmol) of N,N-bis-(5-methoxycarbonylpentyl)-amine hydrochloride (4), was added 125 mL of anhydrous acetonitrile followed by 7.5 mL of triethylamine. The mixture was stirred at room temperature for 22 h and then concentrated via rotary evaporation. The residue was diluted with 300 mL of ethyl acetate and washed with 2×100 mL aliquots of 0.1N aqueous HCl, 100 mL of de-ionized water and 100 mL of 5% aqueous sodium bicarbonate. The organic phase was dried over magnesium sulfate, vacuum filtered and concentrated, first via rotary evaporation and then under full vacuum pump pressure (<0.5 mm Hg) to afford 10.5 g of product (15) as a near colorless oil (97%): ^{1}H NMR (d_6-DMSO) d 3.57 (6H, s) 3.07 (4H, t), 2.28 (4H, t), 1.60-1.10 and 1.37 (21H, m and s) ppm; Thin Layer Chromatography (Visualization with ninhydrin spray and heat); Silica Gel, R_f=0.33 (2⁰⁄₁₀ ethyl acetate/hexane); RP-18 Silica Gel, R_f=0.17 (7⁰⁄₃₀ methanol/water).

Preparation of N-BOC-N,N-Bis-(5-Hydroxycarbonylpentyl)amine (16)

To a 500 mL round bottom flask, charged with 10.5 g of bis-methyl ester 15, was added 75 mL of methanol followed by 75 mL of 1N aqueous sodium hydroxide. The mixture was stirred at room temperature for 16 h and then concentrated via rotary evaporation. The residue was diluted with 75 mL of de-ionized water and the pH of the resultant solution adjusted to 2.0-2.5 by slow addition of approximately 75 mL of 1N aqueous HCl. Then, 200 mL of ethyl acetate was added and the mixture stirred vigorously for 3 minutes. The mixture was transferred to a separatory funnel and the layers separated. The aqueous phase was extracted with 2×150 mL aliquots of ethyl acetate. The organic extracts were combined, dried over anhydrous magnesium sulfate, and vacuum filtered. The filtrates were concentrated, first via rotary evaporation and then under full vacuum pump pressure (<0.5 mm Hg),, to afford 9.52 gof the product as a viscous, nearly colorless oil (98%): ^{1}H-NMR (d_6-DMSO) d 3.07 (4H, t), 2.28 (4H, t), 1.58-1.10 and 1.37 (21H, m and s) ppm; Thin Layer Chromatography (Visualization with ninhydrin spray and heat); RP-18 Silica Gel, R_f=0.44 (7⁰⁄₃₀ methanol/water).

Preparation of N-BOC-N,N-Bis-(N',N'-Bis(5-Methoxycarbonylpentyl)-5-Carbamyl pentyl)Amine (17)

To a 1 liter round bottom flask, charged with 9.52 g (27.6 mmol) of bis-acid 16 in 250 mL of anhydrous dimethylformamide, was added 19.0 (61.3 mmol) of N,N-bis-(5-methoxycarbonylpentyl)amine hydrochloride (4) followed by 30 mL of triethylamine. While the mixture was stirred, 25.7 g (58.1 mmol) of BOP was added. The resulting mixture was stirred at room temperature for 14 h and then concentrated via rotary evaporation. The residue was diluted with 750 mL of ethyl acetate and washed with 250 mL of 0.2N aqueous HCl, 100 mL of 0.1N aqueous HCl, 100 mL of de-ionized water, and 2×100 mL aliquots of 5% aqueous sodium bicarbonate. The organic phase was dried over anhydrous magnesium sulfate, vacuum filtered, and concentrated via rotary evaporation. The residue was chromatographed on 9×21 cm of silica gel, eluting first with 70% ethyl acetate/hexane and then with 100% ethyl acetate. The fractions containing product (17) were combined and concentrated via rotary evaporation. The residue was chromatographed on 7×23 cm of RP-18 silica gel, eluting with first with 75:25 methanol/water. The fractions containing product were combined and concentrated, first via rotary evaporation and then under full vacuum pump pressure. The residue was diluted with 500 mL of diethyl ether and the resulting solution was dried with anhydrous magnesium sulfate. The mixture was vacuum filtered and the filtrate was concentrated, first via rotary evaporation and then under full vacuum pump pressure (<0.5 mm Hg), to afford 17.80 g of product (17) as a near colorless, viscous, oil (75%): ^{1}H-NMR (d_6-DMSO) d 3.57 (12H, s), 3.18 and 3.07 (12H, 2 t's), 2.32-2.16 (12H, m), 1.61-1.09 and 1.37 (45H, m and s) ppm; Thin Layer Chromatography (Visualization with ninhydrin spray and heat); Silica Gel, R_f=0.50 (ethyl acetate); RP-18 Silica Gel, R_f=0.30 (8⁵⁄₁₅ methanol/water).

Preparation of N-BOC-N,N-Bis-(N',N'-Bis(5-Hydroxycarbonylpentyl)-5-Carbamyl pentyl)Amine (18)

To a 500 mL round bottom flask, charged with 7.88 g (9.20 mmol) of the tetramethyl ester (18) in 75 mL of methanol, was added 70 mL of 1N aqueous sodium hydroxide. The mixture was stirred at room temperature for 16 h and then concentrated via rotary evaporation to a thick syrup. The residue was diluted with 50 mL of de-ionized water and, with vigorous stirring, the pH of the solution was adjusted to 2–2.5 by slow addition of approximately 70 mL of 1N aqueous HCl, the product (18) oiling out (one liquid phase separates from another liquid phase) in the process. The mixture was extracted with 200 mL of 3:12-propanol/methylene chloride, and then 3×100 mL aliquots of 3:12-propanol/methylene chloride. The organic extracts were combined, dried over anhydrous magnesium sulfate, filtered and concentrated, first via rotary evaporation and then under full vacuum pump pressure (<0.5 mm Hg) to afford 7.70 g of a near colorless, thick syrup, consisting (by NMR integration) of 6.93 g of the desired product (18, 94%) and 0.77 g of 2-propanol: ^{1}H-NMR (d_6-DMSO) d 3.18 and 3.07 (12H, 2 t's), 2.37-2.12 (12H, m), 1.60-1.10 and 1.37 (45H, m and s) ppm; Thin Layer Chromatography (Visualization with ninhydrin spray and heat); RP-18 Silica Gel, R_f=0.50 (7⁰⁄₃₀ methanol/water).

Preparation of N-BOC-Tet-Gal-NAc-1-a-S-C5 Branch (20)

To a 250 mL round bottom flask, charged with 4.05 g (7.38 mmol) of 3,4,6-tri-O-acetyl-N-acetyl-galactosamine-1-a-S[5'-thiopentyl-N-BOC-amine] (11), was added 20 mL of methylene chloride followed by 20 mL of trifluoroacetic acid. The mixture was stirred at room temperature for 15 minutes. The mixture was concentrated via rotary evaporation and the residue was thrice diluted with 75 mL of methylene chloride and re-concentrated to afford 6.27 g of residue, a mixture of desired product (19) and residual trifluoroacetic acid: ^{1}H-NMR (CD_3OD) d 5.61 (1H, d), 5.41 (1H, dd), 5.01 (1H, dd), 4.62-4.47 (2H, m), 4.11 (2H, d), 2.91 (2H, t), 2.74-2.48 (2H, m), 2.11 (3H, 2s), 2.00 (3H, s), 1.93 and 1.91 (6H, 2 s), and 1.37-1.10 (6H, m) ppm. To a separate 250 mL round bottom flask, charged with 1.33 g of the syrup containing 90% 18 by weight (net 1.20 g, 1.50 mmol), was added 50 mL of anhydrous dimethylformamide. In order to remove residual 2-propanol, the mixture was concentrated first via rotary evaporation and then under full vacuum pump pressure (<0.5 mm Hg). To the residue was added 20 mL of anhydrous dimethylformamide and 10 mL of dry triethylamine. To the resultant, stirred, solution was added a dimethylformamide solution of the crude 19 (in a total of 30 mL of anhydrous dimethylformamide) and the resultant mixture stirred at room temperature for 2 h. The mixture was then concentrated via rotary evaporation. The residue was then diluted with 250 mL of methylene chloride and washed with 2×100 mL aliquots of 1N aqueous HCl, 100 mL of de-ionized water, and then with 100 mL of saturated aqueous sodium bicarbonate. The organic phase was dried over anhydrous magnesium sulfate, vacuum filtered, and concentrated via rotary evaporation. The residue was chromatographed on 5.5×19 cm of RP-18 silica gel, eluting with 250 mL each of 65:35 methanol/water, 70:30 methanol/water, 75:25 methanol/water, and then with 800 mL of 80:20 methanol/water. The fractions containing product were combined, and concentrated, first via rotary evaporation and then under full vacuum pump pressure to afford 3.55 g of a foamy white solid (94%). this material was then chromatographed on 5.5×20 cm of silica gel, eluting with 80:20 ethyl acetate/methanol. The fractions containing only the desired product (20) were combined and concentrated, first via rotary evaporation and then under full vacuum pump pressure (<0.5 mm Hg), to afford 2.83 g of the desired product as a pure white foamy solid (75%): ^{1}H-NMR (CD_3OD) d 5.58 (4II, d), 5.42 (4II, dd), 5.01 (4II, dd), 4.63-4.51 (8H, m), 4.20-4.00 (8H, m), 3.35-3.10 (20H, m), 2.73-2.47 (8H, m), 12.32 (4H, t), 2.25-2.08 (20H, m and s), 2.00 (12H, s), 1.93 and 1.91 (24H, 2 s), 1.71-1.20 (69H, m and s) ppm; Thin Layer Chromatography (Visualization with ninhydrin spray and heat); Silica Gel, R_f=0.47 (75:25 ethyl acetate/methanol); RP-18 Silica Gel, R_f=0.33 (80% methanol/water).

Preparation of N-Methyl-N-(((N",N"-Bis(5-Methoxycarbonylpentyl)-N',N'-Bis-(5-Carbamylpentyl))-5-Carbamylpentyl)Biotinamide(22)

To a 250 mL round bottom flask, charged with 1.50 g (1.75 mmol) of N-BOC-N,N-bis-(N',N'-bis(5-methoxycarbonylpentyl)-5-carbamyl pentyl)-amine (17) in 15 mL of methylene chloride, was added 15 mL of trifluoroacetic acid. The mixture was stirred at room temperature for 15 minutes and then concentrated. The residue was diluted with 50 mL of methylene chloride and then concentrated via rotary evaporation. The residue was then diluted with 50 mL of methanol and re-concentrated via rotary evaporation. The residue was again re-diluted with 50 mL of methylene chloride and re-concentrated, first via rotary evaporation and then under full vacuum pump pressure (<0.5 mm Hg). to the residue was added 30 mL of anhydrous dimethylformamide, 4 mL of dry triethylamine, 715 mg (1.90 mmol) of N-methyl-N-(5-methoxycarbonylpentyl)-biotinamide (13), and finally 840 mg (1.90 mmol) of BOP. The mixture was stirred at room temperature for 3 h and then concentrated via evaporation. The residue was chromatographed on 4.5×18 cm of RP-18 silica gel, eluting with 200 mL each of 55:45 methanol/water, 60:40 methanol/water, 70:30 methanol/water, and 600 mL of 80/20 methanol/water. The fractions containing product were combined and concentrated, first via rotary evaporation and then under full vacuum pump pressure (<0.5 mm Hg), to afford 1.75 g of the product as a near colorless oil (90%): ^{1}H-NMR (d_6-DMSO) d 6.43 (1H, s), 6.34 (1H, s), 4.29 (1H, m), 4.11 (1H, m), 3.57 (12H, s), 3.29-2.99 (15H, m), 2.90 and 2.78 (3H, 2 s's), 2.81 (1H, dd), 2.55 (1H, d), 2.35-2.12 (16H, m), and 1.65-1.10 (48H, m) ppm; Thin Layer Chromatography (Visualization with p-aminocinnimaldehyde spray); RP-18 Silica Gel, R_f=0.48 (85% methanol/water).

Preparation of N-Methyl-N-(((N"N"-Bis(5-Hydroxycarbonylpentyl)-N',N'-Bis-(5-Carbamylpentyl))-5-Carbamylpentyl)Biotinamide(23)

To a 250 mL round bottom flask, charged with 1.75 g (1.58 mmol) of N-methyl-N-(((N",N"-bis-(5-methoxycarbonylpentyl)-N',N'-bis-(5-carbamylpentyl))-5-carbamylpentyl)-biotinamide (22) in 30 mL of methanol, was added 20 mL of 1N aqueous sodium hydroxide. The mixture was stirred at room temperature for 14 h and then concentrated via rotary evaporation. The residue was diluted with 30 mL of de-ionized water and then the vigorously stirred solution was acidified to pH 1.5–2 with the slow addition of approximately 20 mL of 1N aqueous HCl, the product (23) oiling out of solution in the process. The mixture was concentrated via rotary evaporation and the residue was chromatographed on 4.5×18 cm of RP-18 silica gel, eluting with 200 mL each of 55:45 methanol/water, 60:40 methanol/water, 65:35 methanol/water, 70:30 methanol/water and 75:25 methanol/water. The fractions containing product were combined and concentrated, first via rotary evaporation and then under full vacuum pump pressure (<0.5 mm Hg), to give 1.57 g of the product (23) as a glassy solid (95%): ^{1}H-NMR (d_6-DMSO) d 6.43 (1H, s), 6.35 (1H, s), 4.29 (1H, m), 4.11 (1H, m), 3.29-2.99 (15H, m), 2.90 and 2.78 (3H, 2 3's), 2.81 (1H, dd), 2.55 (1H, d), 2.30-2.12 (16H, m), and 1.65-1.10 (48H, m) ppm; Thin Layer Chromatography (Visualization with p-aminocinnimaldehyde spray); RP-18 Silica Gel, R_f=0.56 (80% methanol/water.)

Preparation of Hexadecyl-N-Acetyl-Galactosamine-Biotin Cluster (25)

To a 100 mL round bottom flask, charged with 790 mg (0.313 mmol) of the N-BOC-Tet-Gal-NAc-1-a-S-C5 Branch (20), was added 10 mL of methylene chloride followed by 10 mL of trifluoroacetic acid. The mixture was stirred at room temperature for 15 minutes and then concentrated via rotary evaporation. The residue was diluted with 150 mL of

methylene chloride and washed with 2×100 mL aliquots of saturated aqueous sodium bicarbonate. The organic phase was dried over magnesium sulfate, vacuum filtered and then concentrated, first via rotary evaporation and then under full pump pressure (<0.5 mm Hg), to afford 690 mg of the product (24) as a foamy off-white solid (91%).

It should be noted that the product (24) is a universal reagent which may be used to derivatize a moiety to be cleared following administration thereof. Note that this compound may be used to derivatize any moiety that bears a functional group reactive with an amine group. Alternatively, product (24) may be modified by reaction with a heterobifunctional group or otherwise to afford an alternative functional group with which to bind this universal reagent to a moiety to be cleared. Use of heterobifunctional agent or other means to alter reactive groups is within the ordinary skill in the art. Functional groups which may be employed in this aspect of this invention include active esters, maleimides, alkyl halides, hydrazides, thiols, imidates, aldehydes or the like.

In practice of this aspect of the present invention, a moiety to be cleared after administration (such as a relatively rapidly accreting imaging agent) may be derivatized to incorporate the sugar cluster of product (24). In this manner, the background of the resulting image will be improved in that the imaging agent will accrete to target sites or be cleared via Ashwell receptor recognition of the component contributed by product (24). Thus, circulating imaging agent will be cleared, thus eliminating the background and improving the image.

In a separate 100 mL round bottom flask, charged with 60 mg (0.057 mmol) N-methyl-N-(((N"N"-bis-(5-hydroxycarbonylpentyl)-N',N'-bis-(5-carbamylpentyl))-5-carbamylpentyl)-biotinamide (23), was added 10 mL of anhydrous dimethylformamide. The mixture was concentrated via rotary evaporation, to drive off any residual moisture. To the residue was added 3 mL of anhydrous dimethylformamide and 300 mL of dry diisopropylethylamine followed by 113 mg (0.255 mmol) of BOP. The mixture was stirred at room temperature for 10 minutes and then the amine 24, in a total of 5 mL of anhydrous dimethylformamide was added. The mixture was stirred at room temperature for 3 h and then an additional 20 mg (0.045 mmol) of BOP was added and the mixture was stirred at room temperature for 14 h more. The mixture was concentrated via rotary evaporation and then diluted with 50 mL of methanol and 50 mL of de-ionized water. The resultant mixture was treated with 10 g of AG-1 X8 anion exchange resin (BioRad; Hydroxide form, 2.6 mequiv./g) and stirred at room temperature for 18 h. The mixture was then vacuum filtered. The residue was rinsed with 50 mL of de-ionized water and then with 50 mL of methanol. The filtrates were combined and concentrated via rotary evaporation. The residue was chromatographed on 3.5×16 cm of RP-18 silica gel, eluting with 100 mL each of 50:50 methanol/water, 55:45 methanol/water, 60:40 methanol/water, 65:35 methanol/water, and 70:30 methanol/water. The fractions containing product were combined and concentrated, first via rotary evaporation and then under full vacuum pump pressure (<0.5 mm Hg) to give 470 mg of partially purified product. This material was further purified on a preparative polyhydroxyethyl aspartamide HPLC column (2.5×30 cm; PolyLC Inc., Columbia Md.), eluting with 70/30 acetonitrile/water at 13 ml/min. The fractions containing product were combined and concentrated, first via rotary evaporation and then under full vacuum pump pressure (<0.5 mm Hg). The residue was diluted with 5–10 mL of de-ionized water, frozen to –70° C., and lyophilized to afford 177 mg of the product (25) as a white solid (36%): ^{1}H-NMR (CD_3OD) d 5.54 (16H, d), 4.55–4.25 (18H, m), 3.90 (16H, m), 3.80–3.65 (48H, m), 3.45–2.80 (99H, m), 2.65–2.45 (33H, m), 2.45–2.27 (32H, m), 2.27–2.05(32H, m), 1.97 (48H, s), and 1.80–1.20 (288H, m) ppm; Thin Layer Chromatography (Visualization with p-aminocinnimaldehyde spray or p-anisaldehyde spray and heat); RP-18 Silica Gel, R_f=0.43 (75/25 methanol/water); Mass Spectrometry—Expected M+H=8652.5 amu, Actual M+H=8657 amu.

B. Preparation of 4-N-AcetylGalactosamine-Biotin-CCA (alpha-oxygen) Corresponding to Compound 28 in FIG. **4**.

Preparation of 3,4,6-Tri-O-Acetyl-N-Acetyl-Galactosamine-1-a-O-[N'-Methyl-4'-N'-Butyl-Trifluoroacetamide] (26)

To a 25 mL round bottom flask, charged with 1.00 g (2.57 mmol) of 1-b, 3, 4, 6-tetra-O-acetyl-N-acetyl-galactosamine (7) and 767 (3.85 mmol, 1.50 equiv) N-methyl-N-(4-hydroxybutyl)-trifluoracetamide (4-(N-Methyl-trifluoroacetamido)-1-butanol discussed in Example IV) in 10 mL of dry nitromethane, was added 325 mL (2.64 mmol, 1.03 equiv) of boron trifluoride etherate. The mixture was stirred at 101° C. for 2 h and then concentrated via rotary evaporation. The residue was diluted with 75 mL of methylene chloride and washed with 50 mL of 0.1 N aqueous HCl. The organic phase was dried over magnesium sulfate, vacuum filtered, and the filtrate concentrated via rotary evaporation. The residue was chromatographed on 3.5×18 cm of silica gel, eluting first with 10% acetone/methylene chloride and then with 15% acetone/methylene chloride. The fractions containing product were combined and concentrated, first via rotary evaporation and then under full vacuum pump pressure (<0.5 mm Hg), to afford 453 mg of the product (26) as a foamy white solid (36%): ^{1}H-NMR (d_6-DMSO) d 7.98 (1H, d), 5.31 (1H, d), 5.01 (1H, dd), 4.82 (1H, d), 4.27–4.10 (2H, m), 4.10–3.93 (2H, m), 3.60 (1H, m), 3.49–3.35 (3H, m), 3.09 and 2.96 (3H, q and s), 2.10 (3H, s), 1.99 (3H, s), 1.90 (3H, s), 1.79 (3H, s), 1.71–1.42 (4H, m) ppm.

Preparation of N-Acetyl-Galactosamine-1-a-O-[N'-Methyl-4'-Butylamine] (27)

To a 250 mL round bottom flask, charged with 12.5 g of AG-1 X8 anion exchange resin (BioRad; Hydroxide form, 2.6 mequiv/g) and 50 mL of de-ionized water was added 830 mg (1.51 mmol) of the starting material (26) in 50 mL of methanol. The mixture was stirred at room temperature for 22 h. The mixture was then vacuum filtered. The resin was rinsed with 50 mL of de-ionized water and 50 mL of methanol. The filtrates were combined and concentrated, first via rotary evaporation and then under full vacuum pump pressure (<0.5 mm Hg), to afford 463 mg of the product (27) as a pale yellow oil (96%): ^{1}H-NMR (D_2O) d 4.83 (1H, d), 4.07 (1H, dd), 3.93–3.80 (3H, m), 3.75–3.57 (3H, m), 3.49–3.36 (1H, m), 2.55 (1H, t), 2.30 (3H, s), 1.97 (3H, s), and 1.65–1.42 (4H, m) ppm.

Preparation of 1-a-O-Tetra-N-Acetyl Galactosamine Biotin Cluster Agent (28)

To a 25 mL round bottom flask, charged with 100 mg (0.0949 mmol) of N-methyl-N-(((N"N"-bis-(5-hydroxycarbonylpentyl)-N',N'-bis-(5-carbamylpentyl))-5-carbamylpentyl)-biotinamide (23), was added 140 mg (0.457 mmol, 4.8 equiv) of amine 27 in 5 ml of anhydrous dimethylformamide followed by 0.5 mL of dry triethylamine and finally 190 mg (0.430 mmol, 4.5 equiv) of BOP. The mixture was stirred at room temperature for 19 h and then concentrated via rotary evaporation. The residue was chromatographed on 2.5×15 cm of RP-18 silica gel, eluting with 50:50 methanol/water, 55:45 methanol/water, and 60:40 methanol/water. The fractions containing product were combined and concentrated, first rotary evaporation and then under full vacuum pump pressure (<0.5 mm Hg). The residue was chromatographed on 2.5×18 cm of silica gel, eluting with methanol, 5:95 water/methanol, and 10:90 water/methanol. The fractions containing product were combined and concentrated, first via rotary evaporation and then under full vacuum pump pressure (<0.5 mm Hg). The residue was diluted with 7 mL of de-ionized water, frozen to −70° C., and lyophilized to afford 158 mg of the product (28) as a fluffy white solid (75%): ^{1}H-NMR (D_2O) d 4.82 (4H, m), 4.54 (4H, dd), 4.35 (4H, dd), 4.07 (4H, dd), 3.95–3.78 (12H, m), 3.72–3.57 (12H, m), 3.48–3.18 (23H, m), 2.99–2.80 (16H, 2 s's and dd), 2.70 (1H, d), 2.43–2.25 (16H, m), 1.98 (12H, s), and 1.75–1.12 (64H, m) ppm.

C. Preparation of 4-N-AcetylGalactosamine-Biotin-CCA (beta-oxygen) Corresponding to Compound 31 in FIG. **5**.

Preparation of 3,4,6-Tri-O-Acetyl-N-Acetyl-Galactosamine-1-b-O-[N'-Methyl-4'-N'-Butyl-Trifluoroacetamide] (29)

To a 100 mL round bottom flask, charged with 1.79 g (6.42 mmol) of trityl chloride and 880 mg (6.46 mmol) of zinc chloride, was added a solution of 2.10 g (5.47 mmol) of 1-a-chloro, 3, 4, 6-tetra-O-acetyl-N-acetyl-galactosamine (8) and 1.28 g (6.43 mmol) of N-methyl-N-(4-hydroxybutyl)-trifluoracetamide in 30 mL of dry methylene chloride. The mixture was stirred at room temperature for 3 h and then concentrated via rotary evaporation. The residue was diluted with 100 mL of ethyl acetate and washed with 50 mL of saturated aqueous sodium bicarbonate. The organic phase was dried over magnesium sulfate, vacuum filtered and concentrated via rotary evaporation. The residue was chromatographed on 4.5×19 cm of silica gel, eluting first with 10% acetone/methylene chloride, then with 15% acetone/methylene chloride, and finally with 20% acetone/methylene chloride. The fractions containing product were combined and concentrated, first via rotary evaporation and then under full vacuum pump pressure (<0.5 mm Hg), to afford 1.00 g of the product (29) as a white foamy solid (34%): ^{1}H-NMR (d_6-DMSO) d 7.80 (1H, d), 5.20 (1H, d), 4.95 (1H, dd), 4.48 (1H, d), 4.02 (3H, s), 3.90 (1H, m), 3.73 (1H, m), 3.50–3.35 (3H, m), 3.08 and 2.93 (3H, q and s), 2.10 (3H, s), 1.99 (3H, s), 1.89 (3H, s), 1.75 (3H, s), and 1.68–1.35 (4H, m) ppm.

Preparation of N-Acetyl-Galactosamine-1-b-O-[N-Methyl-4'-Butylamine] (30)

To a 250 mL Erlenmeyer flask, charged with 20 g of AG-1 X8 resin (BioRad; Hydroxide form; 2.6 mequiv/g) and 50 mL of de-ionized water, was added 1.55 g (2.93 mmol) of 3,4,6-tri-O-acetyl-N-acetyl-galactosamine-1-b-O-[N'-methyl-4'-N'-butyl-trifluoroacetamide] (29) in 30 mL of methanol. The mixture was stirred at room temperature for 15 h and then vacuum filtered. The resin was rinsed with 50 mL of de-ionized water and then with 50 mL of methanol. The filtrates were combined and concentrated, first via rotary evaporation and then under full vacuum pump pressure (<0.5 mm Hg), to afford 880 mg of the product (30) as an off-white foamy solid (98%): ^{1}H-NMR (D_2O) d 4.41 (1H, d), 3.95–3.50 (8H, m), 2.63 (2H, t), 2.38 (3H, s), 2.00 and 1.63–1.45 (4H, m) ppm.

Preparation of 1-b-O-Tetra-N-Acetyl Galactosamine Biotin Cluster Agent (31)

To a 25 mL round bottom flask, charged with 100 mg (0.0949 mmol) of N-methyl-N-(((N"N"-bis(5-hydroxycarbonylpentyl)-N',N'-bis-(5-carbamylpentyl))-5-carbamylpentyl)biotinamide (23) and 140 mg (0.457 mmol) of N-acetyl-galactosamine-1-b-O-[N-methyl-4'-butylamine] (30) in 5 mL of anhydrous dimethylformamide, was added 0.5 mL of dry triethylamine and followed by 192 mg (0.434 mmol) of BOP. The mixture was stirred at room temperature for 2 h and then concentrated. The residue was chromatographed on 2.5×16 cm of RP-18 silica gel, eluting with 100 mL each of 50:50 methanol/water and 55:45 methanol/water, and with 150 mL of 60:40 methanol/water. The fractions containing product were combined and concentrated, first via rotary evaporation and then under full vacuum pump pressure (<0.5 mm Hg). The residue was chromatographed on 2.5×17 cm of silica gel, eluting with methanol, then with 95.5 methanol/water, and finally with 90:10 methanol/water. The fractions containing product were combined and concentrated, first via rotary evaporation and then under full vacuum pump pressure (<0.5 mm Hg). The residue was dissolved in 8 mL of de-ionized, water frozen to −70° C., and lyophilized to afford 156 mg of the product (31) as a fluffy white solid (75%): ^{1}H-NMR (D_2O) d 4.54 (1H, dd), 4.42–4.31 (5H, d and m), 3.95–3.45 (32H, m), 3.43–3.15 (23H, m), 3.03–2.82 (16H, 2 s's and dd), 2.71 (1H, d), 2.43–2.26 (16H, m), 1.96 (12H, s), 1.70–1.15 (64H, m) ppm.

D. Preparation of 4-N-AcetylGalactosamine-Biotin-CCA (beta-sulfur) Corresponding to Compound 36 in FIG. **6**.

Preparation of N-BOC-N-Methyl-4-Aminobutanol (32)

To a 250 mL round bottom flask, charged with 3.00 g (28.5 mmol) of N-methyl-4-aminobutanol in 75 mL of dioxane, was added 5 mL of triethylamine (35.4 mmol) followed by 7.85 g (31.9 mmol) of BOC-ON, 2-(tert-butoxycarbonyloxyimino)-2-phenylacetonitrile. The mixture was stirred at room temperature for 20 h and then concentrated via rotary evaporation. The residue was chromatographed on silica gel, eluting first with 20% ethyl acetate/hexane, then with 40% ethyl acetate/hexane, and finally with 75% ethyl/hexane. The fractions containing product were combined and concentrated via rotary evaporation to afford 4.85 g of the product (32) as a near colorless oil (84%): ^{1}H-NMR ($CDCl_3$) d 3.65 (2H, t), 3.23 (2H, t), 2.81 (3H, s), 1.67–1.45 (4H, m), and 1.42 (9H, s) ppm.

Preparation of N-BOC-N-Methyl-4-Aminobutyl Toluene-sulfonate (33)

To a 500 mL round bottom flask, charged with 4.75 g (23.4 mmol) of N-BOC-N-methyl-4-aminopentanol (32) in 150 mL of methylene chloride, was added 5.25 g (27.5

mmol) of toluenesulfonyl chloride and 7.0 mL (49.6 mmol) of triethylamine. The mixture was stirred at room temperature for 24 h and then washed with 3×75 mL aliquots of 1 N aqueous HCl. The organic phase was dried over anhydrous magnesium sulfate, vacuum filtered, and concentrated via rotary evaporation. The residue was chromatographed on silica gel, eluting first with 20% ethyl acetate/hexane and then with 30% ethyl acetate/hexane. The fractions containing product (33) were combined and concentrated via rotary evaporation to afford 6.95 g of the product as a very pale yellow oil (83%): ^{1}H-NMR ($CDCl_3$) d 7.78 (2H, d), 7.31 (2H, d), 4.03 (2H, t), 3.15 (2H, t), 2.86 (3H, s), 2.42 (3H, s), 1.73–1.47 (4H, m), and 1.41 (9H, s) ppm.

Preparation of N-Acetyl-Galactosamine-1-b-S-[N'-BOC-N'-Methyl-4'-Butylamine] (34)

To a 250 mL round bottom flask, charged with 7.0 g (15.8 mmol) of 3,4,6-tri-O-acetyl-N-acetyl-galactosamine-1-b-pseudothiourea hydrochloride (9), 2.6 g of potassium carbonate (18.8 mmol), and 1.65 g (15.9 mmol) of sodium hydrosulfite in 90 mL of methanol, was added 6.00 g (16.7 mmol) of N-BOC-N-methyl-4-Aminobutyl-toluenesulfonate (33) in 20 mL of methanol. The mixture was stirred at room temperature for 20 h and then concentrated via rotary evaporation. The residue was chromatographed on RP-18 silica gel, eluting first with 40:60 methanol/water, then with 45:55 methanol/water, then with 50:50 methanol/water, then with 55:45 methanol/water, and finally with 60:40 methanol/water. The fractions containing product were combined and concentrated, first via rotary evaporation and then under full vacuum pump pressure (<0.5 mm Hg), to afford 2.18 g of the product (34) as an off-white solid (33%): ^{1}H-NMR (D_2O) d 4.47 (1H, d), 3.95–3.82 (2H, m), 3.77–3.57 (4H, m), 3.20 (2H, t), 2.82–2.55 (5H, s and m), 1.97 (3H, s), 1.67–1.45 (4H, m), and 1.38 (9H, s) ppm.

Preparation of N-BOC-Tet-Gal-NAc-1-b-S-C4-N-Me Branch (35)

To a 25 mL round bottom flask, charged with 679 mg (1.61 mmol) of (34), was added 10 mL of trifluoroacetic acid. The mixture was stirred at room temperature for 15 minutes and then concentrated via rotary evaporation. The residue was twice diluted with 10 mL of methanol and then re-concentrated via rotary evaporation.: ^{1}H-NMR D_2O) d 4.47 (1H, d), 3.95–3.82 (2H, m), 3.78–3.57 (4H, m), 2.97 (2H, t), 2.78–2.58 (5H, s and m), 1.95 (3H, s), and 1.80–1.52 (4H, m), ppm. To a 50 mL round bottom flask, charged with 270 mg (0.337 mmol) of N-BOC-N,N-bis-(N,N'-bis(5-hydroxycarbonylpentyl)-5-carbamyl pentyl)amine (18), was added 1 mL of triethylamine along with the residue in the 25 mL round bottom flask in 15 mL of anhydrous dimethylformamide followed by 670 mg (1.52 mmol) of BOP. The mixture was stirred at room temperature for 4 h and then concentrated via rotary evaporation. The residue was chromatographed on RP-18 silica gel, eluting first with 50:50 methanol/water, then with 55:45 methanol/water, then with 60:40 methanol/water, and finally with 65:35 methanol/water. The fractions containing product were combined and concentrated, first via rotary evaporation and then under full vacuum pump pressure (<0.5 mm Hg), to afford 300 mg of the product (35) as a white foamy solid (44%): H-NMR (D_2O) d 4.47 (4H, d), 3.98–3.83 (8H, m), 3.78–3.56 (16H, m), 3.43–3.08 (20H, m), 2.99 and 2.84 (12H, 2 s's), 2.80–2.55 (8H, m), 2.41–2.25 (12H, m), 1.97 (12H, s), and 1.75–1.13 and 1.38 (61H, m and s) ppm.

Preparation of 1-b-S-Tetra-N-Acetyl Galactosamine Biotin Cluster Agent (36)

To a 25 mL round bottom flask, charged with 100 mg of 35 was added 10 mL of trifluoroacetic acid. The mixture was stirred at room temperature for 10 minutes and then concentrated via rotary evaporation. The residue was twice diluted with 10 mL of methanol and re-concentrated, first via rotary evaporation and then under full vacuum pump pressure (<0.5 mm Hg). The residue was diluted with 5 mL of anhydrous dimethylformamide and then treated with 25 mg (0.067 mmol) of N-methyl-N-(5-hydroxycarbonylpentyl) biotinamide (14), 300 mL of dry triethylamine, and then with 30 mg (0.068 mmol) of BOP. The mixture was stirred at room temperature for 2 h and then concentrated via rotary evaporation. The residue was chromatographed on RP-18 silica gel, eluting first with 50:50 methanol/water, then with 55:45 methanol/water, then with 60:40 methanol/water, and finally with 65:35 methanol/water. The fractions containing product were combined and concentrated, first via rotary evaporation and then under full vacuum pump pressure (<0.5 mm Hg). The residue was diluted with 5 mL of de-ionized water, frozen to −70° C. and lyophilized to afford 77 mg of the product (36) as a white puffy solid (77%): H-NMR (D_2O) d 4.53 (1H, dd), 4.47 (4H, d), 4.34 (1H, dd), 3.98–3.80 (8H, m), 3.77–3.54 (16H, m), 3.40–3.08 (23H, m), 2.98 and 2.82 (15H, 2 s's), 2.91 (1H, dd), 2.78–2.55 (9H, m), 2.40–2.23 (16H, m), 1.93 (12H, s), and 1.72–1.11 (64H, m) ppm.

E. Preparation of 4-N-AcetylGalactosamine-Biotin-CCA (alpha-sulfur) Corresponding to Compound 41 in FIG. 7.

Preparation of 3,4,6-Tri-O-Acetyl-N-Acetyl-Galactosamine-1-b-S-[N'-Methyl-4'-N'-Butyl-Trifluoroacetamide] (38)

To a 100 mL round bottom flask, charged with 2.00 g (4.46 mmol) of 3,4,6-tri-O-acetyl-N-acetyl-galactosamine-1-b-pseudothiourea hydrochloride (9), 690 mg of potassium carbonate (4.99 mmol) of 940 mg (9.04 mmol) of sodium hydrosulfite was added 25 mL of de-ionized water followed by 25 mL of methylene chloride. The mixture was stirred at room temperature for 1 h and the layers then separated. The aqueous phase was extracted with 3×75 mL aliquots of methylene chloride. The organic extracts were combined, dried over sodium sulfate, filtered and then concentrated via rotary evaporation: ^{1}H-NMR (d_6-DMSO) d 7.95 (1H, d), 5.28 (1H, d), 4.96 (1H, dd), 4.73 (1H, dd), 4.13–3.89 (4H, m), 3.33 (1H, d), 2.10 (3H, s), 1.99 (3H, s), 1.89 (3H, s), and 1.79 (3H, s) ppm. The residue, 1.03 g of thiol (37), was diluted with 20 mL, of methanol and treated with 412 mg (2.98 mmol) of potassium carbonate, 619 mg (5.95 mmol) of sodium hydrosulfite and 2.00 g (5.66 mmol) of N-methyl-4-trifluoroacetamido-butyltoluenesulfonate (1-(p-Toluenesulfonyloxy)-4-(N-methyl-trifluoroacetamido) butane discussed in Example IV). The mixture was stirred at room temperature for 2 h and then concentrated via rotary evaporation. The residue was diluted with 75 mL of methylene chloride and washed with 50 mL, of 0.1 N aqueous HCl. The organic phase was dried over magnesium sulfate, vacuum filtered and concentrated via rotary evaporation. The residue was chromatographed on silica gel, eluting first

with 10% acetone/methylene chloride and then with 15% acetone/methylene chloride. The fractions containing product were combined and concentrated, first via rotary evaporation and then under full vacuum pump pressure (<0.5 mm Hg), to afford 683 mg of the product (38) as a foamy white solid (26%): ^{1}H-NMR (d_6DMSO) d 7.88 (1H, d), 5.26 (1H, 2 d), 4.96 (1H, dd), 4.60 (1H, d), 4.09–3.92 (4H, m), 3.39 (2H, t), 3.08 and 2.93 (3H, q and s), 2.77–2.50 (2H, m), 2.10 (3H, s), 1.99 (3H, s), 1.89 (3H, s), 1.77 (3H, s), 1.71–1.42 (4H, m) ppm.

Preparation of 3,4,6-Tri-O-Acetyl-N-Acetyl-Galactosamine-1-a-S-[N'-Methyl-4'-N'-Butyl-Trifluoroacetamide] (39)

To a 50 mL round bottom flask, charged with 620 mg (1.17 mmol) of the 3,4,6-tri-O-acetyl-N-acetyl-galactosamine-1-b-S-[N'-methyl-4'-N'-butyl-trifluoroacetamide] (38) in 10 mL of dry nitromethane was added 145 mL of borontrifluoride etherate (1.17 mmol). The mixture was stirred at 100° C. for 3 h and then allowed to sit at room temperature for 3 weeks. The mixture was concentrated via rotary evaporation. The residue was diluted with 75 mL of methylene chloride and washed with 1 N aqueous HCl. The residue was chromatographed on silica gel, eluting first with 10% acetone/methylene chloride and then with 15% acetone/methylene. The fractions containing product were combined and concentrated, first via rotary evaporation and then under full vacuum pump pressure (<0.5 mm Hg), to afford 254 mg of the product (39) as a very pale yellow oil (41%): ^{1}H-NMR (d_6-DMSO) d 8.17 (1H, d), 5.56 (1H, 2 d's), 5.33 (1H, d), 4.88 (1H, dd), 4.49–4.29 (2H, m), 4.03 (2H, d), 3.38 (2H, t), 3.08 and 2.93 (3H, q and s), 2.55 (2H, m), 2.09 (3H, s), 1.97 (3H, s), 1.90 (3H, s), 1.79 (3H, s), 1.72–1.41 (4H, m) ppm.

Preparation of N-Acetyl-Galactosamine-1-a-S-[N-Methyl-4'-Butylamine] (40)

To a 250 mL Erlenmeyer flask, charged with 15 g of AG-1 X8 anion exchange resin (BioRad; Hydroxide form, 2.6 mequiv/g) and 60 mL of de-ionized water, was added 245 mg (0.450 mmol) of tri-O-acetyl-N-acetyl-galactosamine-1-a-S-[N'-methyl-4'-N'-butyl-trifluoroacetamide] (39) in 40 mL of methanol. The mixture was stirred at room temperature for 22 h and then vacuum filtered. The resin was rinsed with 50 mL of de-ionized water and then with 50 mL of methanol. The filtrates were combined and concentrated, first via rotary evaporation and then under full vacuum pump pressure (<0.5 mm Hg), to afford 143 mg of the product (40) as a pale yellow solid (99%): ^{1}H-NMR (D_2O) d 5.43 (1H, d 4.32–4.17 (2H, m), 3.91 (1H, d), 3.77 (1H, dd), 3.70 (2H, d), 2.70–2.45 (4H, m), 2.29 (3H, s), 1.96 (3H, s), 1.66–1.42 (4H, m) ppm.

Preparation of 1-a-S-Tetra-N-Acetyl Galactosamine Biotin Cluster Agent (41)

To a 50 mL round bottom flask, charged with 80 mg (0.0759 mmol) of N-methyl-N-(((N"N"-bis(5-hydroxycarbonylpentyl)-N',N'-bis-(5-carbamylpentyl))-5-carbamylpentyl)biotinamide (23) in 10 mL of anhydrous dimethylformamide, was added 123 mg (0.379 mmol) of N-acetyl-galactosamine-1-a-S-[N-methyl-4'-butylamine] (40) and 0.5 mL of dry triethylamine. The mixture was stirred at room temperature for 10 minutes and then 152 mg (0.344 mmol) of BOP was added. The mixture was stirred at room temperature for 2 h and then concentrated. The residue was chromatographed on 2.5×20 cm of RP-18 silica gel, eluting with 100 mL of 50:50 methanol/water, 100 mL of 55:45 methanol/water, and then with 200 mL of 60:40 methanol/water. The fractions containing product were combined and concentrated, first via rotary evaporation and then under full vacuum pump pressure (<0.5 mm Hg). The residue was diluted with 6 mL of de-ionized water, water frozen to −70° C., and lyophilized to afford 107 mg of the product (41) as a fluffy white solid (62%): ^{1}H-NMR (D_2O) d 5.42 (4H, t), 4.53 (1H, dd), 4.38–4.14 (9H, m), 3.90 (4H, d), 3.80–3.63 (12H, d and dd), 3.45–3.15 (23H, m), 3.00–2.79 (16H, 2 s's and dd), 2.73–2.45 (9H, d and m), 2.40–2.25 (16H, m), 1.95 (12H, s), 1.75–1.12 (64H, m) ppm.

EXAMPLE VII

Second Generation CCA Evaluation

A. Four Sugar Construct Evaluation.

To determine the optimal properties of second generation CCAs, a series of four sugar-containing CCAs were prepared substantially as described above and tested in three sets (designated a, b and c) as follows: BALB/c female mice (20–25 g) were injected i.v. with 120 micrograms of NR-LU-10-streptavidin conjugate radiolabeled with I-125, and blood was serially collected from n=3 mice. The clearance of the conjugate from the blood was measured in these control mice. Separate groups of mice were injected with either 120 or 12 micrograms of radiolabeled monoclonal antibody-streptavidin conjugate which had been precomplexed with the 4-galactose-biotin or 4-N-acetylgalactosamine-biotin CCAs by mixing the biotin analog at a 20-fold molar excess with the antibody conjugate. Generally, both doses of precomplexed conjugate showed extremely rapid clearance from the blood, relative to the antibody conjugate control.

The test results for clearance study sets a), b) and c) (120 microgram doses only) may be summarized as follows:

Number	Sugar Unit	4 hour Conjugate Level (% ID/g)
1	Gal-β-S-$(CH_2)_4$-N(Me)	a) 31.5 ± 1.0%
2	Gal-NAc-β-S-$(CH_2)_4$-N(Me)	a) 22.6 ± 0.6%
3	Gal-NAc-β-O-$(CH_2)_4$-N(Me)	a) 19.8 ± 0.9%
4	Gal-NAc-α-O-$(CH_2)_4$-N(Me)	a) 14.9 ± 1.9%
5	Gal-NAc-α-S-$(CH_2)_4$-N(Me)	b) 4.5 ± 1.2%
6	Gal-NAc-α-O-$(CH_2)_4$-NH	a) 11.3 ± 1.4%
7	Gal-NAc-α-O$(CH_2)_2$ONH$(CH_2)_2$NH	a) 16.0 ± 2.5%
8	Gal-NAc-α-O-$(CH_2)_6$-NH	a) 8.1 ± 0.2% and 6.7 ± 0.2% @ 24h b) 6.2 ± 0.4% and 6.5 ± 0.4% @ 24h
9	Gal-NAc-α-O-$(CH_2)_8$-NH	b) 4.4 ± 0.7%
10	Gal-NAc-α-O-$(CH_2)_6$-N(Me)	b) 8.1 ± 0.6%
11	Gal-NAc-α-S-$(CH_2)_6$-NH	c) ~3%
12	Gal-NAc-α-S-$(CH_2)_8$-NH	c) ~3%; poor aqueous solubility

NOTE: All of these constructs were bound to aminocaproyl-N(Me)-biotin via a cluster backbone characterized by two sets of two branches, as follows: $((\text{Sugar Unit})_2\text{NCO}—(CH_2)_5)_2—N—$. "Gal-NAc" constitutes N-acetylgalactosamine.

The tested 4-sugar CCAs were prepared substantially as set forth above.

The structures of compounds 11 and 12 are included below for illustrative purposes.

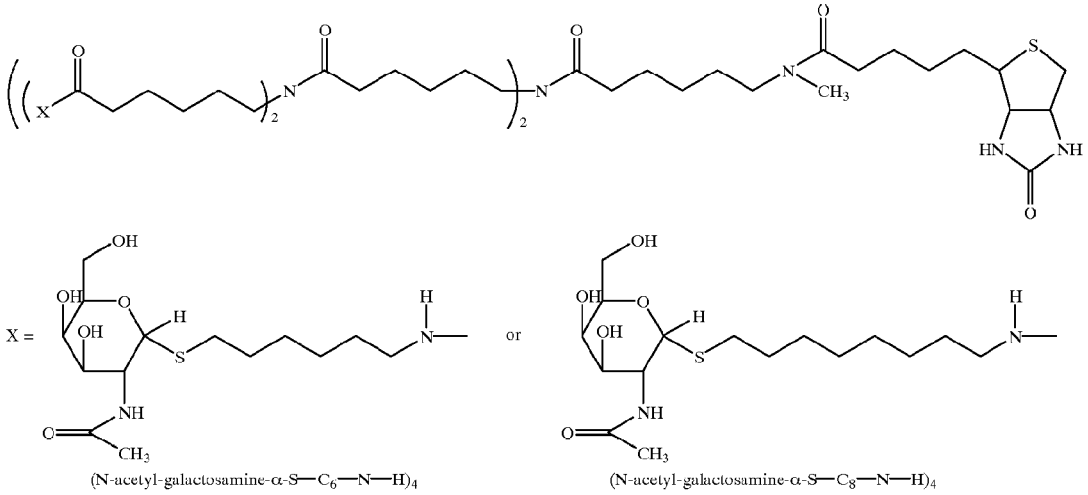

The clearing abilities of compounds 11 and 12 were roughly equivalent to or better than the first generation CCA construct, $(Gal\text{-}1\text{-}\beta\text{-}S\text{—}(CH_2)_4\text{—}N(Me))_{16}$-aminocaproyl-N(Me)-biotin, which is designated $(Galactosyl)_{16}$-LC-biotin in Example V.

B. 16 N-Acetylgalactosamine Construct Evaluation.

The purpose of this study was to investigate and compare the clearing ability and impact on subsequently administered active agent biodistribution of equimolar doses of 3 CCAs containing 16 N-acetylgalactosamines in comparison to a 32-galactose CCA with a $(N\text{-methylaminocaproyl})_2$ linker to biotin:

Sugar Unit	Linker to Biotin
galNAc-α-S-C_6-NH	N-methylaminocaproyl
galNAc-β-S-C_4-NMe	N-methylaminocaproyl
gal-β-S-C_4-NMe	N-methylaminocaproyl

Nude mice bearing s.c. SW-1222 xenografts (n=4 per group per timepoint) were injected at t=0 with 400 μg (1.9 nmol) of NR-LU-10-streptavidin conjugate labeled with PIP-I-125 in accordance with known procedures therefore. After 24 hours, animals were injected with 22.5 nmol (180–360 μg) of each CCA. Four hours later, a tumor-saturating 15 μg (18.6 nmol) dose of In-111-DOTA-biotin was administered. Animals were bled and euthanized by cervical dislocation at 2 and 24 hours post In-111-DOTA-biotin injection. Blood, tail, lung, liver, spleen, stomach, kidney, intestines and tumor were counted in a dual-channel gamma counter to establish the tissue concentrations of In-111 and I-125.

Results of this experiment indicated that the 32-galactose CCA afforded the best clearance (lowest I-125 and In-111 levels in non-tumor tissues). The two N-acetylgalactosamine CCAs performed next best and approximately equivalently. The 16-galactose CCA was the poorest at clearing NR-LU-10-streptavidin, resulting in blood levels of DOTA-biotin that were double those of the N-acetylgalactosamine CCAs and 9 times those of the 32-galactose CCA. As expected with a saturating dose of In-111-DOTA-biotin, tumor targeting of In-111 was equivalent for all groups of animals. Negligible CCA compromise of pretargeted NR-LU-10-streptavidin was observed at the administered doses. Use of the 32-galactose construct resulted in tumor:blood ratios that were 2–4 fold better than for the other tested CCAs and the lowest nadir of NR-LU-10-streptavidin blood concentration. The performance of the 32-galactose CCA was hypothesized to result from either or both of the following: (1) increased sugar density; and (2) the extended linker arm between the cluster and biotin. The extender experimentation is discussed below in Experiment E.

C. Impact of Timing Between CCA and Active Agent Administrations.

This parameter was investigated using a 16-N-acetylgalactosamine construct characterized by a sugar unit of galNAc-α-S-C_6-NH and a N-methylaminocaproyl linker between the cluster and biotin. This construct was chosen, because of its stability with regard to release of biotin and clearing ability over a broad range of doses. In this experiment, dosing was altered slightly to model higher efficiency tumor delivery, as would likely be used in a therapeutic setting. This is done by reducing the dose of DOTA-biotin to 1.0 μg which increases the efficiency of tumor delivery (% ID/g), but places a larger burden on the clearing agent to clear circulating NR-LU-10-streptavidin.

Nude mice bearing s.c. SW-1222 xenografts (n=4 per group per timepoint) were injected at t=0 with 400 μg (1.9 nmol) of NR-LU-10-streptavidin conjugate labeled with PIP-I-125 in accordance with known procedures therefore. After 24 hours, animals were injected with 100 μg (11.25 nmol) of the CCA. At 2, 4, 8 or 24 hours later, 1.0 μg (1.24 nmol) dose of In-111-DOTA-biotin was administered. Animals were bled and euthanized by cervical dislocation at 2 and 24 hours post In-111-DOTA-biotin injection. Blood, tail, lung, liver, kidney and tumor were counted in a dual-channel gamma counter to establish the tissue concentrations of In-111 and I-125.

With each longer interval between CCA and DOTA-biotin injections, the level of In-111-DOTA-biotin in the blood was decreased. This appeared to correlate with circulating NR-LU-10-streptavidin levels in each group of animals. The intervals of 8 and 24 hours yielded both the best tumor targeting and lowest blood levels. The lack of CCA tumor compromise, even at the 24 hour timepoint, was encouraging, and the enhanced blood clearance of conjugate over this extended time period allowed the achievement of markedly improved tumor/blood ratios. Thus, CCAs offer a variety of novel dosing applications which can be exploited to improve blood (and presumably, whale body) clearance of In-111-DOTA-biotin without sacrificing tumor uptake.

D. Impact of Different Doses of Active Agent-Containing Construct.

The low circulating NR-LU-10-streptavidin levels attained in the previous experiment suggested the potential for use of higher specific activity DOTA-biotin to improve tumor efficiency. This experiment was therefore conducted to assess the effect of differing ligand doses on both absolute uptake (% ID/g) and tissue to blood ratios. The rationale for this experiment was that CCAs might allow greater efficiency of tumor targeting with a lower ligand dose due to the lower background of NR-LU-10-streptavidin level using a 24 hour interval between CCA and active agent administration. The CCA employed in this experiment was the same one as employed in Experiment C set forth above.

Nude mice bearing s.c. SW-1222 xenografts (n=4 per group per timepoint) were injected at t=0 with 400 g (1.9 nmol) of NR-LU-10-streptavidin conjugate labeled with PIP-I-125 in accordance with known procedures therefore. After 24 hours, animals were injected with 100 μg (11.25 nmol) of the CCA. Twenty-four hours later, 0.1, 0.5, 1.0, 2.0 or 5.0 μg (0.12–6.19 nmol) of In-111-DOTA-biotin were administered. Animals were bled and euthanized by cervical dislocation at 2 and 24 hours post In-111-DOTA-biotin injection. Blood, tail, lung, liver, spleen, stomach, kidney, intestines and tumor were counted in a dual-channel gamma counter to establish the tissue concentrations of In-111 and I-125.

At the lowest DOTA-biotin dose, 0.1 μg, a significant increase in blood retention of In-111-DOTA-biotin was observed, with a somewhat decreased tumor uptake compared to other doses. The blood values decreased significantly over the next 24 hours with a concomitant rise in tumor localization, probably due to tumor uptake of NR-LU-10 -streptavidin that had been labeled with DOTA-biotin in the blood compartment. The overall biodistribution of In-111-DOTA-biotin in all groups was similar, showing decreasing blood levels between the 2 and 24 hour biodistributions without significant loss of tumor activity. Tumor uptake was good for all ligand doses tested, but decreased somewhat for the higher doses of 2.0 and 5.0 μg. On a % ID/g basis, these two doses showed the lowest levels of non-target retention of DOTA-biotin. Tumor to blood ratios for DOTA-biotin increased markedly with increasing ligand dose. Values at 2 hours increased with ligand dose from approximately 7 to greater than 88, while values at 24 hours ranged form 74 to 172. By utilizing CCAs with modified dose-timing parameters, consistently high efficiency tumor delivery of DOTA-biotin was achieved over a broad range of DOTA-biotin doses. Low levels of blood and non-target organ DOTA-biotin retention were also consistently observed.

E. Aqueous Solubility at Physiological Temperature (37° C.) and Extenders Between Cluster and Binding Moiety.

The 16-N-acetylgalactosamine CCA used in Experiments C and D above, characterized by a sugar unit of galNAc-α-S-C_6-NH and a N-methylaminocaproyl linker between the cluster and biotin, had poor aqueous solubility at physiological temperature (less than 2 mg/mL). Also, it was hypothesized that residual NR-LU-10-streptavidin in the circulation represented a subfraction which either does not efficiently bind to the CCA, due for example to steric constraints, or binds to the CCA, but the sugars of the CCA-containing construct are not effectively presented to Ashwell receptors. To address these two issues, alternative constructs were prepared and evaluated. Those constructs may be described as follows:

Sugar Unit	Linker between Cluster and Biotin
1. $(galNAc\text{-}\alpha\text{-}S\text{-}C_5\text{-}NH)_{16}$	N-methylaminocaproyl
2. $(galNAc\text{-}\alpha\text{-}S\text{-}C_5\text{-}NH)_{16}$	$(N\text{-methylaminocaproyl})_3$
3. $(galNAc\text{-}\alpha\text{-}S\text{-}C_5\text{-}NH)_{32}$	$(N\text{-methylaminocaproyl})_3$
4. $(galNAc\text{-}\alpha\text{-}S\text{-}C_6\text{-}NH)_{16}$	N-methylaminocaproyl
5. $(galNAc\text{-}\alpha\text{-}S\text{-}C_4\text{-}NH)_{32}$	$(N\text{-methylaminocaproyl})_2$

In the first three constructs, the methylene group in the sugar unit was decreased from 6 carbons to 5 carbons in an effort to improve solubility. Also, the extended linker between the cluster and biotin in constructs 2, 3 and 5 was introduced in order to address the difficulty in clearing a subfraction of NR-LU-10-streptavidin conjugate. Construct number 5 also incorporates a four carbon sugar unit methylene group. Initial analysis of these constructs was carried out in a precomplexation experiment in Balb C mice, substantially similar to the precomplexation experiments described above. I-125-labeled NR-LU-10-streptavidin was treated with a 20-fold excess of the CCA and then introduced i.v. The clearance profiles of these precomplexed constructs revealed that the conjugate-CCA 3 complex cleared to the lowest serum levels followed by conjugate-CCA 2 complex; followed by conjugate-CCA 5 complex; followed by conjugate-CCA 4 complex; and lastly by conjugate-CCA1 complex. The CCA1 agent was determined to have been contaminated with a small amount of biotin, so that the reliability of this data with respect to that construct is questionable. However, the results with CCA2 and CCA3 indicate that the design changes were positive. Because the synthesis of the 32-sugar construct is more difficult, further CCA work focused on CCA2.

It should be noted that the solubility of CCA2 at physiological temperature was determined to be greater than 50 mg/mL.

F. Further Characterization of CCA2 of Experiment E.

CCA2 was further characterized by utilization thereof in tumored nude mice in the full pretargeting regimen with escalating CCA doses to assess tumor to blood ratios and CCA compromise (either direct by CCA binding thereto or indirect by biotin-containing CCA metabolite binding thereto) of pretargeted NR-LU-10-streptavidin.

Nude mice bearing s.c. SW-1222 xenografts (n=4 per group per timepoint) were injected at t=0 with 400 μg 1.9 nmol) of NR-LU-10-streptavidin conjugate labeled with PIP-I-125 in accordance with known procedures therefore.

After 24 hours, animals were injected with 50 μg (1×), 250 μg (5×) or 500 μg (10×) of CCA. Four hours later, a saturating dose 15 μg of In-111-DOTA-biotin was administered. Animals were bled and euthanized by cervical dislocation at 2 and 24 hours post In-111-DOTA-biotin injection. Tumor and normal tissues were counted in a dual-channel gamma counter to establish the tissue concentrations of In-111 and I125.

NR-LU-10-streptavidin conjugate concentrations at the tumor were roughly equivalent for all groups. DOTA-biotin concentrations at the tumor decreased with increasing CCA dose, falling to about 50% at the 10× dose in comparison to the concentration at the 1× dose. As illustrated in the following table, tumor to blood values of ligand were modest in association with the lowest does of clearing agent, but superb for the higher two doses at the 2 hour timepoint and even better at the 24 hour timepoint.

^{111}In-DOTA-BT localization

Dose of cluster CA	tu/bl (avg tu/avg bl) @ 2h	tu/bl (avg tu/avg bl) @ 24h
50 μg	9.7 (7 68/0.79)	18.6 (9.75/0.53)
250 μg	52.6 (5.56/0.11)	125.2 (5.39/0.05)
500 μg	53.6 (4.11/0.08)	94.0 (3.71/0.04)

G. Further Characterization of Purified CCA1 of Experiment E.

Because administration of very high doses of CCA2 appeared to result in partial compromise of pretargeted conjugate, further evaluation of highly purified CCA1 was undertaken. Evaluation consisted of determining efficacy in clearance of pre-complexed conjugate and clearance of conjugate in the pretargeting schema. An evaluation of the extent of compromise of pretargeted conjugate was also undertaken. These evaluations were conducted using a control of CCA4 of Experiment E (also a construct used in Experiment B and the construct used in Experiments C and D set forth above).

Both precomplexation and pretargeted clearing experiments were carried out as earlier described. In precomplexation experiments, purified CCA1 and CCA4 of Experiment E appeared to function analogously. Both agents were also found to function nearly identically in clearing conjugate administered in the pretargeting schema. Use of high doses of the two CCAs in tumored mice in the pretargeting schema resulted in little CCA compromise of the binding capacity of the pretargeted streptavidin, wherein the ratio of conjugate to DOTA-biotin being about 5.5:1. This ratio is likely to be within 10% of the theoretical maximum ligand binding capacity of the conjugate, consisting of (on average) between 1–2 streptavidin molecules/antibody.

Kits containing one or more of the components described above are also contemplated. For instance, galactose cluster-biotin conjugate may be provided in a sterile container for use in pretargeting procedures. Alternatively, such a galactose cluster-biotin conjugate may be vialed in a non-sterile condition for use as a research reagent.

From the foregoing, it will be appreciated that, although specific embodiments of the invention have been described herein for purposes of illustration, various modifications may be made without deviating from the spirit and scope of the invention. Accordingly, the invention is not limited except as by the appended claims.

What is claimed is:

1. A clearing agent comprising:

(a) a hepatic clearance directing moiety comprising an iterative, two branch chemical framework to which a plurality of 1-desoxy-1-thio-N-acetylgalactosamine residues are bound; and

(b) one or two binding moieties directly or indirectly attached to the hepatic clearance directing moiety, wherein the binding moieties bind in vivo a compound to be cleared,

wherein the clearing agent is characterized by a molecular mass between about 2,000 and about 20,000 daltons, and directs clearance of the compound by a hepatic pathway.

2. A clearing agent comprising:

(a) a hepatic clearance directing moiety comprising an iterative, two branch chemical framework to which a plurality of N-acetyl-galactosamine hexose residues are bound; and

(b) one or two binding moieties directly or indirectly attached to the hepatic clearance directing moiety, wherein the binding moieties bind in vivo a compound to be cleared,

wherein the clearing agent is characterized by a molecular mass between about 2,000 and about 20,000 daltons, and directs clearance of the compound by a hepatic pathway, and

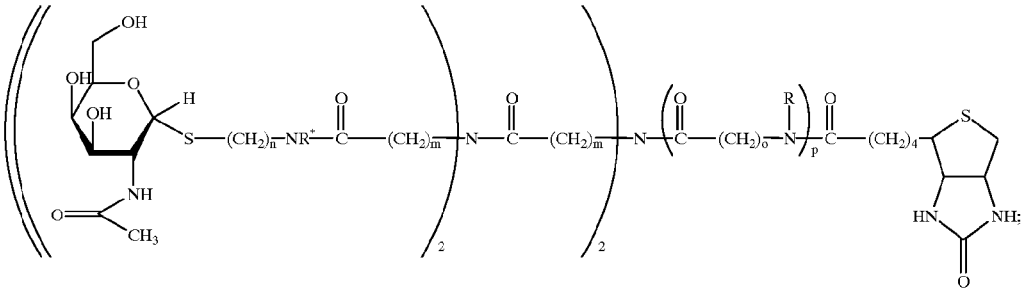

-continued

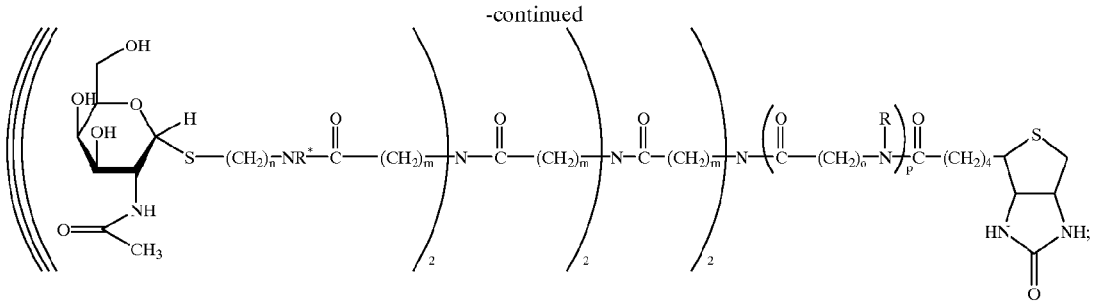

or

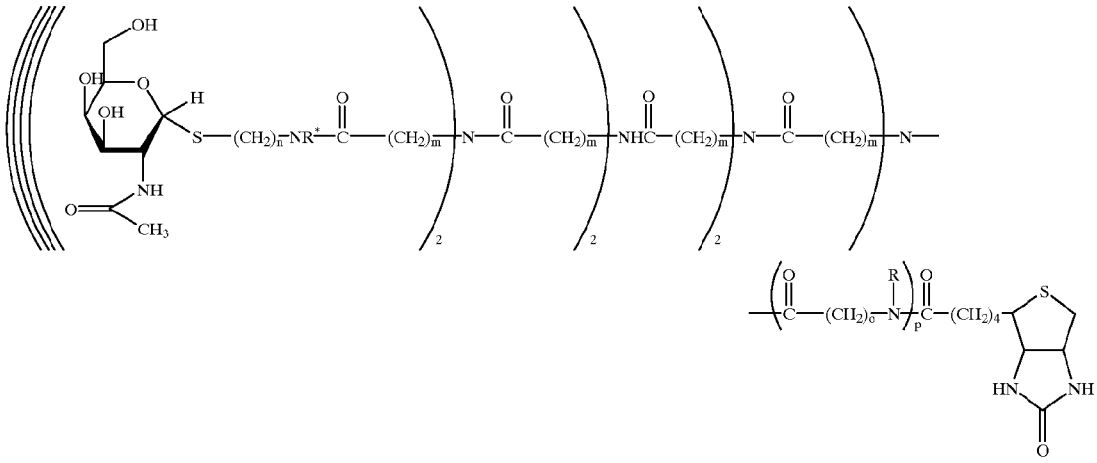

wherein n ranges from about 4 to about 8; m and o range from about 3 to about 6; p ranges from about 1 to about 10; R' is H or lower alkyl of from 1 to about 6 carbon atoms; and R is lower alkyl from about 1 to about 6 carbon atoms, phenyl, benzyl or C_{2-6} lower alkyl substituted with phenyl.

3. A clearing agent of claim **2** wherein p is 2 or 3; and R are a straight chain lower alkyl of 2 carbon atoms.

4. A clearing agent of claim **3** wherein n is 5; m is 5; o is 5; and R' is H.

5. A clearing agent of claim **2** wherein p is 2 or 3; and R are a straight chain lower alkyl of 1 carbon atom.

6. A clearing agent of claim **2** wherein p is 2 or 3; and R are a straight chain lower alkyl of 1 carbon atom and a straight chain lower alkyl of 2 atoms.

7. A clearing agent of claim **6** wherein n is 5; m is 5; o is 5; and R' is H.

8. A clearing agent of claim **2** selected from the third chemical formula of claim **2**, wherein n is 5, m is 5, o is 5, p is 1, R' is H, and R is methyl.

* * * * *

EXHIBIT 8

Design and Synthesis of Novel *N*-Acetylgalactosamine-Terminated Glycolipids for Targeting of Lipoproteins to the Hepatic Asialoglycoprotein Receptor

Patrick C. N. Rensen,*,† Steven H. van Leeuwen,† Leo A. J. M. Sliedregt, Theo J. C. van Berkel, and Erik A. L. Biessen

Division of Biopharmaceutics, Leiden/Amsterdam Center for Drug Research, University of Leiden, Gorlaeus Laboratory, P.O. Box 9502, 2300 RA Leiden, The Netherlands

Received June 30, 2004

A novel glycolipid has been prepared that contains a cluster glycoside with an unusually high affinity for the asialoglycoprotein receptor (ASGPr) and a bile acid moiety that mediates stable incorporation into lipidic particles. The glycolipid spontaneously associated with low-density lipoproteins (LDL) and high-density lipoproteins (HDL) within human and murine plasma, and loading of lipoproteins with this glycolipid resulted in an efficient dose-dependent recognition and uptake of LDL and HDL by the liver (and not by spleen) upon intravenous injection into wild-type mice. Preinjection with asialoorosomucoid largely inhibited the uptake, establishing that both HDL and LDL were selectively recognized and processed by the ASGPr on liver parenchymal cells. Finally, repeated intravenous administration of the glycolipid to hyperlipidemic LDL receptor-deficient mice evoked an efficient and persistent cholesterol-lowering effect. These results indicate that the glycolipid may be a promising alternative for the treatment of hyperlipidemic patients who do not respond sufficiently to current cholesterol-lowering therapies.

Introduction

Clinical data indicate a positive correlation between LDL cholesterol levels and the occurrence of arteriosclerosis,[1,2] while a strong inverse correlation has been demonstrated between HDL cholesterol levels and cardiovascular disease.[3,4] However, recent insights indicate that the antiatherogenic properties of HDL are not dictated by its plasma levels, but rather by its functionality (i.e. capability to deliver cholesteryl esters to the liver). In fact, increasing the flux of HDL to the liver may also be atheroprotective, as it has been shown that overexpression of the hepatic HDL receptor SR-BI in heterozygous LDLr-deficient ($ldlr^{-/-}$) mice on a high fat/high cholesterol diet resulted in strong reduction in plasma HDL cholesterol and concomitantly reduced atherosclerotic lesion area.[5,6] Thus, these studies clearly illustrate that stimulation of the hepatic uptake of LDL and HDL will be an effective entry to antiatherosclerotic therapy and led us to explore the feasibility to induce effective clearance of these lipoproteins via the asialoglycoprotein receptor (ASPGr).[7]

The ASGPr is a high-capacity receptor uniquely expressed on the surface of hepatocytes to mediate the hepatic uptake and subsequent lysosomal processing of galactose (Gal)- and *N*-acetylgalactosamine (GalNAc)-terminated substrates from the serum,[8] at which the affinity for GalNAc is approximately 50-fold higher than for Gal.[9] In addition to the ASGPr on hepatocytes, a second receptor recognizing galactose and fucose groups is present in the liver on Kupffer cells (galactose particle receptor, galactose/fucose receptor)[10,11] and preferentially recognizes a high density of either fucose or galactose on either proteins[11−13] or particles.[14,15] Previous proof-of-concept studies already showed that the bifunctional glycolipid TG(20Å)C (glycolipid **1**, Figure 1), consisting of a cholesteryl moiety for anchorage to lipoproteins and a triantennary Gal-terminated glycoside with moderate affinity for the ASGPr, was able to associate with LDL and HDL and induce their liver uptake in rodents. However, due to the relatively high hydrophilicity of the glycolipid, rapid exchange of the glycolipid occurred in the blood, leading to only a moderate 20% liver uptake of these lipoproteins after preloading with TG(20Å)C.[16] To stabilize incorporation of the glycolipid into lipoproteins, the lipophilicity of the anchoring moiety was increased by adding a fatty acid chain to the steroid core structure. In addition, the intrinsically labile methylene acetals connecting the glycol spacers to the tris cluster core in TG(20Å)C were replaced by more stable ether bonds.[17] The resulting glycolipid compound (glycolipid **2**, Figure 1) indeed showed a very stable interaction with lipidic particles which was retained in the blood and resulted in an effective targeting of liposomes to the ASGPr on hepatocytes.[17,18] However, a major setback still was that high glycolipid surface densities resulted in elimination of liposomes by the galactose particle receptor,[17,18] and preliminary data showed that glycolipid **2** redirected LDL almost exclusively to Kupffer cells.

In this paper, we introduce an improved amphiphilic glycolipid, **3** (see Figure 1), in which, with respect to **2**, two important modifications are present. A tyrosine moiety was introduced to allow for trace labeling with ^{125}I, providing the possibility to perform kinetic studies in vivo. In addition, the galactose residues within the triantennary cluster glycoside were replaced by GalNAc

* Corresponding author's present address: Department of General Internal Medicine, LUMC, Leiden, and TNO-Prevention and Health, Gaubius Laboratory, P.O. Box 2215, 2301 CE Leiden, The Netherlands. Telephone: + 31 71 51 81406. Fax: + 31 71 51 81904. E-mail: pcn.rensen@pg.tno.nl.
† Both authors contributed equally to this work.

10.1021/jm049481d CCC: $27.50
Published on Web 10/06/2004

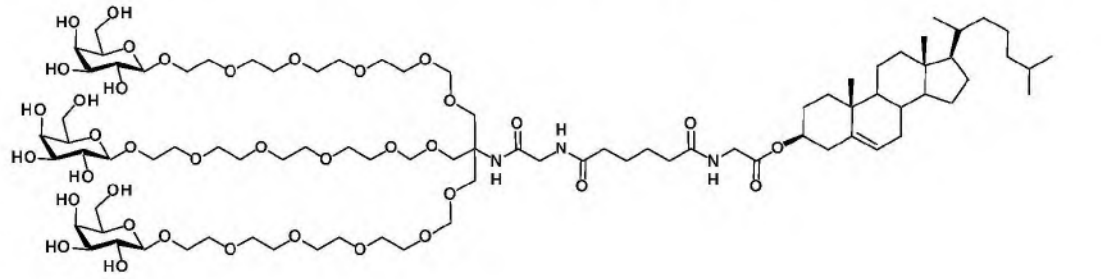

glycolipid **1**

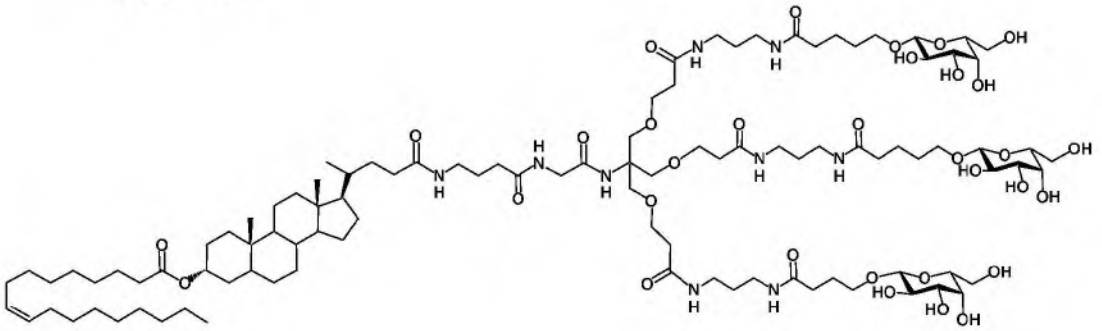

glycolipid **2**

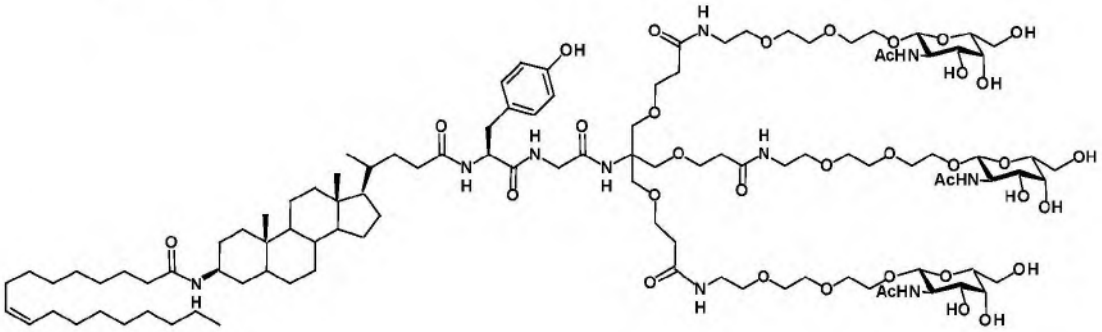

glycolipid **3**

Figure 1. Chemical structures of glycolipids TG(20Å)C (**1**), (3α(oleoyloxy)-5β-cholanoyl)-GABA-Gly-tris(Gal)$_3$ (**2**), and (3β-(oleoylamido)-5β-cholanoyl)-Tyr-Gly-tris(GalNAc)$_3$ (**3**).

residues, which led to a 50-fold increased affinity of the cluster glycoside toward the ASGPr on hepatocytes (K_i 2 nM).[18] The resulting compound was tested for its ability to associate with plasma lipoproteins and to induce their liver uptake and for its cholesterol-lowering capacity in hyperlipidemic *ldlr*$^{-/-}$ mice. We conclude from these data that glycolipid **3** is very effective in promoting cholesterol transport to hepatocytes and thus may be a promising alternative for hyperlipidemic individuals who do not respond sufficiently to current cholesterol-lowering therapies, such as familial hypercholesterolemic patients.[19,20]

Results and Discussion

Synthesis. Previously, we synthesized glycolipid **1**, which only modestly induced the hepatic uptake of lipoproteins, as its cholesterol moiety afforded an only weak association with lipoproteins.[16,21] Replacement of cholesterol by the highly lipophilic lithocholic oleate (LCO) residue yielded glycolipid **2**, which showed a markedly improved association with lipidic particles, but the galactose-exposing cluster glycoside still induced particle uptake by Kupffer and splenic cells via the galactose particle receptor depending on substrate size and substrate surface density of the glycolipid.[17] Previous studies by us[22,23] and others[24] have established that triantennary GalNAc-containing ligands displayed a higher affinity for the ASGPr than the corresponding diantennary GalNAcs or triantennary galactosides. Therefore, we now synthesized a third-generation glycolipid by combining the lipophilic LCO unit possessing high affinity for lipidic particles with a triantennary GalNAc-containing glycoside (glycolipid **3**). This novel triantennary glycoside with 20 Å-spaced terminal GalNAc residues appeared to display a low nanomolar affinity for the ASGPr (2 nM) and to redirect differently sized stable unilamellar liposomes to hepatocytes in vitro and in vivo.[18]

In this study we describe the synthesis of this novel glycolipid **3** and present new biological data indicating

Scheme 1. Synthesis of the Cluster Galactoside Synthon 13[a]

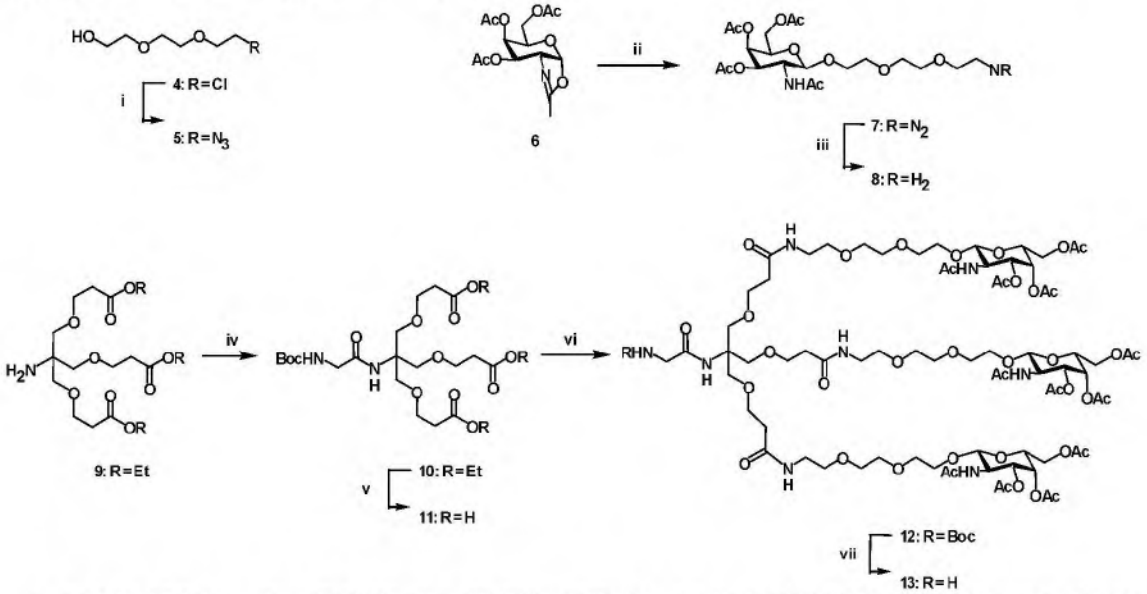

[a] Reagents: (i) NaN_3, NaI, 62%; (ii) **5**, TMSOTf, 58%; (iii) PPh_3, THF, 49%; (iv) BocGlyOH, BOP, DiPEA, 93%; (v) aq NaOH, dioxane, 100%; (vi) **8**, HOBt, PyBOP, DiPEA, DMF; (vii) TFA/DCM 1/4, 100%.

that this improved glycolipid is able to direct both LDL and HDL to the ASGPr on hepatocytes in vivo, thereby avoiding lipoprotein uptake by the galactose particle receptor on Kupffer cells and spleen. In analogy to glycolipid **1**, we have attached the GalNAc units to the tris core by a flexible ethylene glycol linker to warrant an optimal orientation and thus recognition of the terminal sugar moieties by the ASGPr. Given this galactosamine synthon terminus at each dendrimer arm, an eight-atom spacer moiety sufficed to establish a 20 Å long connection between the separate GalNAcs and the tris branching point. Thus, 2-(2-(2-chloroethoxy)ethoxy)ethanol **4** was converted to its corresponding azido-derivative **5** and the galactosamine building-unit **8** was synthesized by glycosylation of the known[25] oxazoline **6** with derivative **5** (see Scheme 1). Condensation in the presence of trimethylsilyl triflate (TMSOTf) gave compound **7** in good yield, while subsequent reduction of the azido moiety with triphenylphosphine afforded the terminal amine derivative **8**.

The triantennary core-unit, which has been described earlier,[17] was smoothly functionalized by a *N*-Boc-glycine under standard amino acid coupling conditions to furnish compound **10**. Hydrolysis of the terminal ethyl esters rendered the trivalent carboxylic acid **11**. Purified **11** was condensed with excess of GalNAc **8** in order to afford compound **12**. Removal of the Boc-protecting group with TFA furnished the trivalent galactosamine **13** with a free amine, which allowed functionalization of the cluster with a tyrosine moiety. The incorporation of this amino acid was performed to enable the ready introduction of a ^{125}I radiolabel and thus to enable us track the incorporation efficacy and pharmacokinetics of the glycolipid per se. Thus, Fmoc-protected tyrosine(OtBu) was reacted with amine **13** under the agency of TBTU and HOBt to afford compound **21**. Subsequent treatment with piperidine (20% in DMF) provided galactoside **22**.

Having the required key synthon **22** in hand, attention was focused on the construction of the lipophilic component of the target glycolipid. Lithocholic acid was converted into its methyl ester **15**, followed by the introduction of a mesyl protecting group at the 3-hydroxyl position. The mesylated methyl ester was reacted with sodium azide to afford, by a nucleophilic substitution reaction, the required azido derivative **17** under inversion of the stereochemistry. Reduction of the azide group readily furnished amine **18**. Freshly distilled oleoyl chloride was used to acylate the free amino group of compound **18**, followed by saponification of the methyl ester to furnish 3-oleoylamidolithocholic acid, synthon **20** (Scheme 2).

The bile oleoylamido acid **20** was joined in moderate yield to the cluster GalNAc via TBTU/HOBt-aided coupling. Deprotection of the fully protected compound **23** was achieved in two steps. The *tert*-butyl ester was removed from the tyrosine by acid treament, while deprotection of the acetyl groups of GalNAc was accomplished by incubation with sodium methanolate. Purification of the target compound was performed by gel filtration over Sephacryl S100 in methanol. The homogeneity and identity of **3** was fully confirmed by NMR spectroscopy and mass spectrometry (Scheme 3). Glycolipid **3** forms stable micelles with a slightly larger size than HDL (8−10 nm) as judged from size exclusion chromatography on a Superose 6 column.[18]

Association of Glycolipids with Lipoproteins. Previously, we showed by FPLC that the presently applied hydrophobic bile acid residue **20** (see Scheme 2) mediates rapid incorporation of glycolipids **2**[17] and **3**[18] into liposomes by intercalation into the liposomal phospholipid bilayer. We now demonstrate using agarose gel electrophoresis that glycolipid **3** avidly and quantitatively incorporated into HDL and LDL at all glycolipid concentrations tested, leading to a reduced electrophoretic mobility of the lipoproteins by shielding off their negative surface charge (Figure 2). Since glycolipid **3** incorporates instantaneously and quantitatively into lipoproteins, even without the need for incubation at 37 °C (not shown), it indeed has a very

Scheme 2. Synthesis of the Lipophilic Anchor Synthon 20[a]

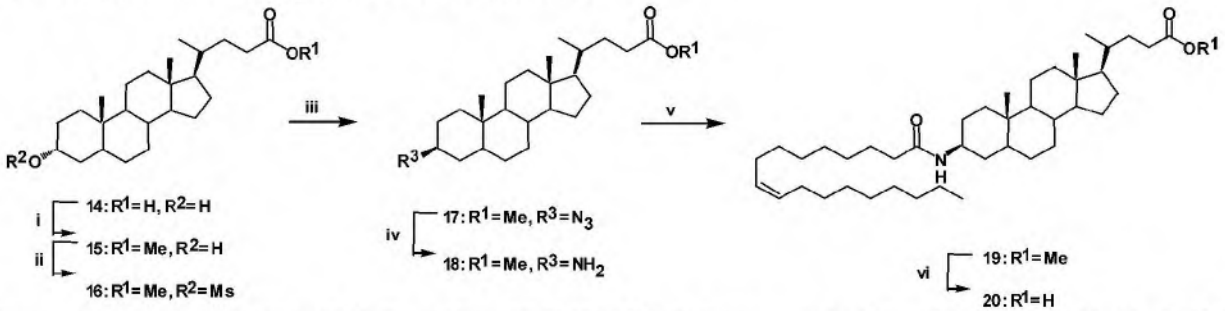

[a] Reagents: (i) MeOH, HCl, 100%; (ii) MsCl, pyridine; (iii) NaN_3, DMF, 70% two steps; (iv) PPh_3, THF; (v) oleoyl chloride, Et_3N, DCE, 86%; (iv) NaOH, dioxane, H_2O, 100%.

Scheme 3. Synthesis of Glycolipid 3[a]

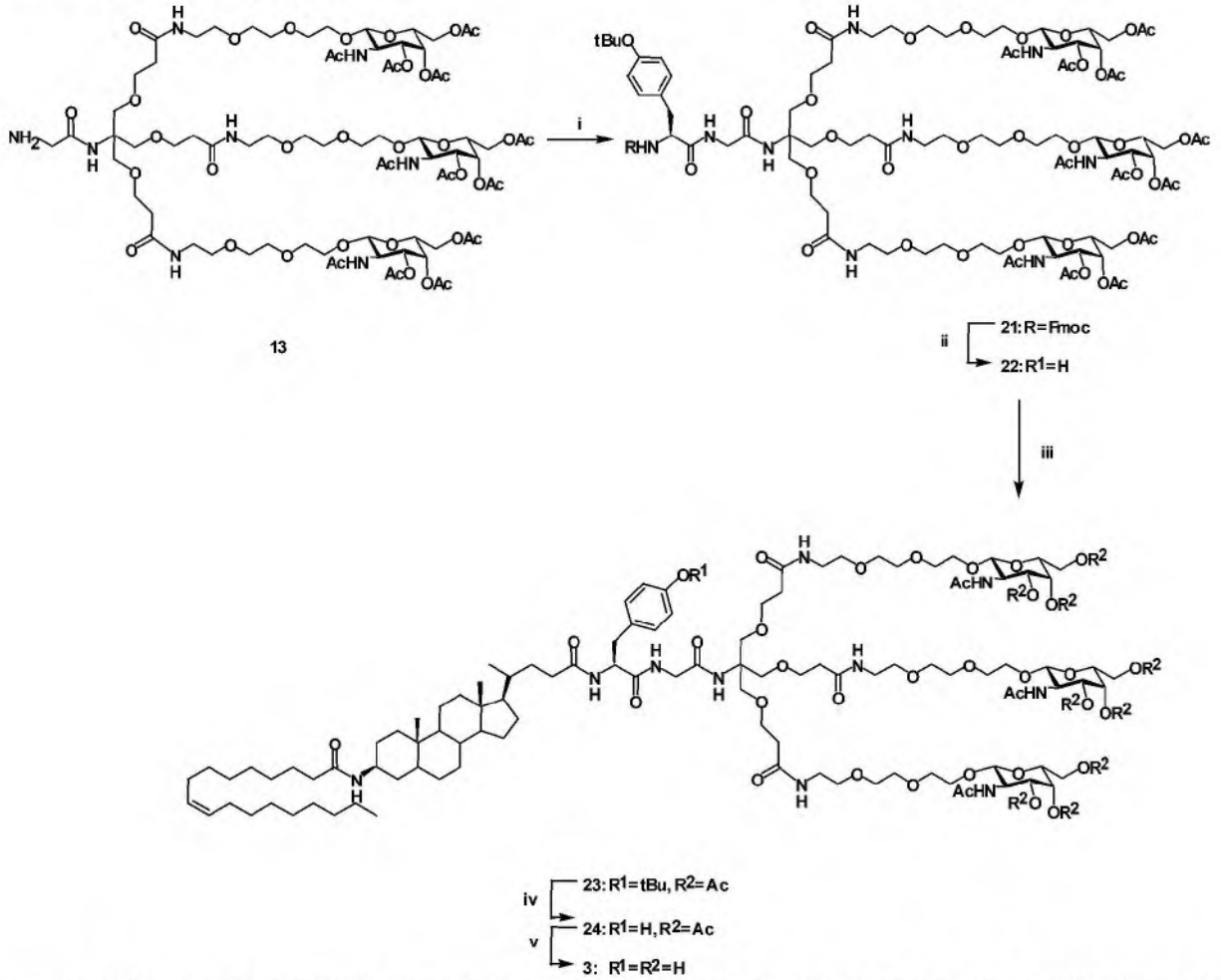

[a] Reagents: (i) FmocTyr(tBu)OH, TBTU, HOBt, DiPEA, DMF, 70%; (ii) 20% piperidine/DMF, 75%; (iii) **20**, TBTU, HOBt, DiPEA, DMF, 80%; (iv) DCM/TFA, 100%; (v) NaOMe, MeOH, 90%.

high affinity for lipoproteins. Since glycolipid **2** induced similar effects on LDL and HDL (not shown), the orientation of the oleoyl moiety relative to the steroid skeleton (α for glycolipid **2** and β for glycolipid **3**) apparently does not affect the distribution of glycolipid over LDL and HDL. Incorporation of the glycolipid did not significantly alter the lipoprotein size, as judged from Sepharose 6 elution profiles (not shown). At the applied amounts of lipoproteins (i.e. equal protein weight of HDL and LDL), the glycolipid displayed an increased association with LDL. This enhanced binding to LDL probably reflects the presence of a larger total phospholipid surface area (i.e. 1.7-fold) of LDL versus HDL at the applied particle ratio. Therefore, the glycolipid does not show preference for association with either lipoprotein. Indeed, the glycolipid induced a similar dose-dependent reduction in the mobility of both lipoproteins, and the relative distribution of the glycolipid over HDL and LDL remained constant over the whole glycolipid concentration range (Figure 2). At the highest amount tested, glycolipid **3** did not affect the composition of LDL (27.2 ± 1.7% protein, 3.3 ± 0.3% triglycerides, 18.8 ± 1.5% phosphatidylcholine, 42.1 ± 1.4% cholesteryl esters, and 8.5 ± 0.2% free cholesterol)

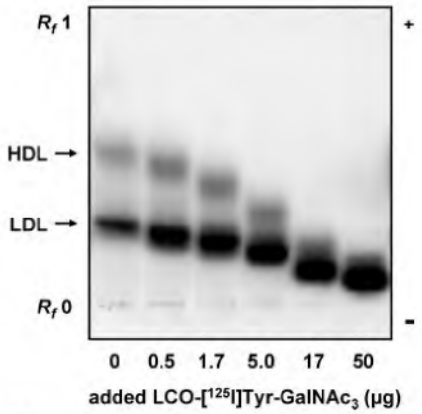

Figure 2. Association of the glycolipid with isolated lipoproteins. Glycolipid **3** (0−50 μg) mixed with a trace amount of [^{125}I]glycolipid **3** (20 ng) was incubated with HDL and LDL (5 μg of protein each) for 30 min at 37 °C. The mixtures were subjected to agarose gel electrophoresis, and radioactivity was visualized. +, anode; -, cathode; R_f 0, position application slots; R_f 1, position front marker bromophenol blue.

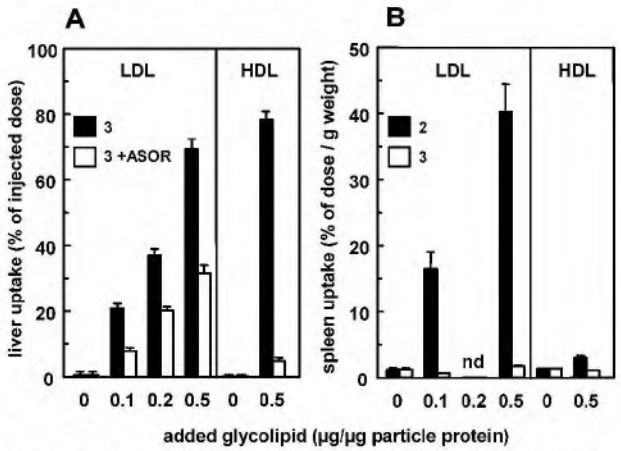

Figure 3. Liver uptake of control and glycolipid-laden lipoproteins in mice. [^{125}I]LDL (5 μg of protein) or [^{3}H]HDL (10 μg of protein) were incubated with the indicated amounts of glycolipid **3** (A, B) or **2** (B) and injected into anaesthetized C57Bl/6J mice, without or with previous injection of ASOR (25 mg/kg) at 1 min before injection of the lipoproteins (A). At 10 min after injection, liver lobules (A) and spleen (B) were taken, and the amount of radioactivity was determined. Values are means ± variation of two experiments.

or HDL (54.9 ± 1.3% protein, 2.2 ± 0.4% triglycerides, 22.9 ± 1.2% phosphatidylcholine, 17.7 ± 1.0% cholesteryl esters, and 2.4 ± 0.4% free cholesterol), as determined by incubation of isolated lipoproteins with the glycolipid and subsequent reisolation of lipoproteins by density gradient ultracentrifugation.

Liver Uptake of Glycolipid/Lipoprotein Complexes. We have recently shown that the novel triantennary GalNAc-terminated cluster glycoside **13** has a 50-fold increased affinity toward the ASGPr on hepatocytes as compared to triantennary galactose-terminated glycosides (K_i 2 vs 100 nM).[18] We now evaluated the effect of the increased affinity of glycolipids **3** over **2** on the induction of the hepatic uptake of lipoproteins. Upon intravenous injection into C57BL/6J mice, the hepatic uptake of [^{125}I]LDL and [^{3}H]HDL was negligible (<1% of the dose at 10 min after injection) (Figure 3A). Prior incubation of LDL or HDL with the novel glycolipid **3** caused a dose-dependently enhanced liver uptake, reaching 70 ± 3% and 78 ± 2% of the dose, respectively, at 0.5 μg of glycolipid per μg of particle protein (Figure 3A), similar to the effect of glycolipid **2** on the hepatic clearance of both lipoproteins. At this glycolipid loading, the ASGPr-specific inhibitor ASOR[26] inhibited the glycolipid-induced hepatic clearance of LDL and HDL for 63% and 94%, respectively. In contrast, the enhanced liver uptake of glycolipid **2**-laden LDL could not be inhibited by ASOR (not shown). These data indicate that the triantennary galactose moiety of glycolipid **2** mediates the uptake of LDL exclusively via the galactose particle receptor on liver macrophages (i.e. Kupffer cells), while replacement of the galactose groups by GalNAcs within the novel glycolipid **3** results in prominent uptake of both HDL and LDL by the ASGPr on hepatocytes. This observation is of major importance for application of glycolipids in cholesterol-lowering therapy, since only hepatocytes are able to directly excrete cholesterol from the body via the bile. Also, whereas glycolipid **2** enhanced the association of LDL with the spleen by 33.5-fold, glycolipid **3** did not affect the splenic uptake (and extrahepatic accumulation in general) of both lipoproteins (Figure 3B). The application of glycolipid **3** in cholesterol-lowering therapy will thus not result in unwanted cholesterol delivery to tissues other than the liver.

We have previously observed that a high surface density of glycolipid **2** leads to a shift in uptake of liposomes from hepatocytes to Kupffer cells,[17] whereas glycolipid **3** induced the uptake of liposomes by hepatocytes, irrespective of its surface density.[18] A similar phenomenon may underlie the different effect of the glycolipids on the intrahepatic distribution of LDL over hepatocytes and Kupffer cells. Whereas glycolipids can evenly distribute over the phospholipid surface of liposomes, the surface of LDL is largely covered by its protein constituent apolipoprotein B-100,[27,28] leaving relatively small clefts for the association of glycolipid. Therefore, the glycolipids will accumulate in these clefts, resulting in a local high glycolipid density, which, for glycolipid **2**, may lead to the induced LDL uptake by Kupffer cells. In contrast, the affinity of glycolipid **3** for the ASGPr is sufficiently high and selective to still induce the uptake of LDL by hepatocytes.

Association of Glycolipid with Lipoproteins In Vivo. To evaluate whether glycolipid **3** is able to spontaneously associate with plasma lipoproteins upon injection prior to elimination by the ASGPr, the tyrosine moiety of glycolipid **3** was radioiodinated, which allowed for kinetic studies in mice. The serum decay of glycolipid **3** upon iv injection (3.33 mg/kg) in C57BL/6J mice was relatively slow ($t_{1/2}$ ~30 min) and could be mainly attributed to a gradually increasing uptake by the liver (44 ± 3% at 60 min after injection) (Figure 4A). At 60 min after injection, glycolipid **3** was almost completely (>95%) associated with HDL (1.063 < d < 1.21 g/mL), as can be appreciated from the overlapping [^{125}I]glycolipid and HDL-cholesterol profiles (Figure 4B). Apparently, the affinity of the bile acid anchoring moiety of the glycolipid for lipoproteins is sufficiently high to overcome rapid elimination of the glycolipid by the liver. Instead, the glycolipid selectively accumulated in lipoproteins, which thus enables the subsequent delivery of lipoproteins to hepatocytes.

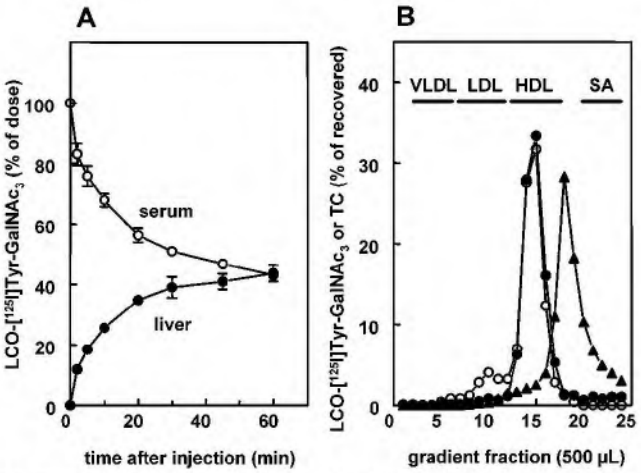

Figure 4. Association of the glycolipid with lipoproteins in plasma in vivo. [^{125}I]Glycolipid **3** (75 μg) was injected into the vena cava inferior of anaesthetized C57Bl/6J mice, and the liver uptake and serum decay were determined. Values are means ± variation of two experiments (A). At 60 min after injection, the mice were bled, and serum samples (100 μL; circles) or pure [^{125}I]glycolipid **3** (5 μg; triangles) were subjected to density gradient ultracentrifugation. The gradients were subdivided from top (fraction 1) to bottom (fraction 24), and the fractions were assayed for ^{125}I-activity (●, ▲) and total cholesterol (TC) (○) (B).

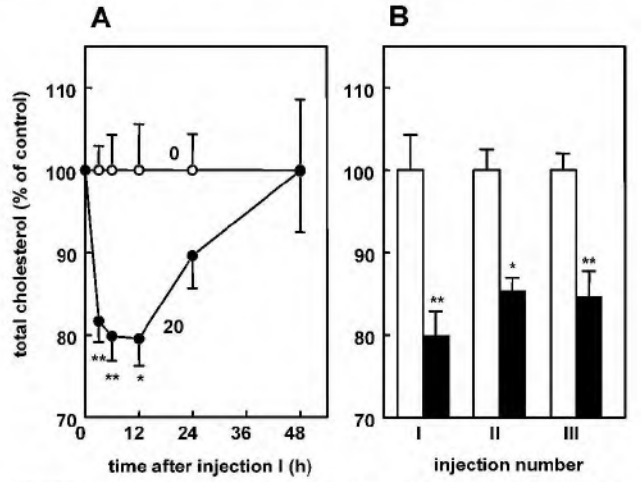

Figure 5. Hypocholesterolemic effect of the glycolipid in mice. Glycolipid **3** (20 mg/kg; ●) or PBS (○) was injected via the tail vein into *ldlr*$^{-/-}$ mice, and plasma samples were taken at the indicated times (A). Subsequently, mice received two additional injections of glycolipid **3** (closed bars) or PBS (open bars) at 72 h intervals, and additional plasma samples were taken at 6 h after injection (B). Total cholesterol levels in the plasmas were determined and expressed as percentage of control values. The initial cholesterol values (100%) in plasma samples taken before injection of glycolipids were 37.9 ± 3.6 mmol/L. Values are means ± SEM (n = 6). *P < 0.05, **P < 0.01

Cholesterol-Lowering Effect of Glycolipids. Since glycolipid **3** appeared superior to glycolipid **2** with respect to its ability to target lipoproteins specifically to hepatocytes, the ability of glycolipid **3** to reduce plasma cholesterol (i.e. lipoprotein) levels was evaluated in hyperlipidemic *ldlr*$^{-/-}$ mice as a model of familial hypercholesterolemia. Upon iv injection of glycolipid **3** into *ldlr*$^{-/-}$ mice, a marked lipoprotein-lowering effect was detected (Figure 5A). The effect peaked already at 3−6 h (20%; P < 0.01) and was still significant (P < 0.05) up to 12 h after injection. Baseline levels were reached only after 48 h after injection. For clinical application of glycolipids in hyperlipidemia, glycolipids should be able to show consistent effects upon repeated administration. Importantly, three consecutive injections of glycolipid **3** mice at 72 h time intervals resulted in consistent reductions in total cholesterol levels (Figure 5B). The glycolipid showed no sign of toxicity at the applied dose as compared to saline injection. At 3 or 24 h after iv injection into mice, no effects were observed on the weight of several organs (liver, heart, kidneys, spleen) and plasma levels of enzymes that would indicate systemic toxicity (lactate dehydrogenase) or liver toxicity (alanine aminotransferase, aspartate aminotransferase, γ-glutamyl transferase). In addition, the glycolipid did not cause hemolysis after incubation with heparinized blood at concentrations equivalent to doses of 100 mg/kg (not shown).

In conclusion, we have prepared glycolipid **3** with an unusually high affinity and specificity for the hepatic ASGPr. The glycolipid is capable of associating with plasma lipoproteins and thereby induces the uptake of LDL and HDL by hepatocytes, which are able to secrete excess cholesterol from the body via the bile as neutral sterols and bile acids, rather than by Kupffer and splenic cells. In this respect, the glycolipid presented here is superior to the latest glycolipid introduced by our group for hepatocyte-directed targeting purposes.[17] Importantly, injection of glycolipid **3** resulted in a prolonged and repeated cholesterol-lowering in a mouse model of familial hypercholesterolemia. This advantageous property of glycolipid **3** opens the way for the employment of glycolipids for cholesterol-lowering therapy in those hypercholesterolemic patients who do not respond to conventional cholesterol-lowering therapies.

Experimental Section

General. Pyridine, *N,N*-dimethylformamide (DMF), 1,2-dichloroethane (DCE), dichloromethane (DCM), 1,4-dioxane, ethanol, tetrahydrofuran (THF), toluene, *N,N*-diisopropylethylamine (DIPEA), trifluoroacetic acid (TFA), piperidine, triethylamine (Et_3N), and methanol were from Biosolve (Valkenswaard, The Netherlands). Methanol was stored over 3 Å molecular sieves, and DMF, DCE, DCM, and THF were stored over 4 Å molecular sieves. Trimethylsilyl trifluoromethanesulfonate (TMSOTf, Fluka), triphenylphosphine (Acros), *N*-Boc-L-glycine (NovaBiochem), (benzotriazol-1-yloxy)tris(dimethylamino)phosphonium hexafluorophosphate (BOP, NovaBiochem), 1-hydroxybenzotriazole (HOBt, NovaBiochem), *O*-(benzotriazol-1-yl)-*N,N,N′,N′*-tetramethyluronium tetrafluoroborate (TBTU, NovaBiochem), *N*-Fmoc-*O*-*tert*-butyl-L-tyrosine (NovaBiochem); mesyl chloride (Merck); sodium azide (Acros); and 1,3-dipropanedithiol (Aldrich) were used as received. Before use oleoyl chloride (Fluka) was distilled under reduced pressure to afford a colorless oil. [1α,2α-^{3}H]cholesteryl oleate and ^{125}I (carrier-free) were from Amersham Biosciences (Little Chalfont, UK). Asialoorosomucoid (ASOR) was prepared by enzymatic desialylation (approximately 70%, as judged by the extent of sialic acid release) of human α_1-acid glycoprotein (orosomucoid) from Cohn Fraction VI (99%; Sigma) as described.[29] All other chemicals were of analytical grade. Merck Kieselgel 60 F_{254} DC Alufolien was used for TLC analysis. Compounds were visualized with UV light (254 nm). Carbohydrate compounds were visualized by charring with sulfuric acid/ethanol (1/4, v/v) at ~150 °C and bile acid esters[30] by charring with $MnCl_2$ at ~150 °C. Compounds containing NH groups were visualized after treatment of the plates with chlorine, spraying with a solution of TDM,[31] and subsequent heating to ~150 °C or by spraying with a solution of ninhydrine in acetic acid/water and subsequent heating. Column

chromatography was performed with Kieselgel 60, 230–400 mesh (Merck). Gel filtration was performed with Sephadex LH-20 (Pharmacia). $^{13}C\{^1H\}$ NMR spectra (75 MHz) and ^1H NMR spectra (300 MHz) were recorded using a Bruker WM-300 spectrometer. Chemical shifts are given in ppm (δ) relative to tetramethylsilane as an internal standard. Fast atom bombardment (FAB) mass spectrometry was carried out using a JEOL JMS SX/SX102A four-sector mass spectrometer, coupled to a JEOL MS-MP7000 data system.

2-(2-(2-Azidoethoxy)ethoxy)ethanol (5). 2-(2-(2-Chloroethoxy)ethoxy)ethanol **4** (10 g, 59.3 mmol) was dissolved in dry ethanol (50 mL), and sodium iodide (0.9 g, 6 mmol) and sodium azide (4.55 g, 70 mmol; preactivated with hydrazine monohydrate) were added. The resulting mixture was refluxed for 5 days until TLC analysis (DCM/methanol 9/1, v/v) showed one product. The reaction mixture was filtered (salts) and concentrated. The residue was dissolved in DCM (50 mL) and stored for 16 h at 4 °C. After filtration and concentration, compound **5** was obtained as clear oil. Yield: 6.42 g (36.6 mmol, 62%). $^{13}C\{^1H\}$ NMR ($CDCl_3$): δ 50.0 (CH_2–N_3), 60.6 (CH_2OH), 69.2, 69.5, 69.8 (3 × CH_2O). ^1H NMR ($CDCl_3$): δ 3.44 (m, 2H, CH_2N_3), 3.68 (m, 10H, CH_2O).

2-(2-(2-Azidoethoxy)ethoxy)ethyl 2-Acetamido-3,4,6-tri-*O*-acetyl-2-deoxy-β-D-galactopyranoside (7). The known oxazoline **6**[25] (1.04 g, 3.0 mmol) and 2-(2-(2-azidoethoxy)-ethoxy)ethanol **5** (0.80 g, 4.6 mmol) were dissolved in 1,2-dichloroethane (DCE) (10 mL). Molecular sieves (4 Å) were added and the mixture was stirred for 30 min. Then, TMSOTf[23] (0.27 mL, 1.5 mmol) was added, and the reaction was stirred overnight. According to TLC analysis (DCM/methanol 9/1, v/v), the oxazoline **6** was completely converted into a lower running product. The mixture was filtered over Hyflo. The filtrate was taken up in DCM (50 mL), washed with aq $NaHCO_3$ (1 M, 50 mL) and water (50 mL), dried over $MgSO_4$, and concentrated to an oil. The crude product was purified by silica gel column chromatography, with DCM/methanol (1/0 → 94/6, v/v) as eluent. Yield: 1.29 g (2.56 mmol, 85%). $^{13}C\{^1H\}$ NMR ($CDCl_3$): δ 20.3 (CH_3 Ac), 22.8 (CH_3 NHAc), 50.2 (C-2 Gal), 50.3 (CH_2–N_3), 61.1 (CH_2O), 61.3 (C-6 Gal), 68.2–72.2 (4 × CH_2O), 66.4, 70.2, 70.5 (C-3,4,5 Gal), 101.7 (C-1 Gal), 169.7, 170.1 (C=O). ^1H NMR ($CDCl_3$): δ 1.99, 2.00, 2.05 (3 × s, 9H, CH_3, Ac), 2.16 (s, 3H, CH_3, NHAc), 3.48 (t, 2H, CH_2N_3), 3.61–3.76 (m, 8H, CH_2O), 3.89 (m, 1H, H-5 Gal), 3.90 (t, 2H, CH_2O), 4.15 (t, 2H, H-6a, H-6b Gal), 4.22 (m, 1H, H-2 Gal, J_{N-2} = 9.3 Hz), 4.78 (d, 1H, H-1 Gal, J_{1-2} = 8.6 Hz), 5.06 (dd, 1H, H-3 Gal, J_{3-4} = 3.3 Hz, J_{3-2} = 11.2 Hz), 5.32 (d, 1H, H-4 Gal), 6.15 (d, 1H, N*H*).

2-(2-(2-Aminoethoxy)ethoxy)ethyl 2-Acetamido-3,4,6-tri-*O*-acetyl-2-deoxy-β-D-galactopyranoside (8). The azide **7** (314 mg, 622 μmol) was dissolved in THF (10 mL), and triphenylphosphine (196 mg, 746 μmol) was added. The mixture was stirred for 48 h, until TLC analysis (toluene/methanol 1/1, v/v) showed the absence of starting material. Water (32 μL, 1.8 mmol) was added to the reaction, and stirring was continued for another 24 h. TLC analysis (toluene/methanol 1/1, v/v and 2-propanol/water 4/1, v/v) showed one product that was both H_2SO_4- and ninhydrine-positive. Trifluoroacetic acid (TFA, 96 μL, 1.25 mmol) and toluene (10 mL) were added, the mixture was concentrated to near dryness and finally coevaporated with toluene (2 × 10 mL). The crude amine **8** thus obtained was used immediately for the synthesis of the protected cluster **12**. $^{13}C\{^1H\}$ NMR ($CDCl_3$): δ 20.2 (CH_3 Ac), 22.6 (CH_3 NHAc), 42.4 (CH_2NH_2), 49.9 (C-2 Gal), 61.3 (C-6 Gal), 68.5–70.2 (CH_2O), 66.5, 69.9 (C-3,4,5 Gal), 101.1 (C-1 Gal), 169.6, 169.8, 169.9 (C=O), 170.9 (C=O, NHAc). ^1H NMR ($CDCl_3$): δ 1.88, 1.94, 2.03 (3 × s, 9H, CH_3, Ac), 2.09 (s, 3H, CH_3, NHAc), 3.20 (m, 2H, CH_2NH_2), 3.47 (m, 4H, 2 × CH_2O), 3.61 (t, 2H, CH_2O), 3.66 (t, 2H, CH_2O), 3.75 (m, 2H, CH_2O), 3.91 (m, 2H, H-5 Gal, N*H*), 4.11 (m, 3H, H-2, H-6a, H-6b Gal), 4.87 (d, 1H, H-1 Gal, J_{1-2} = 8.5 Hz), 5.20 (dd, 1H, H-3 Gal, J_{3-4} = 3.3 Hz, J_{3-2} = 11.2 Hz), 5.34 (d, 1H, H-4 Gal).

***N*-(*tert*-butoxycarbonylglycinyl)tris(carboxyethoxymethyl)aminomethane triethyl ester (10).** Tris(carboxyethoxyethyl)aminoethane triethyl ester **9**[17] (729 mg, 1.73 mmol), *N*-*tert*-butoxycarbonyl-glycine (*N*-BocGlyOH) (306 mg, 1.73 mmol), and BOP (920 mg, 2.08 mmol) were dissolved in DCE (15 mL), and acylation was started by addition of DIPEA (0.72 mL, 4.15 mmol). The resulting mixture was stirred overnight at 20 °C. According to TLC analysis (DCM/methanol 9/1, v/v), the reaction was complete. The mixture was taken up in DCM (50 mL); washed with H_2O (50 mL), $NaHCO_3$ (1 M, 50 mL), and brine (50 mL); dried ($MgSO_4$); and concentrated. The resulting oil was applied to a silica gel column, using ethyl acetate/hexane (1/2 → 1/0, v/v) as eluent, affording compound **10**. Yield: 0.90 g (1.61 mmol, 93%). $^{13}C\{^1H\}$ NMR ($CDCl_3$): δ 14.0 (CH_3 OEt), 28.1 (CH_3 Boc), 34.7 (CH_2C=O), 44.2 (CH_2 Gly), 59.6 (C_q tris), 60.2 (OCH_2CH_3), 66.6 (OCH_2), 68.9 (CH_2 tris), 80.5 (C_q Boc), 156.4 (C=O Boc), 169.1 (C=O ester), 171.4 (C=O amide). ^1H NMR ($CDCl_3$): δ 1.26 (t, 9H, CH_3 ethyl), 1.45 (s, 9H, CH_3 Boc), 2.03 (d, 2H, CH_2 Gly, J_{H-NH} = 0.6 Hz), 2.53 (t, 6H, CH_2C=O, J = 6.2 Hz), 3.70 (m, 12 H, OCH_2), 4.13 (dq, 6H, OCH_2, J = 7.1 Hz), 5.38 (bs, 1H, N*H* Boc), 6.39 (d, 1H, N*H* Gly).

***N*-(*tert*-butoxycarbonylglycinyl)tris(carboxyethoxymethyl)aminomethane (11).** The triester **10** (0.85 g, 1.52 mmol) was dissolved in a mixture of 1,4-dioxane (90 mL) and water (27 mL), and aqueous NaOH (4 M, 3 mL) was added. After stirring for 16 h, TLC analysis (DCM/methanol/acetic acid 18/2/1, v/v/v) showed complete conversion of the starting material into one product. The mixture was carefully neutralized by the addition of Dowex (50 W x 8, H^+ form). The mixture was filtered, and the filtrate concentrated. The residue was coevaporated with toluene (2 × 10 mL) and purified by means of a silica gel column using DCM/methanol/acetic acid (100/0/1 → 95/5/1, v/v/v) as eluent. Yield: 0.75 g (1.52 mmol, 100%). $^{13}C\{^1H\}$ NMR ($CDCl_3$): δ 28.7 (CH_3 Boc), 36.7 (CH_2C=O), 44.9 (CH_2 Gly), 61.2 (C_q tris), 68.2 (OCH_2), 70.0 (CH_2 tris), 80.7 (C_q Boc), 156.5 (C=O Boc), 172.2 (C=O amide), 176.0, 176.3 (C=O, carboxyl). ^1H NMR ($CDCl_3$): δ 1.44 (s, 9H, CH_3 Boc), 2.09 (s, 2H, CH_2 Gly), 2.57 (t, 6H, CH_2C=O), 3.71 (bs, 14 H, OCH_2), 6.59 (bs, 1H, N*H* Gly).

***N*-(*tert*-butoxycarbonylglycinyl)tris{(1-[2-(2-aminoethoxy)ethoxy]ethoxy-2-acetamido-3,4,6-tetra-*O*-acetyl-2-deoxy-β-D-galactosamine)(carboxyethoxymethyl)}methane (12).** To a solution of the tricarboxylate **11** (74 mg, 149 μmol) and the crude amine **8** (<622 μmol) in DMF (5 mL) were added DIPEA (188 μL, 1.08 mmol), HOBt (73 mg, 0.54 mmol), and TBTU (173 mg, 0.54 mmol). The mixture was stirred overnight, after which an extra amount of DIPEA (188 μL, 1.08 mmol) was added and the mixture was stirred again for another 18 h. According to TLC analysis (DCM/methanol 4/1, v/v), the reaction was complete. The reaction mixture was taken up in DCM (40 mL); washed with dilute H_3PO_4 (1 M, 40 mL), aq $NaHCO_3$ (1 M, 40 mL), and water (40 mL); dried ($MgSO_4$); and concentrated to an oil. This oil was applied to a silica gel column, and elution was performed with DCM/methanol (1/0 → 84/16, v/v). The crude product thus obtained was further purified by Sephadex LH20 gel filtration, using DCM/methanol (1/1, v/v) as eluent. Yield: 161 mg (86 μmol, 58%). $^{13}C\{^1H\}$ NMR ($CDCl_3$): δ 20.3 (CH_3 Ac), 22.7 (CH_3 NHAc), 27.9 (CH_3 Boc), 34.1, 36.1, 38.8 (CH_2C=O), 43.1 (CH_2 Gly), 50.2 (C-2 Gal), 51.3 (CH_2–NH), 59.4 (CH_2O), 61.2 (C-6 Gal), 66.4, 70.1 (C-3,4,5 Gal), 67.0–70.0 (CH_2O), 79.2 (C_q, Boc), 101.0 (C-1 Gal), 155.7 (C=O Boc), 169.5, 169.9, 170.6 (C=O ester, amide), 171.3 (C=O NHAc). ^1H NMR ($CDCl_3$): δ 1.44 (s, 9H, CH_3 Boc), 1.96, 1.99, 2.05 (3 × s, 27H, CH_3 Ac), 2.09 (s, 2H, CH_2 Gly), 2.15 (s, 9H, CH_3 NHAc), 2.43, 2.55 (m, 6H, CH_2C=O), 2.97, 3.05, 3.25 (m, 6H, CH_2NH), 3.46–3.94 (m, 24H, OCH_2, H-5 Gal), 4.13 (m, 9H, H-6a, H-6b, H-2 Gal), 4.79 (d, 3H, H-1 Gal), 5.21 (dd, 3H, H-3 Gal), 5.34 (d, 3H, H-4 Gal, $J_{4,3}$ = 3.0 Hz).

Glycinyltris{(1-[2-(2-aminoethoxy)ethoxy]ethoxy-2-acetamido-3,4,6-tetra-*O*-acetyl-2-deoxy-β-D-galactosamine)-(carboxyethoxymethyl)}methane (13). The fully protected derivative **12** (155 mg, 83 μmol) was dissolved in TFA/DCM (1/4, v/v; 5 mL). After the mixture was stirred for 60 min, toluene (20 mL) was added. The mixture was concentrated and the residue coevaporated with toluene (3 × 10 mL). According

to TLC analysis (DCM/methanol 9/1, v/v), the starting material was completely converted into a lower running product. The thus obtained crude **13** was used without prior purification for the synthesis of compound **21**. $^{13}C\{^1H\}$ NMR ($CDCl_3$): δ 20.2 (CH_3 Ac), 22.5 (CH_3 NHAc), 34.3, 35.9, 38.9 ($CH_2C{=}O$), 44.7 (CH_2 Gly), 50.1 (C-2 Gal), 51.4 ($CH_2{-}N_3$), 60.2, 66.4, 67.0, 68.5, 69.8 (CH_2O), 61.3 (C-6 Gal), 66.5, 70.3 (C-3,4,5 Gal), 101.2 (C-1 Gal), 170.2, 170.4 ($C{=}O$ ester, amide), 171.9 ($C{=}O$ NHAc).

Lithocholic Acid Methyl Ester (15).[32] Lithocholic acid (3.77 g, 10 mmol) was dissolved in methanol (25 mL). Concentrated HCl (0.5 mL, 36−38%) was added, and the solution was heated at reflux temperature (65 °C). After 30 min, TLC analysis (toluene/ethanol 85/15, v/v; $MnCl_2$ staining) showed that the ester formation was complete. The reaction mixture was cooled overnight at 0 °C. The crystallized solid was collected by filtration and washed with cold methanol (25 mL). The white solid **15** was dried at room temperature. Yield: 2.97 g (7.6 mmol, 76%). $^{13}C\{^1H\}$ NMR ($CDCl_3$): δ 11.9 (CH_3 C18), 18.1 (CH_3 C21), 20.7 (CH_2), 23.3 (CH_3 C19), 24.1, 26.3, 27.1, 28.0, 30.4, 30.8, 30.9, 34.4, 35.3 (CH_2), 35.2 (*C*H C20), 35.7 (*C*H C8), 40.0 (C_q C10), 40.3 (*C*H C9), 42.0 (*C*H C5), 42.6 (C_q C13), 51.4 (O*C*H3), 55.8 (*C*H C17), 56.3 (*C*H C14), 71.6 (*C*HOH C3), 174.7 ($C{=}O$ C24). ^1H NMR ($CDCl_3$): δ 0.64 (s, 3H, CH_3 C18), 0.90 (s, 3H, CH_3 C21), 0.92 (s, 3H, CH_3 C19), 0.97−1.98 (m, 27H, *C*H, CH_2), 2.28 (m, 2H, $CH_2C{=}O$ C23), 3.33 (bs, 1H, O*H*), 3.66 (s, 3H, OCH_3).

3-Azidolithocholic Acid Methyl Ester (17). Lithocholic acid methyl ester **15** (0.78 g, 2.0 mmol) was dissolved in DCE (10 mL) and concentrated. Next, the methyl ester was dissolved in pyridine (20 mL) and cooled to 0 °C, and following addition of mesyl chloride (186 μL, 2.4 mmol), the resulting mixture was allowed to warm to room temperature. After incubation for 3 h, TLC analysis (toluene/ethanol 85/15, v/v; $MnCl_2$ staining) showed complete disappearance of the starting compound **15**. The reaction mixture was concentrated and coevaporated with toluene (3 × 10 mL). The intermediate compound **16** was dissolved in DMF (20 mL), sodium azide (156 mg, 2.4 mmol) was added, and the mixture was subsequently heated overnight at 100 °C. The reaction mixture was concentrated in vacuo and taken up in DCM (30 mL). The organic layer was washed with water (20 mL), $NaHCO_3$ (1 M, 20 mL), and brine (20 mL); dried ($MgSO_4$); and concentrated. The crude brown solid was recrystallized from DCM/hexane, affording a white solid. Yield: 0.67 g (1.62 mmol, 81%). $^{13}C\{^1H\}$ NMR ($CDCl_3$): δ 11.8 (CH_3 C18), 18.1 (CH_3 C21), 20.8 (CH_2), 23.6 (CH_3, C19), 23.9, 24.5, 26.1, 26.3, 28.0, 30.0, 30.5, 30.8, 34.7 (CH_2), 35.1 (*C*H C20), 35.4 (*C*H C8), 37.1 (*C*H, C9), 39.9 (*C*H C5), 40.0 (C_q C10), 42.5 (C_q C13), 51.2 (*C*H, C17), 55.8 (*C*H C14), 56.4 (O*C*H3), 58.5 (*C*H C3 *C*H-N_3), 174.4 ($C{=}O$ C24). ^1H NMR ($CDCl_3$): δ 0.65 (s, 3H, CH_3 C18), 0.90 (d, 3H, CH_3 C21 J = 6.4 Hz), 0.95 (s, 3H, CH_3 C19), 1.03−2.00 (m, 27H, *C*H, CH_2), 2.28 (m, 2H, $CH_2C{=}O$ C23), 3.66 (s, 3H, OCH_3).

3-Aminolithocholic Acid Methyl Ester (18). The azido derivative **17** (0.15 g, 0.36 mmol) was dissolved in methanol (1.8 mL) to a concentration of 0.2 M. Et_3N (0.25 mL, 1.8 mmol) and 1,3-propanedithiol (0.18 mL, 1.8 mmol) were added, and the resulting mixture was heated at 60 °C for 2 days. TLC analysis (hexane/diethyl ether 3/1, v/v) established that the conversion was complete. After addition of toluene (2 mL) the reaction mixture was concentrated and coevaporated with toluene (3 × 10 mL), resulting in a yellowish solid. The crude product was purified by means of silica gel chromatography using hexane/diethyl ether (5/1 → 1/1, v/v) as eluent, affording **18** as a white solid. Yield: 101 mg (0.26 mmol, 72%). $^{13}C\{^1H\}$ NMR ($CDCl_3$): δ 11.7 (CH_3 C18), 18.0 (CH_3 C21), 20.8 (CH_2), 23.6 (CH_3 C19), 23.9, 26.0, 26.4, 27.5, 28.9, 29.6, 30.7, 33.2, 34.7, 36.6 (CH_2), 35.0 (*C*H C20), 35.3 (*C*H C8), 36.2 (*C*H C9), 39.5 (*C*H C5), 39.9 (C_q C10), 42.4 (C_q C13), 51.1 (O*C*H3), 55.7 (*C*H C17), 56.3 (*C*H C14), 66.5 (*C*H C3 *C*H-NH_2), 174.4 ($C{=}O$ C24).

3-Oleoylamidolithocholic Acid Methyl Ester (19). The amine **18** (156 mg, 400 μmol) was dissolved in dry DCE (10 mL). The solution was cooled to 0 °C, and triethylamine (88 μL, 0.60 mmol) and oleoyl chloride (0.20 mL, 0.60 mmol) were added. After the mixture had been stirred for 3 h, TLC analysis (hexane/diethyl ether 2/3, v/v) revealed complete conversion of starting material. The reaction mixture was taken up in DCM (40 mL), washed with aq $NaHCO_3$ (1 M, 40 mL) and water (40 mL), dried ($MgSO_4$), and concentrated to an oil. This oil was applied to a silica gel column, and elution was performed with hexane/diethyl ether (4/1 → 3/1, v/v). Yield: 225 mg (344 μmol, 86%). $^{13}C\{^1H\}$ NMR ($CDCl_3$): δ 11.7 (CH_3 C18), 13.7 (CH_3 oleoyl), 17.9 (CH_3 C21), 20.8 (CH_2), 23.5 (CH_3 C19), 22.4, 23.9, 24.7, 24.8, 25.9, 26.2, 26.9, 27.8, 28.8, 28.9, 29.1, 29.3, 29.4, 29.5, 30.4, 30.5, 30.7, 31.6, 34.3, 34.5 (CH_2), 35.0 (*C*H C20), 35.4 (*C*H C8), 37.1 (*C*H C9), 39.6 (*C*H C5), 39.9 (C_q C10), 42.4 (C_q C13), 50.8 (O*C*H3), 55.7 (*C*H, C17), 56.2 (*C*H C14), 69.8 (*C*H C3 *C*H-NH), 129.3, 129.5 (C=*C*H, oleoyl), 172.4, 173.7 ($C{=}O$). ^1H NMR ($CDCl_3$): δ 0.65 (s, 3H, CH_3 C18), 0.83−0.92 (m, 6H, CH_3 C21, oleoyl, 0.96 (s, 3H, CH_3 C19), 1.08−1.16 (m, 8H, CH_2), 1.26−1.43 (m, 30H, CH_2), 1.52−1.73 (m, 8H, CH_2), 1.75−2.05 (m, 7H, *C*H), 2.17−2.38 (m, 4H, $CH_2C{=}O$), 3.66 (s, 3H, OCH_3), 5.07 (bs, 1H, N*H*), 5.34 (m, 2H, C=*C*H oleoyl).

3-Oleoylamidolithocholic Acid (20). The methyl ester **19** (200 mg, 306 μmol) was dissolved in a mixture of 1,4-dioxane (30 mL) and water (9 mL), and deprotection was started by adding aq NaOH (4 M, 1 mL). The mixture was stirred overnight. TLC analysis (hexane/diethyl ether 2/3, v/v) revealed that the starting material was completely converted into a product with zero mobility. The mixture was carefully neutralized by the addition of Dowex (50 W x 8, H^+ form) and then filtered. The filtrate was concentrated to a small volume and applied to a silica gel column. Elution with hexane/diethyl ether (1/0 → 1/1, v/v) furnished pure **20** as a white solid. Yield: 196 mg (306 μmol, >99%). $^{13}C\{^1H\}$ NMR ($CDCl_3$): δ 12.0 (CH_3 C18), 14.1 (CH_3 oleoyl), 18.2 (CH_3 C21), 20.8 (CH_2), 23.3 (CH_3 C19), 22.7, 24.2, 24.7, 25.1, 26.3, 26.7, 27.0, 27.2, 28.1, 29.1, 29.3, 29.5, 29.7, 30.8, 31.0, 31.9, 32.3, 34.0, 34.6, 34.8, 35.0 (CH_2), 35.3 (*C*H C20), 35.8 (*C*H C8), 40.1 (C_q C10), 40.4 (*C*H, C9), 41.9 (*C*H C5), 42.7 (C_q C13), 56.0 (*C*H, C17), 56.5 (*C*H C14), 74.1 (*C*H C3 *C*H-NH), 129.7, 130.0 (C=*C*H oleoyl), 179.9, 180.4 ($C{=}O$). ^1H NMR ($CDCl_3$): δ 0.65 (s, 3H, CH_3 C18), 0.86−0.91 (m, 9H, CH_3), 1.07−1.11 (m, 8H, CH_2), 1.26−1.30 (m, 30H, CH_2), 1.61−1.63 (m, 8H, CH_2), 1.80−1.83 (m, 2H, *C*H), 2.00−2.05 (m, 5H, *C*H), 2.23−2.37 (m, 4H, $CH_2C{=}O$), 5.35 (m, 2H, C=*C*H oleoyl).

***O*-*tert*-Butyl-*N*−Fmoc-tyrosinyl-glycinyl-tris{(1-[2-(2-aminoethoxy)ethoxy]ethox y-2-acetamido-3,4,6-tetra-*O*-acetyl-2-deoxy-β-D-galactosamine)(carboxyethoxymethyl)}methane (21).** The crude amine **13** (155 mg, <83 μmol) and *N*-FmocTyr(tBu)OH (57 mg, 125 μmol) were dissolved in DMF (10 mL). To the solution were added DIPEA (30 μL, 170 μmol), HOBT (17 mg, 125 μmol), and TBTU (40 mg, 125 μmol), and the mixture was stirred for 3 h until TLC analysis (DCM/methanol 85/15, v/v) indicated the reaction to be complete. The reaction mixture was taken up in DCM (40 mL); washed with dilute H_3PO_4 (1 M, 40 mL), aq $NaHCO_3$ (1 M, 40 mL), and water (40 mL); dried ($MgSO_4$); and concentrated to an oil. This oil was applied to a silica gel column, and elution was performed with DCM/methanol (1/0 → 88/12, v/v), followed by Sephadex LH-20 gel filtration, using DCM/methanol (1/1, v/v) as eluent. Yield: 129 mg (58 μmol, 70%). $^{13}C\{^1H\}$ NMR ($CDCl_3$): δ 20.4 (CH_3 Ac), 22.8 (CH_3 NHAc), 28.5 (CH_3 tBu), 34.4, 36.4, 39.0 ($CH_2C{=}O$), 37.7 (CH_2 Tyr), 43.1 (CH_2 Gly), 50.3 (C-2 Gal), 51.6 ($CH_2{-}$NH), 56.2 (*C*H Tyr), 59.9 (CH_2O), 61.4 (C-6 Gal), 66.7, 70.4 (C-3,4,5 Gal), 66.9−70.3 (CH_2O), 79.2 (C_q tBu), 101.4 (C-1 Gal), 119.8, 124.9, 126.9, 127.6 (*C*H Fmoc), 124.0, 129.6 (*C*H Tyr), 131.3, 154.1 (C_q Tyr Fmoc), 141.1, 143.6 (C_q Fmoc), 155.9 ($C{=}O$ Fmoc), 170.3, 170.5, 170.6 ($C{=}O$ ester, amide), 171.6 ($C{=}O$ NHAc). ^1H NMR ($CDCl_3$): δ 1.28 (s, 9H, CH_3 tBu), 1.94, 1.98, 2.02 (3 × s, 27H, CH_3 Ac), 2.07 (s, 2H, CH_2 Gly), 2.13 (s, 9H, CH_3 NHAc), 2.41−2.53 (m, 6H, $CH_2C{=}O$), 2.92−3.05 (m, 6H, CH_2NH), 3.14 (m, 2H, βCH_2 Tyr), 3.59−3.92 (m, 45H, OCH_2, H-5 Gal), 4.14 (m, 9H, H-6a, H-6b, H-2 Gal), 4.36 (m, 2H, α*C*H Tyr, *C*H Fmoc), 4.49 (m, 2H, OCH_2 Fmoc), 4.74 (d, 3H, H-1 Gal J = 8.3 Hz), 5.18 (dd, 3H, H-3 Gal

J_{3-2} = 10.5 Hz), 5.33 (d, 3H, H-4 Gal), 6.86−7.11 (4H, C*H* Tyr), 7.30−7.76 (8H, C*H* Fmoc).

***O*-*tert*-Butyl-*N*-tyrosinylglycinyltris{(1-[2-(2-aminoethoxy)ethoxy]ethoxy-2-acetamido-3,4,6-tetra-*O*-acetyl-2-deoxy-*β*-D-galactosamine)(carboxyethoxymethyl)}methane (22).** The fully protected derivative **21** (120 mg, 54 μmol) was dissolved in piperidine/THF (5/95, v/v; 10 mL) and the mixture was stirred for 1 h. TLC analysis (DCM/methanol 85/15, v/v) revealed complete conversion of starting material into a single ninhydrine-positive product with lower mobility. Toluene (10 mL) was added, the mixture was concentrated to a small volume and coevaporated with toluene (2 × 10 mL). The residue was purified by means of silica gel column using DCM/methanol (100/1 → 8/2) as eluent. Yield: 81 mg (41 μmol, 75%). $^{13}C\{^1H\}$ NMR ($CDCl_3$): δ 20.4 (*C*H_3 Ac), 22.9 (*C*H_3 NHAc), 28.5 (*C*H_3 tBu), 34.3, 36.2, 38.9 (*C*H_2C=O), 37.3 (*C*H_2 Tyr), 44.3 (*C*H_2 Gly), 50.2 (C-2 Gal), 51.4 (*C*H_2−NH), 56.1 (*C*H Tyr), 59.8 (*C*H_2O), 61.3 (C-6 Gal), 67.1, 70.2 (C-3,4,5 Gal), 66.5−69.9 (*C*H_2O), 78.1 (*C*$_q$ tBu), 101.2 (C-1 Gal), 124.0, 124.9, (*C*H Tyr), 131.3, 153.9 (*C*$_q$ Tyr), 170.1, 170.2, 170.8 (*C*=O ester, amide), 171.5 (*C*=O, NHAc). ^1H NMR ($CDCl_3$): δ 1.34 (s, 9H, C*H*$_3$ tBu), 1.96, 1.99, 2.04 (3 × s, 27H, C*H*$_3$ Ac), 2.09 (s, 2H, C*H*$_2$ Gly), 2.14 (s, 9H, C*H*$_3$ NHAc), 2.35−2.58 (m, 6H, C*H*$_2$C=O), 2.92−3.05 (m, 6H, C*H*$_2$NH), 3.25 (m, 2H, *β*C*H*$_2$ Tyr), 3.57−4.16 (m, 54H, OC*H*$_2$, H-5, H-6a, H-6b, H-2 Gal), 4.23 (m, 1H, αC*H* Tyr), 4.80 (m, 3H, H-1 Gal), 5.20 (m, 3H, H-3 Gal), 5.35 (m, 3H, H-4 Gal), 6.93 (d, 2H C*H* Tyr), 7.12 (d, 2H, C*H* Tyr).

3-Oleoylamidolithocholic Acid [*O*-*tert*-Butyl-*N*-tyrosinylglycinyltris{(1-[2-(2-aminoethoxy)ethoxy]ethoxy-2-acetamido-3,4,6-tetra-*O*-acetyl-2-deoxy-*β*-D-galactosamine)(carboxyethoxymethyl)}methane] (23). Amine **22** (75 mg, 38 μmol) and acid **20** (36 mg, 57 μmol) were dissolved in DMF (5 mL), and acylation was commenced by addition of DIPEA (14 μL, 80 μmol), HOBT (8 mg, 56 μmol), and TBTU (18 mg, 56 μmol). The mixture was stirred overnight after which TLC analysis (DCM/methanol 85/15, v/v) showed that the reaction has completed. The reaction mixture was taken up in DCM (40 mL); washed with dilute H_3PO_4 (1 M, 40 mL), aq $NaHCO_3$ (1 M, 40 mL), and water (40 mL); dried ($MgSO_4$); and concentrated to an oil. This oil was applied to a silica gel column, and elution was performed with DCM/methanol (1/0 → 88/12, v/v). The crude product thus obtained was further purified by Sephadex LH20 gel filtration, using DCM/methanol (1/1, v/v) as eluent. Yield: 80 mg (30 μmol, 80%). $^{13}C\{^1H\}$ NMR ($CDCl_3$): δ 11.7 (C18 LCO), 13.8 (CH_3 oleoyl), 18.0 (C21 LCO), 20.3 (CH_3, Ac), 20.7 (CH_2 LCO), 22.8 (CH_3, NHAc), 23.5 (C19 CH LCO), 23.8, 24.8, 25.3, 25.8, 26.1, 26.8, 27.8 (CH_2 LCO), 28.5 (CH_3 tBu), 28.7, 28.8, 28.9, 29.1, 29.3, 29.4, 30.4, 31.3, 31.5, 32.8 (CH_2 LCO), 34.5, 36.2, 38.8 (CH_2C=O), 35.1 (C20 CH LCO), 35.3 (C8 CH LCO), 37.2 (CH_2 Tyr), 39.5 (C9 CH LCO), 39.8 (C10 C_q LCO), 42.4 (C13 C_q LCO), 43.1 (CH_2 Gly), 50.2 (C-2 Gal), 51.3 (CH_2−NH), 55.5 (C17 CH LCO), 55.8 (CH, Tyr), 56.2 (C14 CH LCO), 59.7, 60.2 (CH_2O), 61.3 (C-6 Gal), 66.5, 70.0, 70.2 (C-3,4,5 Gal), 67.1−70.1 (CH_2O), 77.9 (C_q tBu), 101.2 (C-1 Gal), 123.8, 129.4, 129.6 (CH Tyr, C=CH oleoyl), 131.3, 153.8 (C_q Tyr), 170.0, 170.1, 170.6, 171.4, 173.0 (C=O). ^1H NMR ($CDCl_3$): δ 0.63 (s, 3H, C18), 0.88 (s, 3H, CH_3 oleoyl), 0.89 (d, 3H, C21 J = 6.6 Hz), 0.96 (s, 3H, C19), 1.13−1.63 (m, 53H, CH, CH_2 LCO), 1.28 (s, 9H, CH_3 tBu), 1.95, 1.99, 2.04 (3 × s, 27H, CH_3 Ac), 2.08 (s, 2H, CH_2 Gly), 2.14 (s, 9H, CH_3 NHAc), 2.27−2.54 (m, 10H, CH_2C=O), 2.93−3.44 (m, 8H, CH_2NH, βCH_2 Tyr), 3.62−3.95 (m, 45H, OCH_2, H-5 Gal), 4.13−4.19 (m, 9H, H-6a, H-6b, H-2), 4.77 (m, 3H, H-1 Gal J_{1-2} = 8.3 Hz), 5.16 (dd, 3H, H-3 Gal J_{3-4} = 2.2 Hz, J_{3-2} = 11.3 Hz), 5.35 (m, 5H, C=CH LCO, H-4 Gal), 6.90 (d, 2H CH Tyr), 7.09 (d, 2H, CH Tyr).

3-Oleoylamidolithocholic Acid [Tyrosinylglycinyltris-{(1-[2-(2-aminoethoxy)ethoxy]ethoxy-2-acetamido-2-deoxy-*β*-D-galactosamine)(carboxyethoxymethyl)}methane] (3). The fully protected glycolipid **23** (32 mg, 12 μmol) was dissolved in DCM/TFA (4/1, v/v; 5 mL). The mixture was stirred for 1 h, when TLC analysis (DCM/methanol 85/15, v/v) revealed the reaction to be complete. The mixture was diluted with toluene (10 mL), concentrated to a small volume, and coevaporated with toluene (2 × 10 mL). The crude product **24** was applied to a silica gel column, using DCM/methanol (1/0 → 82/18, v/v) as eluent. Yield: 27 mg (11 μmol, 91%). $^{13}C\{^1H\}$ NMR ($CDCl_3$): δ 11.8 (C18 LCO), 13.9 (CH_3 oleoyl), 18.0 (C21 LCO), 20.4 (CH_3 Ac), 22.4 (CH_3 NHAc), 23.7 (C19 CH LCO), 23.9, 24.9, 25.4, 25.9, 26.3, 27.0, 27.9, 28.9, 29.1, 29.3, 29.5, 30.5, 31.7, 32.9 (CH_2 LCO), 34.6, 36.1, 39.3 (CH_2C=O), 35.4 (C20 CH LCO), 37.2 (C8 CH LCO), 37.9 (CH Tyr), 39.6 (C9 CH LCO), 39.9 (C10 C_q LCO), 42.5 (CH_2 Gly), 43.1 (C13 C_q LCO), 50.7 (C-2 Gal), 51.6 (CH_2−NH), 54.7, 55.6, 56.3 (C14, C17 CH LCO, CH Tyr), 57.9, 60.1, 60.5 (CH_2O), 61.4 (C-6 Gal), 66.5, 70.4 (C-3,4,5 Gal), 63.4−70.2 (CH_2O), 101.2 (C-1 Gal), 115.4 (CH Tyr), 129.5, 129.8, 130.1 (CH Tyr, C=CH oleoyl), 155.7, 159.0 (C_q Tyr), 170.3, 170.5, 172.6, 172.9, 173.5 (C=O).

Compound **24** was dissolved in methanolic sodium methanolate (0.05 M, 2 mL). After overnight stirring, TLC analysis (DCM/methanol 85/15, v/v and 2-propanol/25% NH_4OH 1/1, v/v) showed complete conversion of the starting material into a single product (compound **3**). The crude deprotected product thus obtained was purified using a Sephacryl S100 gel filtration column, with water as eluent. The product fractions were pooled, concentrated, and lyophilized. Yield: 8.2 mg (3.8 μmol, 32% based on **23**). $^{13}C\{^1H\}$ NMR ($CDCl_3$): δ 12.2 (C18 LCO), 14.2 (*C*H_3 oleoyl), 18.4 (C21 LCO), 23.0 (*C*H_3 NHAc), 24.1 (C19 *C*H LCO), 21.9, 22.9, 25.4, 26.4, 26.8, 27.4, 28.4, 29.3, 29.5, 29.9, 30.0, 31.0, 32.1, 33.4 (*C*H_2 LCO), 34.0, 35.6, 36.9, 40.4 (*C*H_2C=O), 35.8 (C20 *C*H LCO), 35.9 (C8 *C*H LCO), 38.0 (*C*H Tyr), 40.2 (C9 *C*H LCO), 41.5 (*C*H_2, Gly), 41.9 (C10 *C*$_q$ LCO), 43.5 (C13 *C*$_q$ LCO), 52.2 (C-2 Gal), 54.3 (*C*H_2−NH), 56.2 (C17 *C*H LCO), 57.4 (*C*H Tyr), 57.9 (C14 *C*H LCO), 60.5 (*C*H_2O), 61.7 (C-6 Gal), 68.6, 72.7, 75.3 (C-3,4,5 Gal), 67.0−70.8 (*C*H_2O), 101.8 (C-1 Gal), 115.6 (*C*H Tyr), 127.8 (*C*$_q$ Tyr), 129.9, 130.2 (C=*C*H oleoyl), 130.5 (*C*H Tyr), 156.1 (*C*$_q$ Tyr), 169.8, 172.9, 173.4, 174.4, 175.2 (*C*=O).^1H NMR ($CDCl_3$): δ 0.65 (s, 3H, C18), 0.87−1.61 (m, 63H, C*H*$_3$, C*H*$_2$ LCO), 2.01 (s, 9H, C*H*$_3$, NHAc), 2.33 (t, 3H, C*H*$_3$ LCO), 2.43−2.55 (m, 8H, C*H*$_2$C=O), 2.93−3.27 (m, 6H, C*H*$_2$NH), 3.34−3.83 (48H, OC*H*$_2$, Gal), 4.43 (d, 3H, H-1 Gal, J = 8.4 Hz), 4.54 (m, 3H, H-5 Gal), 5.05 (m, 3H, H-3 Gal), 5.33 (m, 5H, H-4 Gal, C=C*H* LCO), 6.69 (d, 2H C*H* Tyr), 7.04 (d, 2H, C*H* Tyr). Mass (FAB$^+$): *m/e* 2206.6 [M + Na]$^+$.

Animals. Male C57Bl/6J mice (12−14 week old, 24−28 g) were obtained from Broekman Instituut BV (Someren, The Netherlands) and fed ad libitum with standard rat/mouse chow (SRM-A, Hope Farms). Homozygous LDL-receptor deficient (*ldlr*$^{-/-}$) mice have originally been obtained from the Jackson Laboratory (Bar Harbor, ME) and are maintained as a colony at our local housing facility at the Gorlaeus Laboratory. Three weeks before use, female *ldlr*$^{-/-}$ mice (20 week old, 25−30 g) were fed a Western-type diet (Hope Farms) ad libitum for three weeks. All experiments were approved by the Ethics Committee on Animal Experiments of the University of Leiden.

Isolation of Lipoproteins. Human LDL and HDL were isolated from freshly isolated serum of healthy volunteers as described[33] and dialyzed at 4 °C against PBS, 1 mmol/L EDTA, pH 7.4. Protein concentrations were determined according to Lowry et al.[34] using BSA as a standard.

Glycolipid. The freeze-dried glycolipids **2** and **3** were dissolved in phosphate-buffered saline (PBS) at a final concentration of 50 μg/μL and stored at −80 °C under Argon. Their stability was routinely checked by TLC (*n*-butanol/*n*-propanol/25% NH_4OH/H_2O = 15/40/30/15, v/v/v/v) and subsequent staining for cholesterol ($MnCl_2$) and sugar (H_2SO_4) moieties.

Radiolabeling of Lipoproteins and Glycolipids. HDL was labeled with [^{3}H]cholesteryl oleate (~25 dpm/ng protein) and LDL was radioiodinated and purified as described,[35] while glycolipid **3** was radiolabeled by the Iodogen method using a Iodogen (10 μg)-coated reaction tube. More than 97% of the radiolabel in [^{125}I]TC-LDL was 10% TCA precipitable, and the specific ^{125}I-activity was ~150 dpm/ng of protein. [^{125}I]glycolipid **3** (1300 dpm/ng) migrated as a single band (R_f 0.64) on TLC (*n*-butanol/*n*-propanol/25% NH_4OH/H_2O = 15/40/30/15, v/v/v/v).

Association of Glycolipids with Lipoproteins. Human HDL and LDL (5 μg of protein each) were incubated (30 min

at 37 °C) with ^{125}I-labeled or unlabeled glycolipid **3** in PBS, pH 7.4. The mixtures were electrophoresed on a 0.75% (w/w) agarose gel at pH 8.8, and the gels were fixed and dried. Lipids were visualized by Sudan Black and ^{125}I-activity was monitored using a Packard Instant Imager (Hewlett-Packard Co., Palo Alto, CA).

Kinetic Studies in Mice. Mice were anesthetized,[17] and the abdomens were opened. [^{125}I]glycolipid **3** or radiolabeled lipoproteins, previously incubated with PBS or glycolipid **3** (30 min at 37 °C), were injected via the inferior vena cava. Blood and liver samples were taken and processed as previously described.[36] When indicated, mice received a preinjection of ASOR (25 mg/kg) at 1 min before injection of the lipoproteins. At 60 min after injection of [^{125}I]glycolipid **3**, mice were bled, and 100 μL serum samples were subjected to density gradient ultracentrifugation.[33] Tubes were fractionated (24 × 0.5 mL) using a Multiprobe 104DT Robotic System (Packard Instrument Co.), and fractions were assayed for ^{125}I-activity and for cholesterol using the Roche Molecular Biochemicals enzymatic kit for cholesterol.

Cholesterol-Lowering Effect of Glycolipids. PBS or glycolipid **3** (20 mg/kg) was injected via the tail vein into conscious *ldlr*$^{-/-}$ mice. Blood samples (25 μL) were taken from the tail vein by heparin-coated capillaries, and the plasmas were analyzed for total cholesterol as described above. Alternatively, mice were sacrificed at 3 or 24 h after injection, and the weight of several organs was determined. Plasma levels of lactate dehydrogenase (LDH), alanine aminotransferase (ALAT), aspartate aminotransferase (ASAT), and γ-glutamyl transferase (γGT) were determined using SYS-3 BM/Hitachi 747 kits from Roche Molecular Biochemicals.

Acknowledgment. This study was supported by a grant from The Netherlands Heart Foundation (NHS grant 95.128) and The Netherlands Organization for Scientific Research (NWO STIGON grant 014-81-102). We thank Roel H. Fokkens (Institute of Mass Spectometry, University of Amsterdam, The Netherlands) for performing MALDI-TOF mass spectometry, and Marijke Frölich (Central Clinical Chemical Laboratory, Leiden University Medical Center, The Netherlands) for measuring plasma enzymes.

References

(1) Lipid Research Clinics Program. The Lipid Research Clinics Coronary Primary Prevention Trial Results. I. Reduction in incidence of coronary heart disease. *JAMA* **1984**, *251*, 351−364.
(2) Lipid Research Clinics Program. The Lipid Research Clinics Coronary Primary Prevention Trial Results. II. The relationship of reduction in incidence of coronary heart disease to cholesterol lowering. *JAMA* **1984**, *251*, 365−374.
(3) Gordon, D. J.; Rifkind, B. M. High-density lipoprotein: The clinical implications of recent studies. *N. Engl. J. Med.* **1989**, *321*, 1311−1316.
(4) Rubins, H. B.; Robins, S. J.; Collins, D.; Fye, C. L.; Anderson, J. W.; Elam, M. B.; Faas, F. H.; Linares, E.; Schaefer, E. J.; Schectman, G.; Wilt, T. J.; Wittes, J.; for the Veterans Affairs High-Density Lipoprotein Cholesterol Intervention Trial Study Group. Gemfibrozil for the secondary prevention of coronary heart disease in men with low levels of high-density lipoprotein cholesterol. *N. Engl. J. Med.* **1999**, *341*, 410−418.
(5) Arai, T.; Wang, N.; Bezouevski, M.; Welch, C.; Tall, A. R. Decreased atherosclerosis in heterozygous low-density lipoprotein receptor-deficient mice expressing the scavenger receptor BI transgene. *J. Biol. Chem.* **1999**, *274*, 2399−2371.
(6) Kozarsky, K. F.; Donahee, M. H.; Glick, J. M.; Krieger, M.; Rader, D. J. Gene transfer and hepatic overexpression of the HDL receptor SR−BI reduces atherosclerosis in the cholesterol-fed LDL receptor-deficient mouse. *Arterioscler. Thromb. Vasc. Biol.* **2000**, *20*, 721−727.
(7) Ashwell, G.; Harford, J. Carbohydrate-specific receptors of the liver. *Annu. Rev. Biochem.* **1982**, *51*, 531−554.
(8) Spiess. M. The asialoglycoprotein receptor: A model for endocytotic transport receptors. *Biochemistry* **1990**, *29*, 10009−10018.
(9) Baenziger, J. U.; Maynard, Y. Human hepatic lectin: Physicochemical properties and specificity. *J. Biol. Chem.* **1980**, *255*, 4607−4613.
(10) Lehrman, M. A.; Hill, R. L. The binding of fucose-containing glycoproteins by hepatic lectins. Purification of a fucose-binding lectin from rat liver. *J. Biol. Chem.* **1986**, *261*, 7419−7425.
(11) Lehrman, M. A.; Haltiwanger, R. S.; Hill, R. L. The binding of fucose-containing glycoproteins by hepatic lectins. The binding specificity of the rat liver fucose lectin. *J. Biol. Chem.* **1986**, *261*, 7426−7432.
(12) Hoyle, G. W.; Hill, R. L. Molecular cloning and sequencing of a cDNA for a carbohydrate binding receptor unique to rat Kupffer cells. *J. Biol. Chem.* **1988**, *263*, 7487−7492.
(13) Biessen, E. A. L.; Bakkeren, H. F.; Beuting, D. M.; Kuiper, J.; Van Berkel, T. J. C. Ligand size is a major determinant of high-affinity binding of fucose- and galactose-exposing (lipo)proteins by the hepatic fucose receptor. *Biochem. J.* **1994**, *299*, 291−296.
(14) Bijsterbosch, M. K.; Van Berkel, T. J. C. Uptake of lactosylated low-density lipoprotein by galactose-specific receptors in rat liver. *Biochem. J.* **1990**, *270*, 233−239.
(15) Kuiper, J.; Bakkeren, H. F.; Biessen E. A. L.; Van Berkel, T. J. C. Characterization of the interaction of galactose-exposing particles with rat Kupffer cells. *Biochem. J.* **1994**, *299*, 285−290.
(16) Biessen, E. A. L.; Vietsch, H.; Van Berkel, T. J. C. Cholesterol derivative of a new triantennary cluster galactoside directs low- and high-density lipoproteins to the parenchymal liver cell. *Biochem. J.* **1994**, *302*, 283−289.
(17) Sliedregt, L. A. J. M.; Rensen, P. C. N.; Rump, E. T.; Van Santbrink, P. J.; Bijsterbosch, M. K.; Valentijn, A. R. P. M.; Van der Marel, G. A.; Van Boom, J. H.; Van Berkel, Th. J. C.; Biessen, E. A. L. Design and synthesis of novel amphiphilic dendritic galactosides for selective targeting of liposomes to the hepatic asialoglycoprotein receptor. *J. Med. Chem.* **1999**, *42*, 609−618.
(18) Rensen, P. C. N.; Sliedregt, L. A. J. M.; Ferns, M.; Kievit, E.; Van Rossenberg, S. M. W.; Van Leeuwen, S. H.; Van Berkel, Th. J. C.; Biessen, E. A. L. Determination of the upper size limit for uptake and processing of ligands by the asialoglycoprotein receptor on hepatocytes in vitro and in vivo. *J. Biol. Chem.* **2001**, *276*, 37577−37584.
(19) Karayan, L.; Qiu, S.; Betard C.; Dufour, R.; Roederer, G.; Minnich, A.; Davignon, J.; Genest, J., Jr. Response of HMG CoA reductase inhibitors in heterozygous familial hypercholesterolemia due to the 10-kb deletion ("French Canadian Mutation") of the LDL receptor gene. *Arterioscler. Thromb.* **1994**, *14*, 1258−1263.
(20) Pazzucconi, F.; Dorigotti, F.; Gianfranceschi, G.; Campagnoli, G.; Sirtori, M.; Franceschini, G.; Sirtori, C. R. Therapy with HMG CoA reductase inhibitors: Characteristics of the long-term permanence of hypocholesterolemic activity. *Atherosclerosis* **1995**, *117*, 189−198.
(21) Biessen, E. A. L.; Broxterman, H.; van Boom, J. H.; van Berkel, Th. J. C. The Cholesterol derivative of a triantennary galactoside with high affinity for the hepatic asialoglycoprotein receptor: A potent cholesterol lowering agent. *J. Med. Chem.* **1995**, *38*, 1846−1852.
(22) Biessen, E. A. L.; Beuting, D. M.; Roelen, H. C. P. F.; van der Marel, G. A.; van Boom, J. H.; van Berkel, Th. J. C. Synthesis of cluster galactosides with high affinity for the hepatic asialoglycoprotein receptor. *J. Med. Chem.* **1995**, *38*, 1538−1546.
(23) Valentijn, A. R. P. M.; Van der Marel, G. A.; Sliedregt, L. A. J. M.; Van Berkel, Th. J. C.; Biessen, E. A. L.; Van Boom, J. H. Solid-phase synthesis of lysine-based cluster galactosides with high affinity for the asialoglycoprotein receptor. *Tetrahedron* **1997**, *53*, 759−770.
(24) Lee R. T.; Lee, Y. C. Facile synthesis of a high-affinity ligand for mammalian hepatic lectin containing three terminal *N*-acetylgalactosamine residues. *Bioconjugate Chem.* **1997**, *8*, 762−765.
(25) Nakabayashi, S.; Warren, C. D.; Jeanloz, R. W. A new procedure for the preparation of oligosaccharide oxazolines. *Carbohydr. Res.* **1986**, *150*, C7.
(26) Tozawa, R.; Ishibashi, S.; Osuga. J.; Yamamoto, K.; Yagyu, H.; Ohashi, K.; Tamura, Y.; Yahagi, N.; Iizuka, Y.; Okazaki, H.; Harada, K.; Gotoda, T.; Shimano, H.; Kimura, S.; Nagai, R.; Yamada, N. Asialoglycoprotein receptor deficiency in mice lacking the major receptor subunit. *J. Biol. Chem.* **2001**, *276*, 12624−12628.
(27) Orlova, E. V.; Sherman, M. B.; Chiu, W.; Mowri, H.; Smith, L. C.; Gotto, A. M., Jr. Three-dimensional structure of low-density lipoproteins by electron microscopy. *Proc. Natl. Acad. Sci. U.S.A.* **1999**, *96*, 8420−8425.
(28) Segrest, J. P.; Jones, M. K.; De Loof, H.; Dashti, N. Structure of apolipoprotein B-100 in low-density lipoproteins. *J. Lipid Res.* **2001**, *42*, 1346−1367.
(29) Whitehead, P. H.; Sammons, H. G. 1966 A simple technique for the isolation of orosomucoid from normal and pathological sera. *Biochim. Biophys. Acta* **1966**, *124*, 209−211.
(30) Goswami, S. K.; Frey, C. F. Manganous chloride spray reagent for cholesterol and bile acids on thin-layer chromatograms. *J. Chromatogr.* **1970**, *53*, 380−390.

(31) Von Arx, E.; Faupel, M.; Brugger, M. Das 4,4′-tetramethyldiamino-diphenylmethan reagens (TDM); eine modifikation der chlor-o-tolidin farbereaktion für die dünnschicht-chromatographie. *J. Chromatogr.* **1976**, *120*, 224−228.
(32) Gouin, S.; Zhu, X. X. Synthesis of 3-alpha and 3-beta-dimers from selected bile acids. *Steroids* **1996**, *61*, 664−669.
(33) Redgave, T. G.; Roberts, D. C.; West, C. E. Separation of plasma lipoproteins by density-gradient ultracentrifugation. *Anal. Biochem.* **1975**, *65*, 42−49.
(34) Lowry, O. H.; Rosebrough, N. J.; Farr, A. L.; Randall, R. J. Protein measurement with the Folin phenol reagent. *J. Biol. Chem.* **1951**, *93*, 265−275.
(35) Rensen, P. C. N.; Jong, M. C.; Van Vark, L. C.; Van der Boom, H.; Hendriks, W. L.; Van Berkel, T. J. C.; Biessen, E. A. L.; Havekes, L. M. Apolipoprotein E is resistant to intracellular degradation in vitro and in vivo: Evidence for retroendocytosis. *J. Biol. Chem.* **2000**, *275*, 8564−8571.
(36) Rensen, P. C. N.; Herijgers, N.; Netscher, M. H.; Meskers, S. C. J.; Van Eck, M.; Van Berkel, T. J. C. Particle size determines the specificity of apolipoprotein E-containing triglyceride-rich emulsions for the LDL receptor versus hepatic remnant receptor in vivo. *J. Lipid. Res.* **1997**, *38*, 1070−1084.

JM049481D

EXHIBIT 9

ChemRxiv 10.26434/chemrxiv.7927061.v1

Lysosome Targeting Chimeras (LYTACs) for the Degradation of Secreted and Membrane Proteins

Steven Banik, Kayvon Pedram, Simon Wisnovsky, Nicholas Riley, Carolyn Bertozzi

Submitted date: 29/03/2019 • Posted date: 29/03/2019

Citation information: Banik, Steven; Pedram, Kayvon; Wisnovsky, Simon; Riley, Nicholas; Bertozzi, Carolyn (2019): Lysosome Targeting Chimeras (LYTACs) for the Degradation of Secreted and Membrane Proteins. ChemRxiv. Preprint.

Targeted protein degradation is a powerful strategy to address the canonically undruggable proteome. However, current technologies are limited to targets with cytosolically-accessible and ligandable domains. Here, we designed and synthesized conjugates capable of binding both a cell surface lysosome targeting receptor and the extracellular domain of a target protein. These lysosome targeting chimeras (LYTACs) consist of an antibody fused to agonist glycopeptide ligands for the cation-independent mannose-6-phosphate receptor (CI-M6PR). LYTACs enabled a CRISPRi knockdown screen revealing the biochemical pathway for CI-M6PR-mediated cargo internalization. We demonstrated that LYTACs mediate efficient degradation of Apolipoprotein-E4, epidermal growth factor receptor (EGFR), CD71, and programmed death-ligand 1 (PD-L1). LYTACs represent a modular strategy for directing secreted and membrane proteins for degradation in the context of both basic research and therapy.

File list (3)

Combined.pdf (26.74 MiB)	view on ChemRxiv • download file
Supplemental Data 1.xlsx (10.29 MiB)	view on ChemRxiv • download file
Supplemental Data 2.xlsx (572.50 KiB)	view on ChemRxiv • download file

Title: Lysosome Targeting Chimeras (LYTACs) for the Degradation of Secreted and Membrane Proteins

One Sentence Summary: Chemically reprogrammed antibodies capable of bridging an antigen and a lysosomal shuttling receptor enable targeted protein degradation.

Authors: Steven M. Banik[1], Kayvon Pedram[1], Simon Wisnovsky[1], Nicholas M. Riley[1], Carolyn R. Bertozzi[1,2]*

Affiliations:
[1]Department of Chemistry, Stanford University, Stanford, California 94305, USA.
[2]Howard Hughes Medical Institute, Stanford, California 94305, USA.
*Correspondence should be addressed to C.R.B. (bertozzi@stanford.edu).

Abstract: Targeted protein degradation is a powerful strategy to address the canonically undruggable proteome. However, current technologies are limited to targets with cytosolically-accessible and ligandable domains. Here, we designed and synthesized conjugates capable of binding both a cell surface lysosome targeting receptor and the extracellular domain of a target protein. These lysosome targeting chimeras (LYTACs) consist of an antibody fused to agonist glycopeptide ligands for the cation-independent mannose-6-phosphate receptor (CI-M6PR). LYTACs enabled a CRISPRi knockdown screen revealing the biochemical pathway for CI-M6PR-mediated cargo internalization. We demonstrated that LYTACs mediate efficient degradation of Apolipoprotein-E4, epidermal growth factor receptor (EGFR), CD71, and programmed death-ligand 1 (PD-L1). LYTACs represent a modular strategy for directing secreted and membrane proteins for degradation in the context of both basic research and therapy.

Main Text: Most protein-directed therapeutics act by obstructing target function, as is the case with enzyme inhibitors and receptor blockers, or by recruiting immune effectors, as with many monoclonal antibody drugs. However, many potential therapeutic targets have molecular functions that are either incompletely understood or not readily druggable by these mechanisms (e.g., transcription factors, scaffolding proteins, aggregate-forming proteins, lipid carriers, mucins, orphan receptors, and polyfunctional molecules). Proteolysis targeting chimeras (PROTACs) (*1*, *2*) and conceptually related degradation platforms (e.g., dTAGs (*3*), Trim-Away (*4*), chaperone-mediated autophagy targeting (*5*) and SNIPERs(*6*)) have emerged as elegant strategies to address these canonically "undruggable" targets. PROTACs form a bridge between an E3 ubiquitin ligase and their target of interest, thereby facilitating ubiquitination and degradation by the proteasome (*7*). Despite their transformative power, state-of-the-art protein degradation technologies are, by their mechanism, fundamentally limited to targets with cytosolic domains, leaving secreted and many membrane proteins inaccessible. Reflecting ~40% of protein-encoding genes (*8*), secreted and membrane proteins play key roles in many disease states, including cancer, neurodegeneration, autoimmunity and infectious disease (*9*). Therefore, a general strategy for targeting secreted and plasma membrane proteins for degradation remains an unmet need that could dramatically impact human health.

Unlike the proteasomal pathway, the lysosomal pathway for protein degradation is not limited to proteins with intracellular domains. In addition, families of cell surface lysosomal targeting receptors (LTRs) have been discovered which facilitate transport of proteins to lysosomes (*10*). We hypothesized that chimeric molecules capable of binding both a cell surface LTR and an extracellular protein would induce internalization and lysosomal degradation of the target.

The prototypical LTR is the cation-independent mannose-6-phosphate receptor (CI-M6PR, also called IGF2R), which endogenously transports proteins bearing N-glycans capped

with mannose-6-phosphate (M6P) residues to lysosomes (*11*). The receptor cycles constitutively between endosomes, the cell surface, and the Golgi complex. Upon engagement by multivalent ligands, CI-M6PR shuttles cargo efficiently to prelysosomal compartments where a lower pH allows cargo to dissociate and progress to the lysosome while CI-M6PR recycles. Based on its ability to efficiently deliver cargo to lysosomes and its widespread tissue expression, CI-M6PR has been exploited to deliver therapeutic enzymes for treatment of lysosomal storage disorders (*12*). Here, we present the lysosome targeting chimera (LYTAC) platform, which enables depletion of secreted and membrane proteins via a mechanism of action that is orthogonal and complementary to existing technologies (Fig. 1A). Herein, LYTACs comprise antibodies conjugated with agonist multivalent glycopolypeptide ligands for CI-M6PR. We show that LYTACs can be used as biochemical probes to study receptor trafficking and protein degradation, and are capable of degrading both secreted and membrane proteins of therapeutic interest.

In our effort to develop CI-M6PR agonist ligands, we leveraged precedents from work aimed at enhancing lysosomal enzyme replacement therapies and drug delivery platforms. This prior work included biosynthetic engineering of M6P-bearing glycans (*13*) as well as chemical synthesis of oligomeric M6P-containing scaffolds (*14*). A recurring design parameter from these studies was the requirement of ligand multivalency to achieve optimal CI-M6PR agonism (*15*–*17*). Prior work had also revealed that the 6-phosphoester can undergo hydrolysis in human serum (*18*), leading to rapid endocytosis by macrophages bearing mannose receptors (*19*). We reasoned that *N*-carboxyanhydride (NCA)-derived glycopolypeptides (*20*) bearing multiple serine-*O*-mannose-6-phosphonate (M6Pn) residues would enable multivalent presentation on a biocompatible, phosphatase-inert (*21*), and modular scaffold. We synthesized M6Pn glycopolypeptides starting with conversion of mannose pentaacetate to M6Pn-NCA **1** in 13 steps (Fig. 1B). Subsequent copolymerization of **1** and alanine-NCA (1:1 ratio, for the purpose of spacing and polymerization kinetics) provided access to M6Pn glycopolypeptides (post-deprotection Đ = 1.3-1.5). The living nature of NCA polymerization allowed us to generate M6Pn glycopolypeptides of various lengths; for this study we made short (20 M6Pn) and long (90 M6Pn) variants to test in protein degradation assays. We also synthesized the corresponding M6P-containing copolymers bearing the natural phosphorylated glycan structure (Fig. S1), as well as copolymers with similar molecular weights and dispersities to those obtained with M6Pn monomers.

To demonstrate the feasibility of CI-M6PR-driven LYTACs, we designed an assay to measure uptake of NeutrAvidin-647 (NA-647) using conjugates comprising biotin N-terminally fused to glycopolypeptides (Fig. 1C). Additionally, we synthesized and biotinylated poly(GalNAc), and poly(Mannose) as control polymers (Fig. 1D and Fig. S2). K562 cells were incubated with NA-647 or NA-647 and biotinylated glycopolypeptide for 1 hour, then washed and analyzed by flow cytometry. Co-incubation with M6P and M6Pn polymers increased cellular fluorescence 5-6 fold over background, with only minor differences in uptake efficiency observed as a result glycopolypeptide length (short versus long, Fig. 1E). M6Pn-polymers performed equivalently or superior to M6P polymers of similar length, while incubation with mannose or GalNAc containing glycopolypeptides had no effect. NA-647 uptake mediated by poly(M6Pn) was attenuated by co-incubation with excess exogenous M6P. Further, uptake remained continuous over time (Fig. S3), consistent with surface receptor recycling acting as the rate-limiting step (*22*). Note that AF647 is reported to be stable in endosomes and lysosomes, consistent with steadily increasing fluorescent signal arising from intracellular fluorophore accumulation (*23*). In addition, live cell fluorescence microscopy revealed that AF647 signal co-localized with acidic endosomes and lysosomes after just 1 hour (Fig. 1F, Figs. S4–S5). Finally, biotin LYTACs mediated NA-647 uptake in a variety of cell lines, including those derived from breast cancer, cervical cancer, lymphoma, and leukemia, demonstrating the generality of CI-M6PR-targeting (Fig. 1G).

We performed a CRISPRi pooled genetic screen with the aim of identifying genes whose knockdown ablated intracellular delivery of LYTAC-conjugated NA-647 (*24*, *25*) (Fig. 2A). K562

cells expressing dCas9-KRAB were transduced with a genome-wide library of CRISPRi sgRNAs and incubated with LYTAC and NA-647. A population of cells exhibiting a significant decrease in NA-647 labeling was isolated by fluorescence-activated cell sorting (FACS). Next-Gen sequencing was performed to identify sgRNAs constitutively overrepresented in this population. Guide RNAs to CI-M6PR were highly enriched in the sorted pool, providing unbiased confirmation of selective receptor targeting (Fig. 2B, full dataset available in Supplementary Data 1). Other significantly enriched guides (FDR < 5%) targeted genes that regulate endosomal acidification, vesicle trafficking, endosome-lysosome fusion, and clathrin-dependent endocytosis (Fig. 2C), consistent with a CI-M6PR-driven endocytic pathway to lysosomes (*11*). Components of the exocyst complex, which is reported to mediate vesicle localization to the plasma membrane (*26*), were also identified as essential for M6Pn-mediated delivery of NA-647. We hypothesized that the exocyst complex could be involved in cell surface presentation of CI-M6PR, a biochemical pathway which has yet to be elucidated (*11*). We performed CRISPRi knockdown of EXOC1 and EXOC2 in K562 cells using CRISPRi library guides and measured cell-surface CI-M6PR levels by flow cytometry. Strikingly, we observed a 60% decrease in cell surface CI-M6PR (Fig. 2D). We replicated these results in HeLa cells (75% decrease, Fig. 2E), and found that total CI-M6PR as read out by Western blot did not change upon knockdown of EXOC1 in either cell line (Fig. 2F and Fig. 2G, respectively). Further, no change in surface expression of epidermal growth factor receptor (EGFR) in HeLa cells was observed (Fig. S6), indicating global cell surface protein trafficking remained unperturbed. Together these data indicate that surface presentation of CI-M6PR is mediated in part by the exocyst complex, and more broadly, that LYTACs can be used to study the molecular pathways involved in cell surface receptor regulation.

We next sought to determine if conjugation of a poly(M6Pn)-bearing glycopeptide to an antibody would reprogram the antibody to rapidly direct extracellular agents to the lysosome. As proof-of-principle, we non-specifically labeled lysines on a polyclonal anti-mouse IgG with bicyclononyne-NHS (BCN-NHS), and subsequently conjugated this antibody to azide-terminated glycopolypeptides via Cu-free strain-promoted azide-alkyne cycloaddition (Fig. 3A), generating LYTAC **Ab-1**. The conjugation reaction was readily monitored by native gel electrophoresis as covalent attachment of the highly anionic polypeptides caused a characteristic enhancement in migration compared to non-charged polypeptide-conjugated antibodies (i.e. GalNAc) (Fig. 3B). Incubation of K562 cells with mouse IgG labeled with AlexaFluor-488 (AF488) and **Ab-1** (Fig. 3C), resulted in a 40-fold increase in lysosomal AF488 signal relative to controls (Fig 3D and Fig. S7).

Given that **Ab-1** efficiently trafficked IgG molecules to lysosomes, we reasoned it could function as a LYTAC for a primary IgG antibody bound to its antigen (Fig. 3E). Co-incubation of cells with mCherry, mouse-anti mCherry, and **Ab-1** resulted in 10-100-fold increases in uptake relative to non-M6Pn bearing antibodies in all cell lines tested (Fig. 3 F–H). To expand this strategy to a clinically relevant target, we chose Apolipoprotein E4 (ApoE4), which has been implicated in the pathogenesis of neurodegenerative disease (*27*). A 13-fold increase in uptake was observed using **Ab-1** along with a mouse-anti-ApoE4 primary antibody (Fig. 3I), with uptake continuous over the course of the incubation (Fig. 3J). Co-localization of AF647 signal with lysosomes was observed at both 1 and 24 hours (Fig. S8), replicating our findings with NeutrAvidin and mCherry. Importantly, non-specific inhibition of serine and cysteine proteases using leupeptin resulted in accumulation of intracellular AF647-labeled ApoE (ApoE4-647), which was substantially increased in the presence of anti-ApoE4 with **Ab-1** (Fig. 3K and Fig. S9). These data demonstrate that LYTAC-mediated target enrichment at the lysosome is coupled with increased target degradation. More broadly, conjugation of a lysosomal targeting ligand to an antibody can reprogram the antibody to direct an extracellular antigen for degradation.

We next asked if LYTACs could be used to accelerate the degradation of membrane-associated extracellular proteins. In principle, this requires simultaneous binding of a surface-associated protein and stimulation of CI-M6PR, an interaction which would also benefit from increased effective molarity upon target binding. EGFR, a known driver of cancer proliferation,

which can perform multiple scaffolding functions regardless of kinase inhibition, served as the first target. LYTACs constructed using cetuximab (ctx), an FDA-approved EGFR-blocking antibody, were generated using a similar scheme to **Ab-1** (Fig. 4A). HeLa cells were incubated for 24 hours with 100 nM ctx, ctx functionalized with either long or short M6Pn glycopolypeptides, or GalNAc-functionalized ctx as a control (Fig. 4B). Cells were then lysed and assayed for total EGFR levels by Western blot (Fig. 4C). Substantial degradation of EGFR was observed only with ctx conjugates bearing M6Pn glycopolypeptides (>70% degradation, comparable to EGF-induced downregulation), while no change in CI-M6PR levels were observed. There was no apparent difference in degradation ability between LYTACs bearing short or long M6Pn glycopolypeptides. Analogous results were obtained with concentrations of ctx-M6Pn between 100 nM and 10 nM (Fig. S10). To confirm that depletion of EGFR was mediated by CI-M6PR, we compared the degrading ability of ctx-M6Pn **Ab-2** (Fig. S11) to unmodified ctx in dCas9-KRAB HeLa lines stably expressing a non-targeting or CI-M6PR-targeting sgRNA. Accelerated degradation of EGFR was only observed in non-targeting sgRNA-expressing HeLa cells, while knockdown of CI-M6PR completely abrogated the degradation ability of **Ab-2** (Fig. 4D). EGFR degradation reached maximum between 12-24 hours and persisted for at least 72 hours (Fig. S12). To rule out the possibility that EGFR crosslinking by ctx contributed to target downregulation (*28*, *29*), we digested ctx with papain to obtain ctx-Fab, a monovalent binder of EGFR, and conjugated it to poly(M6Pn-co-Ala) to generate **Fab-1** (Fig. 4E). **Fab-1** accelerated degradation of EGFR in a CI-M6PR-dependent manner to levels comparable with **Ab-2** (Fig. 4F), demonstrating that monovalent binders can be used as LYTACs. In a mixed cell assay with HeLa (CI-M6PR$^+$EGFR$^+$) and Jurkat (CI-M6PR$^+$EGFR$^-$) cells, the ctx-M6Pn conjugate exhibited a similar binding profile to ctx alone, suggesting that LYTACs with dual affinities for target and CI-M6PR can maintain high on-target specificity (Fig. S13). EGFR degradation was also observed in breast cancer (BT474, MDA-MB-361) and lung cancer (A549) cell lines (Fig. S14).

Next, proteome-wide characterization of LYTAC degradation specificity was evaluated via quantitative mass spectrometry analysis of cells treated with ctx or **Ab-2**. Significant reduction of EGFR levels was effected by **Ab-2**, while ctx did not affect EGFR levels significantly (Fig. 4G). CI-M6PR levels were unchanged, further supporting catalytic CI-M6PR-mediated degradation of EGFR. Changes in the expression levels of other proteins as a result of EGFR degradation were also observed (Fig. S15, full dataset in Supplementary Data 2). These co-degraded proteins may represent EGFR interaction partners or co-regulated molecules. For example, treatment with **Ab-2** caused significant downregulation of CD99, dihydropteridine reductase, 7,8-dihydro-8-oxoguanine triphosphatase, and transcription factor Dp-1, and resulted in upregulation of glucose-1,6-bisphosphate synthase and COPRS. While the precise mechanism for these changes remains to be elucidated, these data suggest that LYTACs may provide a new means to monitor cellular changes in response to protein degradation.

To demonstrate the generality of the LYTAC platform, we targeted several additional membrane-associated proteins for degradation. CD71 (transferrin receptor-1), a therapeutic cancer target progressing to clinical trials, is known to cycle between early endosomes and the cell surface, avoiding trafficking to the lysosome for degradation (*30*). Upon incubation of Jurkat cells with a mouse-anti-CD71 antibody and **Ab-1** (Fig. 4H), significant degradation of CD71 was observed (>80%, Fig. 4I). Note the anti-CD71 antibody alone is reported to induce partial CD71 downregulation (*31*). After 24 hours incubation, cells treated with anti-CD71 and **Ab-1** exhibited a decrease in transferrin-647 uptake compared to no treatment or treatment with non-M6Pn bearing antibodies (Fig. 4J), highlighting the functional consequences of target degradation in this system.

Finally, we investigated whether LYTACs could degrade PD-L1, a driver of cancer cell immune evasion. In order for PD-L1 to undergo accelerated degradation, the LYTAC must override the PD-L1 recycling pathway (*32*). MDA-MB-231 cells, which are PD-L1 positive, were treated with anti-PD-L1, anti-PD-L1 functionalized with GalNAc glycopolypeptides, or anti-PD-L1-

M6Pn LYTAC (**Ab-3**, Fig. S16). Treatment with **Ab-3** resulted in a significant decrease (average 33%) in cell-surface PD-L1 levels compared to unfunctionalized anti-PD-L1 or anti-PD-L1-poly(GalNAc) (Fig. 4K); the observed decrease was sustained over the course of 72 hours. At 48 hours, PD-L1 levels were reduced only in cells treated with **Ab-3,** as assayed by Western blot (Fig. 4L). As MDA-MB-231 express low levels of CI-M6PR, we next tested degradation of PD-L1 in the Hodgkin's lymphoma cell line HDLM-2 which expresses higher levels of CI-M6PR. After 36 hours, 50% downregulation of PD-L1 was observed (Fig. 4M). Together, these data demonstrate proof-of-principle that LYTACs can alter the endogenous recycling programs of cell-surface proteins and accelerate their lysosomal degradation.

In summary, LYTACs are a platform for targeting extracellular molecules directly for lysosomal degradation. The success of a particular LYTAC likely results from a combination of factors, including the endogenous kinetics of protein trafficking and turnover, amount of surface localization, inherent susceptibility to lysosomal transportation through clathrin-mediated endocytosis, and stoichiometry relative to the lysosome targeting receptor. While the LYTACs described above take advantage of CI-M6PR, in principle other recycling receptors could be coopted. We anticipate the chemical tunability and modularity of LYTACs will offer new opportunities in targeted protein degradation for both research and translational applications.

References

1. K. M. Sakamoto *et al.*, Protacs: Chimeric molecules that target proteins to the Skp1–Cullin–F box complex for ubiquitination and degradation. *Proc. Natl. Acad. Sci.* **98**, 8554–8559 (2001).

2. G. E. Winter *et al.*, Phthalimide conjugation as a strategy for in vivo target protein degradation. *Science*. **348**, 1376–1381 (2015).

3. B. Nabet *et al.*, The dTAG system for immediate and target-specific protein degradation. *Nat. Chem. Biol.* **14**, 431 (2018).

4. D. Clift *et al.*, A Method for the Acute and Rapid Degradation of Endogenous Proteins. *Cell*. **171**, 1692-1706.e18 (2017).

5. X. Fan, W. Y. Jin, J. Lu, J. Wang, Y. T. Wang, Rapid and reversible knockdown of endogenous proteins by peptide-directed lysosomal degradation. *Nat. Neurosci.* **17**, 471–480 (2014).

6. M. Naito, N. Ohoka, N. Shibata, SNIPERs—Hijacking IAP activity to induce protein degradation. *Drug Discov. Today Technol.* (2019), doi:10.1016/j.ddtec.2018.12.002.

7. G. M. Burslem, C. M. Crews, Small-Molecule Modulation of Protein Homeostasis. *Chem. Rev.* **117**, 11269–11301 (2017).

8. M. Uhlén *et al.*, Tissue-based map of the human proteome. *Science*. **347**, 1260419 (2015).

9. K. J. Brown *et al.*, The human secretome atlas initiative: Implications in health and disease conditions. *Biochim. Biophys. Acta*. **1834**, 2454–2461 (2013).

10. M. F. Coutinho, M. J. Prata, S. Alves, A shortcut to the lysosome: The mannose-6-phosphate-independent pathway. *Mol. Genet. Metab.* **107**, 257–266 (2012).

11. P. Ghosh, N. M. Dahms, S. Kornfeld, Mannose 6-phosphate receptors: new twists in the tale. *Nat. Rev. Mol. Cell Biol.* **4**, 202–213 (2003).

12. M. Gary-Bobo, P. Nirdé, A. Jeanjean, A. Morère, M. Garcia, Mannose 6-phosphate receptor targeting and its applications in human diseases. *Curr. Med. Chem.* **14**, 2945–2953 (2007).

13. L. Liu, W.-S. Lee, B. Doray, S. Kornfeld, Engineering of GlcNAc-1-Phosphotransferase for Production of Highly Phosphorylated Lysosomal Enzymes for Enzyme Replacement Therapy. *Mol. Ther. - Methods Clin. Dev.* **5**, 59–65 (2017).

14. Y. Zhu *et al.*, Conjugation of Mannose 6-Phosphate-containing Oligosaccharides to Acid α-Glucosidase Improves the Clearance of Glycogen in Pompe Mice. *J. Biol. Chem.* **279**, 50336–50341 (2004).

15. L. Beljaars *et al.*, Albumin modified with mannose 6-phosphate: A potential carrier for selective delivery of antifibrotic drugs to rat and human hepatic stellate cells. *Hepatology*. **29**, 1486–1493 (1999).

16. D. B. Berkowitz, G. Maiti, B. D. Charette, C. D. Dreis, R. G. MacDonald, Mono- and Bivalent Ligands Bearing Mannose 6-Phosphate (M6P) Surrogates: Targeting the M6P/Insulin-Like Growth Factor II Receptor. *Org. Lett.* **6**, 4921–4924 (2004).

17. S. Das, N. Parekh, B. Mondal, S. S. Gupta, Controlled Synthesis of End-Functionalized Mannose-6-phosphate Glycopolypeptides for Lysosome Targeting. *ACS Macro Lett.* **5**, 809–813 (2016).

18. A. Jeanjean, M. Garcia, A. Leydet, J.-L. Montero, A. Morère, Synthesis and receptor binding affinity of carboxylate analogues of the mannose 6-phosphate recognition marker. *Bioorg. Med. Chem.* **14**, 3575–3582 (2006).

19. W. S. Sly *et al.*, Enzyme therapy in mannose receptor-null mucopolysaccharidosis VII mice defines roles for the mannose 6-phosphate and mannose receptors. *Proc. Natl. Acad. Sci.* **103**, 15172–15177 (2006).

20. J. R. Kramer, B. Onoa, C. Bustamante, C. R. Bertozzi, Chemically tunable mucin chimeras assembled on living cells. *Proc. Natl. Acad. Sci.* **112**, 12574–12579 (2015).

21. A. Jeanjean *et al.*, Synthesis of new sulfonate and phosphonate derivatives for cation-independent mannose 6-phosphate receptor targeting. *Bioorg. Med. Chem. Lett.* **18**, 6240–6243 (2008).

22. T. E. Ritter, O. Fajardo, H. Matsue, R. G. Anderson, S. W. Lacey, Folate receptors targeted to clathrin-coated pits cannot regulate vitamin uptake. *Proc. Natl. Acad. Sci.* **92**, 3824–3828 (1995).

23. D. E. Johnson, P. Ostrowski, V. Jaumouillé, S. Grinstein, The position of lysosomes within the cell determines their luminal pH. *J Cell Biol*. **212**, 677–692 (2016).

24. M. Kampmann, M. C. Bassik, J. S. Weissman, Functional genomics platform for pooled screening and generation of mammalian genetic interaction maps. *Nat. Protoc.* **9**, 1825–1847 (2014).

25. M. A. Horlbeck *et al.*, Compact and highly active next-generation libraries for CRISPR-mediated gene repression and activation. *eLife*. **5**, e19760 (2016).

26. M. R. Heider, M. Munson, Exorcising the Exocyst Complex. *Traffic*. **13**, 898–907 (2012).

27. Y. Yamazaki, M. M. Painter, G. Bu, T. Kanekiyo, Apolipoprotein E as a Therapeutic Target in Alzheimer's Disease: A Review of Basic Research and Clinical Evidence. *CNS Drugs*. **30**, 773–789 (2016).

28. J. Y. Li *et al.*, A Biparatopic HER2-Targeting Antibody-Drug Conjugate Induces Tumor Regression in Primary Models Refractory to or Ineligible for HER2-Targeted Therapy. *Cancer Cell*. **29**, 117–129 (2016).

29. J. B. Spangler *et al.*, Combination antibody treatment down-regulates epidermal growth factor receptor by inhibiting endosomal recycling. *Proc. Natl. Acad. Sci.* **107**, 13252–13257 (2010).

30. Y. Shen *et al.*, Transferrin receptor 1 in cancer: a new sight for cancer therapy. *Am. J. Cancer Res.* **8**, 916–931 (2018).

31. A. M. Weissman, R. D. Klausner, K. Rao, J. B. Harford, Exposure of K562 cells to anti-receptor monoclonal antibody OKT9 results in rapid redistribution and enhanced degradation of the transferrin receptor. *J. Cell Biol.* **102**, 951–958 (1986).

32. M. L. Burr *et al.*, CMTM6 maintains the expression of PD-L1 and regulates anti-tumour immunity. *Nature*. **549**, 101–105 (2017).

33. W. B. Cowden, Phosphosugars and phosphosugar-containing compounds having anti-inflammatory activity (2001), (available at https://patents.google.com/patent/US6294521B1/en).

34. K. Lin, A. M. Kasko, Effect of Branching Density on Avidity of Hyperbranched Glycomimetics for Mannose Binding Lectin. *Biomacromolecules*. **14**, 350–357 (2013).

35. M. N. Zhou *et al.*, N-Carboxyanhydride Polymerization of Glycopolypeptides That Activate Antigen-Presenting Cells through Dectin-1 and Dectin-2. *Angew. Chem. Int. Ed Engl.* **57**, 3137–3142 (2018).

36. W. Li *et al.*, MAGeCK enables robust identification of essential genes from genome-scale CRISPR/Cas9 knockout screens. *Genome Biol.* **15**, 554 (2014).

37. E. Eden, R. Navon, I. Steinfeld, D. Lipson, Z. Yakhini, GOrilla: a tool for discovery and visualization of enriched GO terms in ranked gene lists. *BMC Bioinformatics*. **10**, 48 (2009).

38. A. S. Hebert *et al.*, Improved Precursor Characterization for Data-Dependent Mass Spectrometry. *Anal. Chem.* **90**, 2333–2340 (2018).

39. S. Tyanova, T. Temu, J. Cox, The MaxQuant computational platform for mass spectrometry-based shotgun proteomics. *Nat. Protoc.* **11**, 2301–2319 (2016).

40. J. Cox *et al.*, Andromeda: a peptide search engine integrated into the MaxQuant environment. *J. Proteome Res.* **10**, 1794–805 (2011).

41. J. E. Elias, S. P. Gygi, Target-decoy search strategy for increased confidence in large-scale protein identifications by mass spectrometry. *Nat. Methods*. **4**, 207–214 (2007).

42. J. Cox *et al.*, Accurate proteome-wide label-free quantification by delayed normalization and maximal peptide ratio extraction, termed MaxLFQ. *Mol. Cell. Proteomics MCP*. **13**, 2513–26 (2014).

43. S. Tyanova *et al.*, The Perseus computational platform for comprehensive analysis of (prote)omics data. *Nat. Methods*. **13**, 731–740 (2016).

Acknowledgements

We thank Michael Bassik (Stanford) for the CRISPRi library and dCas9-KRAB expressing cell lines. We thank Thomas Waldmann (National Institutes of Health) for a gift of the HDLM-2 cell line. We thank Green Ahn (Stanford) for recombinant mCherry protein. We thank Eric Appel (Stanford) for use of aqueous gel permeation chromatography. This work was supported in part by National Institutes of Health grant P30CA124435 utilizing the Stanford Cancer Institute Proteomics/Mass Spectrometry Shared Resource. This work was supported in part by National Institutes of Health grant R01CA227942 to C.R.B. S.M.B was supported by a National Institute of General Medical Sciences F32 Postdoctoral Fellowship. K.P. was supported by a National Science Foundation Graduate Research Fellowship, a Stanford Graduate Fellowship, and the Stanford ChEM-H Chemistry/Biology Interface Predoctoral Training Program. S.W. was supported by a Banting Postdoctoral Fellowship from the Canadian Institutes of Health. N.M.R. was supported by National Institutes of Health grant K00CA21245403.

Author contributions

S.M.B, K.P., and C.R.B. conceived the project. S.M.B., K.P., S.W., and N.M.R. carried out experiments and interpreted data. S.M.B and C.R.B. wrote the manuscript with input from all authors. C.R.B. provided supervision.

Competing interests

A patent application relating to lysosome targeting chimeras has been filed by Stanford University (docket number STAN-1497PRV). C.R.B. is a co-founder and Scientific Advisory Board member of Palleon Pharmaceuticals, Enable Bioscience, Redwood Biosciences (a subsidiary of Catalent) and InterVenn Biosciences, and a member of the Board of Directors of Eli Lilly & Company.

List of Supplementary materials

Materials and Methods
Fig. S1-S16
Supplemental Data 1
Supplemental Data 2

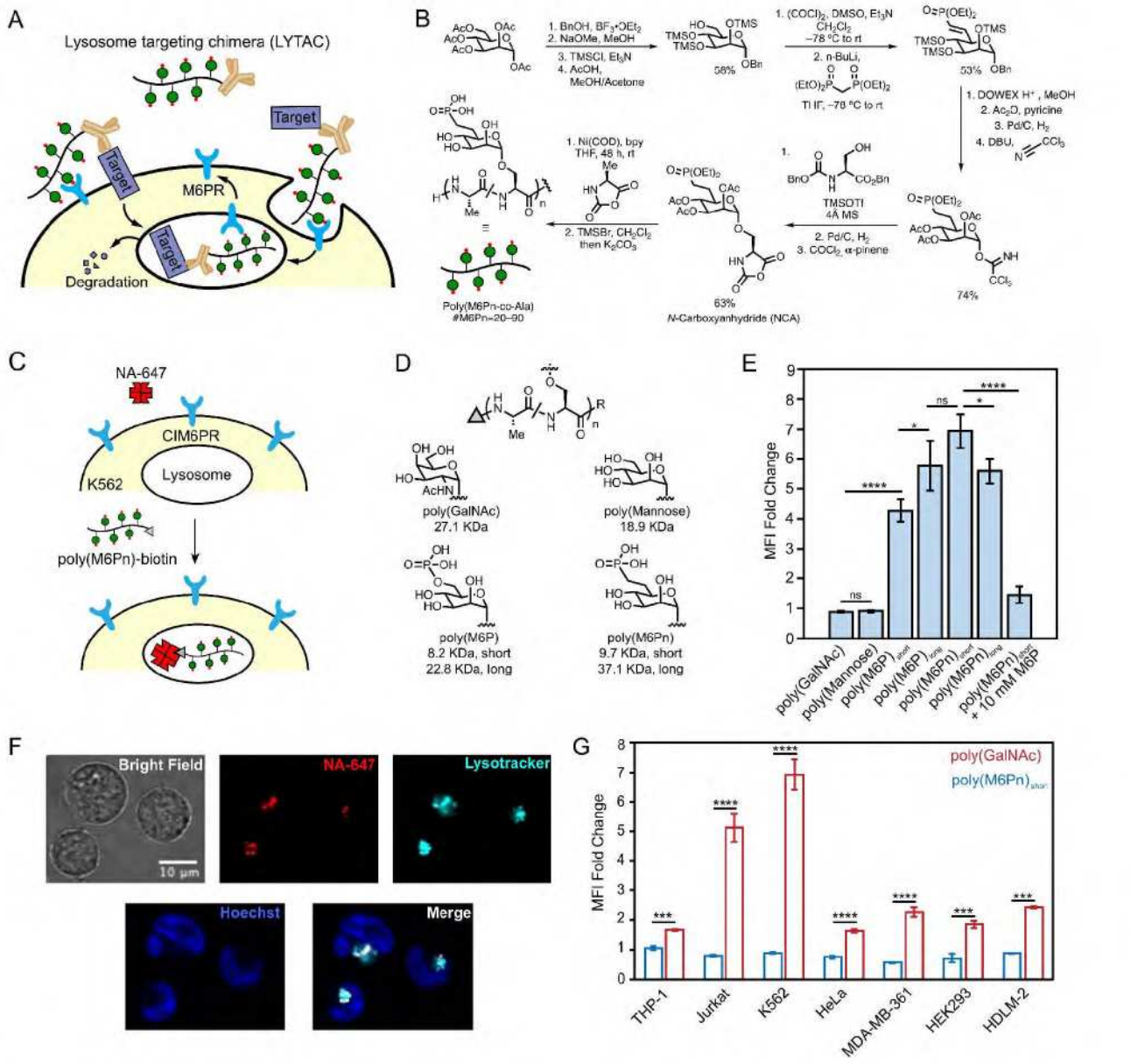

Fig. 1. Lysosomal targeting chimeras (LYTACs) utilizing the cation-independent mannose-6-phosphate receptor (CI-M6PR) traffic proteins to lysosomes. (A) LYTAC concept where a glycopolypeptide ligand for CI-M6PR is conjugated to an antibody to traffic secreted and membrane proteins to lysosomes. (B) Synthesis of mannose-6-phosphonate (M6Pn) glycopolypeptide agonists for CI-M6PR. (C) NeutrAvidin-647 (NA-647) internalization assay for biotin-based LYTACs. (D) Panel of synthetic M6P and M6Pn glycopolypeptides and controls. GalNAc = *N*-acetylgalactosamine. (E) Mean fluorescence intensity (MFI) fold changes for K562 cells incubated at 37 °C for 1 hour with 500 nM NA-647 or 500 nM NA-647 and 2 μM biotinylated glycopolypeptide in complete growth media. MFI determined by live cell flow cytometry and values are the average of three independent experiments ± SD. Fold change is relative to NA-647 uptake alone. (F) Live cell confocal microscopy images of K562 cells treated as in (E), then labeled with Lysotracker Green for 30 minutes. (G) Cell line panel for NA-647 uptake performed as in (E),

depicted values are the average of three independent experiments ± SD. *P < 0.05; **P < 0.01; ***P < 0.001; ****P < 0.0001, determined by Student's two-tailed t-test.

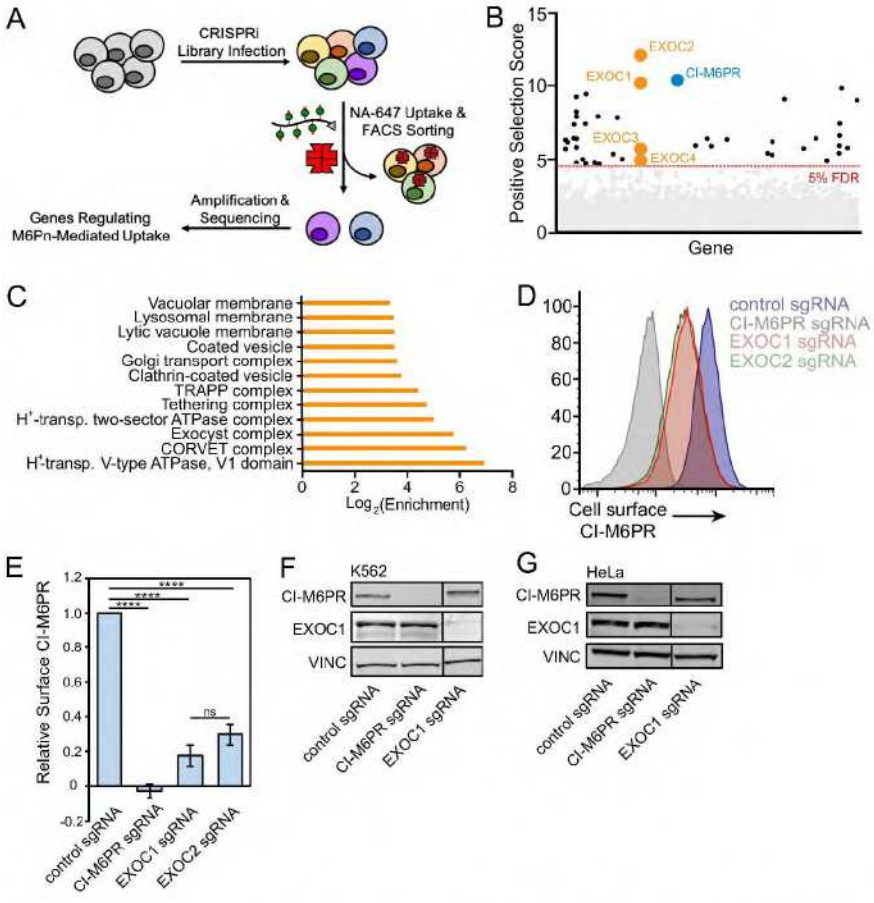

Fig. 2. CRISPRi screen identifies key cellular machinery for LYTACs. (A) CRISPRi screen in K562 cells stably expressing dCas9-KRAB and a library of sgRNAs with genome-wide coverage. (B) Gene hits for regulation of NA-647 internalization by LYTACs. (C) Gene ontology (GO) annotation for significant hits (< 5% FDR). (D) and (E) Cell surface expression levels of CI-M6PR in dCas9-KRAB K562 cells (D) or HeLa cells (E) transfected with control sgRNA, CI-M6PR-targeting sgRNA, EXOC1-targeting sgRNA, or EXOC2-targeting sgRNA. Cells were stained for CI-M6PR and subjected to live cell flow cytometry. (D) is representative of two measurements for K562 cells, which rapidly lost the exocyst knockdown phenotype; (E) is the average of three independent experiments in HeLa ± SD and normalized to control sgRNA. *P < 0.05; **P < 0.01; ***P < 0.001; ****P < 0.0001, determined by Student's two-tailed t-test. (F) and (G) Western blot analysis of EXOC1 and CI-M6PR in K562 (F) and HeLa (G) CRISPRi knockdown lines.

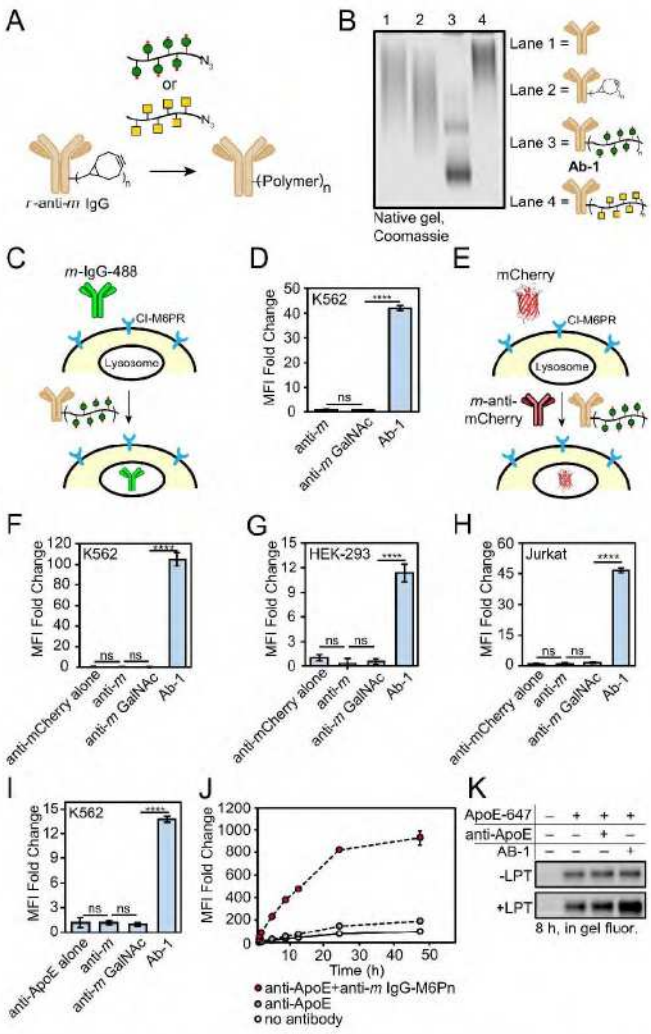

Fig. 3. LYTACs target soluble proteins to lysosomes for degradation. (A) Synthetic scheme for antibody-based LYTACs. (B) Native gel of polyclonal rabbit anti-mouse IgG conjugates. (C) Uptake of an AlexaFluor-488 labeled mouse IgG (m-IgG-488) into K562 cells using antibody LYTACs. (D) Mean fluorescence intensity fold change over background uptake measured by live cell flow cytometry. K562 cells were incubated at 37 °C for 1 hour with 50 nM IgG-488 or 50 nM IgG and 25 nM of anti-mouse or **Ab-1**. Values represent averages of three independent experiments ± SD. (E) Uptake of mCherry antigen and its antibody by a LYTAC into (F) K562 cells, (G) HEK-293 cells, or (H) Jurkat cells measured by live cell flow cytometry after 1 hour incubation as in (D). (I) Uptake of ApoE-647 into K562 cells, performed as in (D). Median fluorescence intensity was measured by live cell flow cytometry. Values represent averages of three independent experiments ± SD. (J) ApoE-647 uptake over time. K562 cells were incubated with 50 nM ApoE-647 in the presence or absence of anti-ApoE4 and **Ab-1**. At the indicated time point, cells were aliquoted and MFI measurements were taken as in (D). (K) Cells were incubated as in (D) for 8 hours in the presence or absence of 0.1 mg/mL leupeptin (LPT), then lysed. Lysates were separated by SDS-PAGE, and ApoE-647 was detected via in-gel fluorescence. *P < 0.05; **P < 0.01; ***P < 0.001; ****P < 0.0001, determined by Student's two-tailed t-test, fold changes are reported relative to incubation with protein targets alone.

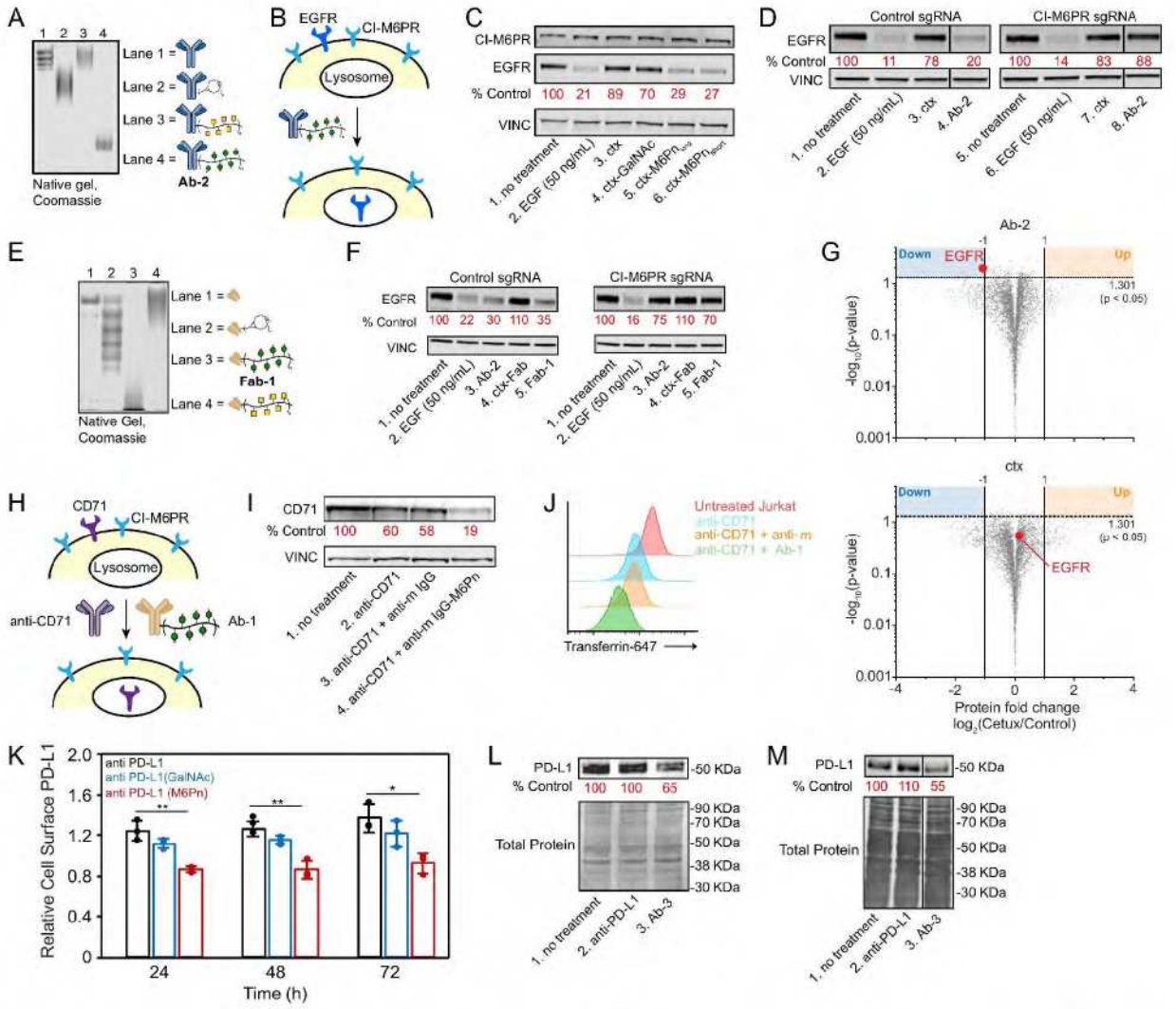

Fig. 4. LYTACs accelerate degradation of membrane proteins. (A) Native gel of cetuximab(ctx)-based LYTACs. (B) EGFR degradation using antibody LYTACs. (C) Western blot of HeLa cells treated with 100 nM ctx (lane 3), ctx-GalNAc (lane 4), ctx-M6Pn$_{long}$ (lane 5) or ctx-M6Pn$_{short}$ (lane 6) for 24 hours in complete growth media. EGF stimulation is a positive control for EGFR downregulation. (D) Western blot of EGFR degradation with 10 nM **Ab-2** for 24 hours in HeLa dCas9-KRAB cells expressing a control sgRNA or sgRNA targeting CI-M6PR. (E) Native gel of ctx-Fab-based LYTACs. (F) Western blot of EGFR degradation with **Fab-1** in HeLa dCas9-KRAB cells expressing a control sgRNA or sgRNA targeting CI-M6PR. (G) Fold change abundance of 3877 HeLa proteins detected via quantitative MS analysis following 24-hour treatment with either 10 nM **Ab-2** (top) or ctx (bottom). (H) Degradation of CD71 mediated by a primary antibody and **Ab-1**. (I) Western blot analysis of CD71 degradation in Jurkat cells after 24 hours. (J) Uptake of transferrin-647 in Jurkat cells treated with anti-CD71 or anti-CD71 and **Ab-1** for 24 hours. (K) Cell surface PD-L1 determined by live cell flow cytometry after incubation with anti-PD-L1 or conjugates (50 nM). At each time point, cells were lifted, brought to 4 °C, then stained for PD-L1. Cell surface PD-L1 is reported relative to untreated and PD-L1 stained cells. (L) and (M) Western blot analysis of total PD-L1 in MDA-MB-231 after 48 hours (L) and HDLM-2 after 36 hours (M). Percent control values were calculated via densitometry and normalized to

loading control or total protein. *P < 0.05; **P < 0.01; ***P < 0.001; ****P < 0.0001, determined by Student's two-tailed t-test.

Supplementary Materials for

Lysosome Targeting Chimeras (LYTACs) for the Degradation of Secreted and Membrane Proteins

Steven M. Banik, Kayvon Pedram, Simon Wisnovsky, Nicholas M. Riley, Carolyn R. Bertozzi*

*Correspondence should be addressed to C.R.B. (bertozzi@stanford.edu).

This PDF file includes:

Materials and Methods
Fig. S1-S16

Other Supplementary Materials for this manuscript include the following:

Supplemental Data 1
Supplemental Data 2

Materials and Methods

General Synthetic Chemistry Procedures and Materials: All reactions were performed in standard, dry glassware fitted with rubber septa under an inert atmosphere of nitrogen unless otherwise described. Stainless steel syringes or cannulae were used to transfer air- and moisture-sensitive liquids. Reported concentrations refer to solution volumes at room temperature. Column chromatography was performed with ZEOprep® 60 (40–63 micron) silica gel from American Scientific. Thin layer chromatography (TLC) was used for reaction monitoring and product detection using pre-coated glass plates covered with 0.20 mm silica gel with fluorescent indicator; visualization by UV light, $KMnO_4$, or 5% H_2SO_4 in MeOH. Reagents were purchased in reagent grade from commercial suppliers and used as received, unless otherwise described. Anhydrous solvents (acetonitrile, benzene, dichloromethane, diethyl ether, *N*,*N*-dimethylformamide, tetrahydrofuran, and toluene) were prepared by passing the solvent through an activated alumina column.

Chemical Analysis Instrumentation: Proton nuclear magnetic resonance (^{1}H NMR) spectra were recorded on an Inova-600 spectrometer or a Varian-400 spectrometer at 25 °C, are reported in parts per million downfield from tetramethylsilane, and are referenced to the residual protium resonances of the NMR solvent ($CDCl_3$: 7.26 [$CHCl_3$], CD_3OD: 4.87 [MeOH], D_2O: 3.31 [H_2O]). Proton-decoupled carbon-13 nuclear magnetic resonance (^{13}C {^{1}H} NMR) spectra were recorded on an Varian-400 spectrometer at 25 °C, are reported in parts per million downfield from tetramethylsilane, and are referenced to the carbon resonances of the NMR solvent ($CDCl_3$: 77.16, CD_3OD: 49.00). Chemical shifts for phosphorus-31 nuclear magnetic resonance (^{31}P NMR) were recorded on a Varian Mercury-400 spectrometer at 25 °C, are reported in parts per million downfield from H_3PO_4 (δ = 0). Data are represented as follows: chemical shift, multiplicity (br = broad, s = singlet, d = doublet, t = triplet, q = quartet, quin = quintet, sept = septet, m = multiplet), coupling constants in Hertz (Hz), integration. High-resolution mass spectrometric data were obtained on a Thermo Exactive benchtop Orbitrap.

Synthesis of Mannose-6-Phosphonate *N*-Carboxyanhydride Monomers:

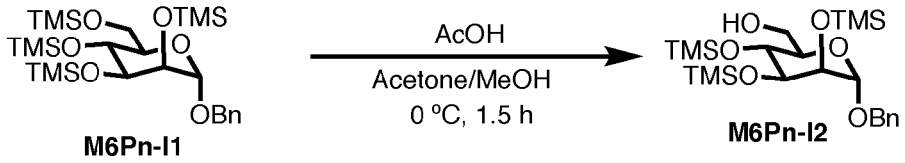

M6Pn-I2. To **M6Pn-I1** (*33*) (5.65 g, 10.1 mmol, 1.0 equiv.) was added acetone (22 mL) and methanol (30 mL). The mixture was cooled to 0 °C, and acetic acid (1.11 mL) was added. The reaction was stirred for 1.5 hours at 0 °C, after which solid $NaHCO_3$ (1.79 g, 21.3 mmol, 2.10 equiv.) was added. The reaction mixture was concentrated under reduced pressure and the resulting residue was purified by flash column chromatography on silica gel (0 to 15% ethyl acetate in hexanes) to give a colorless oil (2.80 g, 58%). ^{1}H NMR (400 MHz, $CDCl_3$) δ 7.38–7.28 (m, 5H), 4.73–4.70 (d, *J* = 12.2 Hz, 1H), 4.69 (s, 1H), 4.51–4.48 (d, *J* = 12.2 Hz, 1H), 3.92–3.59 (m, 6H), 2.01 (s, 1H), 0.17 (s, 9H), 0.16 (s, 9H), 0.12 (s, 9H). ^{13}C NMR (101 MHz, $CDCl_3$) δ 137.6, 128.4, 127.7, 127.6, 100.3, 74.1, 73.7, 72.5, 69.0, 68.1, 62.2, 0.66, 0.58, 0.35. ESI-HRMS Calc'd [$M+NH_4^+$]=504.2633; found 504.2627.

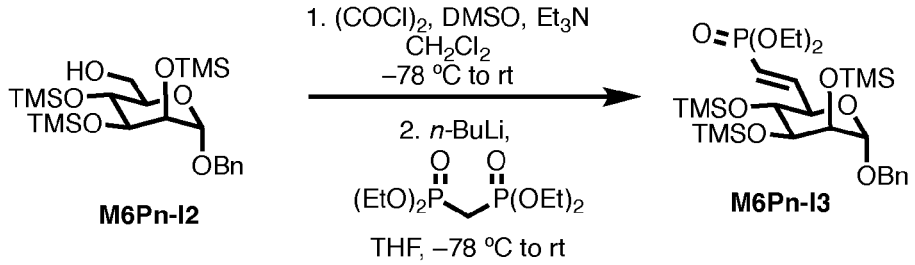

M6Pn-I3. To oxalyl chloride (0.649 mL, 5.87 mmol, 1.1 equiv.) was added dichloromethane (10 mL), and the mixture was cooled to -78 °C. To the reaction mixture was added DMSO (0.834 mL, 11.74 mmol, 2.2 equiv.), and the reaction was stirred for 10 minutes at -78 °C. To the reaction mixture was added a solution of **M6Pn-I2** (2.60 g, 5.34 mmol, 1.0 equiv.) in dichloromethane (10 mL) dropwise, and the reaction was stirred at -78 °C. After 45 minutes, triethylamine (3.72 mL, 26.7 mmol, 5.0 equiv) was added, and the mixture was allowed to warm to room temperature and stirred for 1 hour. The reaction mixture was diluted with dichloromethane (150 mL) and washed with water (3 X 50 mL). The organic layer was dried with $MgSO_4$ and concentrated under reduced pressure to give an orange residue. To tetraethyl methylenediphosphonate (2.31 g, 8.01 mmol, 1.5 equiv.) was added tetrahydrofuran (30 mL) and the reaction mixture was cooled to –78 °C. To the reaction mixture was added *n*-BuLi (2.5 M in hexanes, 2.67 mL, 6.67 mmol, 1.25 equiv.). After 45 minutes, the orange residue obtained above was added slowly as a solution in tetrahydrofuran (10 mL), and the reaction mixture was stirred at -78 °C for two hours, then allowed to warm to room temperature overnight. The reaction mixture was diluted with ethyl acetate (250 mL) and washed with water (2 X 50 mL). The organic layer was dried with $MgSO_4$ and concentrated under reduced pressure. The resulting residue was purified by flash column chromatography on silica gel (0 to 40% ethyl acetate in hexanes) to give a colorless oil (1.93 g, 53% over two steps). ^{1}H NMR (400 MHz, $CDCl_3$) δ 7.44–7.21 (m, 5H), 6.85 (ddd, *J* = 22.8, 17.2, 4.2 Hz, 1H), 6.05 (ddd, *J* = 22.0, 17.2, 1.8 Hz, 1H), 4.70 (m, 1H), 4.67–4.45 (d, *J* = 12.2 Hz, 1H), 4.48–4.45 (d, *J* = 12.2 Hz, 1H), 4.14 – 4.05 (m, 6H), 3.83 – 3.80 (m, 2H), 3.69 (app. t, *J* = 9.6 Hz, 2H), 1.33 (td, *J* = 7.1, 1.3 Hz, 4H), 0.16 (s, 9H), 0.13 (s, 9H), 0.10 (s, 9H). ^{13}C NMR (101 MHz, $CDCl_3$) δ 148.9 (d, J = 5.9 Hz), 137.5, 128.4, 127.7, 127.6, 117.0 (d, *J* = 189.2 Hz), 100.2, 73.5, 73.3, 72.8, 71.5, 69.1, 61.6 (t, *J* = 6.1 Hz), 16.4 (d, *J* = 6.2 Hz), 0.74, 0.56, 0.32. ^{31}P NMR (162 MHz, $CDCl_3$) δ 18.5. ESI-HRMS Calc'd [M+H$^+$, -3 X TMS]=403.1522; found 403.1514.

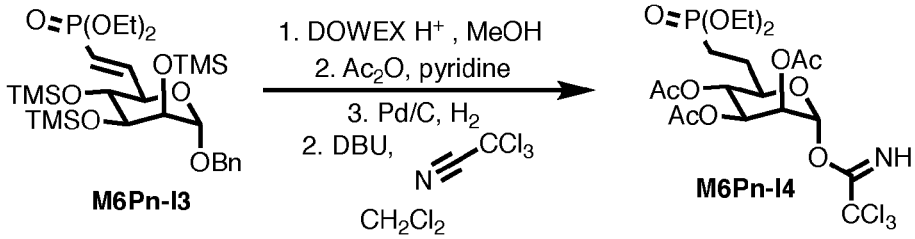

M6Pn-I4. To **M6Pn-I3** (1.93 g, 3.12 mmol, 1.0 equiv) was added methanol (40 mL) and DOWEX 50 WX8-200 (1.0 g). The mixture was stirred for 1 hour at room temperature. The reaction mixture was filtered and concentrated under reduced pressure. The resulting residue was dissolved in pyridine (20 mL), and acetic anhydride (10 mL) was added. The reaction was allowed to stir overnight, then concentrated under reduced pressure. The residue was dissolved in dichloromethane (100 mL) and washed with 1M HCl (50 mL) and water (50 mL). The organic layer was dried with anhydrous $MgSO_4$ and concentrated under reduced pressure. To the

resulting residue was added 10% Pd/C (666 mg, 0.624 mmol, 0.2 equiv.), and methanol (40 mL), and the reaction mixture was degassed and placed under an atmosphere of hydrogen. After 24 hours, additional Pd/C was added (2.00 g), and the reaction was stirred under an atmosphere of hydrogen for an additional 24 hours. Upon completion, the reaction mixture was filtered through celite and concentrated. To the resulting residue was added dichloromethane (50 mL), trichloroacetonitrile (3.12 mL, 31.2 mmol, 10.0 equiv.), and DBU (0.046 mL, 0.0312 mmol, 0.1 equiv.). The reaction mixture was allowed to stir for 1 hour at room temperature, then concentrated under reduced pressure. The resulting residue was purified by flash column chromatography on silica gel (30 to 100% ethyl acetate in hexanes) to give a pale yellow foam (1.35 g, 74% over 4 steps). ^{1}H NMR (400 MHz, $CDCl_3$) δ 8.70 (s, 1H), 6.09 (s, 1H), 5.33–5.31 (m, 1H), 5.22 (dd, *J* = 10.0, 3.4 Hz, 1H), 5.07 (app. t, *J* = 10.0 Hz, 1H), 4.00–3.88 (m, 4H), 3.82 (app. t, *J* = 8.1 Hz, 1H), 2.06 (s, 3H), 1.95 (s, 3H), 1.87 (s, 3H), 1.82–1.43 (m, 4H), 1.18 (t, *J* = 7.1 Hz, 6H). ^{13}C NMR (101 MHz, $CDCl_3$) δ 169.6, 169.5, 169.5, 159.5, 94.2, 90.4, 72.2 (d, *J* = 18.0 Hz), 68.7, 67.9 (d, *J* = 16.8 Hz), 61.5 (d, *J* = 6.9 Hz), 61.4 (d, *J* = 7.0 Hz), 24.1 (d, *J* = 4.0 Hz), 21.6, 20.6, 20.6, 20.5, 20.1, 16.4 (d, *J* = 5.9 Hz). ^{31}P NMR (162 MHz, $CDCl_3$) δ 31.2. ESI-HRMS Calc'd [M+H$^+$]=584.0622; found 584.0607.

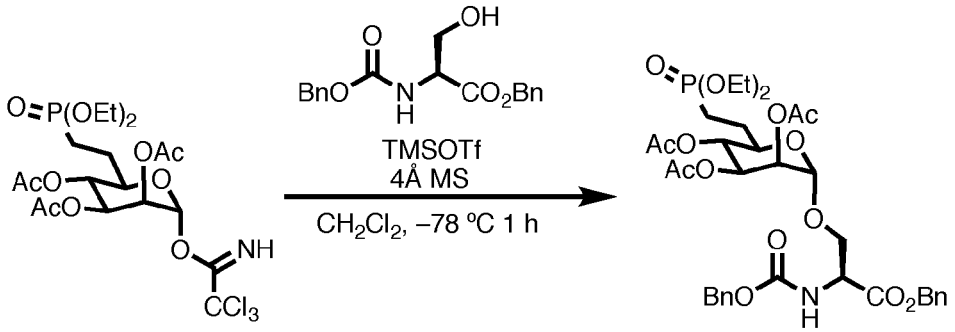

M6Pn-I4 **M6Pn-I5**

M6Pn-I5. To **M6Pn-I4** (1 g, 1.71 mmol, 1.25 equiv.) was added Z-Ser-OBn (451 mg, 1.37 mmol, 1.0 equiv.), 3 g freshly activated 4Å MS, and dichloromethane (50 mL). The reaction mixture was cooled to -78 °C and TMSOTf (0.060 mL, 0.342 mmol, 0.2 equiv.) was added and the reaction mixture was stirred at -78 °C for 1 h. Triethylamine (1 mL) was added to reaction mixture, and the resulting mixture was filtered over celite and concentrated. The resulting residue was purified by flash column chromatography on silica gel (30 to 100% ethyl acetate in hexanes) to give a white foam (1.02 g, 79%). ^{1}H NMR (400 MHz, $CDCl_3$) δ 7.34–7.28 (m, 10H), 5.84 (d, *J* = 8.0 Hz, 1H), 5.31 – 4.95 (m, 8H), 4.63 (s, 1H), 4.55 (d, *J* = 7.7 Hz, 2H), 4.09–3.95 (m, 4H), 3.92–3.90 (m, 2H), 3.72–3.68 (m, 1H), 2.10 (s, 3H), 2.00 (s, 3H), 1.95 (s, 3H), 1.84–1.66 (m, 4H), 1.27 (t, *J* = 7.1 Hz, 6H). ^{13}C NMR (101 MHz, $CDCl_3$) δ 169.7, 169.6, 169.3, 155.8, 136.0, 135.0, 128.5, 128.4, 128.4, 128.3, 128.1, 128.0, 97.7, 69.8 (d, *J* = 17.2 Hz), 68.5 (d, *J* = 40.4 Hz), 67.5, 67.1, 61.5 (d, *J* = 4.6 Hz), 61.5 (d, *J* = 5.4 Hz), 54.2, 24.1 (d, *J* = 4.1 Hz), 20.8 (d, *J* = 143.3 Hz), 20.6, 20.6, 20.5, 20.1, 16.3 (d, *J* = 6.0 Hz). ^{31}P NMR (162 MHz, $CDCl_3$) δ 31.3. ESI-HRMS Calc'd [M+H$^+$]=752.2683; found 752.2670.

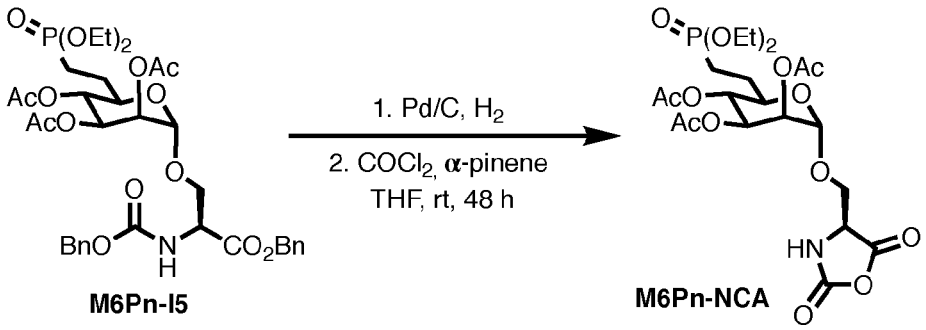

M6Pn-I5 **M6Pn-NCA**

M6Pn-NCA. To **M6Pn-I5** (500 mg, 0.665 mmol, 1.0 equiv.) was added 10% Pd/C (71 mg, 0.067 mmol, 0.1 equiv.), and methanol (15 mL), and the reaction mixture was degassed and placed under an atmosphere of hydrogen. After 12 hours, the reaction mixture was filtered over celite and concentrated to give the corresponding amino acid. The resulting residue was dissolved in tetrahydrofuran (15 mL), and α-pinene (422 µL, 2.66 mmol, 4.00 equiv), and phosgene (950 µL, 1.33 mmol, 2.00 equiv.) were added. The reaction mixture was allowed to stir for 48 hours, then concentrated under reduced pressure into a cold trap in a fumehood. The resulting tan residue was purified by flash column chromatography on anhydrous silica gel (0 to 30% anhydrous tetrahydrofuran in anhydrous dichloromethane) to give a white foam (420 mg, 80%). ^{1}H NMR (400 MHz, $CDCl_3$) δ 8.76 – 8.73 (m, 1H), 5.24 (dd, *J* = 3.4, 1.8 Hz, 1H), 5.11 (dd, *J* = 10.1, 3.4 Hz, 1H), 5.02 (app. t, *J* = 9.9 Hz, 1H), 4.79 (d, *J* = 1.8 Hz, 1H), 4.36 (app. t, *J* = 2.3 Hz, 1H), 4.25–3.96 (m, 6H), 3.85 (dd, *J* = 9.6, 2.2 Hz, 1H), 2.11 (s, 3H), 2.05 (s, 3H), 1.94 (s, 3H), 1.92–1.60 (m, 4H), 1.35 (t, *J* = 7.0 Hz, 3H), 1.31 (t, *J* = 7.1 Hz, 3H). ^{13}C NMR (101 MHz, $CDCl_3$) δ 170.2, 169.9, 169.3, 168.9, 152.2, 96.8, 69.9, 69.3, 68.7, 68.5 (d, *J* = 2.6 Hz), 64.2, 62.5 (d, *J* = 7.0 Hz), 62.1 (d, *J* = 6.7 Hz), 58.1, 25.3 (d, *J* = 5.7 Hz), 20.9, 20.9, 20.7, 20.3 (d, *J* = 143.1 Hz), 16.6 (d, *J* = 5.9 Hz), 16.5 (d, *J* = 6.1 Hz) ^{31}P NMR (162 MHz, $CDCl_3$) δ 29.4. ESI-HRMS Calc'd $[M+H^+]$=554.1639; found 554.1627.

Synthesis of Mannose-6-Phosphate *N*-Carboxyanhydride Monomers:

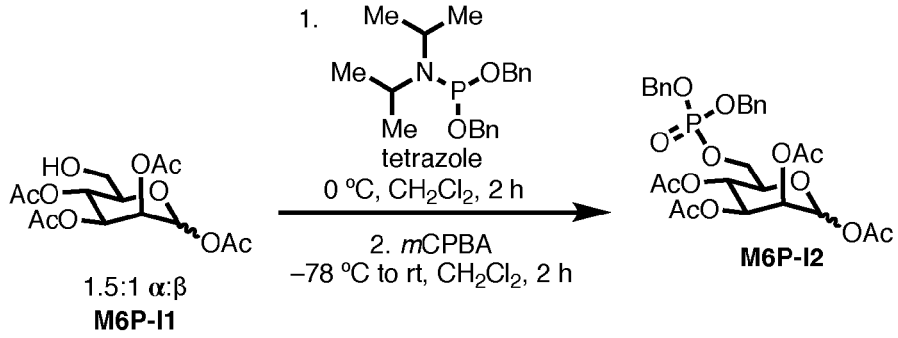

1.5:1 α:β
M6P-I1 **M6P-I2**

M6P-I2. To **M6P-I1** (*34*) (5.00 g, 14.4 mmol, 1.00 equiv.) was added 1*H*-tetrazole (2.03 g, 28.8 mmol, 2.00 equiv.) and dichloromethane (288 mL). The mixture was cooled to 0 °C, and dibenzyl *N,N*-diisopropylphosphoramidite (7.26 mL, 21.6 mmol, 1.5 equiv.) was added dropwise over 5 minutes. After 2 hours, the reaction mixture was cooled to -78 °C, and *m*CPBA (12.91 g of 77% *m*CPBA, 57.6 mmol, 4 equiv.) was added as a solid. The reaction was allowed to warm to 0 °C. After two hours, saturated $Na_2S_2O_3$ (100 mL) was added, and the organic layer was removed, washed 2X with saturated $NaHCO_3$ (150 mL), dried with $MgSO_4$, and concentrated under reduced pressure. The resulting residue was purified by flash column chromatography on silica gel (10 to 90% ethyl acetate in hexanes) to give a colorless, viscous oil (8.01 g, 91%). ^{1}H NMR (400 MHz,

$CDCl_3$, two diastereomers) 7.31–7.23 (m, 10H), 6.25 (d, *J* = 3.7 Hz, 1H), 5.66 (d, *J* = 8.3 Hz, 1H), 5.39 (t, *J* = 9.9 Hz, 1H), 5.18 (t, *J* = 9.4 Hz, 1H), 5.09 – 4.90 (m, 8H), 4.16 – 3.93 (m, 3H), 3.73 (dd, *J* = 9.9, 1.6 Hz, 1H), 2.06 (s, 3H), 1.97 (s, 3H), 1.96 (s, 3H), 1.95 (s, 6H), 1.93 (s, 3H), 1.92 (s, 3H). ^{13}C NMR (101 MHz, $CDCl_3$) δ 170.1, 170.0, 169.5, 169.2, 169.1, 168.7, 168.6, 135.7, 135.6, 128.5, 128.5, 127.9, 127.9, 127.8, 91.5, 88.8, 73.0 (d, *J* = 8.1 Hz), 72.7, 70.2 (d, *J* = 8.1 Hz), 70.1, 69.7, 69.4 (d, *J* = 1.6 Hz), 69.4, 69.0, 67.7, 67.6, 65.0 (d, *J* = 5.2 Hz), 64.9 (d, *J* = 5.8 Hz), 20.7, 20.6, 20.5, 20.4, 20.3. ^{31}P NMR (162 MHz, $CDCl_3$) δ -1.3, -1.5. ESI-HRMS Calc'd $[M+H^+]$=609.1737; found 609.1728.

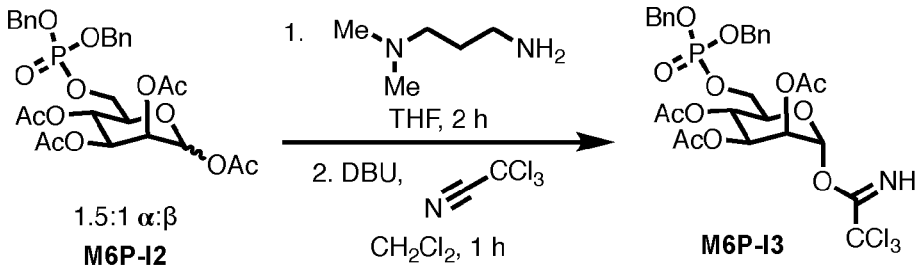

M6P-I3. To **M6P-I2** (8.01 g, 13.2 mmol, 1.00 equiv.) was added tetrahydrofuran (66 mL), followed by 3-(dimethylamino)-1-propylamine (4.15 mL, 33.0 mmol, 2.5 equiv.). The reaction was allowed to stir 1.5 hours until complete consumption of the starting material was observed. The reaction mixture was diluted with dichloromethane (250 mL) and washed with 1M HCl (100 mL) and water (100 mL). The organic layer was dried with $MgSO_4$ and concentrated under reduced pressure. To the resulting residue was added dichloromethane (250 mL), trichloroacetonitrile (6.62 mL, 66.0 mmol, 5.0 equiv.), and DBU (0.197 mL, 1.32 mmol, 0.1 equiv.). The reaction mixture was allowed to stir for 1 hour at room temperature, then concentrated under reduced pressure. The resulting residue was purified by flash column chromatography on silica gel (10 to 85% ethyl acetate) to give a pale yellow, viscous oil (6.10g, 65% over two steps). ^1H NMR (400 MHz, $CDCl_3$) δ 8.70 (s, 1H), 6.20 (s, 1H), 5.38 (s, 1H), 5.36 – 5.27 (m, 2H), 4.97 (app. t, *J* = 6.8 Hz, 4H), 4.25 – 3.89 (m, 3H), 2.02 (s, 3H), 1.96 (s, 3H), 1.94 (d, *J* = 6.8 Hz, 3H). ^{13}C NMR (101 MHz, $CDCl_3$) δ 169.7, 169.6, 169.4, 159.4, 135.7 (d, *J* = 4.1 Hz), 135.6 (d, *J* = 4.1 Hz), 128.5, 128.4, 127.9, 127.8, 94.3, 71.7 (d, *J* = 7.8 Hz), 69.4 (d, *J* = 2.2 Hz), 69.3 (d, *J* = 2.1 Hz), 68.7, 67.7, 65.4 (d, *J* = 5.2 Hz), 65.1, 20.6, 20.6, 20.6. ^{31}P NMR (162 MHz, $CDCl_3$) δ -1.35. ESI-HRMS Calc'd $[M+H^+]$=710.0728; found 710.0714.

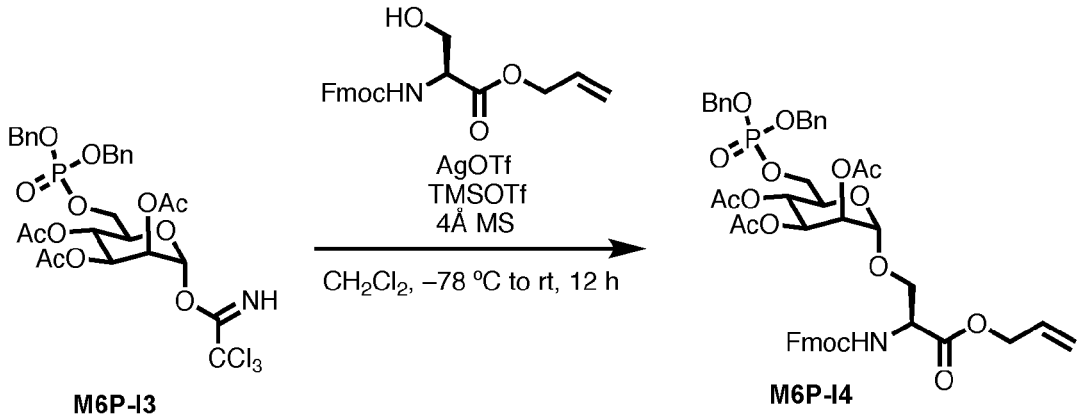

M6P-I4. To **M6P-I3** (4.00 g, 5.63 mmol, 1.0 equiv.) was added Fmoc-Ser allyl ester (2.48 g, 6.76 mmol, 1.2 equiv.), AgOTf (2.89 g, 11.26 mmol, 2.0 equiv.), freshly activated 4Å MS (12.0 g), and dichloromethane (320 mL). The reaction mixture was cooled to -78 °C and TMSOTf (0.255 mL, 1.41 mmol, 0.25 equiv.) was added. The reaction was allowed to warm to -40 °C, stirred at that temperature for 1 h, then allowed to warm to room temperature over 12 hours. Triethylamine (1.0 mL) was added to reaction mixture, and the resulting mixture was filtered over celite and concentrated. The resulting residue was purified by flash column chromatography on silica gel (10 to 100% ethyl acetate in hexanes) to give a white foam (2.33g, 45%). ESI-HRMS Calc'd [M+H$^+$]=916.2945; found 916.2925.

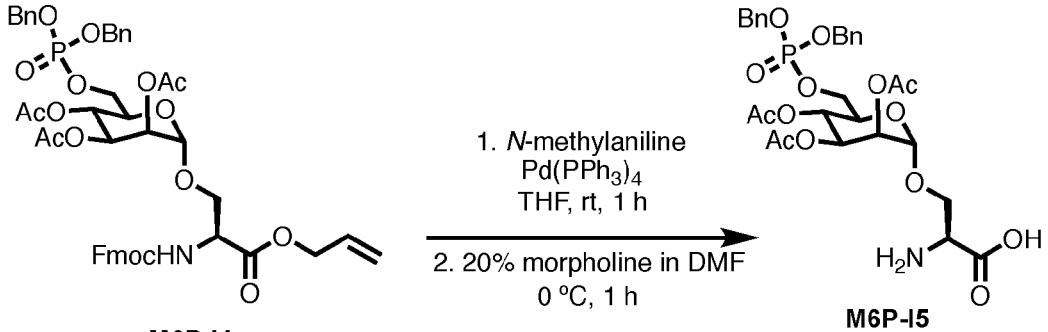

M6P-I4 **M6P-I5**

M6P-I5. To **M6P-I4** (2.33 g, 2.54 mmol, 1.0 equiv.) was added tetrahydrofuran (109 mL), $Pd(PPh_3)_4$ (210 mg, 0.181 mmol, 0.071 equiv.), and *N*-methylaniline (2.75 mL, 25.4 mmol, 10.0 equiv.). The reaction mixture was stirred for 1 hour at room temperature, then concentrated under reduced pressure. The resulting residue was purified by flash column chromatography on silica gel (20 to 100% ethyl acetate in hexanes) to give a light brown foam, which was dissolved in *N*,*N*-dimethylformamide (48.0 mL) and cooled to 0 °C. Morpholine (12.0 mL) was added, and the reaction was stirred at 0 °C for 1 hour. The reaction mixture was concentrated under reduced pressure and purified by flash column chromatography on silica gel (100% ethyl acetate to 33% MeOH in ethyl acetate to 33% MeOH in ethyl acetate with 17% H_2O) to give a tan foam (743 mg, 45% over two steps). ^{1}H NMR (400 MHz, CD_3OD) δ 7.55 – 7.11 (m, 10H), 5.39–5.34 (m, 1H), 5.31 (s, 1H), 5.30–5.28 (m, 1H), 5.10–5.00 (m, 4H), 4.20–4.14 (m, 2H), 4.11–4.04 (m, 2H), 3.81–3.71 (m, 2H), 1.96 (s, 3H), 1.95 (s, 3H), 1.92 (s, 3H). ^{13}C NMR (101 MHz, CD_3OD) δ 171.8, 171.4, 171.2, 137.2 (m), 129.8 (d, *J* = 1.2 Hz), 129.7, 129.2, 129.2, 99.5, 71.0, 70.9, 70.9, 70.8, 70.5 (d, *J* = 7.8 Hz), 70.2, 68.2, 66.9 (d, *J* = 5.3 Hz), 66.5, 55.0, 20.7, 20.6, 20.6. ^{31}P NMR (162 MHz, CD_3OD) δ -1.87. ESI-HRMS Calc'd [M+H$^+$]=654.1952; found 654.1941.

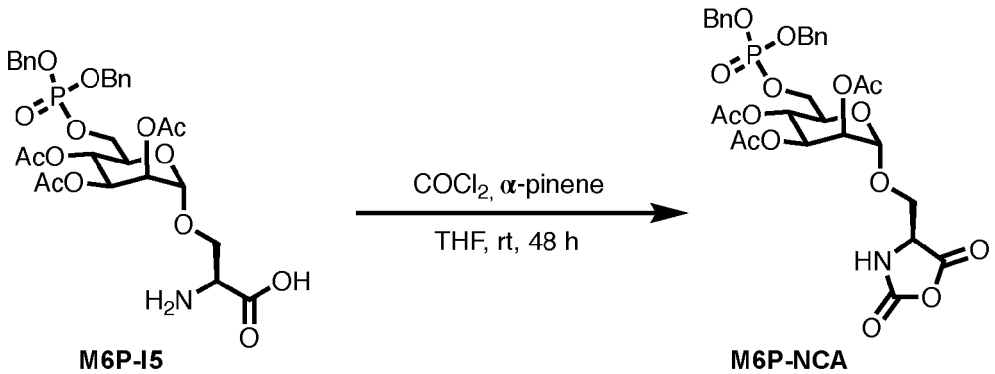

M6P-I5 **M6P-NCA**

M6P-NCA. To **M6P-I5** (350 mg, 0.536 mmol, 1.0 equiv.) was added 12 mL tetrahydrofuran, α-pinene (340 µL, 2.14 mmol, 4.00 equiv.), and phosgene (765 µL, 1.07 mmol, 2.00 equiv.). The reaction mixture was allowed to stir for 48 hours, then concentrated under reduced pressure into a cold trap in a fumehood. The resulting tan residue was purified by flash column chromatography on anhydrous silica gel (0 to 30% anhydrous tetrahydrofuran in anhydrous dichloromethane) to give a white foam (290 mg, 80%). ^{1}H NMR (400 MHz, $CDCl_3$) δ 8.19 (s, 1H), 7.40–7.25 (m, 10H), 5.25 (dd, *J* = 3.5, 1.8 Hz, 1H), 5.17–4.95 (m, 6H), 4.80 (s, 1H), 4.33–4.30 (m, 1H), 4.25–4.18 (m, 1H), 4.11–3.95 (m, 3H), 3.82 (dd, *J* = 10.1, 2.8 Hz, 1H), 2.09 (s, 3H), 1.95 (s, 3H), 1.88 (s, 3H). ^{13}C NMR (101 MHz, $CDCl_3$) 170.3, 169.8, 169.4, 168.3, 152.1, 135.4 (d, *J* = 6.7 Hz), 135.3 (d, *J* = 6.9 Hz), 129.0, 129.0, 128.9, 128.8, 128.3, 128.0, 97.1, 70.2 (d, *J* = 1.0 Hz), 70.12 (d, *J* = 1.9 Hz), 69.5 (d, *J* = 1.8 Hz), 69.0, 68.5, 67.70 (d, *J* = 6.3 Hz), 66.6, 64.7, 58.0, 20.8, 20.7, 20.6. δ ^{31}P NMR (162 MHz, $CDCl_3$) δ -3.18. ESI-HRMS Calc'd $[M+H^+]$=680.1744; found 680.1735.

General Procedure for M6Pn/M6P-containing Glycopolypeptide Synthesis: Polymerization is performed in a glovebox under a N_2 atmosphere. The polymerization catalyst was prepared fresh following the procedure of Kramer *et al*. (*20*), using Ni(COD) and 2,2'-bipyridyl. To an oven dried 1-mL vial was added 20 mg M6Pn-NCA, 4.2 mg Alanine NCA, and 161 µL freshly prepared catalyst mixture (stoichiometry relative to initiator = 5:5:1). The reaction mixture turned from deep purple to red, and was incubated for 48 hours at ambient temperature in the glovebox. After 48 hours, the vial was removed from the glovebox and the reaction mixture quenched with acidic methanol and evaporated under reduced pressure. For both M6Pn and M6P containing polymerization reactions, reactions proceeded slowly without alanine-NCA used as a comonomer, while reaction completion of 1:1 mixtures was obtained within 48 hours.

General Procedure for M6Pn-Containing Polymer Deprotection: To the resulting residue obtained above was added 1 mL anhydrous DCM, 50 µL TMSBr (10 equiv. per phosphonate group), and 30 µL pyridine (10 equiv. per phosphonate). The reaction mixture was stirred at room temperature overnight sealed under N_2. After concentrating under vacuum, the reaction mixture was suspended in a 1:1:1 mixture of 2 mL MeOH with 2 mL THF and 2 mL saturated aqueous K_2CO_3. After 48 hours, 2 mL H_2O was added, in which some of the precipitate dissolved to yield a cloudy solution that was further stirred for 24 hours. The reaction mixture was neutralized to pH = 7 using concentrated HCl, and evaporated to dryness under reduced pressure. The resulting residues and salts were dissolved in H_2O and dialyzed in a 3.5 KDa MWCO dialysis cassette against H_2O for 3 days, with H_2O changes every 8 hours for the first 24 hours, followed by every 12 hours subsequently. The dialysate was removed from the cassette and any precipitate was removed by filtration through a 0.2 µM filter. The resulting solution was lyophilized to yield white solids.

General Procedure for M6P-Containing Polymer Deprotection: To the residue obtained above was added Pd/C (100 mol% Pd per phosphate group) and a dichloromethane/methanol mixture (1:1, 2 mL total/20 mg NCA used in polymerization), and the reaction was stirred under a balloon of H_2 for 48 hours. After filtration through a 0.2 µM filter, the resulting residue was concentrated under vacuum and resuspended in a 1:1:1 mixture of 2 mL MeOH with 2 mL THF and 2 mL saturated aqueous K_2CO_3. After 48 hours, 2 mL H_2O was added, in which some of the precipitate dissolved to yield a cloudy solution that was further stirred for 24 hours. The reaction mixture was neutralized to pH = 7 using concentrated HCl, and evaporated to dryness under reduced pressure. The resulting residues and salts were dissolved in H_2O and dialyzed in a 3.5 KDa MWCO dialysis cassette against H_2O for 3 days, with H_2O changes every 8 hours for the first 24 hours, followed

by every 12 hours subsequently. The contents of the cassette were removed and filtered through a 0.2 µM filter. The resulting solution was lyophilized to yield a white solid.

Synthesis of Poly(GalNAc-co-Ala) and poly(Mannose-co-Ala): As previously described. (*20*, *35*).

Glycopolypeptide Molecular Weight Analysis with Aqueous GPC: Gel permeation chromatography (GPC) was carried out in aqueous 0.1M $NaNO_3$ + 0.01M NaN_3 or PBS using an OHpak SB-803 HQ Shodex column with the dimensions 8.0 x 300 mm a particle size of 6 µm connected in series with a DAWN multiangle laser light scattering (MALLS) detector and an Optilab T-rEX differential refractometer (both from Wyatt Technology), dn/dc values were obtained for each injection by assuming 100% mass elution from the columns.

Glycopolypeptide GPC Molecular Weights, Dispersities, and ^{1}H NMR Glycosylated Serine:Alanine Ratios:

poly(Mannose-co-Ala): M_n=18.9 KDa, Đ = 1.51, 2.4:1
poly(GalNAc-co-Ala): M_n=27.1 KDa, Đ = 1.24, 1.2:1
poly(M6Pn-co-Ala)$_{short}$: M_n=9.75 KDa, Đ = 1.32, 1:1.6
poly(M6Pn-co-Ala)$_{long}$: M_n=37.1 KDa, Đ = 1.42, 1:0.9
poly(M6P-co-Ala)$_{short}$: M_n=8.20 KDa, Đ = 1.58, 1:1.2
poly(M6P-co-Ala)$_{long}$: M_n=24.7 KDa, Đ = 1.75, 1:1.2

Representative Procedure for Polymer N-terminal Biotinylation: To 1.0 mg of poly(M6Pn)$_{short}$ (M_n = 9.7 KDa, 103 nmoles) was added PBS (0.5 mL), and 40 equiv. Biotin-Sulfo-NHS (1.8 mg). The reaction was allowed to incubate for 12 hours at room temperature, then purified with a NAP-25 column, eluting with water. The eluent was then dialyzed against H_2O for 48 hours, with 6 water changes. Yield: 896 µg. The resulting material was dissolved in 231 µL PBS to make a 400 µM stock solution.

Representative Procedure for Polymer N-terminal Azide-Functionalization: To 1.0 mg of poly(M6Pn)$_{short}$ (M_n = 9.7 KDa, 103 nmoles) was added PBS (0.5 mL), and 50 equiv. NHS-PEG_4-N_3 (100 µL of a 20 mg/mL stock) was added. The reaction was allowed to incubate for 12 hours at room temperature, then purified with a NAP-25 column, eluting with water. The eluent was then dialyzed against water for 48 hours, with 6 water changes.

Representative Procedure for Polymer N-terminal BCN-Functionalization: To 500 µg of poly(M6Pn)$_{short}$ (M_n = 9.7 KDa, 51.5 nmoles) was added PBS (1.0 mL) and 25 equiv. BCN-NHS (360 µL of a 1 mg/mL stock in DMSO). The reaction was allowed to incubate for 12 hours at room temperature, then purified with a NAP-25 column, eluting with water. The eluent was then dialyzed against H_2O for 48 hours, with 6 water changes. Yield: 424 µg.

Representative Procedure for Antibody Labeling with BCN-NHS (Cetuximab): 1 mL of a 2 mg/mL solution of cetuximab was concentrated with a 30K spin filter and subsequently diluted to 1000 µL with PBS. 100 µg (25 equiv.) of NHS-BCN in DMSO (1 mg/mL solution, 100 uL) was

added, and the reaction was allowed to incubate at rt overnight. After incubation, the reaction mixture was filtered and diluted eight times using a 500 µL, 30 KDa Amicon Centrifugal Filter.

Representative Procedure for Antibody Labeling with NHS-PEG$_4$-N$_3$ (Cetuximab): 1 mL of a 2 mg/mL solution of cetuximab was concentrated with a 30K spin filter and subsequently diluted with 1000 µL PBS. 137 µg (25 equiv., 14 µL) of NHS-PEG4-N3 in DMSO (10 mg/mL, 137 uL) was added, and the reaction was allowed to incubate at rt overnight. After incubation, the reaction mixture was filtered and diluted eight times using a 500 µL, 30 KDa Amicon Centrifugal Filter.

Representative Procedure for Antibody-Glycopolypeptide Conjugation: To poly(M6Pn)$_{short}$-N$_3$ (136 µg, 20 equiv.) was added ctx-BCN (100 µg, 50 µL in PBS) and the reaction was allowed to incubate for 3 days at room temperature. The reaction mixture was filtered 9X with a 50 KDa Amicon Centrifugal Filter, then resuspended in 100 µL 1X PBS to give a 5.94 µM solution in PBS (89% recovery). Protein concentration was determined by A_{280} absorbance.

Cell Lines: Cells were grown in T75 flasks (Thermo Fisher) and maintained at 37 °C and 5% CO_2. K562 and Jurkat cells were grown in RPMI supplemented with 10% fetal bovine serum (FBS) and 1% penicillin/streptomycin. THP-1 were grown in RPMI supplemented with 10% FBS, 1% penicillin/streptomycin, and 0.05 mM 2-mercaptoethanol. HeLa, MDA-MB-361, HEK293, A549, BT474, and MDA-MB-231 were grown in DMEM supplemented with 10% fetal bovine serum (FBS) and 1% penicillin/streptomycin. HDLM-2 were grown in RPMI supplemented with 20% heat-inactivated FBS and 1% penicillin/streptomycin. HeLa and K562 cells stably expressing dCas9-KRAB were a generous gift from Michael Bassik, Stanford University.

General Procedure for NeutrAvidin-647 Uptake Experiments: Cells (70% confluent in 24-well plate for adherent cells, 1×10^6 cells/mL for suspension cells) were incubated in complete growth medium supplemented with 500 nM NA-647, or NA-647 and 2 µM glycopolypeptide. Addition was performed sequentially, with NA-647 added first followed by glycopolypeptide and immediate transfer to 37 °C.

General Procedure for Protein Uptake and Degradation Experiments: Cells (70% confluent in 24-well plate for adherent cells, 2×10^6 cells/mL for suspension cells) were incubated in complete growth medium supplemented with 50 nM target protein, or 50 nM target protein and 25 nM of each antibody. Addition was performed sequentially, with target protein added first followed by secondary antibodies, followed by primary antibodies, and subsequent immediate transfer to 37 °C.

CRISPRi Screen Procedure: The hCRISPRi-v2 library was a generous gift from Jonathan Weissman (Addgene ID #83969). K562 cells stably expressing dCas9-KRAB were infected with the 104,535 sgRNA library described in Horlbeck *et al.* (*25*), targeting the transcriptional start sites of 18,905 annotated genes at a redundancy of 5 sgRNA/start site. Infectivity was titrated such as to transduce the library at an MOI of 0.3-0.4. Cells were selected with puromycin for 96 h and then allowed to expand in puromycin-free media for 48 h. Staining and FACS was performed within seven days of completion of puromycin selection. On the day of sorting, two replicates of $50x10^6$ library-infected cells (4×10^6 cells/mL) were incubated with NA-647 (500 nM)

and poly(M6Pn)$_{long}$ (2 μM) for 1 hour at 37 °C. Cells were washed three times with PBS at 4 °C. Cells were then resuspended in PBS with Sytox Green (according to manufacturer's specifications) and FACS sorted using a BD Aria II. Intact, viable cells were selected by gating on FSC/SSC and Sytox Green channels. A population of cells representing the bottom 15% of the fluorescence distribution in the NA-647 channel was then selected for and sorted. Sorting was conducted until 25x10^6 events had been processed, corresponding to a ~250-fold library coverage. Sorted cells were then pelleted and frozen for subsequent downstream processing. Aliquots of 50x10^6 unsorted cells from each replicate were also pelleted and frozen down in parallel for normalization.

CRISPRi Screen DNA Extraction and Data Analysis: Frozen cell pellets were thawed and genomic DNA extraction was performed using either the QIAamp DNA Blood Maxi Kit (for unsorted samples) or the Sigma GeneElute Mammalian Genomic DNA Miniprep kit (for sorted samples) according to manufacturer's specifications. The sgRNA-encoding regions were amplified via nested PCR and sequenced on an Illumina NextSeq500. Alignment of sequencing reads to sgRNA library and statistical comparison of positively selected genes in sorted vs. unsorted samples was performed using MaGeCK (*36*). MaGeCK returned a statistical score for gene enrichment in the sorted population and genes were ranked by a positive selection score corresponding to the -log(PosScore). GO enrichment analysis was performed using GOrilla (*37*).

Generation of CRISPRi Knockdown Cell Lines: K562 or HeLa cell stably expressing dCas9-KRAB were infected with lentivirus encoding guide sgRNAs obtained from the CRISPRi screen. Lentivirus was produced by co-transfection of HEK-293T cells with a lentiviral transfer vector and packaging plasmids (pGag/pol, pREV, pTAT, pVSVG). Transfection was performed using Lipofectamine 2000 reagent as recommended by the manufacturer. Viral supernatants were collected 48 h following transfection, filtered through a 0.45 μm filter, and added to target cells (400 μL viral supernatant/well in a 6-well plate) along with polybrene (8 μg/mL). 48-hours post infection, cell media was replaced and cells were placed under puromycin selection (2 μg/mL).

sgRNA guides:
CI-M6PR 5'-GAGGTGAGCGCGGCTCGACT-3'
EXOC1 5'-GGGCGGACAGACGAGCTGAC-3'
EXOC2 5'-GGGCGGAAGTGAGGTGCCGG-3'

Flow Cytometry for Surface Staining and Uptake Measurements: For protein uptake experiments in suspension cell lines, cells were incubated for the indicated time with proteins and conjugates, then washed three times with PBS at 4 °C. Cells were then incubated with either Sytox Green or Sytox Red according to the manufacturer's specifications for 15 minutes on ice. For protein uptake experiments in adherent cell lines, cells were incubated for the indicated time with proteins and conjugates, then washed two times quickly with PBS and lifted with trypsin. Cells were transferred to a 96-well V-bottom plate and washed three times with PBS, then incubated with either Sytox Green or Sytox Red according to the manufacturer's specifications for 15 minutes on ice.

For surface staining experiments, adherent cells were lifted with non-enzymatic cell dissociation buffer (Gibco) and transferred to a 96-well V-bottom plate, and suspension cells were transferred to a 96-well V-bottom plate. After washing three times with 0.5% BSA in PBS, cells were incubated with primary antibody for 30 minutes on ice. Cells were subsequently washed three times with 0.5% BSA in PBS, then incubated with secondary antibodies for 30 minutes on ice. After incubation, cells were washed three times with 0.5% BSA in PBS and incubated with

either Sytox Green or Sytox Red according to the manufacturer's specifications for 15 minutes on ice. Flow cytometry was performed on either a BD-Accuri C6 Plus or DxP FACScan flow cytometer, and analysis was performed using the FlowJo software package. Gating was performed on single cells and live cells.

Cell Surface Degradation Experiment: Adherent cells (70% confluency for 24-hour experiments, 50% confluency for 48-hour experiments) were treated with antibodies or conjugates in complete growth media. At the indicated time, cells were washed three times with DPBS, then lysed as detailed below. Suspension cells were suspended in complete growth media in a flat bottom plate, and at the indicated time transferred to a 96-well V-bottom plate and washed three times with PBS, then lysed as detailed below.

Western Blotting: Cell culture experiments with adherent cells conducted in 24-well plates were washed three times with DPBS, then lysed with RIPA buffer supplemented with protease inhibitor cocktail (Roche), phosphatase inhibitor cocktail (Cell Signaling Technologies) and 0.1% benzonase (Millipore-Sigma) on ice for 30 minutes. The lysates were spun at 21,000*g* for 15 minutes at 4 °C and protein concentration was determined using BCA assay (Pierce). Suspension cell lines were transferred to a 96-well V-bottom plate, washed three times with PBS, then lysed with RIPA buffer supplemented as above. Adherent cells in 6-well plates were washed three times with DPBS then lysed with 1X Laemmli buffer containing protease inhibitor cocktail (Roche) and phosphatase inhibitor cocktail (Cell Signaling Technologies). Lysates were then sonicated on ice using a microtip sonicator for 30 seconds, with 10 second sonication intervals and rest intervals, and protein concentration was determined using BCA assay (Pierce). Equal amounts of lysates were separated by sodium dodecyl sulfate-polyacrylamide gel electrophoresis (4-12% Bis-Tris gel), then transferred to a nitrocellulose membrane. After transfer, the membrane was stained for total protein using REVERT Total Protein Stain (LI-COR), then blocked in TBS-T with 5% non-fat dried milk or Odyssey Blocking Buffer (TBS) (LI-COR) for 1 hour at room temperature with gentle shaking. Membranes were incubated overnight with primary antibody at 4 °C with gentle shaking, then washed three times with TBS-T for five minutes each. The membrane was then incubated with 800CW goat anti-mouse IgG, 800CW goat anti-rabbit IgG, 800CW donkey anti-goat IgG, or 680LT goat anti-rabbit IgG secondary antibodies (1:10,000) in Odyssey Blocking Buffer (TBS) for one hour at room temperature with gentle shaking. Membranes were washed three times with TBS-T, then imaged using an OdysseyCLxImager (LI-COR). Quantification of band intensities was performed using Image Studio Software (LI-COR).

Confocal microscopy: A Nikon A1R confocal microscope equipped with a Plan Fluor 60x oil immersion 1.30–numerical aperture objective was used. This instrument is equipped with a 405-nm violet laser, 488-nm blue laser, 561-nm green, and a 639-nm red laser.

Antibodies and Usage:

Antibody	Source (#)	Usage and dilution
Rabbit anti-EGFR	CST (D38B1)	WB, 1:1000
Goat anti-EGFR	R&D Systems (AF231)	WB, 1:1000
Mouse anti-CD71	Bio-Rad (VMA00037)	WB, 1:1000
Rabbit anti-PD-L1	CST (E1L3N)	WB, 1:500
Mouse anti-Vinculin	Bio-Rad (V284)	WB, 1:1000

Mouse anti-α-Tubulin	Millipore Sigma (T5168)	WB, 1:5000
Rabbit anti-EXOC1	Abcam (ab118798)	WB, 1:2500
Rabbit anti-CIM6PR	CST (D3V8C)	WB, 1:1000
Mouse anti-CD71	BioXCell (BE0023)	Functional
Mouse anti-PD-L1	BioXCell (BE0285)	Functional
Mouse anti-mCherry	Biorbyt (orb66657)	Functional
Mouse anti-ApoE4	Novus Biologicals (4E4)	Functional
Goat anti-Mouse IgG	Jackson ImmunoResearch (115-005-062)	Functional
Mouse anti-biotin-Alexa Fluor 488	Jackson ImmunoResearch (200-542-211)	Functional
Cetuximab	Eli Lilly	Flow cytometry, Functional
Mouse anti-CIM6PR	Abcam (2G11)	Flow cytometry, 1:500
Goat anti-mouse IgG-Alexa Fluor 488	Jackson ImmunoResearch (115-545-008)	Flow cytometry, 1:375
Goat anti-mouse IgG-Alexa Fluor 647	Jackson ImmunoResearch (115-605-071)	Flow cytometry, 1:375
Goat anti-human IgG-Alexa Fluor 647	Jackson ImmunoResearch (109-605-003)	Flow cytometry, 1:375

Mass Spectrometry:

Sample Preparation: Samples were prepared for proteomic analysis using a previously described method with methanol precipitation to extract proteins, followed by tryptic digestion (*38*). Briefly, HeLa cells from each treatment condition were lysed by suspension in 6 M guanidine, total protein concentration was measured using BCA (Thermo Fisher Scientific), and 100 µg of protein was extracted via precipitation in 90% methanol for each sample. Supernatants were decanted and protein pellets were suspended in a buffer comprising 8 M urea, 100 mM tris pH 8, 10 mM tris(2-carboxyethyl)phosphine, and 40 mM chloroacetamide. Following incubation at room temperature for 30 minutes, samples were diluted to 1.5 M urea with 100 mM tris pH 8 and digested with trypsin (50:1 protein to enzyme, Promega, Madison, WI) overnight. Sample cleanup was performed by first quenching with formic acid to a final pH of ~2, followed by desalting over a polystyrene-divinylbenzene solid phase extraction (PS-DVB SPE) cartridge (Phenomenex). Samples were dried with vacuum centrifugation following desalting, and peptide mass was assayed using peptide colorimetric assay (Fisher).

LC-MS/MS: All samples were resuspended in 0.2% formic acid in water at ~ 500 ng/µL, and 500 ng of total peptide mass was injected on column for each sample. Peptides were separated over a 25 cm EasySpray reversed phase LC column (75 µm inner diameter packed with 2 µm, 100 Å, PepMap C18 particles, Thermo Fisher Scientific). The mobile phases (A: water with 0.2% formic acid and B: acetonitrile with 0.2% formic acid) were driven and controlled by a Dionex Ultimate 3000 RPLC nano system (Thermo Fisher Scientific). Gradient elution was performed at 300 nL/min. Mobile phase B was increased to 5% over 6 min, followed by an increase to 40% at 76 min, a ramp to 90% B at 77 min, and a wash at 90% B for 10 min. Flow was then ramped back to 0% B over the course of 1 min, and the column was re-equilibrated at 0% B for 12 min, for a total analysis of 100 minutes. Eluted peptides were analyzed on an Orbitrap Fusion Tribrid MS system (Thermo Fisher Scientific). Precursors were ionized using an EASY-Spray ionization source (Thermo Fisher Scientific) source held at +2.2 kV compared to ground, and the column was held at 40 °C. The inlet capillary temperature was held at 275 °C. Survey scans of peptide precursors were collected in the Orbitrap from 350-1500 Th with an AGC target of 1,000,000, a maximum

injection time of 50 ms, and a resolution of 120,000 at 200 m/z. Monoisotopic precursor selection was enabled for peptide isotopic distributions, precursors of z = 2-5 were selected for data-dependent MS/MS scans for 2 seconds of cycle time, and dynamic exclusion was set to 45 seconds with a ±10 ppm window set around the precursor monoisotope. An isolation window of 0.7 Th was used to select precursor ions with the quadrupole. MS/MS scans were collected using HCD at 30 normalized collision energy (nce) with an AGC target of 30,000 and a maximum injection time of 25 ms. Mass analysis was performed in the linear ion trap using the "Rapid" scan speed while scanning from 200-1500 Th.

Data Analysis: Raw data were processed using MaxQuant version 1.6.3.4 (*39*), and tandem mass spectra were searched with the Andromeda search algorithm (*40*). Oxidation of methionine and protein N-terminal acetylation were specified as variable modifications, while carbamidomethylation of cysteine was set as a fixed modification. A precursor ion search tolerance of 20 ppm and a product ion mass tolerance of 0.3 Da were used for searches, and two missed cleavages were allowed for full trypsin specificity. Peptide spectral matches (PSMs) were made against a target-decoy human reference proteome database downloaded from Uniprot. Peptides were filtered to a 1% false discovery rate (FDR) and a 1% protein FDR was applied according to the target-decoy method (*41*). Proteins were identified and quantified using at least one peptide (razor + unique), where razor peptide is defined as a non-unique peptide assigned to the protein group with the most other peptides (Occam's razor principle). Proteins were quantified and normalized using MaxLFQ (*42*) with a label-free quantification (LFQ) minimum ratio count of 1. LFQ intensities were calculated using the match between runs feature, and MS/MS spectra were required for LFQ comparisons. For quantitative comparisons, protein intensity values were log2 transformed prior to further analysis, and missing values were imputed from a normal distribution with width 0.3 and downshift value of 1.8 (i.e., default values) using the Perseus software suite (*43*). Significance calculations were performed using a two-tailed t-test with heteroscedastic variance (performed in Microsoft Excel).

Supplemental Figures

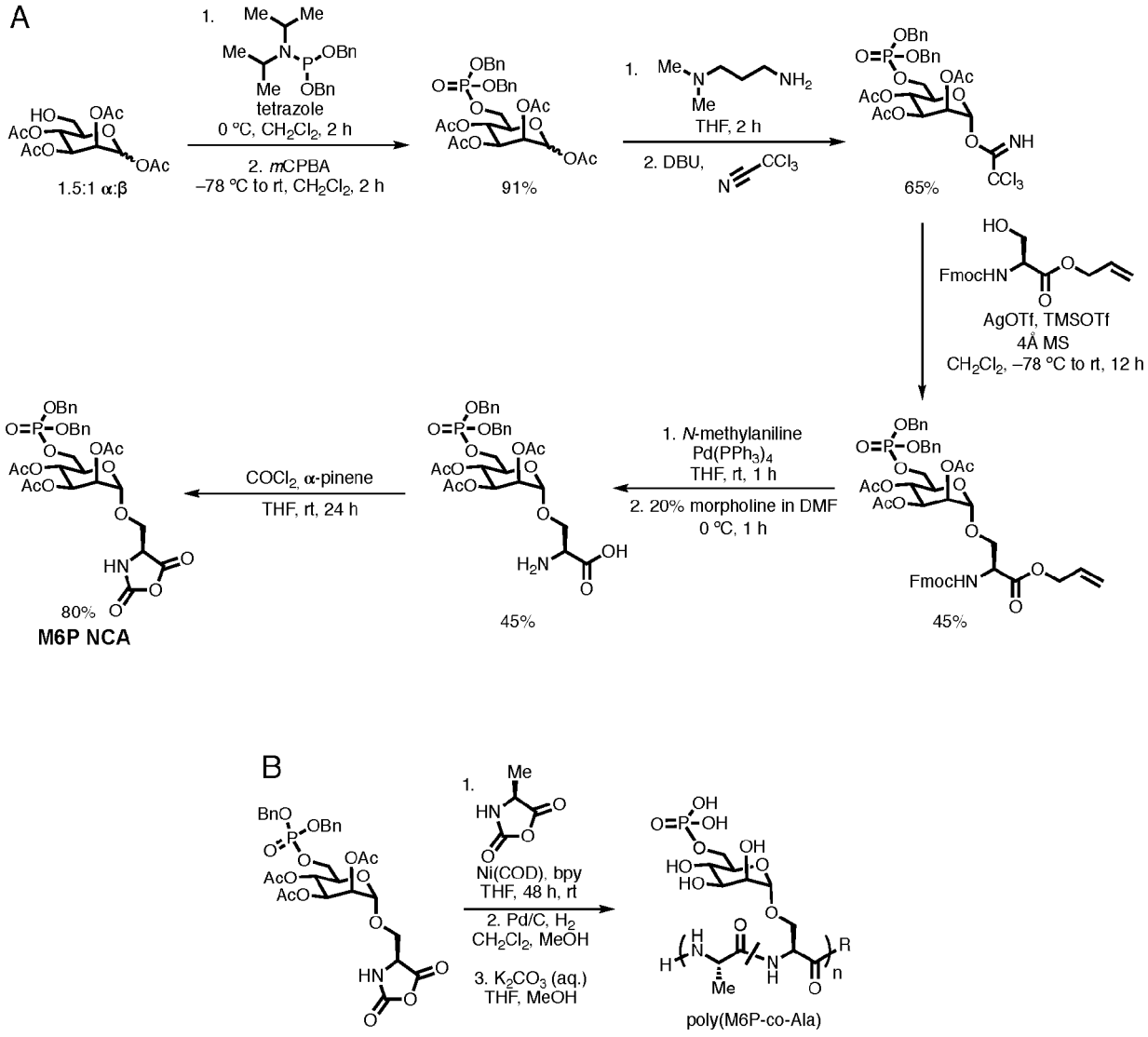

Fig. S1. Synthesis of mannose-6-phosphate (M6P) glycopolypeptides. (A) Synthetic route to mannose-6-phosphate-serine *N*-carboxyanhydride (NCA). (B) General synthetic scheme for poly(M6P) glycopolypeptides. Polymerization reactions were carried out in a N_2 glovebox for 48 hours in THF.

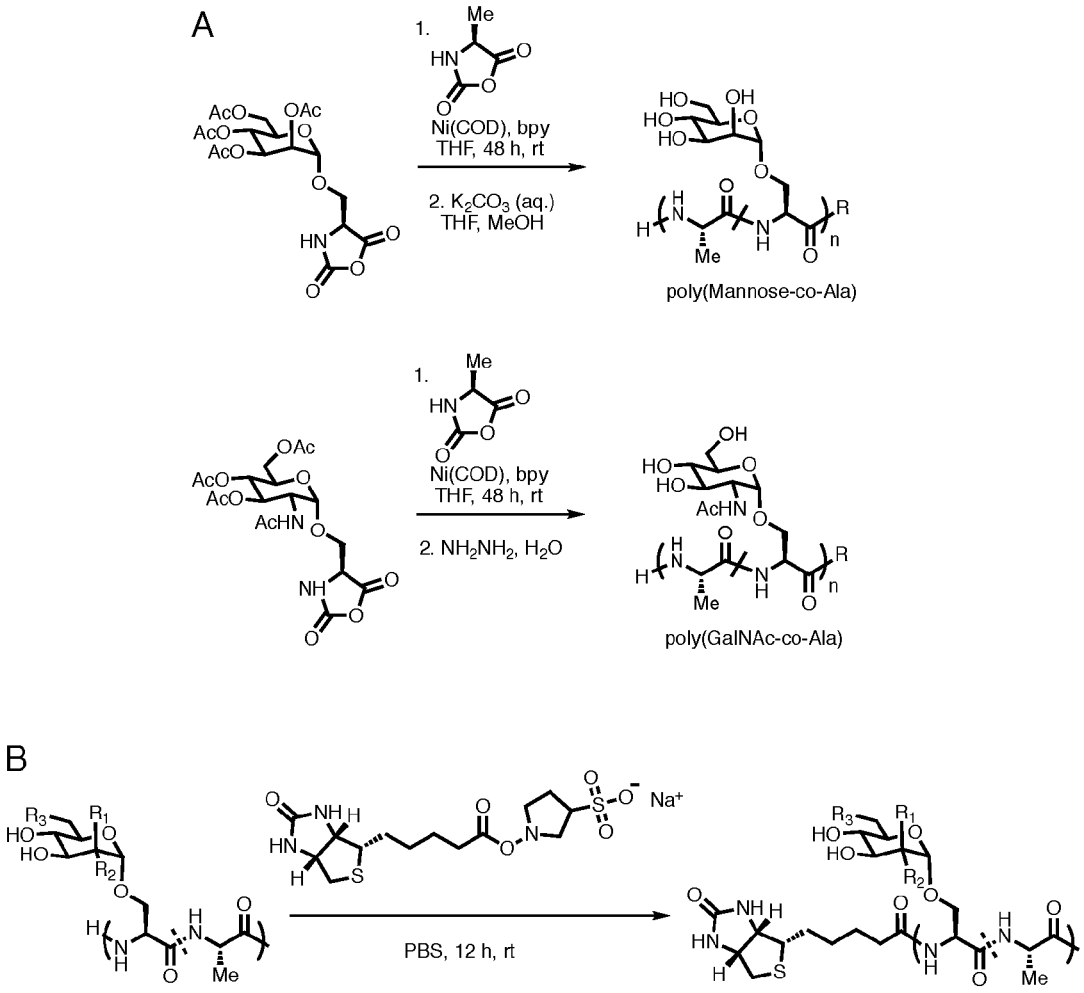

Fig. S2. Synthesis of poly(Mannose-co-Ala), poly(GalNAc-co-Ala) and N-terminal biotinylation of glycopolypeptides. (A) General synthetic schemes for polymerization of Mannose-NCA and GalNAc-NCA. (B) General scheme for biotinylation of glycopolypeptides with sulfo-NHS biotin. Biotinylation reactions were performed in 1X PBS at room temperature overnight.

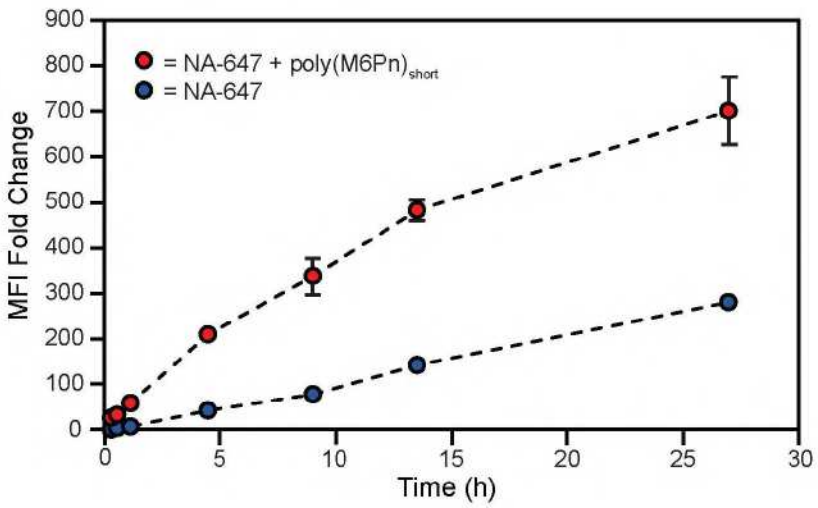

Fig. S3. CIM6PR-mediated NeutrAvidin (NA-647) uptake is continuous over time in K562 cells. K562 cells were incubated at 37 °C in full-serum media with 500 nM NA-647 or 500 nM NA-647 and 2 μM poly(M6Pn)$_{short}$ for the indicated time, then washed and analyzed by live cell flow cytometry. The mean fluorescence intensity (MFI) was measured relative to background fluorescence from untreated K562 cells. Error bars represent standard deviation of three independent experiments.

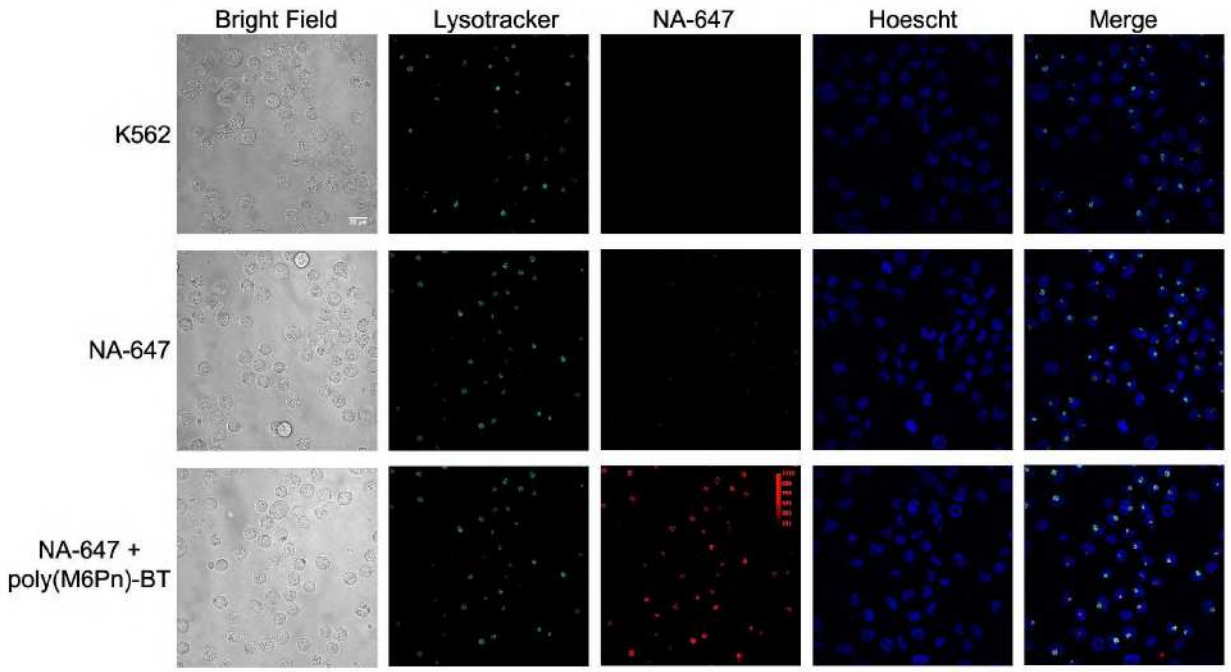

Fig. S4. Biotiylated poly(M6Pn) LYTACs direct NeutrAvidin-647 (NA-647) to lysosomes in K562 cells. K562 cells were incubated with PBS, 500 nM NA-647, or 500 nM NA-647 and 2 μM biotinylated poly(M6Pn)$_{short}$ for 1 h in full-serum media. NA-647 (red) colocalized with acidic endosomes and lysosomes as labeled with Lysotracker Green (turquoise). Scale bar is 20 μM. Fluorescence intensity is normalized in the NA-647 channel for all images.

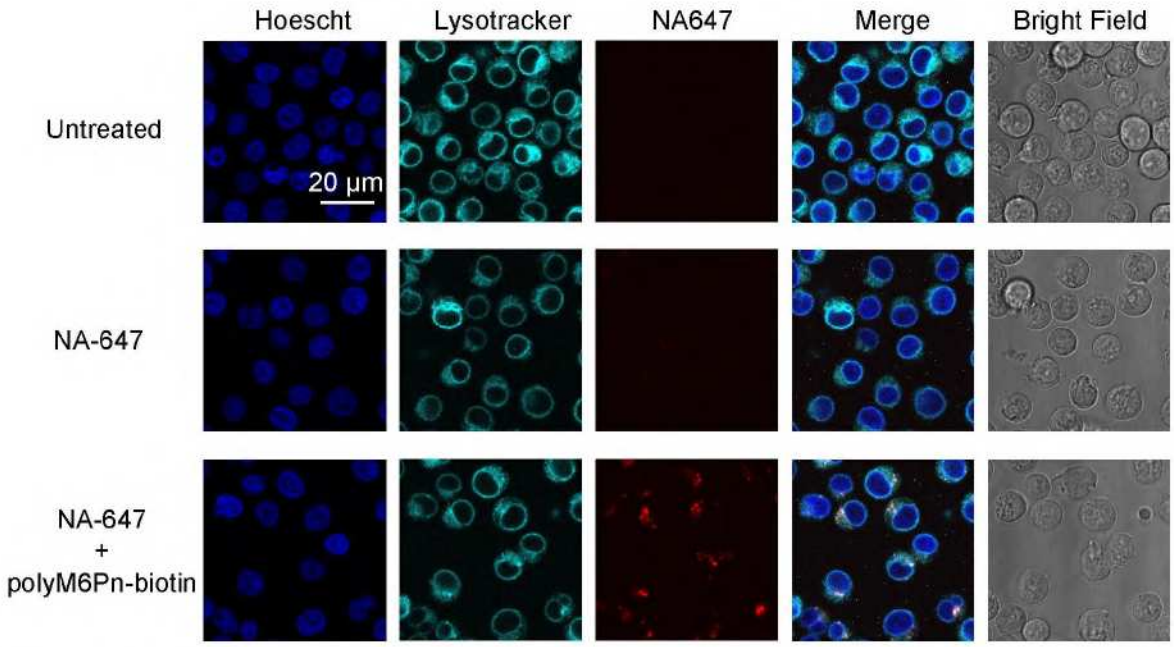

Fig. S5. Biotiylated poly(M6Pn) LYTACs direct NeutrAvidin-647 (NA-647) to lysosomes in Jurkat cells. Jurkat cells were incubated with PBS, 500 nM NA-647, or 500 nM NA-647 and 2 µM biotinylated poly(M6Pn)$_{short}$ for 0.5 h in full-serum media. NA-647 (red) colocalized with acidic endosomes and lysosomes as labeled with Lysotracker Green (turquoise). Scale bar is 20 µM. Fluorescence intensities are normalized for all images.

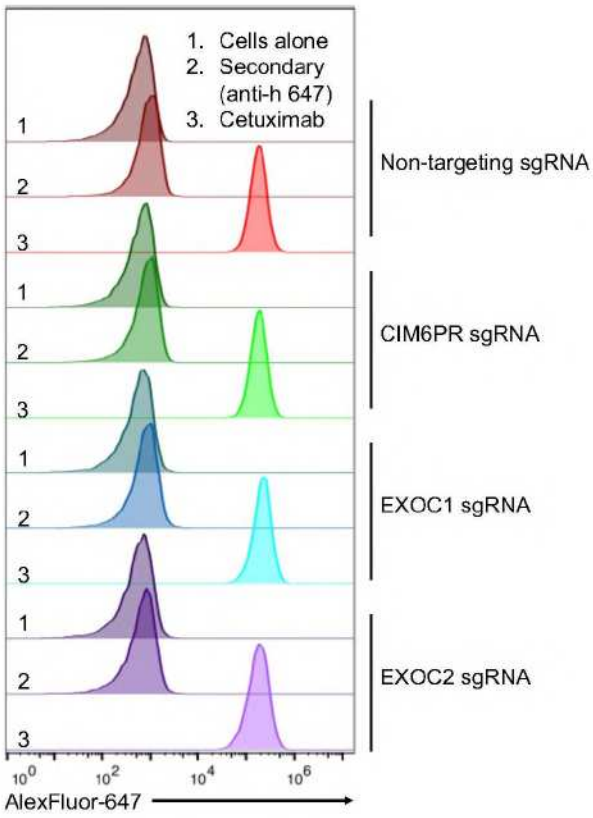

Fig. S6. EGFR surface localization is unchanged in EXOC1 and EXOC2 knockdown HeLa cells. Cetuximab binds equally to dCas9-KRAB HeLa cells transfected with non-targeting sgRNA and cells transfected with sgRNA against CI-M6PR, EXOC1, or EXOC2, indicating no change in EGFR surface transport. Cells were subjected to live cell flow cytometry using cetuximab followed by an anti-human AlexaFluor-647 conjugated anti-human (anti-h 647) secondary antibody.

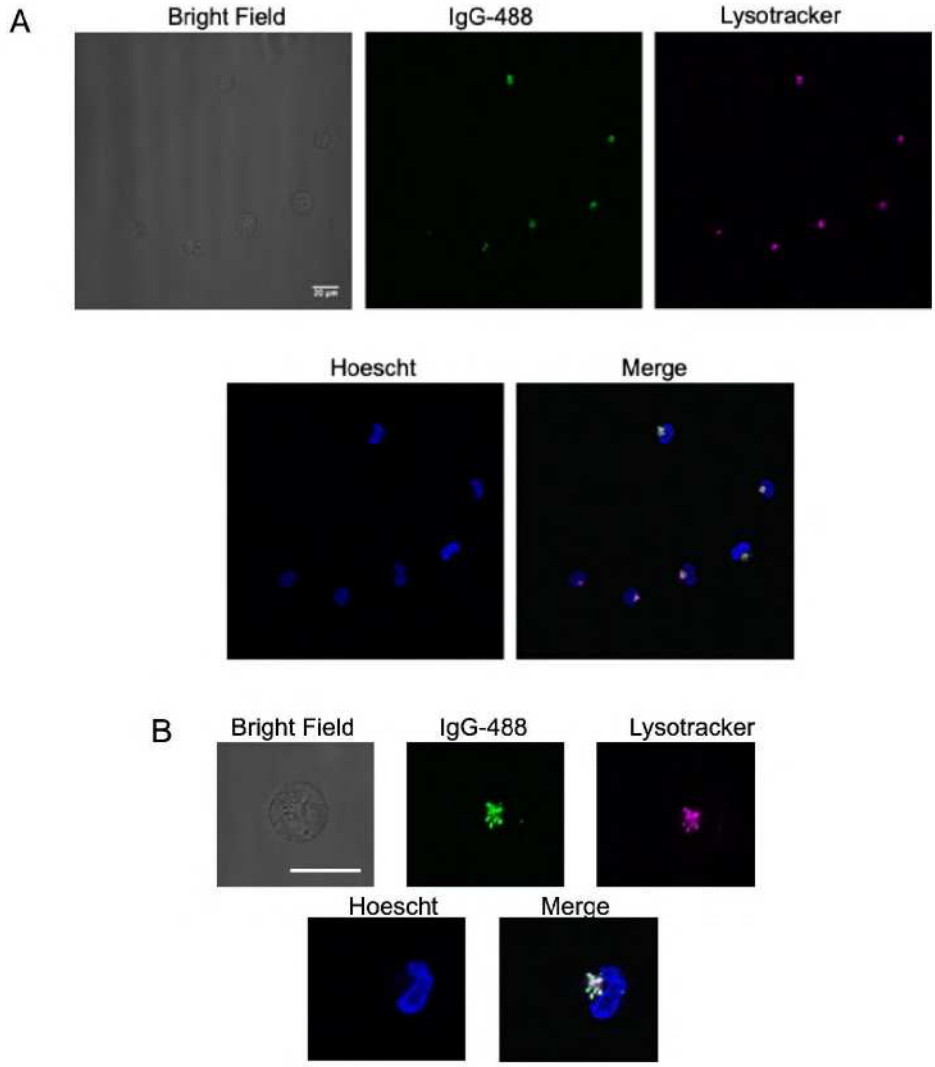

Fig. S7. Ab-1 mediates uptake of soluble proteins to lysosomes. (A) K562 cells were incubated with PBS, 50 nM *m*-IgG-488, or 50 nM *m*-IgG-488 and 25 nM Ab-1 for 1 h in full-serum media at 37 °C. IgG-488 (green) colocalized with acidic endosomes and lysosomes as labeled with Lysotracker Red (magenta). (B) Expanded view of K562 cells containing IgG-488 and Lysotracker Red. Scale bars are 20 μm.

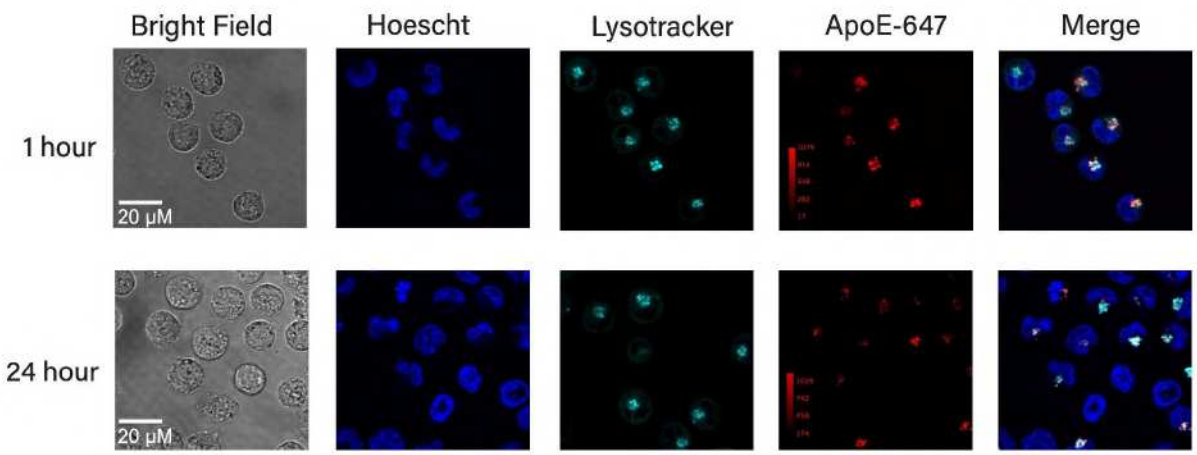

Fig. S8. Ab-1 mediates uptake of ApoE4-647 to lysosomes at both 1 and 24 hours. (A) K562 cells were incubated with PBS, 50 nM ApoE4-647, 25 nM anti-ApoE4, and 25 nM Ab-1 for 1 h or 24 h in full-serum media at 37 °C. AlexaFluor-647 signal (red) colocalizes with acidic endosomes and lysosomes as labeled with Lysotracker Green (turquoise).

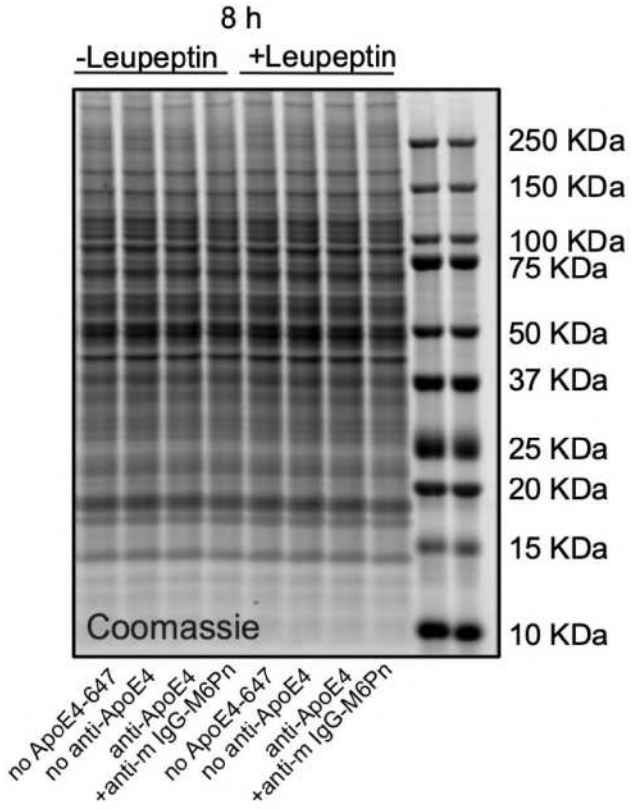

Fig. S9. Total protein levels for leupeptin inhibition of apoE4 degradation in K562 cells, corresponding to lanes shown in Figure 3K. Total protein was visualized by Coomassie stain.

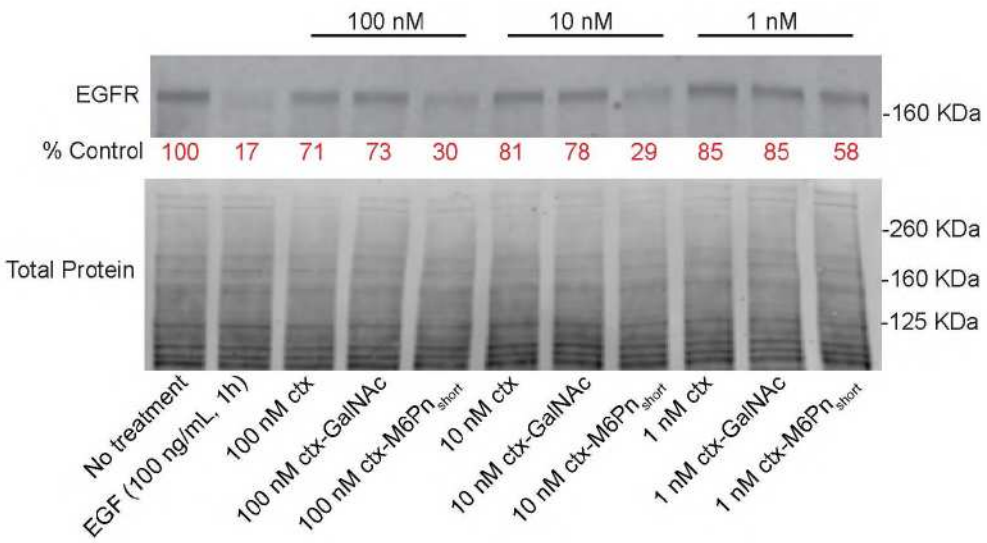

Fig. S10. LYTAC-mediated EGFR degradation occurs in a concentration dependent manner. HeLa cells were incubated with 100 nM, 10 nM, or 1 nM conjugates for 24 hours in full serum media. After 24 hours, cells were lysed, and total EGFR levels were measured by Western blot. Percent control was calculated by densitometry and normalized to total protein.

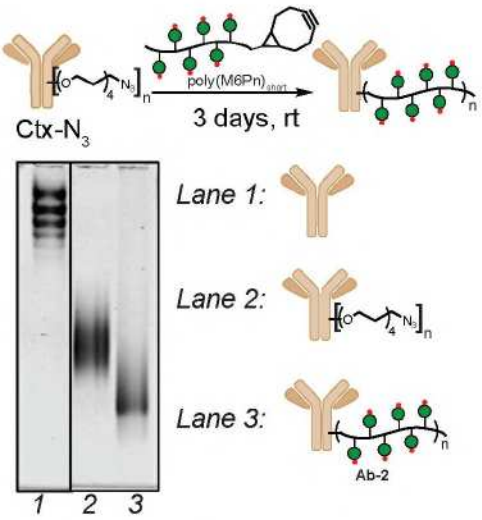

Fig. S11. Synthesis of Ab-2. Cetuximab was labeled with NHS-PEG_4-N_3, then incubated with BCN-functionalized $poly(M6Pn)_{short}$ for 3 days at room temperature. Reaction progress was monitored by native gel electrophoresis and visualized with Coomassie stain.

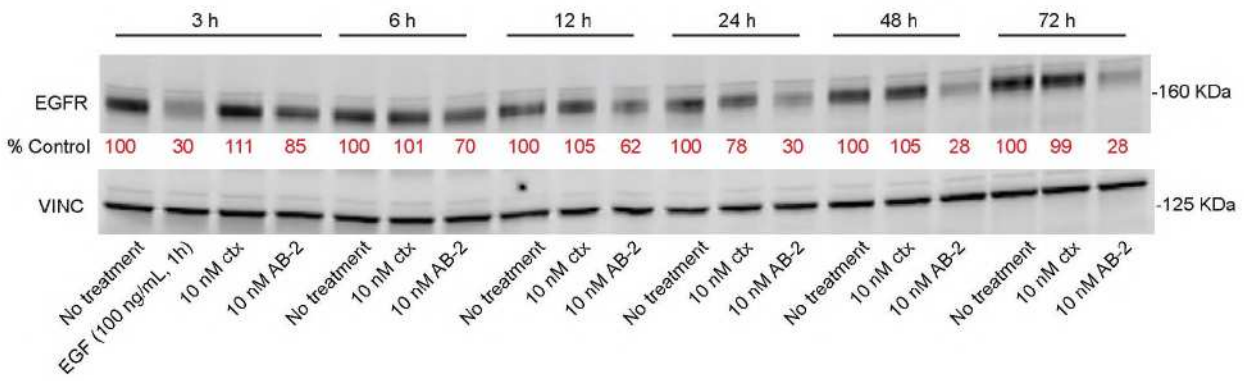

Fig. S12. LYTAC-mediated EGFR degradation increases over time. HeLa cells were incubated with conjugates for the indicated time, then washed and lysed. Total EGFR levels were assayed by Western blot and degradation was calculated by densitometry normalized to vinculin loading control.

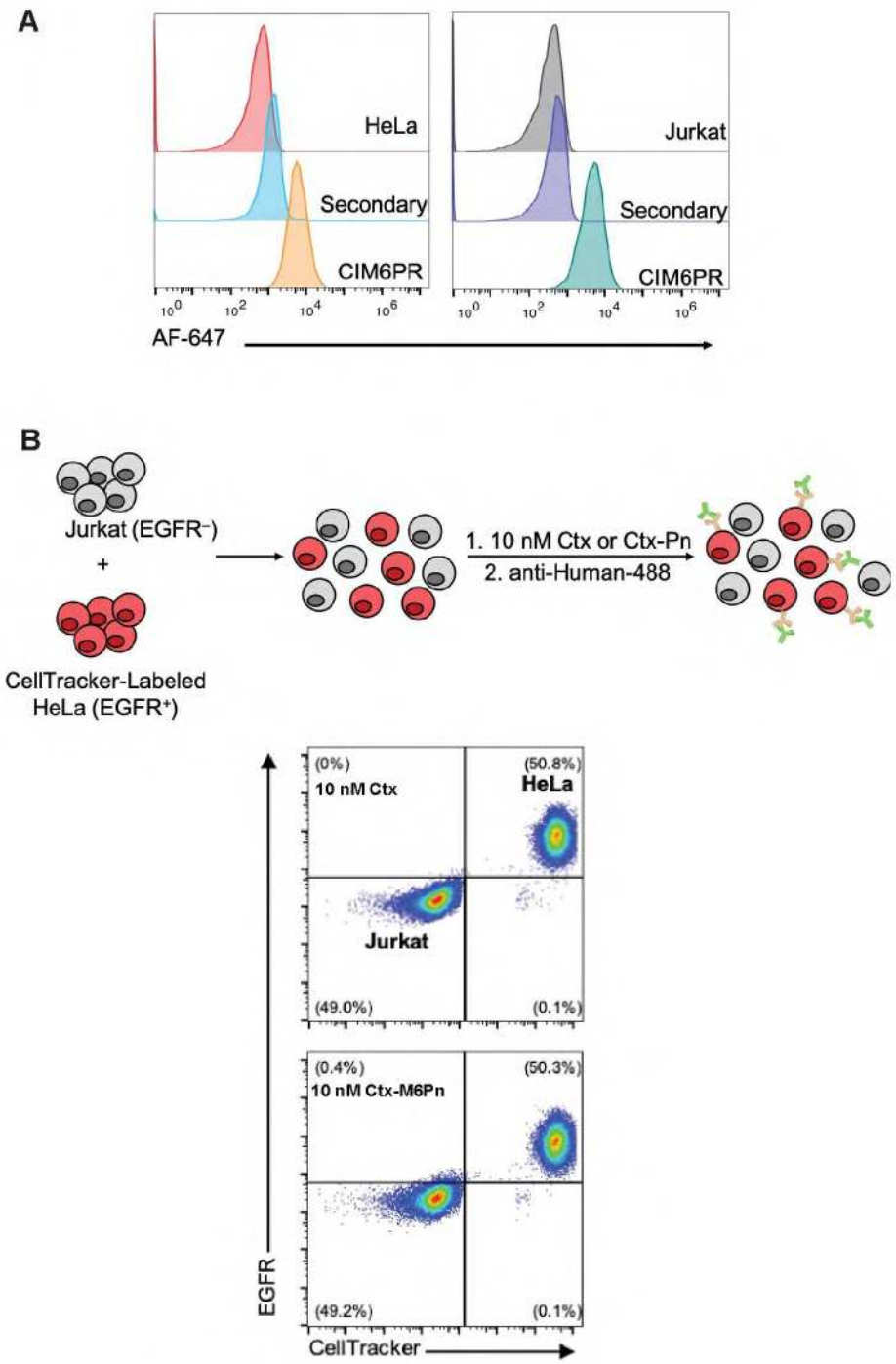

Fig. S13. Mixed-cell assay demonstrates that ctx-M6Pn binding specificity is comparable to ctx. (A) Cell surface CIM6PR levels on HeLa cells (CIM6PR$^+$EGFR$^+$) and Jurkat cells (CIM6PR$^+$EGFR$^-$) was measured by live cell flow cytometry. HeLa and Jurkat exhibited similar levels of cell surface CIM6PR. (B) HeLa cells were lifted and labeled with CellTracker Deep Red, then mixed in a 1:1 ratio with Jurkat cells. The mixed cell sample was stained with 10 nM cetuximab or ctx-M6Pn conjugate and anti-human 488, then subjected to live cell flow cytometry. Ctx and ctx-M6Pn exhibit equivalent binding to HeLa cells, and ctx-M6Pn exhibits < 1% increased binding to Jurkat cells relative to ctx.

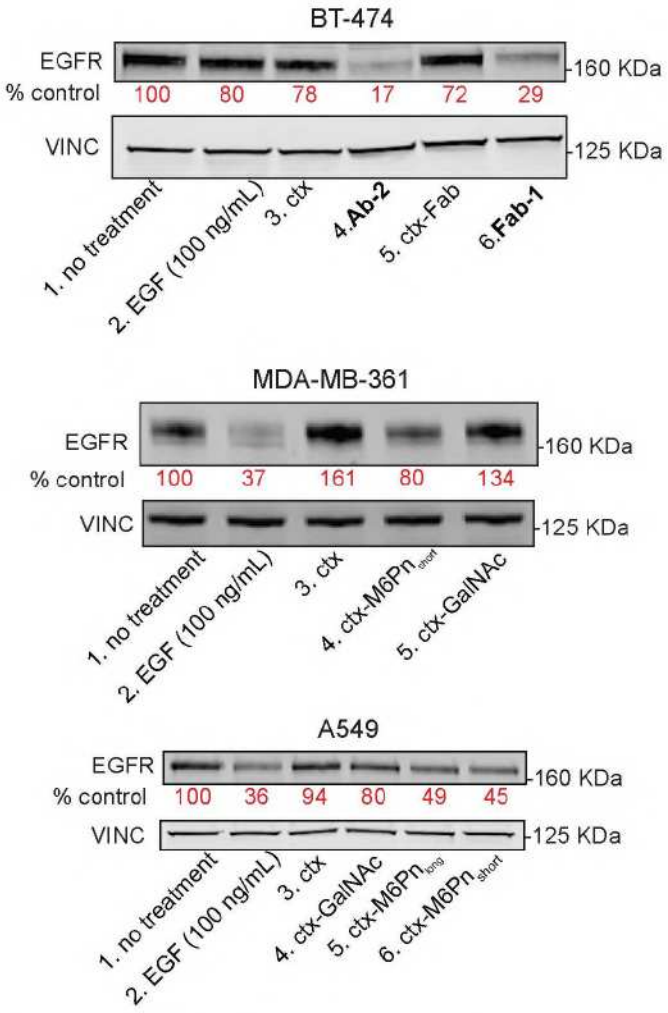

Fig. S14. EGFR is degraded in multiple cell lines. BT-474, MDA-MB-361, or A549 cells were incubated with 20 nM conjugates, then washed and lysed. Total EGFR amounts were assayed by Western blot, and degradation was measured by densitometry normalized to vinculin loading control.

	Ab-2 (ctx-M6Pn)	
	Downregulated	
	Fold Change	p value
DHPR	-3.08	0.023
TFDP1	-2.98	0.039
8ODP	-1.82	0.019
CD99	-1.8	0.051
UBXN6	-1.55	0.043
WDR11	-1.38	0.049
BAG5	-1.35	0.015
AGAP3	-1.31	0.036
SCO2	-1.21	0.017
ORC2	-1.08	0.015
	Upregulated	
	Fold Change	p value
CCD57	3.82	0.046
PGM2L	2.72	0.012
NFIB	2.48	0.003
ALKB5	2.21	0.029
COPRS	2.13	5.4E-05
IGKC	1.99	0.009
FRYL	1.99	0.024
DESP	1.12	0.0006

	Cetuximab	
	Downregulated	
	Fold Change	p value
TF2B	-2.37	0.008
HIF1N	-1.54	0.042
	Upregulated	
	Fold Change	p value
CCD57	3.82	0.036
IGKC	3.15	0.032
NFIB	2.43	0.006
PO2F1	2.06	0.03
NRBP	2.01	0.011

Fig. S15. Examples of proteins with differential abundance following treatment of HeLa cells with ctx. or ctx.-M6Pn. Untreated, ctx-treated, or Ab-2-treated HeLa cells were lysed, digested, and analyzed by quantitative proteomics. Depicted are exemplary hits with fold change values reported relative to untreated samples. Proteins highlighted in gray were found in both ctx and Ab-2 treated cells. For a full list, see Supplementary Data 2.

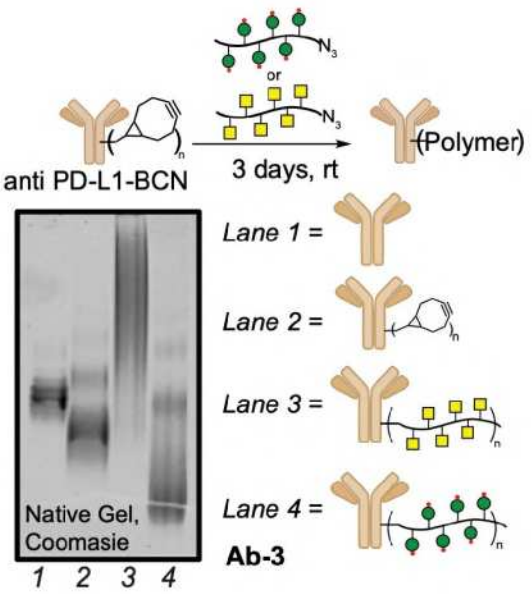

Fig. S16. Synthesis of anti PD-L1 glycopolypeptide conjugates. Anti-PD-L1 was non-specifically labeled with BCN, then incubated with poly(M6Pn)$_{short}$ for 3 days at room temperature. Reaction progress was monitored by native gel electrophoresis and visualized by Coomassie stain.

NMR and FTIR Spectra

^{1}H NMR
400 MHz
$CDCl_3$

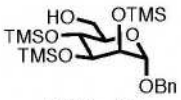

M6Pn-I2

^{13}C NMR
101 MHz
$CDCl_3$

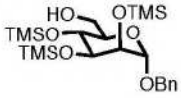

^{1}H NMR
400 MHz
$CDCl_3$

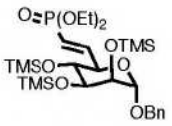

M6Pn-I3

^{13}C NMR
101 MHz
$CDCl_3$

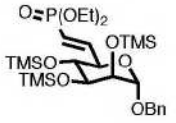

^{31}P NMR
162 MHz
$CDCl_3$

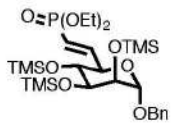

^{1}H NMR
400 MHz
$CDCl_3$

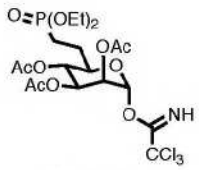

M6Pn-I4

^{13}C NMR
101 MHz
$CDCl_3$

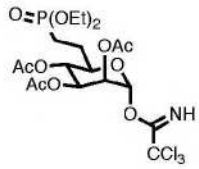

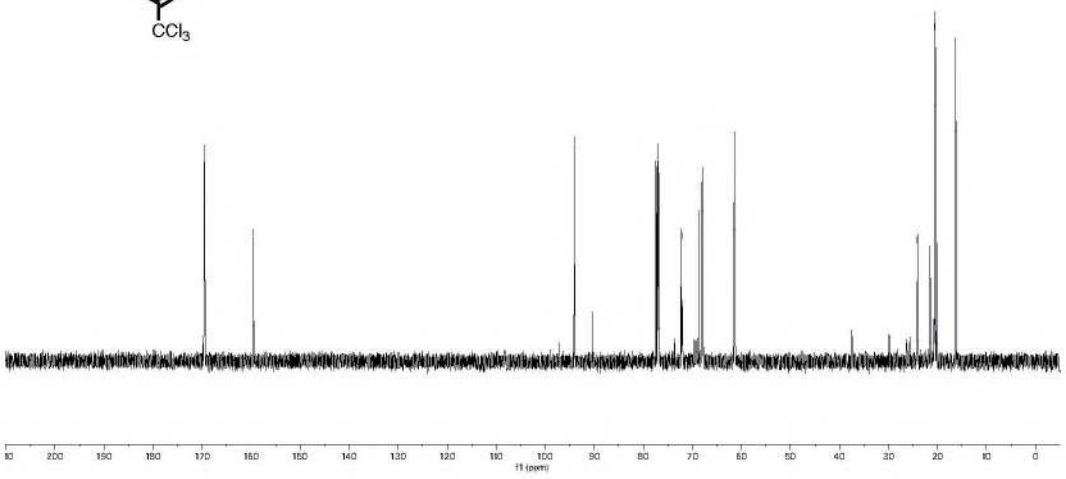

^{31}P NMR
162 MHz
$CDCl_3$

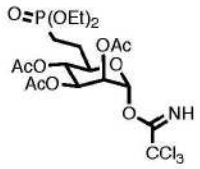

^{1}H NMR
400 MHz
$CDCl_3$

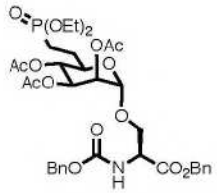

M6Pn-I5

^{13}C NMR
101 MHz
$CDCl_3$

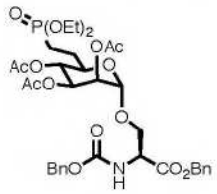

^{31}P NMR
162 MHz
$CDCl_3$

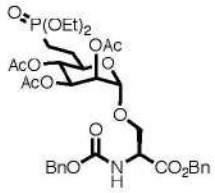

^{1}H NMR
400 MHz
$CDCl_3$

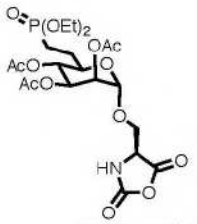

M6Pn-NCA

^{13}C NMR
101 MHz
$CDCl_3$

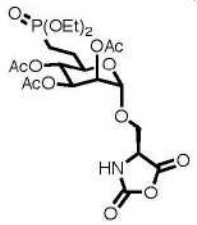

^{31}P NMR
162 MHz
$CDCl_3$

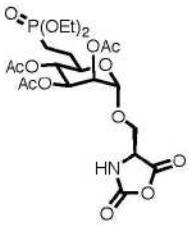

^{1}H NMR
400 MHz
$CDCl_3$

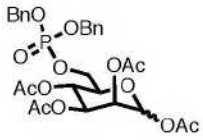

M6P-I2

^{13}C NMR
101 MHz
$CDCl_3$

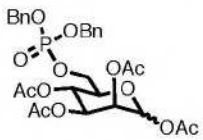

^{31}P NMR
162 MHz
$CDCl_3$

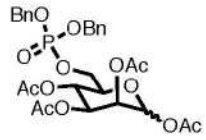

^{1}H NMR
400 MHz
$CDCl_3$

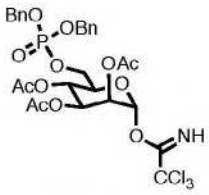

M6P-I3

^{13}C NMR
101 MHz
$CDCl_3$

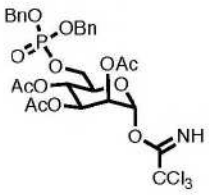

^{31}P NMR
162 MHz
$CDCl_3$

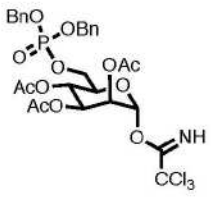

^{1}H NMR
400 MHz
$CDCl_3$

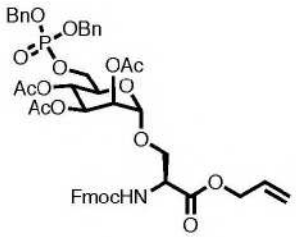

M6P-I4

^{13}C NMR
101 MHz
$CDCl_3$

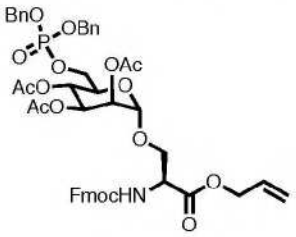

^{31}P NMR
162 MHz
$CDCl_3$

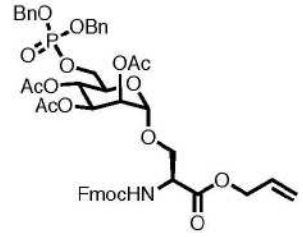

^{1}H NMR
400 MHz
CD_3OD

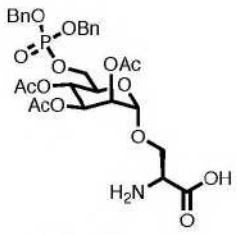

M6P-I5

^{13}C NMR
101 MHz
CD_3OD

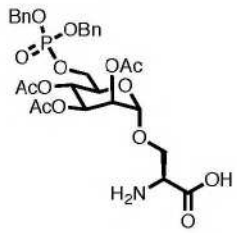

^{31}P NMR
162 MHz
CD_3OD

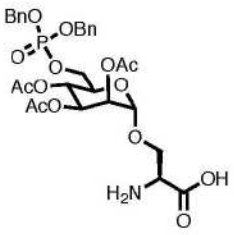

^{1}H NMR
400 MHz
$CDCl_3$

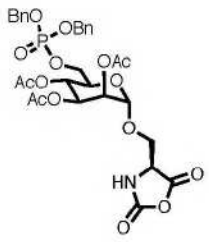

M6P-NCA

^{13}C NMR
101 MHz
$CDCl_3$

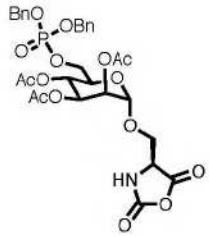

^{31}P NMR
162 MHz
$CDCl_3$

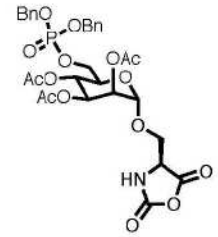

^{1}H NMR
600 MHz
D_2O

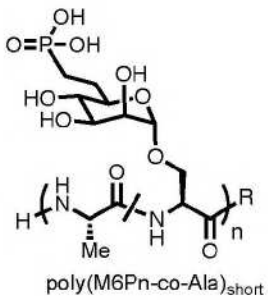

poly(M6Pn-co-Ala)$_{short}$

^{31}P NMR
162 MHz
D_2O

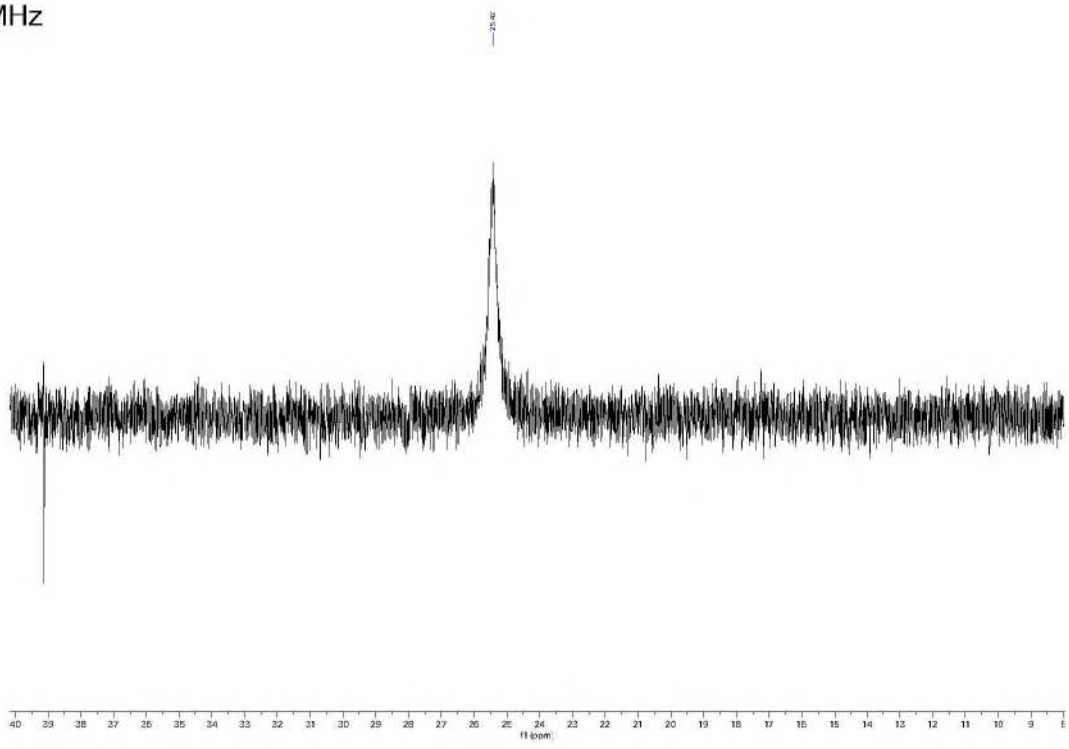

^{1}H NMR
600 MHz
D_2O

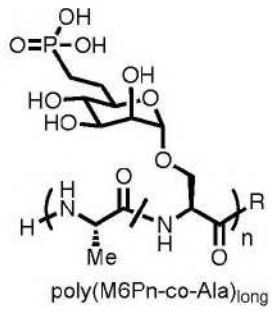

poly(M6Pn-co-Ala)$_{long}$

^{31}P NMR
162 MHz
D_2O

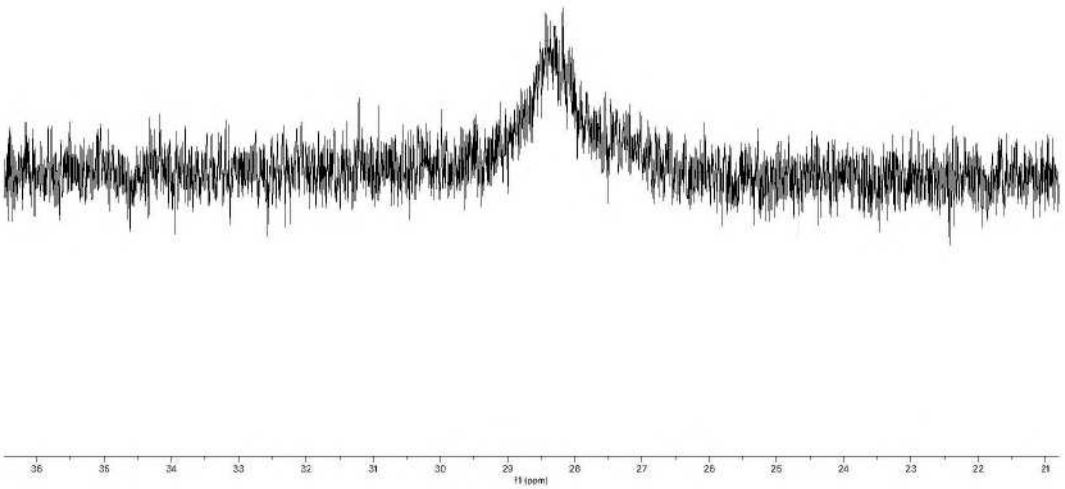

^{1}H NMR
600 MHz
D_2O

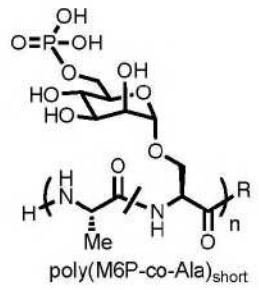

poly(M6P-co-Ala)$_{short}$

^{31}P NMR
162 MHz
D_2O

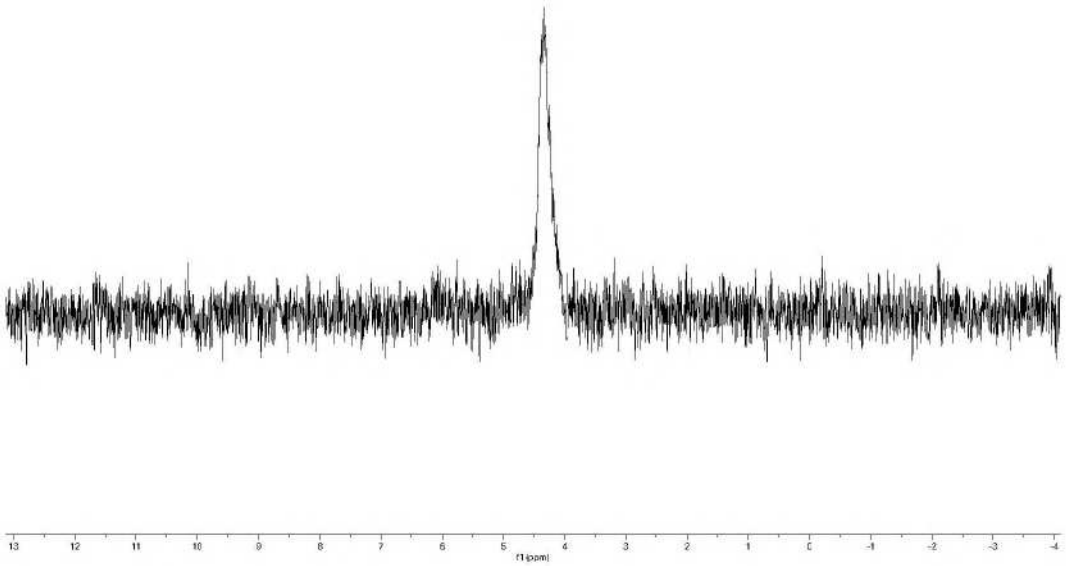

^{1}H NMR
600 MHz
D_2O

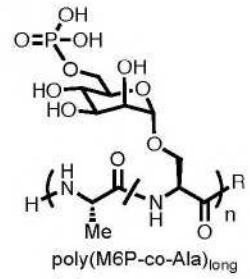

poly(M6P-co-Ala)$_{long}$

^{31}P NMR
162 MHz
D_2O

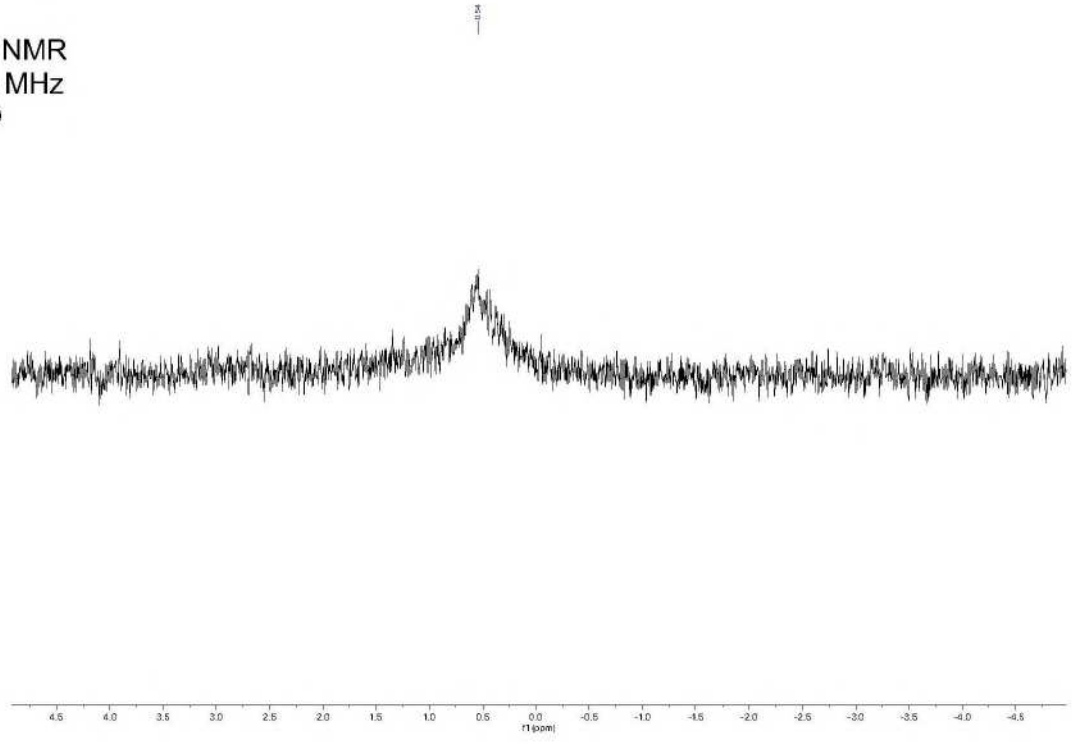

Other files

Supplemental Data 1.xlsx (10.29 MiB)	view on ChemRxiv • download file
Supplemental Data 2.xlsx (572.50 KiB)	view on ChemRxiv • download file